The Late Proterozoic to Palaeozoic Tectonic Evolution of the Long Range Mountains in southwestern Newfoundland

by

Arjan Gerben Brem

A thesis
presented to the University of Waterloo
in fulfillment of the
thesis requirement for the degree of
Doctor of Philosophy
in
Earth Sciences

Waterloo, Ontario, Canada, 2007

Author’s declaration

I hereby declare that I am the sole author of this thesis. This is a true copy of the thesis, including any required final revisions, as accepted by my examiners.

I understand that my thesis may be made electronically available to the public.

Abstract

Ever since the first plate-tectonic model for the Appalachians was proposed, the Laurentian margin has been interpreted as having experienced a collision-related dynamo-thermal event during the Middle Ordovician Taconic orogeny. In the western Newfoundland Appalachians, evidence for this collision is well-preserved in the Dashwoods subzone. Nevertheless, rocks of the neighbouring Corner Brook Lake block (CBLB), which is located in the heart of the Laurentian realm, did not show evidence for such an event. Instead, it was affected by Early Silurian Salinic deformation and associated peak metamorphism. Even though this difference in Early Palaeozoic tectonic history between the Dashwoods and the CBLB is widely known, it has not been satisfactorily explained.

To better understand the Early Palaeozoic history of the region, in particular to test and better explain the lack of a Taconic dynamo-thermal event in the CBLB, field mapping, microscopic work, and U-Pb and $^{40}Ar/^{39}Ar$ geochronological studies were undertaken in the western and northern part of the Dashwoods subzone, and in the southern part of the CBLB. In addition, the kinematic history of the Baie Verte-Brompton Line - Cabot Fault Zone (BCZ), the tectonic zone that separates the two unique tectonic fragments, was studied.

The western and northern parts of the Dashwoods subzone contain variably foliated igneous units of Middle Ordovician age (ca. 460 Ma) that are associated with the regionally voluminous Notre Dame continental arc. A ca. 455 Ma conjugate set of late syn-tectonic pegmatite dykes in the BCZ demonstrates a dextral sense of shear along the BCZ (D_{BCZ-1}) during the Late Ordovician to earliest Silurian, and constrains the minimum age of the main phase of ductile deformation in the Dashwoods subzone.

The fault-bounded CBLB has been affected by a single west-vergent deformational event, constrained between ca. 434 and ca. 427 Ma. More importantly, no evidence – neither petrographic nor

geochronological – is present that would indicate that the CBLB was affected by a significant Taconic dynamo-thermal event. Hence, the CBLB and Dashwoods could not have been juxtaposed until after the late Early Silurian. Furthermore, the basement to the CBLB is devoid of any Grenville (*sensu lato*; ca. 1.0-1.3 Ga) U-Pb ages, which is in sharp contrast with crystalline basement elsewhere in the region, such as the Long Range Inlier. Therefore, it is highly unlikely that the CBLB represents the para-autochthonous leading edge of the Laurentian craton in the Newfoundland Appalachians, as commonly accepted. The CBLB is interpreted as a suspect terrane that has moved over 500 km parallel to the strike of the orogen. Docking to the external Humber Zone is likely to have occurred during the Early Silurian. Final juxtaposition with the Dashwoods took place after the late Early Silurian (post-Salinic) as a result of protracted dextral movement along the BCZ (D_{BCZ-2} and D_{BCZ-5}).

Current tectonic models for the Newfoundland Appalachians mainly focus on well-documented Early Palaeozoic orthogonal convergence of various terranes with the Laurentian margin, but large-scale orogen-parallel movements have rarely been considered. The possibility of large-scale strike-slip tectonics documented here, in addition to the convergent motions, may have significant implications for the tectonic interpretation of the Early Palaeozoic evolution of the Newfoundland Appalachians.

Acknowledgements

The research in this thesis forms part of the “Red Indian Line” project funded by the Geological Survey of Canada’s Targeted Geoscience Initiative (TGI) 000018 and led by Dr. Cees van Staal. It is also supported by Natural Sciences and Engineering Research Council (NSERC) grants to Drs. Shoufa Lin and Don Davis, and an Ontario Premier’s Research Excellence Award to Dr. Shoufa Lin. Additional funding came from the University of Waterloo in the form of International Graduate Student awards and a Doctoral Thesis Completion Award.

I would like to take this opportunity to thank my thesis supervisors, Dr. Shoufa Lin and Dr. Cees van Staal for support, guidance and especially their patience during my years as a graduate student. I am very grateful for the opportunity that I have been able to participate in their personal project. Dr. Shoufa Lin is thanked for the many discussions on various topics of structural geology and tectonics, as well as supporting me in the pursuit of my own ideas. Dr. Cees van Staal is thanked for introducing me to the fascinating geology of the Newfoundland Appalachians and sharing his wealth of knowledge on Appalachian geology.

Next my appreciation goes to Drs. Mario Coniglio, Don Davis, and Bob Linnen for being on my thesis committee and for giving their constructive criticism of this manuscript. Sue Fisher is thanked for helping out with all the bureaucratic issues; without her I would have long been lost in this Department.

This research would not have been possible without the help of many people in the field and laboratory. Melissa Battler, Melodie Stone and Oliver Wendland are thanked for their competent field assistance. Thanks to Drs. Vicki McNicoll and Nancy Joyce at the Geological Survey of Canada in Ottawa for processing the U-Pb SHRIMP and Ar-Ar geochronology samples, respectively. I am very grateful to Dr. Don Davis and his staff at the Jack Satterly geochronology laboratory in Toronto for the many hours that I was allowed to spend in the intricate world of U-Pb (TIMS) geochronology. Special

thanks go to Kim Kwok and Dr. Mike Hamilton for their enthusiastic and sometimes late-night help and admirable patience during the long hours in the chemistry room and behind the mass spectrometer. George Kretschmann and Shawn McConville at the University of Toronto are thanked for their help with BSEM imaging. Greyhound Buslines® is acknowledged for their logistical support. Dr. Sandra Barr, Dr. Greg Dunning, Dr. Johan Lissenberg, Dr. Vicki McNicoll, Dr. Sally Pehrsson, Mr. Jeff Pollock, Dr. Joe Whalen and Dr. Alex Zagorevski are thanked for the numerous discussions on regional Appalachian geology.

I could not have survived every-day life in Kitchener-Waterloo if it was not for my friends and barroom buddies in Canada: Matt Downey, Yvette Kuiper, Chad Macavelia, Jen Parks and many others. Also thanks to my friends back home: Desiree Bakker, Simone de Jong, Paul Mulder, and Martijn Sleutel, whose correspondance have meant a lot to me and who have kept my spirits up. Thanks to Waterloo County RFC and its members; weekdays may be schooldays, but Saturday is a rugby day!

Last but not least, I would like to extend my warmest gratitude to Terri-lyn, as well as my beloved mother and sister for their encouragements and continued loving support. Thank you for believing in me, I could not have accomplished this feat without you.

Dedication

Voor mijn ouders.

Table of Contents

List of Figures

List of Tables

Chapter 1: Introduction

1.1. General Introduction

The Appalachian-Caledonian mountain belt in eastern North America (Figure 1.1) and Western Europe is a narrow linear mountain belt that was formed by the Late Neoproterozoic opening and Palaeozoic closure of the proto-Atlantic Iapetus Ocean and associated basins (Wilson, 1966; Williams, 1995; Waldron and van Staal, 2001; van Staal, 2007). In the original plate-tectonic model proposed for the Newfoundland Appalachians by Dewey (1969), the Laurentian margin, which underlies the western side of the island, was suggested to have experienced a single orogenic event during the Ordovician: the Taconic orogeny. With continued research over the past four decades, this basic model has been shaped into a more complex geodynamic framework that is interpreted as resembling the present-day southwest Pacific Ocean geodynamic setting (Williams and Hatcher, 1982; van Staal et al., 1998). Such a setting is characterized by the presence of numerous individual entities, including continental plates, microcontinents, spreading centres, subduction zones, volcanic arcs, and sedimentary basins. Some of these entities may be very short-lived and regionally discontinuous. During collision, amalgamation of these individual elements takes place in subsequent yet distinct orogenic phases. For the Newfoundland Appalachians, various elements were added to the composite Laurentian margin during the Early Palaeozoic, including the Gander terrane during the Early Silurian Salinic orogeny (Dunning et al., 1990; van Staal, 2007) and the Avalon terrane during the Early-Middle Devonian Acadian orogeny (e.g. Bird and Dewey, 1970).

In spite of numerous modifications and additions, the basic aspect of the original model that the Laurentian margin was strongly deformed during the Taconic orogeny has remained (e.g. Hibbard, 1983; Williams, 1995; Waldron et al., 1998a; van Staal, 2007). Evidence for this can be found in the autochthonous external Humber Zone (Figures 1.1 and 1.2; tectonostratigraphic subdivisions after

Williams, 1979; Williams et al., 1988; Piasecki et al., 1990). The external Humber Zone is underlain by Cambro-Ordovician passive margin carbonates. Overlying sediments of the Llanvirnian Table Head Group demonstrate a complicated record of uplift, faulting, and carbonate platform collapse and show the transition from carbonate platform to deep foreland basin flysch (Waldron et al., 1998a). The Humber Arm Allochthon (Figure 1.2), which is a composite tectonic slice consisting of continental rift, slope and rise sedimentary rocks (Waldron et al., 1998a), was emplaced onto the passive margin carbonates and contains stratigraphic evidence showing that tectonic loading started in the Middle Arenigian[1] (ca. 475 Ma; Waldron and van Staal, 2001). This age is corroborated by the ca. 469 Ma cooling age for the metamorphic sole of the Bay of Islands ophiolite, the upper-most tectonic slice of the Humber Arm Allochthon, suggesting that ophiolite emplacement and associated west-directed deformation is in fact late Early Ordovician (late Arenig) to Middle Ordovician (Llanvirn; Waldron and van Staal, 2001, and references therein; Bradley, 2005). The best evidence for Taconic orogeny is preserved in the Dashwoods subzone of the Notre Dame subzone (Figures 1.1 and 1.2; Williams et al., 1988; Piasecki et al. 1990). The Dashwoods subzone is characterized by the ample presence of metasedimentary rocks overlying an unexposed crystalline basement, and has been intruded by voluminous Ordovician-Silurian continental arc plutons (Notre Dame Arc; Dunning et al., 1989; Whalen et al., 1997; van Staal et al., 2007). Late Middle Ordovician (ca. 460 Ma) tonalite plutons overprint the main phase of deformation and associated amphibolite facies metamorphism in the Dashwoods subzone (Pehrsson et al., 2003; van Staal et al., 2007). Also, unconformably overlying Upper Ordovician to Devonian rocks were only affected by low-grade regional metamorphism and little penetrative deformation (Dubé et al., 1996; Waldron and van Staal, 2001).

Geological evidence from the Corner Brook Lake block (CBLB; after Cawood et al., 1995) of the internal Humber Zone (Williams, 1995) is not consistent with such a Taconic scenario. The CBLB occupies a central position within the Laurentian realm between the external Humber Zone and the Dashwoods subzone (Figure 1.2). It comprises exposures of crystalline basement and overlying

[1] The timescale of McKerrow and van Staal (2000) has been used throughout this thesis.

metasedimentary rocks, which have been deformed and metamorphosed under amphibolite facies conditions (Cawood and van Gool, 1998). Based on regional correlation with less-deformed sedimentary rocks in the external Humber Zone, the CBLB was commonly considered to also have experienced Ordovician Taconic deformation and peak metamorphism (e.g. Hibbard, 1983; Williams, 1995, and references therein). However, petrographic fabrics and $^{40}Ar/^{39}Ar$ and U/Pb geochronological data introduced by Cawood et al. (1994) demonstrated that this important dynamo-thermal event occurred during the Early Silurian Salinic orogeny (Dunning et al., 1990), ca. 30 million years after the main regional Taconic event. Whereas the external Humber Zone is characterized by a mid-Silurian sedimentary hiatus (Waldron et al., 1998a), the Salinic event is only locally developed in the neighbouring Dashwoods subzone (e.g. Pehrsson et al., 2003). Even though this marked difference in Early Palaeozoic tectonic history between the CBLB and the Dashwoods subzone is widely known, it has not been satisfactorily explained.

To understand the relationship between the CBLB and the Dashwoods subzone, it is also important to understand the kinematics of their boundary. The CBLB and Dashwoods are separated by a crustal-scale tectonic zone, compositely termed the Baie Verte-Brompton Line - Cabot Fault Zone (BCZ; Figures 1.2 and 1.4; Wilson, 1962; Hyde et al., 1988; Piasecki, 1995; van der Velden et al., 2004). This regionally extensive tectonic boundary has a long-lived (>150 m.y.) and complex kinematic history. Contradicting ductile senses of shear have been reported and the ages of these ductile movements are poorly constrained. Hence, no clear consensus exists on the pre-Devonian tectonic history of the BCZ in southwest Newfoundland.

1.2. Thesis Objective and Summary of Results

The goal of this thesis is to examine the Early Palaeozoic tectonic history of the region, by characterizing the dynamo-thermal history of the CBLB, examining the dynamo-thermal history of the western and northern part of the Dashwoods subzone, and understanding the kinematic evolution of the

BCZ. For this, I have undertaken fieldwork (mapping and sampling), structural analyses, thin sections studies, $^{40}Ar/^{39}Ar$ and U/Pb geochronological studies (both ID-TIMS [Isotope Dilution - Thermal Ionisation Mass Spectrometry] and SHRIMP [Sensitive High-Resolution Ion MicroProbe]), and – to a lesser extent – geochemical studies. In addition, numerous data are present in the literature, including geochronological, geochemical and seismic data (from Lithoprobe and petroleum industry), as well as field observations and aeromagnetic data.

The results demonstrate that the main dynamo-thermal event is Taconic in the Dashwoods, and Salinic in the CBLB, corroborating previous observations and interpretations. Moreover, the results from the BCZ show that this tectonic zone has facilitated predominant dextral movement throughout the Appalachian orogenic history. Based on this, I propose that, in addition to the well-documented orthogonal convergent movements, large-scale orogen-parallel transcurrent movements in the Appalachian orogen have played an important role in the tectonic history of the region, and therefore should be taken into account in every tectonic model.

1.3. Thesis Outline

This thesis is presented in the paper format. Each of the following chapters is focused on a particular topic, intended for a stand-alone paper. Each chapter contains new field data, geochronological results, interpretations and conclusions. Some repetition of descriptions and discussion of results is inevitable. Paragraphs that were entirely prepared by a co-author have been italicized and appropriately referred to in footnotes. All references and appendices to individual chapters have been combined and added after the final chapter, allowing for a better continuity of the manuscript and avoiding too many unnecessary repetitions.

Chapter 2 is focused on the Dashwoods subzone, and elaborates on the post-Taconic evolution of the Dashwoods microcontinent (Waldron and van Staal, 2001). The results show that during the late Middle Ordovician to earliest Silurian Dashwoods moved southwards with respect to the Laurentian

margin (present-day reference frame). Synchronously, Dashwoods moved up relative to the Notre Dame subzone along the Little Grand Lake Fault.

Chapter 3 elaborates on the timing of Early Palaeozoic orogenic events in the Corner Brook Lake block (CBLB) of the internal Humber Zone. An attempt is made to find evidence for the presence of a pre-Salinic dynamo-thermal event. The results demonstrate that the CBLB has experienced Early Silurian Salinic deformation and peak metamorphism, corroborating previously reported data (Cawood et al., 1994). No evidence was found that would indicate the presence of a significant Taconic dynamo-thermal event in the CBLB area.

Chapter 4 concentrates on the unique signature of the CBLB. A compilation of U-Pb ID-TIMS ages demonstrates that the basement of the CBLB is devoid of a Grenville signature. This is uncharacteristic for true autochthonous Laurentian crystalline basement. When the distinct Early Palaeozoic tectonic history is also taken into consideration, the CBLB is proposed to represent a suspect terrane that may have experienced >500 km orogen-parallel displacement. This new interpretation has profound implications for the tectonic history of the Newfoundland Appalachians.

Chapter 5 is focused on the Baie Verte-Brompton Line - Cabot Fault Zone (BCZ). New data presented here show that the BCZ has experienced episodic yet continuous dextral deformation since the Late Ordovician, most notably during the late Early Silurian, an interpretation that contrasts with that in the current literature (e.g. Piasecki, 1995).

Finally, in Chapter 6, the results (including conclusions and interpretations) from the previous chapters are summarized and a model for the tectonic evolution of the Laurentian margin of the Newfoundland Appalachians is proposed.

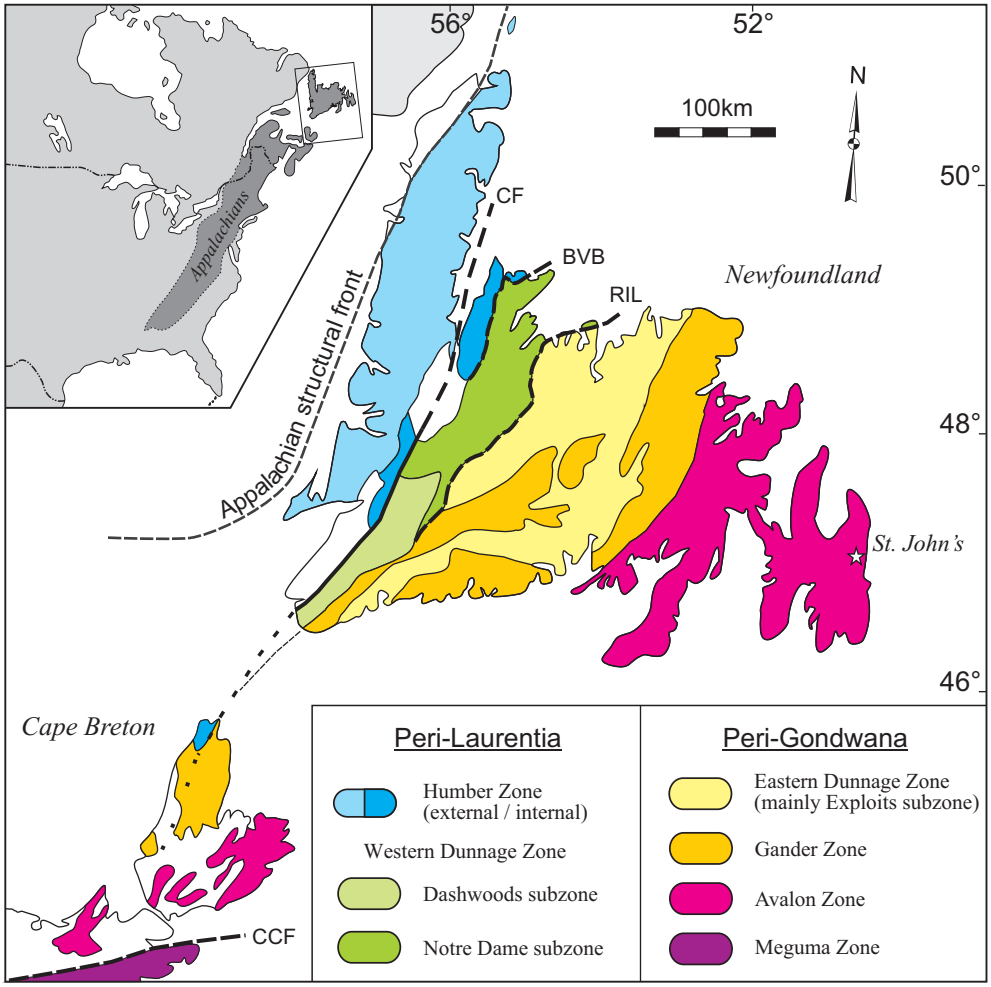

Figure 1.1 Tectono-stratigraphic subdivisions of the Newfoundland and Cape Breton Appalachians. Abbreviations: BVB - Baie Verte-Brompton Line; CF - Cabot Fault; and RIL - Red Indian Line. After Williams (1979), Williams et al. (1988), and Piasecki et al. (1990).

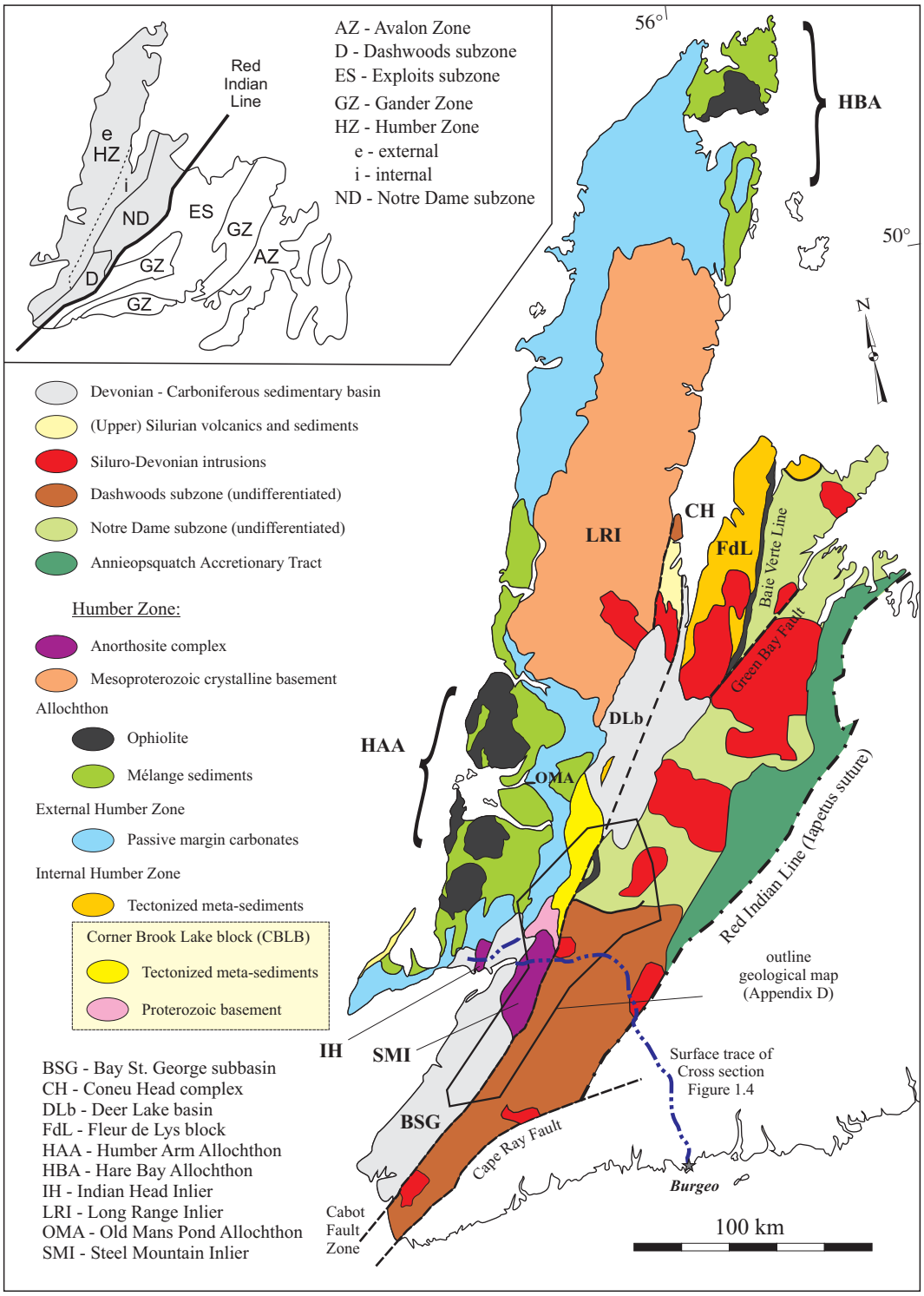

Figure 1.2 Simplified geological map of western Newfoundland, showing the main tectonic elements of the Laurentian realm in the Newfoundland Appalachians. Modified after Waldron et al. (1998). Inset shows the tectono-stratigraphic subdivision of Figure 1.1. Red Indian Line divides elements of Laurentian affinity (grey) from elements of Gondwanan affinity (white).

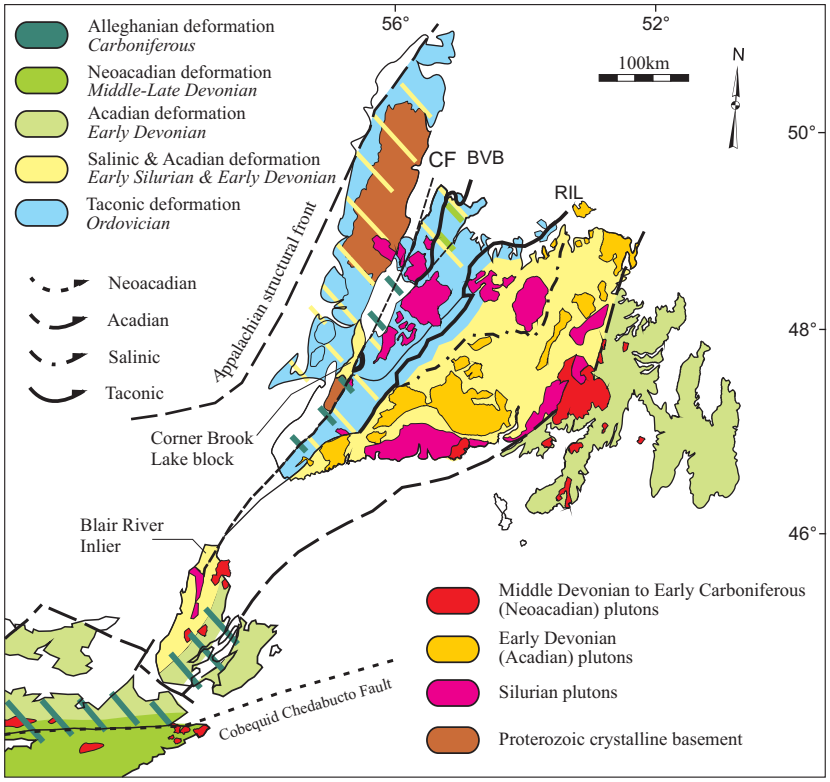

Figure 1.3: Schematic diagram of the Newfoundland and Cape Breton Appalachians showing the spatial and temporal distributions of deformation and associated metamorphism. Diagonal lines indicate a subsequent orogenic overprint. Also shown are suites of Silurian to Carboniferous plutons. Abbreviations: BVB - Baie Verte-Brompton Line; CF - Cabot Fault; and RIL - Red Indian Line. Modified from van Staal (2005).

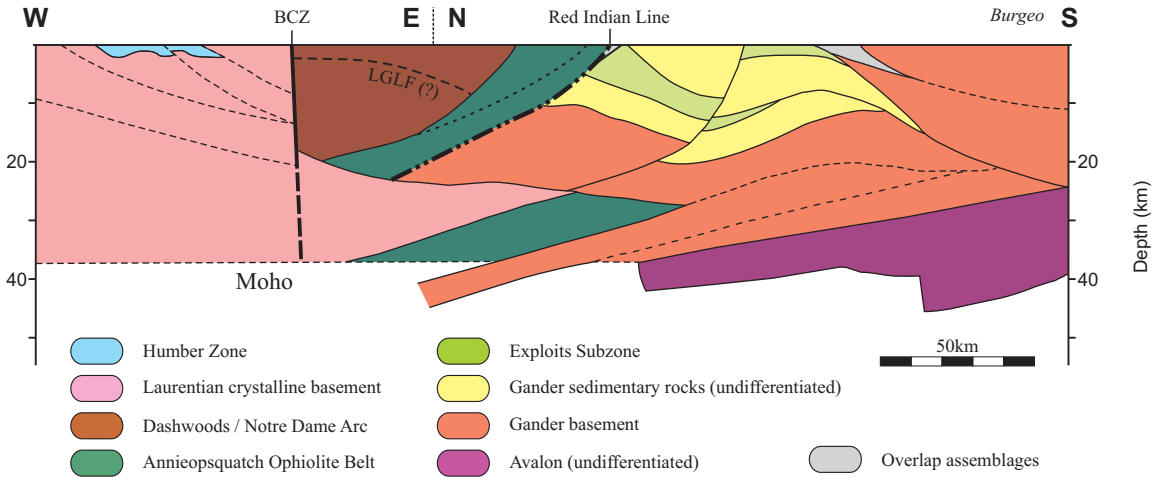

Figure 1.4: Schematic W-E cross section across the Newfoundland Appalachians showing the main tectonic segments discussed in this thesis. Trace of section is shown in Figure 1.2. Abbreviation: BCZ - Baie Verte-Brompton Line - Cabot Fault Zone. Modified from van der Velden et al. (2004).

Chapter 2: The Middle Ordovician to Early Silurian voyage of the Dashwoods microcontinent, west Newfoundland; based on new U/Pb and $^{40}Ar/^{39}Ar$ geochronological, and kinematic constraints[1]

2.1. Abstract

The Dashwoods microcontinent is an important tectonic segment in the peri-Laurentian setting of the Newfoundland Appalachians. To better understand the tectonic history of Dashwoods during the Ordovician Taconic orogeny, field mapping, microscopic studies, and U-Pb and $^{40}Ar/^{39}Ar$ geochronological studies were undertaken along its northern (Little Grand Lake Fault; LGLF) and western (Baie Verte-Brompton Line - Cabot Fault Zone; BCZ) boundaries.

Oblique-dextral ductile deformation in the BCZ occurred from late Middle Ordovician into the Early Silurian, based on the presence of a late syntectonic pegmatite dyke (455 ± 12 Ma) and a foliated granodiorite sheet (445.8 ± 0.6 Ma). Deformation is coeval with oblique-sinistral accretion along the eastern margin of Dashwoods, which means that Dashwoods and its Notre Dame Arc had a southward translation with respect to the Laurentian margin and the then-present Iapetus Ocean during the Late Ordovician. Dextral movement along the BCZ continued after the collision of Dashwoods with the Laurentian margin. Deformation along the Little Grand Lake Fault is bracketed between 463 ± 5 Ma and 440 ± 4 Ma. These ages combined with other geological arguments indicate that motion probably took place during the Late Ordovician to earliest Silurian contemporaneous with the southward translation of Dashwoods. A possible explanation is that the Snooks Arm arc moved independently from and faster southwards than the Notre Dame Arc with its Dashwoods infrastructure, thereby underthrusting the Dashwoods along the Little Grand Lake Fault.

[1] Brem, A.G., Lin, S., van Staal, C.R., Davis, D.W., and McNicoll, V.J. (2007) *American Journal of Science*, Volume 307, in press.

Our new U-Pb geochronological data, including a muscovite granite (463 ± 5 Ma), a schistose muscovite granite (459 $^{+17}/_{-21}$ Ma), and a tectonized tonalite (458 ± 20 Ma), add to the geochronological database of the voluminous second phase of the Notre Dame Arc. Additionally, in all-but-one of the U-Pb samples, inherited grains of Mesoproterozoic age (ca. 1.0 Ga) have been obtained. Their regional presence fortifies the possible relationship of the Dashwoods microcontinent with the Long Range Inlier in western Newfoundland. Furthermore, it introduces a potential link with the Blair River Inlier in Cape Breton Island.

2.2. Introduction

The Appalachian-Caledonian mountain chain is a narrow linear mountain belt, the tectonic evolution of which has been compared to the present-day tectonic setting in southwest Pacific Ocean (van Staal et al., 1998). Such mountain chains consist of numerous along-strike segments, including oceanic tracts and microcontinents, each of which has experienced a distinct history. In the western Newfoundland Appalachians, the Notre Dame subzone (Williams et al., 1988) consists of several tectonic segments (Figure 2.1) that are linked together by their Laurentian affinity and an Ordovician tectono-magmatic event (van Staal, 2007).

The Dashwoods subzone (Piasecki et al., 1990), previously referred to as the Tonalite Terrane (Whalen and Currie, 1983) or Central Gneiss Terrane (Piasecki, 1988; Currie and van Berkel, 1992), represents the southern part of the Notre Dame subzone (Figure 2.1 inset). It is characterized by the ample presence of meta-sedimentary rocks, which are scarce in the northern Notre Dame subzone (Figure 2.1), and the absence of Early Ordovician oceanic arc rocks, which are present throughout the northern Notre Dame subzone. The Dashwoods subzone has been interpreted as representing a microcontinent (Waldron and van Staal, 2001), which formed the basement to an extensive continental arc (Notre Dame Arc; Whalen et al., 1997) that was intermittently active from Early Ordovician to Early Silurian (489-435 Ma; Whalen et al., 1997; van Staal et al., 2007). Collision of Dashwoods with

the Laurentian margin during the Middle to Late Ordovician (Taconic orogeny) resulted in regional deformation and high-grade metamorphism, and was followed by late syn- to post-kinematic magmatism and rapid uplift in the Early Silurian (Pehrsson et al., 2003; Whalen et al., 2006).

In order to comprehend the mosaic of tectonic segments in a mountain belt, it is important to understand the kinematics of boundaries between individual segments. The boundaries of the Dashwoods subzone are all fault zones. The histories of the eastern boundaries of Dashwoods are well documented: the Annieopsquatch Accretionary Tract was accreted to the Dashwoods subzone along the Lloyds River Fault Zone (LRF in Figure 2.1) in Middle Ordovician (468-459 Ma; Lissenberg et al., 2005), and the Cape Ray Fault (CRF in Figure 2.1) has recorded Late Silurian to Early Devonian (Acadian) overthrusting of the Dashwoods subzone by high-grade metamorphic rocks of the Gander Zone (Dubé et al., 1996). The northern boundary, the Little Grand Lake Fault (LGLF; Figure 2.1), is characterized by a marked change in metamorphic grade and has recorded high-angle south-over-north thrusting (Whalen et al., 1993; Piasecki, 1995; Brem et al., 2003). The age of deformation was interpreted as being Middle Ordovician, based on crosscutting relationships, petrographic observations, and regional correlations (Whalen et al., 1993; Piasecki, 1995), but no precise geochronological constraints exist. To the west Dashwoods is separated from the (internal) Humber Zone along the Baie Verte-Brompton Line - Cabot Fault Zone (BCZ; Figure 2.1). The BCZ is a crustal-scale tectonic boundary with a long-lived and complex kinematic history (Wilson, 1962; Hyde et al., 1988; Piasecki et al., 1990; Goodwin and Williams, 1990; van der Velden et al., 2004). Contradicting ductile senses of shear have been reported for the BCZ, and the ages of these ductile movements are poorly constrained. Also, younger (Devonian-Carboniferous) brittle-ductile and brittle movements in the BCZ have overprinted and partly obliterated pre-existing deformation features. Hence, no clear consensus exists on the pre-Devonian tectonic history of the BCZ in southwest Newfoundland.

To better understand the tectonic history of the Dashwoods microcontinent and its associated sediments and arc plutons in the Appalachian mountain belt, we attempt to improve the understanding of the kinematic history of its northern (LGLF) and western (BCZ) boundaries. Detailed field studies

and thin section analysis were conducted to constrain the kinematics of deformation, and U-Pb (ID-TIMS and SHRIMP) and $^{40}Ar/^{39}Ar$ geochronology on selected samples was used to constrain the timing of deformation. The results show that the western, northern and eastern boundaries of Dashwoods were active in Late Ordovician time, but the movements along these tectonic boundaries are difficult to reconcile kinematically with one another. We elaborate on a possible explanation of the latter. The possible link of the Dashwoods microcontinent with nearby basement inliers is also discussed.

2.3. Geological Setting

2.3.1. Dashwoods Subzone - the Dashwoods Microcontinent

The northern and central-western parts of the Dashwoods subzone, which are the focus of this study (Figure 2.1 and 2.2), are dominated by clastic metasediments correlated with those of the Mischief Mélange further to the south (Hall and van Staal, 1999), and tentatively correlated with the Fleur de Lys Supergroup in the internal Humber Zone (Hibbard, 1983; Currie and van Berkel, 1992). They include stromatic to nebulitic migmatites, meta-psammitic schist and gneiss, and rare marble and conglomerate layers. Most units contain sillimanite, biotite, muscovite, garnet, and/or hornblende suggestive of medium-to-high grade amphibolite facies metamorphism. However, they also contain retrograde chlorite. Throughout the area, metamorphosed mélange contains various mafic and ultramafic inclusions, which include amphibolite (potentially disrupted mafic dykes), serpentinized dunite, pyroxenite and gabbro, most of which had been altered prior to incorporation into the mélange (Fox and van Berkel, 1988). The ultramafic inclusions are interpreted as disrupted ophiolitic fragments, and are probably related to the Long Range mafic-ultramafic complex of the southern Dashwoods subzone (Hall and van Staal, 1999).

The meta-sediments and mélange units have been intruded by voluminous tonalite and granodiorite plutons assigned to the Notre Dame Arc (Whalen et al., 1997), which range in age between 489-477 Ma (first phase) and 469-459 Ma (second phase) (van Staal et al., 2007; and references therein). These plutons are strongly foliated to non-foliated and most contain xenoliths of (metamorphosed) mafic to ultramafic composition, including amphibolite, gabbro and pyroxenite. In various places, magma mingling of leucocrate granitoid and mafic compositions has occurred (Brem et al., 2003; Pehrsson et al., 2003). On a local, outcrop scale, granodiorite sills are interlayered with the gneissose meta-sediments. Various pegmatite and aplite dykes are present, most of which apparently cut the gneissic fabric, although at least some of these dykes have been caught up in the deformation.

Several plutons of the Notre Dame Arc have yielded xenocrystic components of Mesoproterozoic (1300-1650 Ma; e.g. Dunning et al., 1989; Dubé et al., 1996) and Paleoproterozoic age (ca. 2090 Ma; Whalen et al., 1987). Additionally, strongly negative Nd isotopic evidence suggests that the Notre Dame Arc plutons were founded on a continental basement (Whalen et al., 1997). This basement was interpreted to be a microcontinent of Laurentian affinity instead of the leading edge of Laurentia, based on the observation that Dashwoods was obducted by an oceanic tract (the Lush's Bight oceanic tract; Figure 2.1) approximately 20 million years before tectonic loading affected the external Humber Zone (Waldron and van Staal, 2001; van Staal et al., 2007).

Regional deformation and peak metamorphism under amphibolite to lower granulite facies conditions in the Dashwoods subzone are Middle Ordovician (ca. 460 Ma; e.g. Dunning et al., 1989; Currie et al., 1992; Pehrsson et al., 2003). This dynamo-thermal event is related to the collision of Dashwoods with the Laurentian margin (van Staal et al., 2007).

2.3.2. Northwestern Notre Dame Subzone - the Baie Verte Oceanic Tract

Rocks immediately north of the LGLF (Figure 2.1; Appendix D) are part of the Glover Group and consist of mafic (pillow basalts) to silicic (felsic tuffs and rhyolite flows) volcanics, high-level mafic

intrusive rocks (mainly gabbro), and sparse sedimentary rocks, including graptolite-bearing Arenig shales (S.H. Williams, 1992). These rocks overlie gabbro, trondhjemite, serpentinized peridotites and other mafic to ultramafic rocks of the Glover Island complex (ca. 490 Ma; Cawood and van Gool, 1998). This complex is interpreted as representing oceanic crust of the Baie Verte oceanic tract (van Staal, 2007) that formed in the Humber seaway, the narrow seaway between the Humber margin and the Dashwoods microcontinent (Waldron and van Staal, 2001). Subsequently, the Baie Verte oceanic tract formed the basement to an Early Ordovician oceanic arc / back arc complex (Bédard et al., 2000), which includes the Glover Group.

Regional deformation and (sub-) greenschist metamorphism of these rocks occurred before the Early Silurian (Cawood and van Gool, 1998). They were subsequently intruded by latest Ordovician to Early Silurian granodiorite plutons (e.g. ca. 440 Ma Glover Island granodiorite; Cawood and van Gool, 1998), and voluminous high-level peralkaline granites (e.g. 427-429 Ma Topsails Igneous Suite; Whalen et al., 1987).

In fact, throughout the Notre Dame subzone (including the Dashwoods subzone), latest Ordovician to Early Silurian plutons of felsic (granodiorite to granite) and mafic compositions (gabbro to quartz diorite, diabase) are exposed (Figures 2.1 and 2.2; Appendix D; Whalen et al., 2006; and references therein). In outcrop, these units commonly appear undeformed and unmetamorphosed (e.g. ca. 431 Ma Main Gut gabbro; Dunning et al., 1989). Some intrusions truncate the strong regional fabric developed in the meta-sediments of the Dashwoods as well as plutons of earlier phases of the Notre Dame Arc.

2.3.3. (Internal) Humber Zone - Humber Margin of the Laurentian Continent

The units west of the BCZ form part of the Humber Zone, which is interpreted as the Laurentian margin (Williams, 1995). The Humber Zone was divided into an external and an internal zone based on a difference in metamorphic grade and style of deformation (Figure 2.1; Cawood et al., 1994). In southwestern Newfoundland, the internal Humber Zone is characterized by a Mesoproterozoic(?)

anorthosite complex that is in structural contactwith Late Neoproterozoic crystalline basement and associated – mainly clastic – metasediments. Regional deformation and peak metamorphism (up to amphibolite facies conditions) of the latter units occurred in the Early Silurian (ca. 430 Ma; Salinic orogeny; Cawood et al., 1994), 30 million years after peak metamorphism and deformation in the Dashwoods subzone. Evidence for large-scale Ordovician (Taconic) deformation, metamorphism and plutonism in the internal Humber Zone is absent. However, some Taconic influence is expected, since the stratigraphic record in the external Humber Zone clearly suggests that the Humber margin was being loaded in the Middle Ordovician (Knight et al., 1995; Waldron et al., 1998). The difference in age and style of deformation and metamorphism between the Dashwoods subzone and internal Humber Zone shows that these segments were not juxtaposed until after the Early Silurian (Cawood and van Gool, 1998; Chapter 3).

2.4. Dashwoods Boundaries - Observations and Interpretations

2.4.1. BCZ - Western Dashwoods Subzone Boundary

2.4.1.1. General

In southwestern Newfoundland the Carboniferous Cabot Fault Zone (Wilson, 1962) coincides with the Ordovician Baie Verte-Brompton Line (Williams and St-Julien, 1982) and separates the Dashwoods subzone of the western Dunnage Zone from the Humber Zone (BCZ in Figure 2.1; Williams and St-Julien, 1982; Williams, 1995); hence the BCZ is a long-lived crustal-scale tectonic zone with a very complex kinematic history (Wilson, 1962; Hyde et al., 1988; Goodwin and Williams, 1990; Brem et al., 2002; van der Velden et al., 2004). In southwestern Newfoundland, the BCZ is also referred to as the Long Range Fault (e.g. Piasecki et al., 1990; Currie and van Berkel, 1992). The generally wide tectonic zone consists of anastomosing ductile and brittle-ductile shear zones that are crosscut and overprinted by intense high-level brittle-ductile and brittle structures (Chapter 5). As a

result, most pre-existing ductile deformation features have been obliterated (e.g. Figure 5.9B). Moreover, rocks caught up in the BCZ have been deformed to the extent that in most places positive identification of a protolith is not possible. However, the brittle overprint is concentrated in a narrow zone along the present-day Humber Zone - Dunnage Zone boundary (Figure 2.2), and the older ductile fabrics away from this zone are relatively undisturbed.

2.4.1.2. Internal geometry and kinematics of the BCZ

The western part of the Dashwoods subzone is characterized by gneissic to migmatitic meta-sediments and variably foliated igneous units. The gneissic foliation and localized high-strain zones are steeply dipping and generally strike NE (orogen parallel), but deviations from this direction to northerly and easterly strikes occur (Figure 2.3A). In the gneissic rocks, the foliation is planar and defined by quartz-feldspar plates and biotite and/or hornblende-rich layers. In areas of lower strain, where individual marble and conglomerate layers could be identified, the foliation has developed parallel to sedimentary layering. In migmatites and high-strain zones, the foliation is commonly curvi-planar and irregular (Figure 2.4A).

Stretching lineations, defined by elongate quartz-feldspar aggregates, and mineral lineations defined by biotite and/or hornblende, vary in orientation, but dominantly plunge moderately to steeply towards the southwest (Figure 2.3B). Shear-sense indicators, such as sheath folds (Figure 2.4A), winged objects (Figure 2.4B), and S-C structures (Passchier and Trouw, 1996) associated with these lineations indicate a prominent dip-slip to oblique-dextral and southeast-side-down movement. This dextral sense of shear is corroborated by Z-folds related to open-to-tight asymmetric folding of the mylonitic foliation (Figure 2.3C). Thus, the Dashwoods subzone moved down and towards the southwest (in present-day reference frame) with respect to the rocks of the adjacent Humber Zone.

Sinistral shear-sense indicators have also been observed, but these are relatively rare, and less pronounced than the dextral shear-sense indicators. Lineations associated with the sinistral shear-sense indicators plunge moderately towards the west, whereas the dominant dextral lineations plunge

towards the southwest (Figure 2.3B). Sinistral movement may have post-dated the main dextral shearing, as observed in one outcrop, where a pegmatite dyke that truncates the gneissosity was sinistrally offset. This interpretation agrees with the one made by Piasecki (1988). The preferred interpretation is that sinistral shearing was synchronous with the pre-dominant dextral shearing. Jiang and White (1995; Case III) demonstrated that within a host shear zone – such as the BCZ – locally induced spin may have been strong enough to induce a sense of non-coaxiality, which resulted in antithetic (here sinistral) shear fabrics that are at low angle to the main dextral shear zone.

2.4.1.3. Late syntectonic pegmatite dykes

As described above, the dominant sense of shear observed along the western boundary of the Dashwoods subzone is oblique-dextral. At an outcrop in close proximity to the BCZ (location 2 in Figure 2.2B) the mylonitic foliation was truncated by a conjugate set of pink pegmatite dykes (Figure 2.5A). The pegmatite dyke that is anti-clockwise from the foliation is stretched and boudinaged, whereas the dyke oriented clockwise from the foliation is shortened and folded. Such geometry is indicative of a dextral sense of shear (Figure 2.5A inset). The dykes intruded the mylonitic foliation either in between two deformational phases (inter-kinematic), or during the latest increments of continuous deformation (late synkinematic). Also at the outcrop, several lithologically similar pegmatite dykes truncate the mylonitic foliation but appear undeformed. If these undeformed pegmatite dykes were emplaced at the same time as the deformed dykes, it can be concluded that deformation occurred during pegmatite emplacement. Since deformation of the paragneisses appears to be relatively homogeneous, the deformed pegmatite dykes are interpreted to have intruded during the latest stages of progressive deformation (syntectonic). Either way, these deformed dykes constrain the minimum age on the main phase of ductile deformation in the BCZ. The folded pegmatite dyke (Figure 2.5A) was sampled for U-Pb TIMS geochronology (see below).

2.4.2. LGLF - Northern Dashwoods Subzone Boundary

2.4.2.1. General

The Little Grand Lake Fault (LGLF) is an east-west trending narrow belt of ductile shear zones that marks a distinct metamorphic break between the low-grade volcanics to the north and the high-grade meta-sediments to the south (Figure 2.2A), although this jump in metamorphic grade is absent east of Little Grand Lake (Piasecki et al., 1990; Whalen et al., 1993; Brem et al., 2003). Previously, the LGLF was interpreted to have experienced two deformational events (Piasecki, 1995). However, field observations show that later brittle deformation on low-angle north-dipping thrust planes is merely spatially coincident with part of the trace of the LGLF and is not developed in the LGLF itself. It is therefore concluded that the LGLF only experienced one deformational event.

The eastern continuation of the LGLF east of Little Grand Lake is not well constrained. The LGLF was previously thought to curve anti-clockwise towards the Lloyds River Fault Zone (Figure 2.1; 'A' in Figure 2.2A; Currie and van Berkel, 1992; Brem et al., 2003). Recently, van Staal et al. (2007) proposed that the LGLF takes a northward swing immediately east of Little Grand Lake and appears to hook up with the Green Bay Fault on the north coast of Newfoundland, thereby separating the Baie Verte oceanic tract from the Dashwoods subzone - Notre Dame Arc (Figure 2.1; 'B' in Figure 2.2A). Due to lack of outcrop east of the Little Grand Lake and overprinting by younger intrusive units, such as the Topsails Igneous Suite, these hypotheses cannot easily be tested. Towards the west, the LGLF is truncated by the BCZ and hence, its continuation west of this lineament could not be established (Figures 2.1 and 2.2A).

2.4.2.2. Internal geometry and kinematics of the LGLF

The LGLF is best observed in granitoid rocks at the eastern end of Little Grand Lake (Figure 2.2A; Whalen et al., 1993; Brem et al., 2003), where several strands of the LGLF are exposed, the main strand (at least 40 m wide) being closest to the lake. Towards the south away from the main strand,

mylonitic shear zones become sparser and narrower. The shear-related foliation on all strands is steeply south-dipping to vertical (Figure 2.3D). Mineral lineations, defined by muscovite grains, and stretching lineations, defined by quartz-feldspar aggregates, plunge down dip on the main strand, but towards the south, away from the main shear zone, these plunge shallowly towards the east (Figure 2.2A inset and 2.3E).

Shear-sense indicators associated with these fabrics include S-C fabrics, shear bands, bookshelf-stacking and winged objects (Figure 2.5B; Passchier and Trouw, 1996), and consistently show a reverse to dextral-reverse, south-side up movement. This sense of shear corroborates the observations and interpretation by Whalen et al. (1993) and Piasecki (1995), and facilitates the juxtaposition of the high-grade amphibolite facies Dashwoods meta-sedimentary rocks to the south with greenschist facies volcanic rocks of the Glover Group to the north of the fault. Thus fault motion – at least in part – must have occurred post peak metamorphism in the Dashwoods meta-sedimentary rocks.

2.4.2.3. Microscopic observations and temperature condition of deformation

The muscovite grains, which define the mylonitic foliation, are both deformed (kinked, bent and fractured) as well as undeformed (Figure 2.5B), suggesting that muscovite growth was predominantly synkinematic, but that some grains may be remnant pre-kinematic grains. In thin section, subgrain domains and undulose extinction characterize the quartz aggregates. These aggregates are surrounded by numerous small, dynamically recrystallized quartz grains giving the fabric a seriate-interlobate texture (Figure 3.30 in Passchier and Trouw, 1996). Feldspar grains are of variable composition, and form characteristic porphyroclasts (Figure 2.5B) of various sizes, and are commonly internally fractured. Different intracrystalline deformation features have developed in feldspar grains, including undulose extinction, kinks and deformation twins in plagioclase, and perthite exsolution structures in K-feldspar. More importantly, a core-mantle texture defined by subgrain rotation and small, recrystallized feldspars around larger feldspar clasts is common throughout the thin section (Regime 2 of Hirth and Tullis, 1992; Vernon, 2005). Dynamic recrystallization of quartz may start at temperatures

above 300°C (Passchier and Trouw, 1996; Hirth et al., 2001), but recrystallization of feldspar starts to become important at low-to-medium grade conditions (>350°C; Pryer, 1993; Passchier and Trouw, 1996). This would suggest that deformation on the LGLF occurred at greenschist facies conditions or higher, i.e. probably at temperature conditions near or above the muscovite closure temperature for argon (ca. 350°C; McDougall and Harrison, 1999).

2.5. Geochronology

2.5.1. Analytical Procedures

This is a summary of the analytical techniques of U-Pb ID-TIMS and SHRIMP, and $^{40}Ar/^{39}Ar$ geochronology. Detailed descriptions of the analytical procedures can be found in Appendix A to C.

Single whole grain zircon and monazite U-Pb analyses were performed at the Jack Satterly Laboratory, University of Toronto (formerly at the Royal Ontario Museum). Standard mineral separation techniques were followed, including methods described by Krogh (1973, 1982). Data were calculated, regressed and plotted using in-house software (UtilAge by D.W. Davis) with regression based on Davis (1982). Results are presented in Table 2.1 and Figures 2.6 and 2.7A.

U-Pb SHRIMP II analyses were conducted at the Geological Survey of Canada (GSC) in Ottawa using analytical procedures described by Stern (1997), with standards and U-Pb calibration methods following Stern and Amelin (2003). Results are presented in Table 2.2 and Figure 2.7B, using Isoplot v. 2.49 (Ludwig, 2001).

Laser $^{40}Ar/^{39}Ar$ step-heating analyses were also performed at the GSC. Data collection protocols of Villeneuve and MacIntyre (1997) and Villeneuve et al. (2000) were followed. Error analysis procedures are outlined in Roddick (1988) and Scaillet (2000). Results are presented in Table 2.3 and Figures 2.7C and D. All age errors are given at the 95% confidence interval.

2.5.2. Sample Description and Results

2.5.2.1. Muscovite granite (AB-01-029; zircon, monazite)

This K-feldspar-rich, schistose muscovite granite is exposed as a small body in a gully west of Little Grand Lake. None of its contacts are exposed, but these are assumed to be tectonic given its position within the cataclastic zone of the BCZ (Figure 2.2A). Previously, this unit was interpreted to be part of a muscovite-bearing phase of the Late Neoproterozoic Hare Hill Complex of the Humber Zone (Currie and van Berkel, 1992), but given its unique lithology, this unit is tentatively assigned to the Dashwoods subzone.

Ample zircon was obtained from this sample, and two distinct populations were observed: a population of well-rounded brownish grains with pitted surfaces; and a euhedral population of variable morphology, from slender elongate and prismatic grains to short stubby grains and fragments, most of which contain round or rod-shaped inclusions. Five fractions of zircon grains were analyzed, yielding various $^{207}Pb/^{206}Pb$ ages between 1128 and 1191 Ma (euhedral population) and one older age of 1462 Ma (Grain A3; rounded population; Table 2.1; Figure 2.6A). Back-scattered SEM-imaging shows that zircon grains from the euhedral population have small overgrowths around their cores (Figure 2.8A). Since all analyzed grains had been abraded, such minor overgrowth could easily have been removed during the abrasion process, thereby exposing the cores. Therefore, the U-Pb zircon ages are most likely to represent ages of xenocrysts.

A few good-quality monazite grains were obtained from the sample. These grains are subhedral, clear to yellowish, and some grains have an orange (iron oxide) coating on their surfaces. Four single monazite grains yielded data that are highly discordant (10.7 and 19.2%; Grains A7 and A8), slightly discordant (-0.4%; Grain A6), as well as negatively discordant (-11.5%; Grain A9). Their $^{207}Pb/^{206}Pb$ ages range between 396 Ma and 808 Ma (Table 2.1). The three older $^{207}Pb/^{206}Pb$ ages (Grains A6 to A8) define a mixing line with a lower intercept at 459 $^{+17}/_{-21}$ Ma and an upper intercept at 1047 $^{+80}/_{-91}$ Ma (78% probability of fit; Figure 2.6B). The large error on the lower intercept is due to the large

$^{207}Pb/^{235}U$ age error, but this lower intercept age is assumed to be fairly accurate, given the near-concordant position (-0.4%) and small error on the $^{206}Pb/^{238}U$ age of Grain A6. Back-scattered SEM-imaging shows that most of the monazite grains are heterogeneous, having a complex core and a featureless grey rim (Figures 2.8B and C).

The schistose granite shows a complex U-Pb history and different explanations for these U-Pb ages are possible. Based on regional correlation, the preferred hypothesis is that the lower intercept of ca. 459 Ma represents the age of emplacement of the granite. The upper intercept of ca. 1047 Ma would indicate that the average age of the inherited monazite grains is Grenvillian. Also, all zircon ages can be interpreted as Mesoproterozoic inheritance and the minor overgrowths are most likely Ordovician in age and magmatic in origin. An alternative interpretation is that the concordant zircon grains around 1130 Ma (Grains A1, A2 and A4) represent the age of emplacement of the granite. The monazite discordia line would represent two distinct metamorphic events: a subsequent Grenvillian and an Ordovician event. In this scenario, the zircon overgrowths can be interpreted as being metamorphic or hydrothermal.

There is no irrefutable evidence to support either interpretation, but the important conclusion that can be drawn from the complex U-Pb ages of this schistose granite is that it has recorded at least one Grenvillian and an Ordovician dynamo-thermal event. The interpretation of this granite is even more complicated by the fact that a fourth monazite grain (Grain A9; Table 2.1) is concordant within error but gives a younger $^{206}Pb/^{238}U$ age of 414 ± 3 Ma. This may reflect lead-loss or monazite growth related to movement in the BCZ after emplacement of the granite.

2.5.2.2. Late syntectonic pegmatite dyke (AB-01-104; zircon)

A sample was taken from the folded, late syntectonic pegmatite dyke described above (Figure 2.5A), in order to constrain the age of medium- to high-grade deformation in the BCZ (Figure 2.2B). The sample yielded a small number of zircon grains, which predominantly have a stubby morphology. The grains are colorless to slightly brownish and have few inclusions. All five analyzed zircon grains

define a best-fit regression line (42% probability of fit; Figure 2.6C) with a lower intercept of 455 ± 12 Ma and an upper intercept of 1039 ± 12 Ma. The lower intercept is interpreted as the age of intrusion of the pegmatite. Moreover, it constrains the minimum age of the main phase of high-grade deformation along the BCZ to be Middle to Late Ordovician (Taconic). Unfortunately, the error on the lower intercept is rather large, because the analyses have limited spread and plot near the middle of the discordia line. The upper intercept shows that the inherited grains in the pegmatite are Mesoproterozoic (Grenvillian) in age.

2.5.2.3. Tectonized tonalite (AB-02-213; zircon)

In the southwestern part of the study area, a tonalite with a strong gneissic fabric is exposed (Figure 2.2B). The tonalite contains mafic and ultramafic xenoliths of variable size and shape, some of which contain a pre-incorporation fabric. The strong tectonic fabric in the tonalite suggests that significant deformation occurred after emplacement of the tonalite. A sample was taken from a relatively homogenous and xenolith-free section of the outcrop.

The sample contains abundant zircons, which were divided into two populations: a euhedral elongate and a multifaceted ovoid population. Zircon grains of the former population are of simple morphology, variable size, elongate, and clear. Most grains contain small melt inclusions, which, when present, are located in the central part of the grains. Some grains have visible cores and associated overgrowths. Back-scattered SEM-imaging of a random population of zircon from the sample shows that most grains have clear subdomains of cores and overgrowths. The cores are characterized by oscillatory zoning and the wide rims, which generally have euhedral crystal faces, occasionally show a faint zoning pattern. Some boundaries between the cores and overgrowths are very irregular, which is indicative of resorption (Figure 2.8D). Based on the morphology of most zircon grains from both populations, heterogeneity within the grains was expected. Three single zircon grains were analyzed: two from the elongate population (Grains C15 and C16), and one from the multi-facetted population (Grain C17; Table 2.1). In addition, one zircon fragment (Grain C20) was analyzed, and two analyses

were done on tips of grains (Grains C18 and C19), which were carefully detached from their respective cores. When constructing a mixing line using all six analyses, the analyses lie scattered, half way between the lower and upper intercept of a discordia line (443 ± 20 and 1017 ± 11 Ma intercepts), but probability of fit is very low. Analyses of the two tips and the fragment actually yielded the oldest $^{207}Pb/^{206}Pb$ ages (Table 2.1). A best-fit regression line that fits four of the data within error (Grains C16 to C19) yields an upper intercept of 1044 ± 14 Ma and a lower intercept of 458 ± 20 Ma (56% probability of fit; Figure 2.6D). The large errors on both intercepts prevent a precise interpretation of the age of emplacement of the tonalite, but the data show that the tonalite was emplaced in the Middle to Late Ordovician. The upper intercept shows that there is an important xenocrystic Grenvillian component that is very similar to the previously discussed samples (ca. 1.04 Ga).

2.5.2.4. Foliated granodiorite sheet (AB-02-229; zircon)

A sample was taken from a foliated granodiorite sheet that is interlayered on a metre- to decametre-scale with strongly deformed mélange metasediments (Figure 2.2B and 2.4B). The coarser-grained and xenolith-free granodiorite has a weak foliation, in contrast with the strongly deformed and heterogeneous paragneiss, which may indicate that the granodiorite intruded syn- or intertectonically. Associated sheath folds (Figure 2.4A) and winged objects (Figure 2.4B) indicate oblique-dextral deformation. Locally, the granodiorite is observed to have commingled with a more mafic magma (diorite).

Two populations of zircon grains were identified in the sample: a population of ovoid, multi-facetted zircons, and a population of large elongate, needle-like zircon grains. The elongate zircon grains are clear, contain some melt inclusions, and are of simple morphology. The grains of the multi-facetted population are of various sizes, stubby in shape, inclusions are absent, and some grains show visible overgrowth. Based on morphology, grains of the former population are interpreted as having formed in the parent magma, whereas the grains of the multi-facetted population would most likely contain inherited cores with younger overgrowth (similar to samples AB-02-213 and AB-02-293).

Three zircon grains were analyzed, two of the elongate morphology (Grains D21 and D22; Table 2.1), and one of the multi-facetted population (Grain D23; Table 2.1). The analyses yielded concordant data with $^{206}Pb/^{238}U$ ages within error. The 2σ-error on the $^{207}Pb/^{235}U$ ages is large, in contrast with the $^{206}Pb/^{238}U$ ages. Therefore, the age of 445.8 ± 0.6 Ma (52% probability of fit; Figure 2.6E) for the foliated granodiorite is based on the average $^{206}Pb/^{238}U$ age and is interpreted to be the age of emplacement of the granodiorite.

2.5.2.5. Mylonitic muscovite granite, Little Grand Lake Fault (AB-02-293; zircon, muscovite)

In order to obtain the age of deformation on the LGLF, a sample from the main strand of the LGLF at the southeastern end of Little Grand Lake was collected (Figure 2.2A). The protolith, in which the shear zone has developed, is a plagioclase-rich muscovite granite that was emplaced into a meta-sedimentary unit. The sample has a strong mylonitic fabric. Both U-Pb (ID-TIMS and SHRIMP) and $^{40}Ar/^{39}Ar$ analyses were performed (Figure 2.7).

U-Pb Geochronology: The sample yielded abundant zircons, most of which are multifaceted and euhedral. Zircon grains are clear, stubby, sometimes distinctly bipyramidal, and some grains contain opaque and melt inclusions. Overgrowths, especially on the larger grains, are commonly visible under a binocular microscope.

Initial U-Pb TIMS analyses of two zircon grains (Table 2.1) gave discordant (9 and 19%) results with different $^{207}Pb/^{206}Pb$ ages (Figure 2.7A). A mixing line based on these analyses has a Late Ordovician lower intercept and a Mesoproterozoic upper intercept, indicative of heterogeneity within the zircon grains. Cores are overgrown by bright rims that are characterized by magmatic oscillatory zoning, which are clearly apparent in back-scattered SEM-images (Figures 2.8E and F). Consequently, in-situ analyses of the overgrowths were undertaken on SHRIMP. Eight of the analyses were pooled and a Concordia age of 463 ± 5 Ma (92% probability of fit; MSWD = 0.33; Figure 2.7B) was

calculated. One SHRIMP analysis yielded a discordant Mesoproterozoic age (1064 Ma $^{207}Pb/^{206}Pb$ age; Table 2.2; Figure 2.7B inset), which is interpreted as an inherited age based on the abundance of heterogeneous grains in this sample. The age (ca. 1.0 Ga) is again similar to the age of inheritance of other samples in this study. All fractions have high uranium content (532-1425 ppm) and Th/U ratios vary between 0.06 and 0.68 (Table 2.2). The date of 463 ± 5 Ma is interpreted as the age of emplacement of the muscovite granite protolith.

$^{40}Ar/^{39}Ar$ Geochronology: Two separate analyses on muscovite separates from the mylonitic muscovite granite sample were completed. The first analysis comprised two aliquots (Table 2.3, Figure 2.7C). The first aliquot analyzed has quite a bit of scatter (Aliquot A; Table 2.3) and all of the steps are radiogenic. The scatter most likely indicates the presence of some sort of contaminant degassing, perhaps K-feldspar inclusions in the muscovite. The second aliquot (Aliquot B; Table 2.3) reveals the presence of excess Ar in the first 2 steps. However, it yields a well-defined plateau, comprising 68% of the total gas and defining the age of the aliquot to be 440 ± 4 Ma (Table 2.3, Figure 2.7C). As the two aliquots from the first analysis were not in agreement, further analysis of muscovite from this sample was undertaken. A second analysis of muscovite yielded a well-defined plateau age, comprising 95% of total gas emitted (Table 2.3, Figure 2.7D) and defining the age of the sample at 445 ± 3 Ma. These $^{40}Ar/^{39}Ar$ cooling ages (Aliquots B and C) are within error.

The temperature condition under which the mylonitic fabric formed (see discussion above) was above or near the muscovite closure temperature for argon (ca. 350°C; McDougall and Harrison, 1999). Therefore the muscovite ages represent either the age at which this mylonitic rock cooled below 350°C, or the actual crystallization age of muscovite and hence the age of deformation on the LGLF. Thus, south-side-up deformation on the LGLF is constrained to have occurred between late Middle Ordovician and the earliest Silurian, between 463 ± 5 Ma and 440 ± 4 Ma. However, considering that most of the motion on the LGLF took place after peak metamorphism in the Dashwoods block (see above), which lasted no later than ca. 456 Ma (van Staal et al., 2007), the synkinematic muscovite is

interpreted to have predominantly grown during retrograde conditions. Hence, the motion along the LGLF mainly took place during the latest Ordovician to earliest Silurian (450-440 Ma).

2.6. Interpretation and Discussion

2.6.1. Ordovician Plutonism in the Dashwoods Subzone

Except for the foliated granodiorite sheet (AB-02-229), all samples yielded late Mesoproterozoic upper intercepts (ca. 1.04 Ga) as well as Ordovician lower intercepts (ca. 0.45 Ga), but unfortunately each sample has a relatively large error on both intercepts. When combining the analyses of these four samples (AB-01-029, AB-01-104, AB-02-213, and ID-TIMS analyses of AB-02-293), a mixing line can be constructed based on 3 monazite (Grains A6 to A8) and 11 zircon data (Grains B10 to B14, C16 to C19, and E24 and E25; Table 2.1; Figure 2.6F), yielding an upper intercept of 1038 ± 6 Ma, and a lower intercept of 453 ± 6 Ma (85% probability of fit).

This diagram demonstrates the regional importance of the late Middle to Late Ordovician magmatic event – the voluminous second phase of the Notre Dame Arc (van Staal, 2007) – that has affected the Dashwoods subzone. This magmatic event is coeval with regional deformation in the Dashwoods subzone and has been interpreted to represent the collision of Dashwoods with the Laurentian margin (van Staal et al., 2007). Additionally, the diagram demonstrates the regional development of a source of Grenvillian affinity to the Dashwoods subzone, which is important for paleogeographical reconstructions (see discussion below). Last of all, the diagram also demonstrates that, based on its U-Pb ages, the schistose muscovite granite (AB-01-029) exposed in the cataclastic zone of the BCZ has a closer relationship with Dashwoods subzone units than with the Neoproterozoic Hare Hill Complex of the internal Humber Zone (Currie and van Berkel, 1992), and therefore the schistose granite is assigned to the Dashwoods subzone.

2.6.2. Oblique-dextral Deformation along the BCZ

In Late Ordovician time (ca. 455 Ma) the western boundary of the Dashwoods subzone experienced oblique-dextral deformation, as exemplified by the syntectonic pegmatite dyke (AB-01-104), under medium- to high-grade conditions. Similar observations have been made along the Humber Zone - Dunnage Zone boundary throughout the northern Appalachians. In the Three Pond area of the Dashwoods subzone (15 km northeast of Figure 2.2B), a belt of anastomosing shear zones, which are spatially related to (ultra) mafic lenses in the metasediments, is exposed. These N-S striking high-strain zones have a predominant dextral sense of shear, were demonstrated to post-date peak regional metamorphism and migmatization (ca. 460 Ma; Piasecki, 1988), and were inferred to be pre-Silurian (Piasecki, 1995). In the Baie Verte peninsula in northern Newfoundland, the Baie Verte-Brompton Line (BBL in Figure 2.1) has registered a complex deformation history that includes ductile transcurrent (both dextral and sinistral), and dip-slip movements (Hibbard, 1983; Goodwin and Williams, 1990; Piasecki, 1995). No direct geochronological ages have been associated with these deformational phases, but recently it was postulated that two ductile dextral strike-slip motions have occurred, the younger of which is associated with greenschist facies deformation and is younger than Early Silurian (Goodwin and Williams, 1996). The older dextral movement in the Baie Verte-Brompton Line is most likely Middle to Late Ordovician and related to the Taconic orogeny (cf. Williams and St-Julien, 1982). To the south in the Québec Appalachians, the Shickshock Sud fault zone, a fault system spatially associated with the BCZ, has also been shown to accommodate oblique-dextral movement during the Late Ordovician (454-456 Ma; Sacks et al., 2004). Thus late Middle to Late Ordovician (oblique-) dextral deformation along the Laurentian (Humber) margin has been recognized throughout the northern Appalachians.

The 445.8 ± 0.6 Ma latest Ordovician granodiorite sheet (AB-02-229) in the western Dashwoods subzone is similar in age and composition to the ca. 449 Ma Pin pluton (Hall and van Staal, 1999) in the southern Dashwoods subzone, and the ca. 440 Ma Glover Island and Burlington granodiorite

bodies in the northern Notre Dame subzone (Cawood and van Gool, 1998). This geographically widespread group of granitoid bodies represents the third phase of the Notre Dame Arc (see Figure 2 in van Staal, 2007), which is interpreted to post-date the Taconic orogeny (*sensu* van Staal et al., 2007). The granodiorite sheet has also been affected by oblique-dextral deformation, and therefore the Late Ordovician deformation in the BCZ continued (possibly intermittently) into the Early Silurian with a similar sense of shear along its boundary. This also implies that oblique-dextral deformation along the western boundary of Dashwoods under medium- to high-grade conditions is not restricted to the Taconic orogeny, but continued after the main collision of Dashwoods with the Laurentian margin. Post-collisional movements along the boundaries of individual tectonic segments, especially lateral movements along crustal-scale boundaries such as the BCZ, are to be expected in a southwest Pacific Ocean type tectonic setting (van Staal et al., 1998).

2.6.3. Regional Tectonic Setting and the LGLF

The late Middle to Late Ordovician oblique-dextral movement along the western boundary of Dashwoods (BCZ) is contemporaneous with oblique-sinistral accretion of the Annieopsquatch Accretionary Tract along its eastern margin (Lissenberg et al., 2005; Zagorevski et al., 2006). However, it is unlikely that these motions were coupled dynamically, since both of them are related to different convergence systems (Waldron and van Staal, 2001; Zagorevski et al., 2006). This implies that during the late Middle to Late Ordovician, the Dashwoods microcontinent moved in a southerly direction with respect to Laurentia (to the west) and the then-present Iapetus Ocean (to the east) (Figure 2.9).

Deformation on the LGLF is probably latest Ordovician to earliest Silurian in age (450-440 Ma) suggesting that the dextral-reverse movement along the LGLF is contemporaneous with the Late Ordovician deformation in the BCZ. If the oceanic Snooks Arm arc and the continental Notre Dame Arc formed part of the same continuous arc system, comparable to the present-day Banda and Sunda

arc system in Indonesia (van Staal, 2007; van Staal et al., 2007), the Snooks Arm arc and its Baie Verte oceanic tract infrastructure may have moved independently and faster southwards than the Notre Dame Arc with its Dashwoods substrate. Such convergence would have made the LGLF a contractional bend in an overall arc-parallel strike-slip fault system (Figure 2.9). Hence a faster moving Snooks Arm arc could have underthrusted the Dashwoods microcontinent with its Notre Dame Arc suprastructure, juxtaposing the higher-grade rocks of the latter with lower grade volcanic rocks of the Snooks Arm arc.

2.6.4. Inherited Grains and Dashwoods Microcontinent Correlatives

The presence of Late Mesoproterozoic (1030-1190 Ma; Figure 2.7) inheritance in several igneous rock units of the Dashwoods subzone (Tables 2.1 and 2.2) has tectonic implications with respect to paleogeographic reconstructions. The fact that a well-defined mixing line can be constructed using the analyses of four different samples (Figure 2.6F) demonstrates the regional presence of a crustal source with a Grenville affinity in the Dashwoods subzone. It is unclear whether the inherited grains from the U-Pb samples were derived from the crystalline basement to the Dashwoods subzone or its overlying sediments.

In addition to previously recognized Early Mesoproterozoic (1300-1650 Ma) inherited ages (e.g. Dunning et al., 1989; Whalen et al., 1997), the presence of Grenvillian inherited ages in the Dashwoods subzone strengthens the argument for relating Dashwoods to the Long Range Inlier of northern Newfoundland, where crystalline units of similar ages (1.5 and 1.0 Ga) are exposed (Figure 2.1; Heaman et al., 2002). To the west, the Long Range Inlier is tectonically emplaced onto 'its' Cambro-Ordovician passive margin sequence, but along its northern and southern margin the rift-drift clastics and subsequent passive margin carbonates are unconformably overlying the Long Range Inlier (Erdmer and Williams, 1995). Therefore, the Long Range Inlier cannot represent the Dashwoods microcontinent *sensu stricto,* but the two crystalline segments appear to have a similar

Mesoproterozoic history and hence may have been adjacent to one another prior to rifting, opening of the Humber seaway and departure of Dashwoods.

Our new ages also introduce a possible connection of the Dashwoods subzone with the Blair River Inlier in Cape Breton Island, Nova Scotia. This crystalline complex is composed of various plutonic rocks of Grenvillian age (978-1080 Ma), and even though no ages older than 1.2 Ga have been identified, Sm-Nd depleted mantle model ages from gneisses in the area suggest the presence of an older Mesoproterozoic component of ca. 1.5 Ga (Dickin and Raeside, 1990; Miller et al., 1996). The Blair River Inlier is generally interpreted, but not definitively confirmed, to be Humber Zone basement. Its isolated position, the absence of overlying Cambro-Ordovician sediments, and its tectonic contact with peri-Gondwanan units allow for different interpretations of its provenance (Miller et al., 1996; and references therein). Could it be possible that the Blair River Inlier formed part of the Dashwoods microcontinent? Both segments have been affected by Silurian (435-425 Ma) magmatism. However, the Ordovician tectono-magmatic event characteristic of the Dashwoods subzone has not been identified in the Blair River Complex. If the Blair River Inlier indeed formed part of the Dashwoods microcontinent, it is important to explain the absence of this Ordovician tectono-magmatic event. The Blair River Inlier could have been: (1) along-strike with the Notre Dame Arc, in a tectonic setting where the subducting crust was situated too shallow or too deep below the overlying crust to allow for arc magmatism to occur (Cross and Pilger, 1982); or (2) in front of the Notre Dame Arc (forearc region). In both locations, these segments would not have been affected by Ordovician magmatism. The absence of an Ordovician dynamo-thermal event could have been attained when, for example, the Blair River Inlier was situated either in or in front of a re-entrant, and Dashwoods was opposed to a promontory. In this scenario, the Blair River Inlier would have escaped the (hard) collision that affected the Dashwoods.

Based on the evidence, it is possible that the Blair River Inlier and/or the Long Range Inlier represents Dashwoods basement. However, important queries, including the marked discrepancy in Nd

isotopic values between the Dashwoods and the two basement inliers (Whalen et al., 1997), have to be addressed in order to allow for a positive correlation.

2.7. Conclusions

The conclusions can be summarized as follows:

1. The western boundary of the Dashwoods microcontinent experienced oblique-dextral deformation from Late Ordovician into Early Silurian either continuously or intermittently, based on the presence of a late syntectonic pegmatite dyke (455 ± 12 Ma) and a precisely dated foliated granodiorite sheet (446 ± 1 Ma). Deformation along the Humber Zone - Dunnage Zone boundary, which has been observed throughout the northern Appalachians, is contemporaneous with oblique-sinistral accretion of peri-Laurentian units (Annieopsquatch Accretionary Tract) to the eastern margin of the Dashwoods microcontinent. This suggests that the Dashwoods microcontinent had a southward translation during the Middle to Late Ordovician (Figure 2.9).
2. U-Pb and $^{40}Ar/^{39}Ar$ geochronology combined with other geological evidence confirms that Late Ordovician-earliest Silurian (ca. 450-440 Ma) dextral-reverse movement along the Little Grand Lake Fault (LGLF), which juxtaposed low-grade oceanic units to the north with medium- to high-grade meta-sedimentary units to the south, is coeval with the southward translation of the Dashwoods microcontinent.
3. New U-Pb geochronology data, including a muscovite granite (463 ± 5 Ma), a schistose muscovite granite (459 $^{+17}/_{-21}$ Ma), and a tectonized tonalite (458 ± 20 Ma), demonstrate the regional importance in the Dashwoods subzone of the voluminous Middle Ordovician magmatic pulse (second phase of the Notre Dame Arc).
4. The presence of numerous ca. 1040 Ma (Grenvillian *sensu stricto*) inherited grains in several igneous units is important for paleogeographical reconstruction of the Dashwoods microcontinent. It reinforces the link of the Dashwoods basement with the Long Range Inlier in western

Newfoundland. Moreover, it introduces a possible link with the Blair River Inlier in Cape Breton. Based on U-Pb ages, it is feasible that this segment formed part of the Dashwoods microcontinent during the Ordovician.

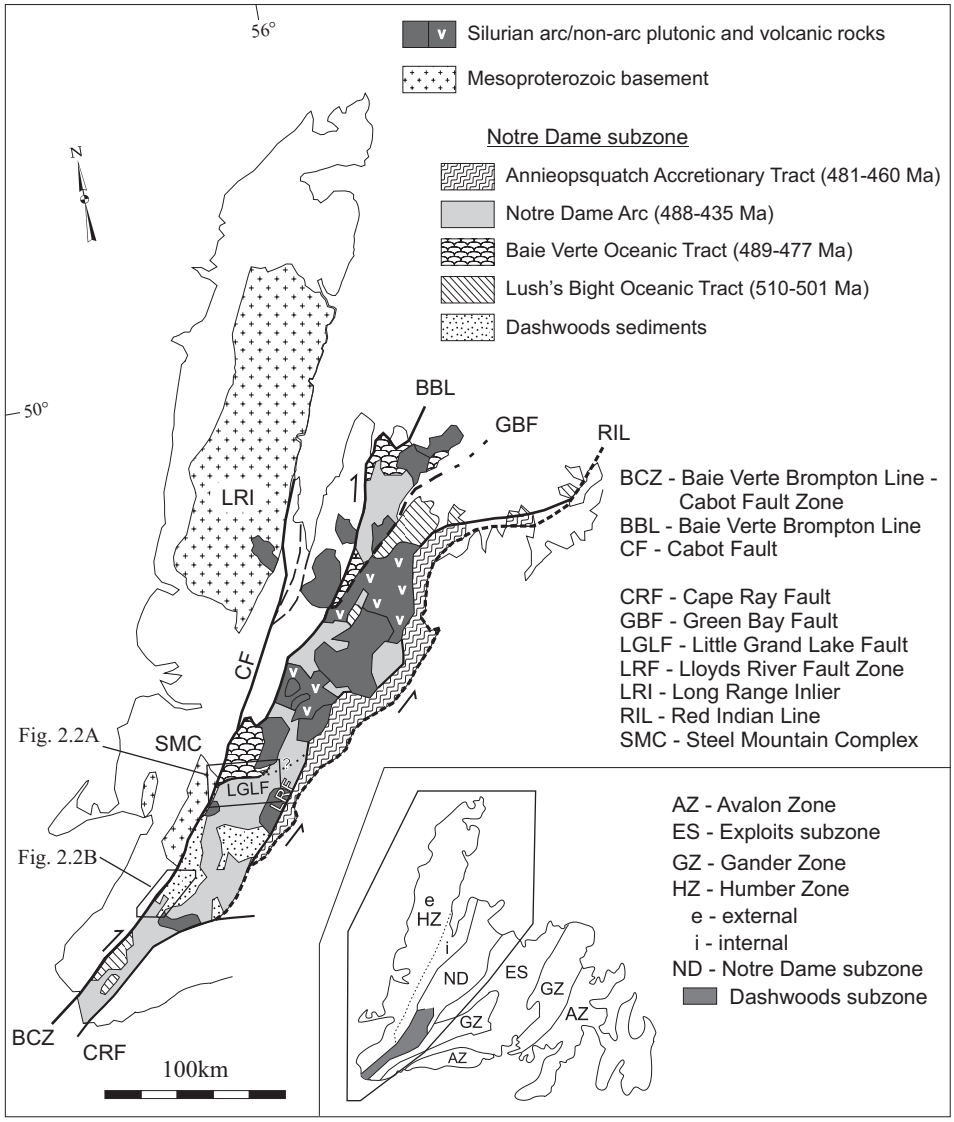

Figure 2.1 Simplified geological map of western Newfoundland, showing the main tectonic elements discussed in the text (modified after van Staal, 2006). Inset shows the tectono-stratigraphic division of the Newfoundland Appalachians and the position of the Dashwoods subzone (modified after Williams et al., 1988).

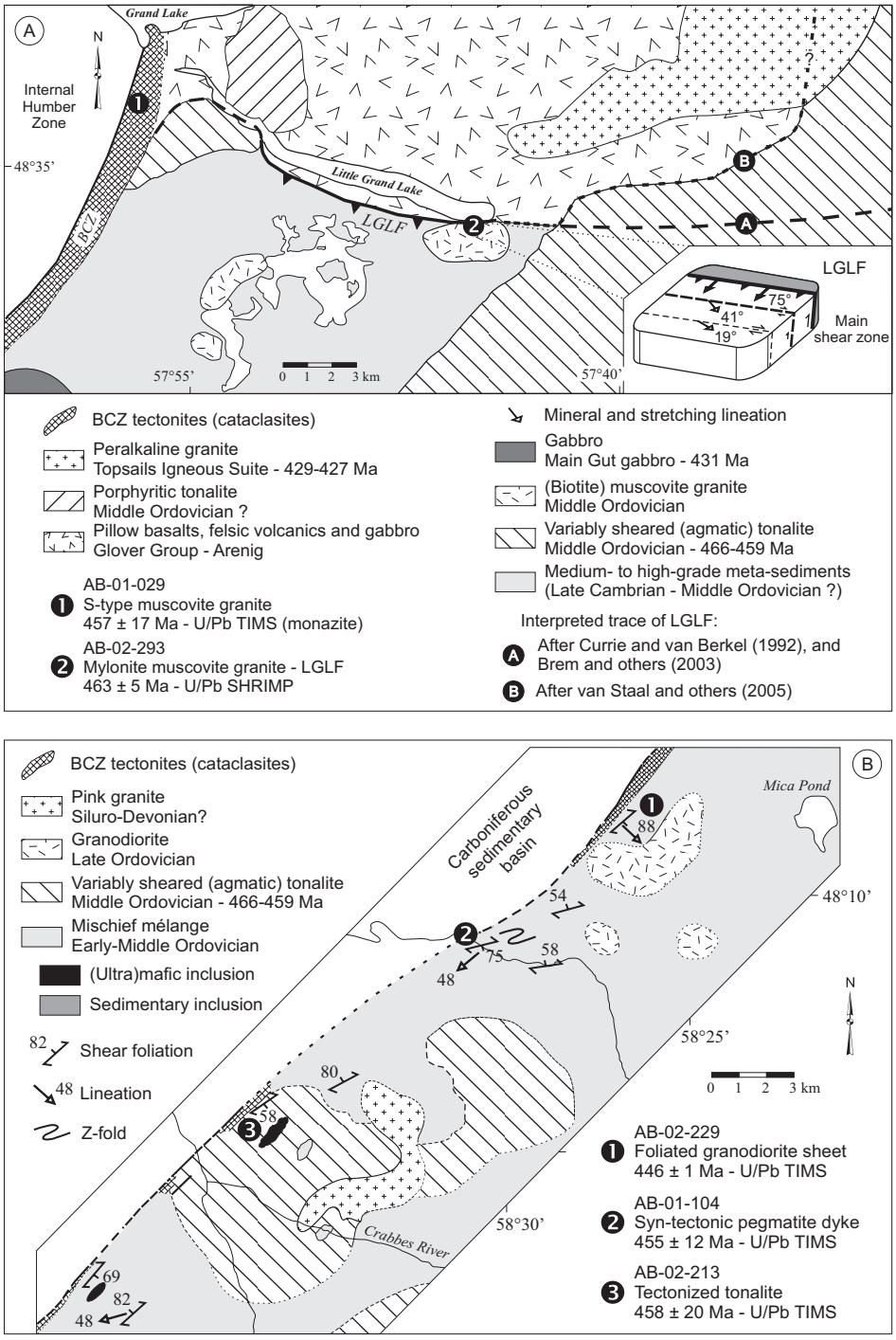

Figure 2.2 Simplified geological maps. (**A**) The LGLF region. Numbers indicate the locations of the geochronological samples of this study; letters indicate the proposed traces of the LGLF east of the Little Grand Lake according to different authors as discussed in the text. Inset shows the heterogeneous slip partitioning in the LGLF. (**B**) The BCZ along the central part of Dashwoods. Numbers indicate the locations of the geochronological samples of this study. See Figure 2.1 for locations of the areas.

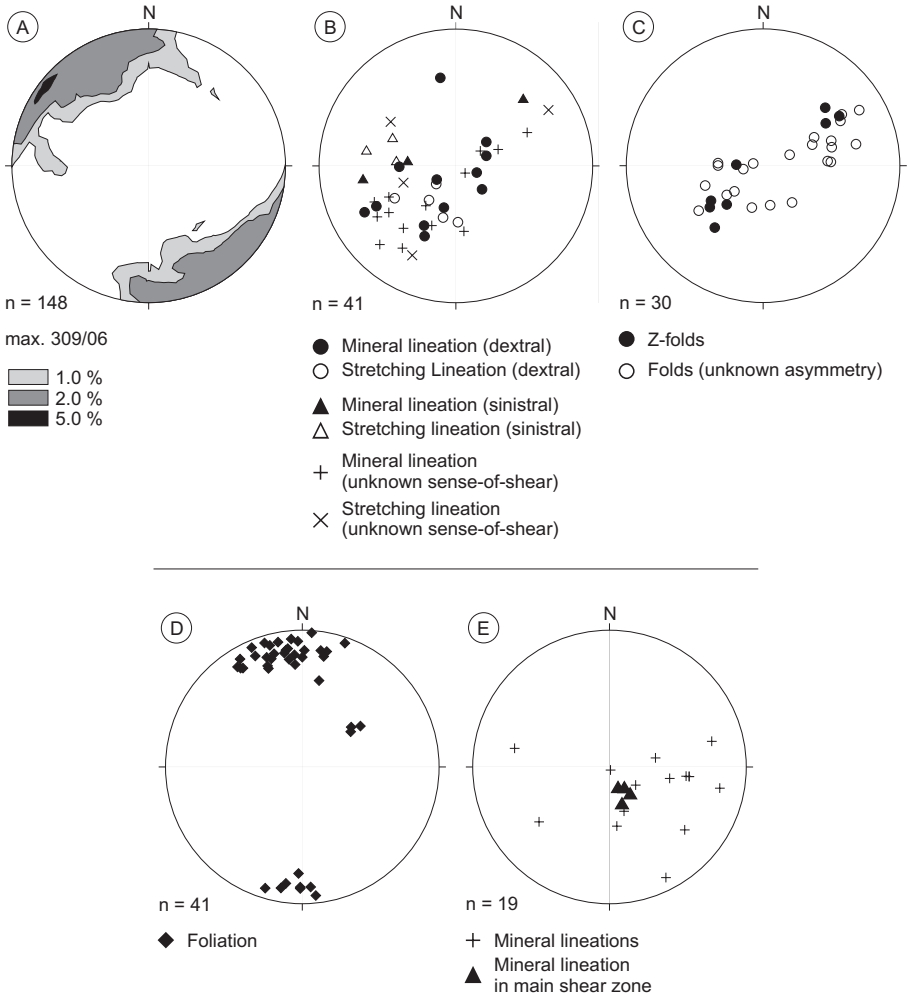

Figure 2.3 Equal-area lower-hemisphere projections of: (**A**) Contours of poles to foliation of the high-strain fabric of the BCZ; (**B**) Lineations associated with the high-strain fabric of the BCZ; (**C**) Fold axes of asymmetric folds in the BCZ; (**D**) Poles to foliation in the LGLF; and (**E**) Mineral and stretching lineations in the LGLF.

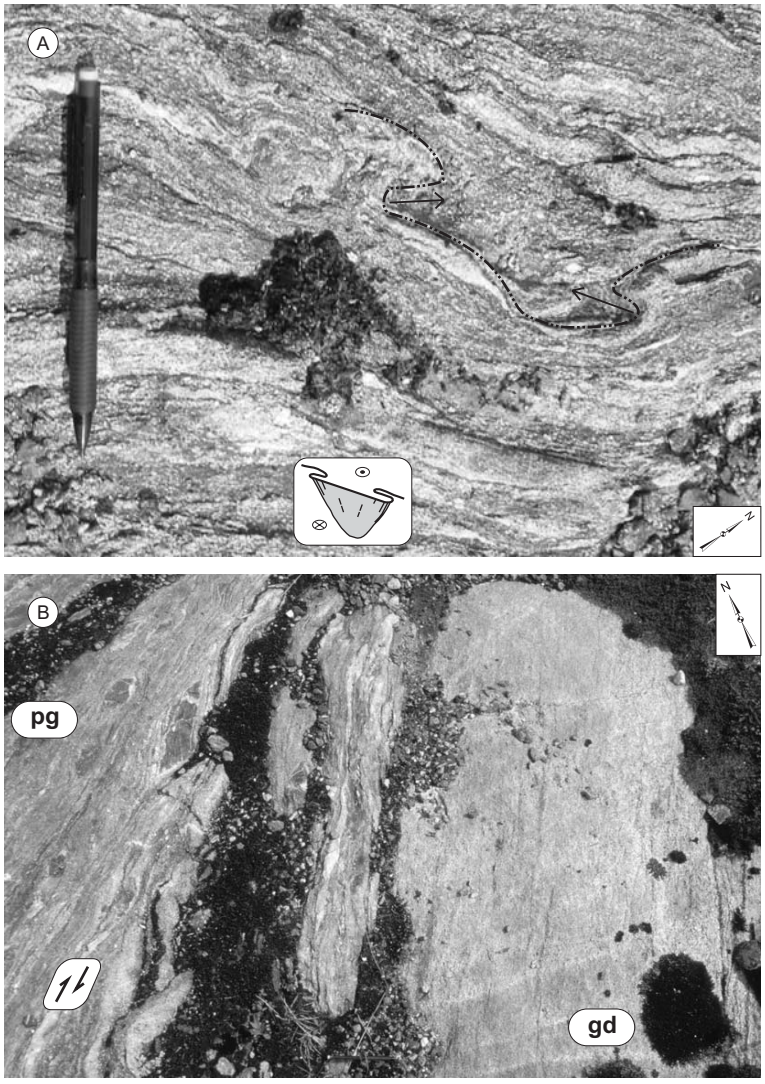

Figure 2.4 Field photographs of the high-strain fabrics in the BCZ. (**A**) Sheath fold in high-strain zone developed in paragneiss, with vertical foliation, down-dip mineral lineation, northeast plunging Z-fold axis and southwest plunging S-fold-axis. Such geometry is indicative of a northwest-side-up movement. (**B**) High-strain fabric in xenolith-bearing paragneisses (pg) intruded by xenolith-free granodiorite sheet (gd). Xenoliths in paragneiss show dextral sense of shear. Granodiorite was sampled for U-Pb geochronology (sample AB-02-229). Width of view is approximately 3 metres.

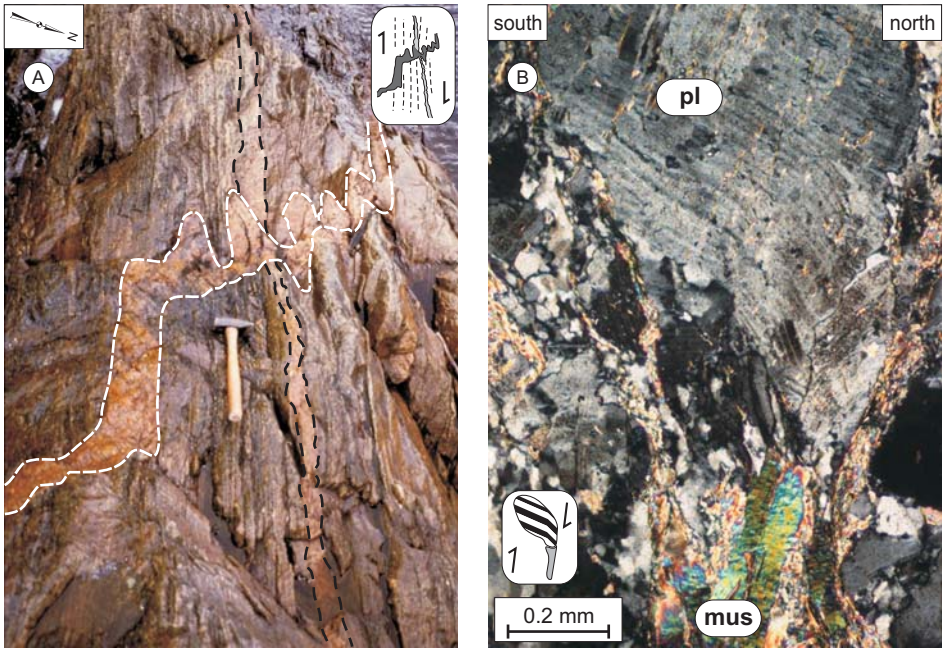

Figure 2.5 (**A**) Field photograph of late syntectonic pegmatite dykes intruding mylonitic paragneisses. The dyke clockwise from the foliation is folded (white dashed lines), and the one counter-clockwise from the foliation is boudinaged (black dashed lines). Such geometry is indicative of a dextral sense of shear. The folded vein was sampled for U-Pb geochronology (sample AB-01-104). (**B**) Photomicrograph of a deformed grain in the main strand of the Little Grand Lake Fault; Plagioclase (pl) porphyroclast with muscovite (mus) tail, indicative of a south-side-up component of movement. Thin section is perpendicular to the foliation and parallel to the down-dip mineral lineation.

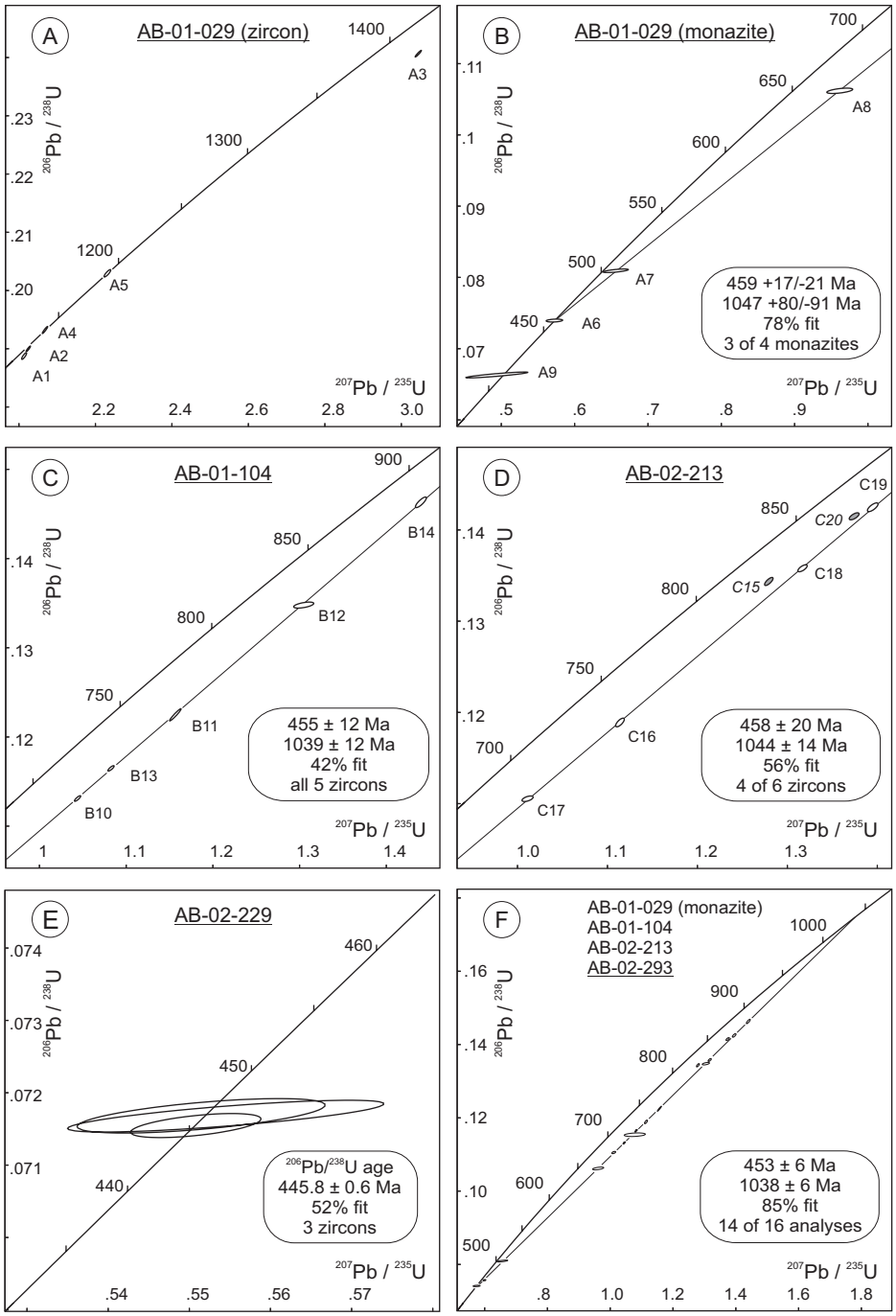

Figure 2.6 U-Pb TIMS Concordia diagrams for samples from the BCZ (results in Table 2.1). (**A**) Sample AB-01-029 (schistose muscovite granite) zircon grains. (**B**) Sample AB-01-029 (schistose muscovite granite) monazite grains. (**C**) Sample AB-01-104 (late syn-tectonic pegmatite dyke). (**D**) Sample AB-02-213 (tectonized tonalite). (**E**) Sample AB-02-229 (foliated granodiorite sheet). (**F**) Compiled diagram including AB-01-029 monazite analyses, and AB-01-104, AB-02-213, and AB-02-293 ID-TIMS zircon analyses.

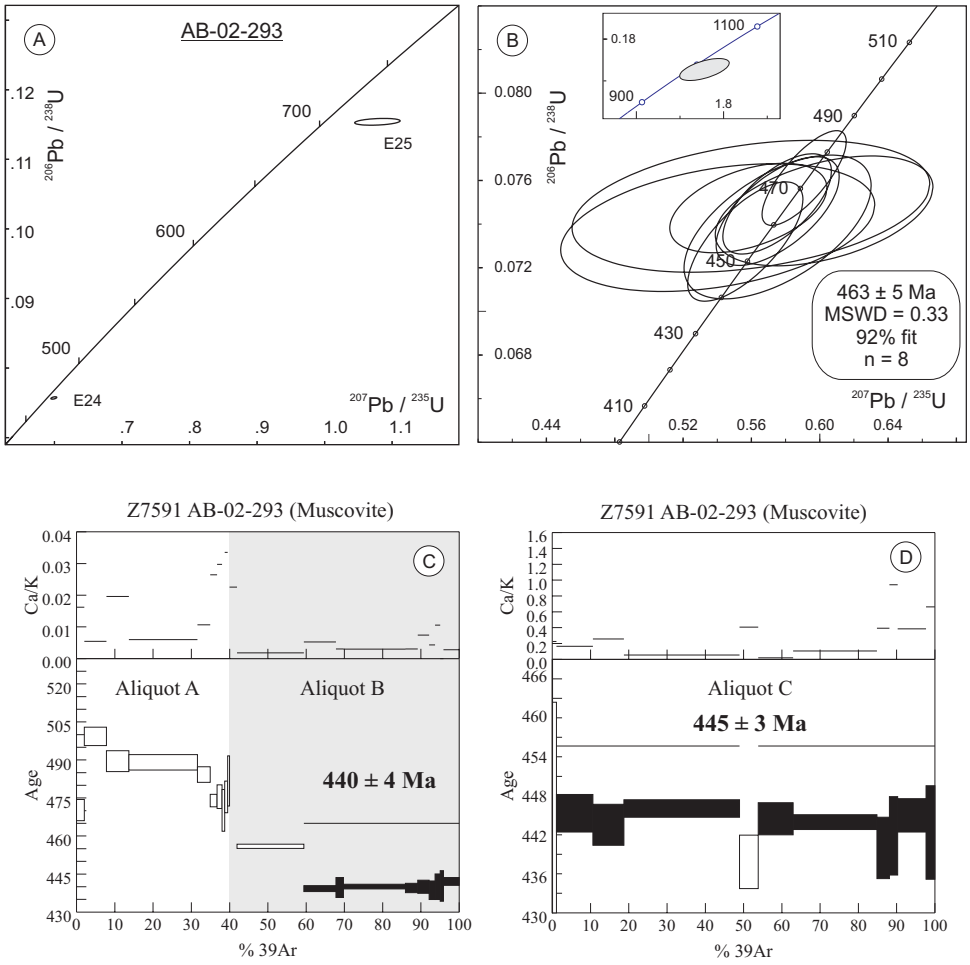

Figure 2.7 Results of various geochronological analyses on the mylonitic muscovite granite (sample AB-02-293) from the main strand of the Little Grand Lake Fault (results in Tables 2.1 to 2.3). (**A**) U-Pb TIMS Concordia diagram of 2 zircon analyses. (**B**) U-Pb SHRIMP Concordia diagram of 8 analyses of tips of zircon grains. Inset shows one analysis yielding an older Grenvillian age, which was omitted from calculations. (**C**) and (**D**) ^{40}Ar/^{39}Ar muscovite geochronology age spectrum.

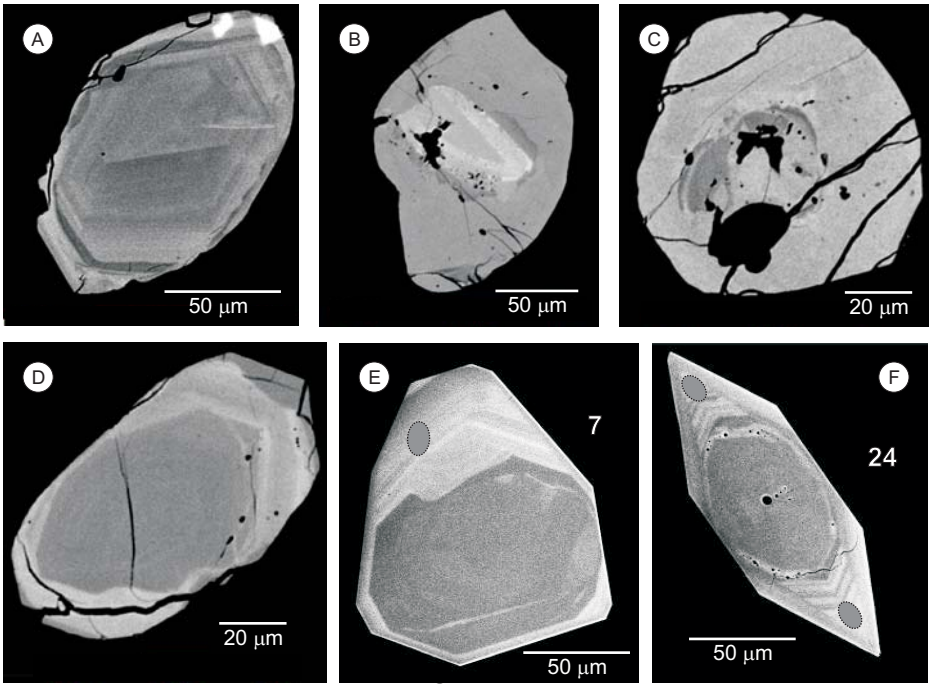

Figure 2.8 Back-scattered electron microscope (BSEM) images of zircon and monazite grains from U-Pb geochronological samples. (**A**) Zircon grain showing an oscillatory zoned core with a narrow overgrowth (schistose muscovite granite, sample AB-01-029). (**B**) Monazite grain showing wide featureless rim around a complex zoned core (schistose muscovite granite, sample AB-01-029). (**C**) Monazite grain showing wide featureless rim around a heterogeneous resorbed (?) core. The large ovoid dark area towards the bottom is a zircon inclusion; the triangular black areas in the core are inclusions of xenotime and feldspar (schistose muscovite granite, sample AB-01-029). (**D**) Zircon grain showing evidence for resorption (lower part of grain), and euhedral overgrowth (top of grain) (tectonized tonalite, sample AB-02-213). (**E**) and (**F**) Zircon grains with euhedral overgrowth with oscillatory magmatic zoning (mylonitic muscovite granite, sample AB-02-293). The grey ellipses mark the location of SHRIMP spot; the numbers refer to the grain analyzed (see Table 2.2).

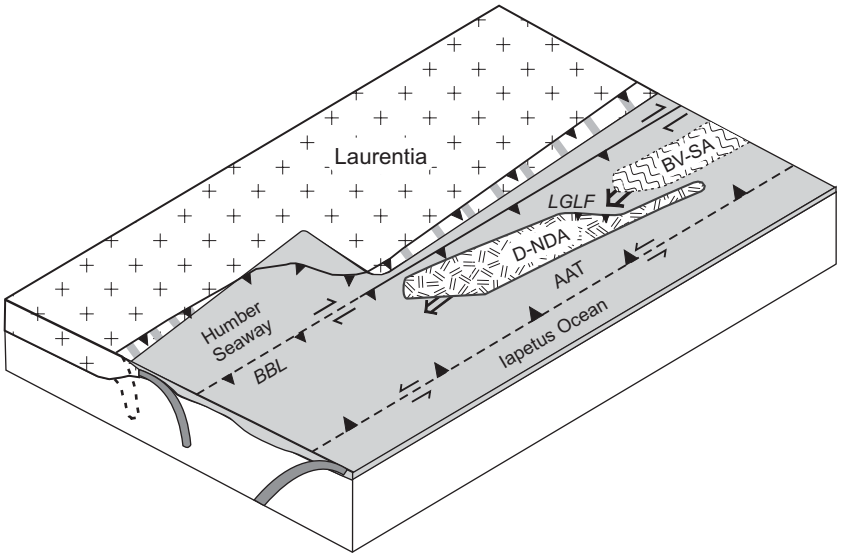

Figure 2.9 A tectonic model for the Dashwoods micro-continent and associated Notre Dame Arc during the Middle to Late Ordovician. The model shows the southward translation of Dashwoods micro-continent and its associated Notre Dame Arc (D-NDA), with respect to the Laurentian margin and the Annieopsquatch Accretionary Tract (AAT). It also shows the interaction along the Little Grand Lake Fault (LGLF) between the Baie Verte Oceanic Tract with its Snooks Arm arc (BV-SA) and the Dashwoods micro-continent (modified from van Staal, 2007).

Table 2.1: U-Pb ID-TIMS isotopic data for zircon and monazite from granitoid rocks of the Dashwoods Subzone, western Newfoundland.

No.	Description	Wt. (mg)	U (ppm)	Th/U	Pbtot (pg)	PbCom (pg)	206Pb/204Pb	206Pb/238U	207Pb/235U
A	**AB-01-029 - Schistose muscovite granite, Cabot Fault Zone (UTM 53843-4288)**								
1	Abr zr, euh, 1 bubble incl	15.2	85.5	0.42	254.1	1.99	7913.2	0.1887	2.0134
2	Abr zr, euh, clr, rod incl	7.7	166.3	0.77	274.2	0.90	17397.0	0.1900	2.0243
3	Abr zr, rnd, clr, no incl	13.8	118.7	0.34	404.0	0.80	31550.3	0.2407	3.0443
4	Abr zr, euh, clr, no incl	12	91.4	0.33	214.7	0.76	17948.5	0.1932	2.0680
5	Abr zr, euh, clr, 1 rod incl	12	29.4	0.26	71.3	0.89	5176.9	0.2030	2.2313
6	Mon, frag, clr, cracked	4	643.2	19.36	1188.4	27.51	447.5	0.0741	0.5743
7	Mon, ylw, equant, clr, 1 white incl	10	65.8	40.40	627.7	7.99	446.7	0.0809	0.6560
8	Mon, rnd, ylw, clr, pitted, *	11.1	21.1	48.56	344.2	2.95	560.8	0.1062	0.9616
9	Mon, ang, ylw, clr, pitted, *	5.9	15.5	41.68	74.4	2.69	163.1	0.0663	0.4940
B	**AB-01-104 - Late syn-tectonic pegmatite dyke, Dashwoods Subzone (UTM 53342-3872)**								
10	Abr zr, best pick, **	1.8	355.5	0.22	72.7	0.72	6667.1	0.1165	1.0825
11	Abr zr, 2nd best, **	3.1	490.3	0.35	188.3	0.97	12327.5	0.1225	1.1567
12	Abr zr, bubble incl, crack	3.5	326.2	0.30	153.5	9.35	1073.8	0.1348	1.3047
13	Abr zr, frag, melt incl, **	1.4	376.4	0.24	58.5	0.66	5832.6	0.1131	1.0443
14	Abr zr, clr, equant, melt incl, **	3.1	195.7	0.27	87.9	0.87	6547.8	0.1463	1.4399
C	**AB-02-213 - Tectonized tonalite, Dashwoods Subzone (UTM 53278-3792)**								
15	Abr zr, stubby, best pick, **	2.9	362.2	0.27	139.6	1.71	5314.2	0.1343	1.2794
16	Abr zr, **	2.5	269.1	0.36	81.0	1.15	4479.0	0.1189	1.1139
17	Abr zr, rnd, 2^{nd} choice	4.1	171.6	0.33	78.1	2.82	1785.6	0.1105	1.0112
18	Abr zr tip, clr, rnd, **	0.9	389.7	0.27	47.2	0.87	3526.1	0.1358	1.3169
19	Abr zr tip, fuzzy, rnd, crack, **	2.2	192.1	0.36	61.2	1.12	3464.0	0.1425	1.3949
20	Abr zr, frag, rnd, clr, dented, **	2.4	183.9	0.35	63.2	1.23	3284.2	0.1415	1.3742
D	**AB-02-229 - Foliated granodiorite sheet, Dashwoods Subzone (UTM 53387-3937)**								
21	Abr zr, needle, multi incl	5.8	140.9	0.65	63.4	9.20	426.6	0.0717	0.5515
22	Abr zr,	1.6	168.8	0.53	20.3	1.55	818.8	0.0715	0.5508
23	Abr zr, 2nd choice, rnd, clr, **	1.9	98.0	0.53	14.0	2.71	333.9	0.0717	0.5545
E	**AB-02-293 - Mylonitic muscovite granite, Little Grand Lake Fault (UTM 53784-4443)**								
24	Abr zr, equant, clr	6.1	207.2	0.41	97.5	3.06	2024.0	0.0757	0.5991
25	Abr zr, equant, opq and bubble incl, **	2.7	261.1	0.26	94.5	24.36	232.2	0.1154	1.0782

UTM measurements are in NAD-27 coordinates
abr = abraded, ang = angular, clr = clear, euh = euhedral, frag = fragment, incl = inclusion, mon = monazite, opq = opaque, rnd = round, ylw = yellow; zr = zircon
* = before dissolution, grain was treated with HNO_3 to remove the hematite (?) coating from the grains
** = no column chemistry (Krogh, 1973) performed on zircons
PbCom is common Pb, assuming the isotopic composition of laboratory blank
Th/U calculated from radiogenic $^{208}Pb/^{206}Pb$ ratio and $^{207}Pb/^{206}Pb$ age assuming concordance
% Disc., is per cent discordance for the given $^{207}Pb/^{206}Pb$ age
Decay constants are from Jaffey and others (1971)

Table 2.1: Continued.

No.	206Pb/238U	2σ	207Pb/235U	2σ	207Pb/206Pb	2σ	Disc %	Error Corr. Coeff.	Lab No.
	age (Ma) calculated								
A	**AB-01-029 - Schistose muscovite granite**								
1	1114.6	3.1	1120.1	2.2	1130.7	3.4	1.5	0.8499	dwd4078
2	1121.3	2.6	1123.7	1.9	1128.4	2.1	0.7	0.9290	dwd4079
3	1390.2	2.9	1418.8	2.0	1462.1	1.6	5.5	0.9507	dwd4080
4	1138.8	3.2	1138.3	2.3	1137.3	2.2	-0.1	0.9416	dwd4102
5	1191.2	3.4	1190.9	2.7	1190.4	4.0	-0.1	0.8592	dwd4103
6	461.0	1.1	460.8	7.3	459.9	42.4	-0.2	0.2675	dwd4114
7	501.7	1.5	512.2	10.6	559.5	53.5	10.7	0.6677	dwd4115
8	650.6	2.2	684.1	9.2	796.0	35.2	19.2	0.5489	dwd4760
9	413.9	2.5	407.6	28.8	372.5	184.0	-11.5	0.8887	dwd4761
B	**AB-01-104 - Late syn-tectonic pegmatite dyke**								
10	710.3	1.8	744.8	1.7	850.2	3.7	17.4	0.8393	dwd4084
11	744.8	3.9	780.4	3.1	883.5	3.2	16.6	0.9617	dwd4085
12	815.1	1.9	847.8	5.1	934.4	16.0	13.6	0.5507	dwd4086
13	690.9	1.7	726.0	1.7	836.0	3.9	18.3	0.8347	dwd4106
14	880.2	3.3	905.7	2.6	968.3	5.0	9.7	0.8308	dwd4107
C	**AB-02-213 - Tectonized tonalite**								
15	812.6	2.5	836.6	2.1	900.7	5.1	10.4	0.7536	dwd4730
16	724.2	2.7	760.1	2.3	867.1	6.4	17.4	0.7221	dwd4731
17	675.8	1.8	709.5	3.1	817.4	10.7	18.2	0.5575	dwd4732
18	820.9	2.2	853.1	2.3	938.1	5.8	13.3	0.6949	dwd4757
19	858.7	2.7	886.8	2.5	957.5	5.9	11.0	0.7297	dwd4758
20	853.1	2.2	878.0	2.3	941.2	6.0	10.0	0.6829	dwd4759
D	**AB-02-229 - Foliated granodiorite sheet**								
21	446.3	1.4	446.0	10.0	444.3	57.9	-0.5	0.6275	dwd4733
22	445.5	1.0	445.5	5.3	445.8	30.0	0.1	0.5545	dwd4734
23	446.3	1.3	447.9	12.8	456.6	73.6	2.3	0.7972	dwd4735
E	**AB-02-293 mylonitic muscovite granite**								
24	470.4	1.0	476.6	2.8	506.7	14.2	7.4	0.5042	dwd4391
25	704.0	2.8	742.8	16.5	861.4	63.3	19.3	0.2872	dwd4393

Table 2.2: U-Pb SHRIMP isotopic data for zircon from a mylonitic muscovite granite from the Little Grand Lake Fault, western Newfoundland

Spot name	U (ppm)	Th (ppm)	Th/U	Pb* (ppm)	^{204}Pb (ppb)	^{204}Pb/^{206}Pb	± ^{204}Pb/^{206}Pb	f(206)^{204}	^{208}Pb/^{206}Pb	± ^{208}Pb/^{206}Pb	^{207}Pb/^{235}U	± ^{207}Pb/^{235}U	^{206}Pb/^{238}U	± ^{206}Pb/^{238}U	Corr Coeff	^{207}Pb/^{206}Pb	± ^{207}Pb/^{206}Pb	^{206}Pb/^{238}U	± ^{206}Pb/^{238}U	^{207}Pb/^{206}Pb	± ^{207}Pb/^{206}Pb
VB02-293 (Z7591): Mylonite muscovite granite, Little Grand Lake Fault (UTM 53784-4443)																					
7591-2.1	532	118	0.229	87	0	0.000002	0.000076	0.0000	0.0709	0.0038	1.7083	0.0460	0.1655	0.0022	0.588	0.0749	0.0016	987	12	1064	45
7591-7.1	542	29	0.056	37	3	0.000100	0.000242	0.0017	0.0158	0.0091	0.5594	0.0430	0.0748	0.0012	0.334	0.0543	0.0040	465	7	382	173
7591-24.1	1243	814	0.676	99	1	0.000010	0.000010	0.0002	0.2044	0.0080	0.5560	0.0139	0.0732	0.0011	0.703	0.0551	0.0010	455	7	417	40
7591-51.1	938	75	0.083	65	1	0.000010	0.000010	0.0002	0.0256	0.0018	0.5748	0.0130	0.0749	0.0009	0.648	0.0557	0.0010	466	6	439	39
7591-50.1	575	32	0.058	40	0	0.000010	0.000010	0.0002	0.0192	0.0022	0.5752	0.0148	0.0746	0.0010	0.629	0.0560	0.0011	464	6	451	45
7591-39.1	1034	66	0.066	71	2	0.000034	0.000093	0.0006	0.0194	0.0041	0.5579	0.0189	0.0747	0.0008	0.445	0.0542	0.0017	464	5	378	70
7591-48.1	1158	182	0.162	82	2	0.000024	0.000054	0.0004	0.0537	0.0033	0.5751	0.0225	0.0738	0.0014	0.570	0.0565	0.0018	459	8	472	73
7591-45.1	1425	144	0.105	100	1	0.000010	0.000010	0.0002	0.0336	0.0019	0.6023	0.0261	0.0746	0.0010	0.432	0.0586	0.0023	464	6	552	88
7591-24.2	763	309	0.418	57	13	0.000276	0.000142	0.0048	0.1258	0.0068	0.5399	0.0377	0.0738	0.0012	0.351	0.0531	0.0035	459	7	331	157

UTM measurements are in NAD-27 coordinates
Notes (see Stern, 1997):
Uncertainties reported at 1sigma (absolute) and are calculated by numerical propagation of all known sources of error
f206^{204} refers to mole fraction of total ^{206}Pb that is due to common Pb, calculated using the ^{204}Pb-method; common Pb composition used is the surface blank
[1] 204-corrected ages (Stern, 1997)

Table 2.3: $^{40}Ar/^{39}Ar$ isotopic data from analyses on muscovite from a mylonitic muscovite granite from the Little Grand Lake Fault, western Newfoundland.

Power[a]	Vol.^{39}Ar	$^{36}Ar/^{39}Ar$	$^{37}Ar/$	$^{38}Ar/$	$^{40}Ar/$	%^{40}Ar	*$^{40}Ar/$	f_{39}[b]	App. Age
	x10^{-11} cc		^{39}Ar	^{39}Ar	^{39}Ar	ATM	^{39}Ar	(%)	Ma[c]
AB-02-293 Muscovite; J=.02344580[d] (Z7591; UTM 53784-4443)									
Aliquot:A									
2.4	7.1375	0.0016±0.0004	0.008±0.002	0.007±0.011	13.170±0.106	3.6	12.701±0.128	2.0	470.22±4.16
2.8	20.6033	0.0000±0.0001	0.003±0.001	0.004±0.011	13.606±0.109	0.0	13.600±0.113	5.8	499.30±3.62
3.0	20.8554	0.0001±0.0001	0.010±0.000	0.003±0.011	13.311±0.124	0.1	13.297±0.128	5.9	489.54±4.13
3.5	63.5564	0.0001±0.0001	0.003±0.000	0.003±0.011	13.303±0.094	0.2	13.281±0.094	17.9	489.05±3.04
3.9	11.9294	0.0001±0.0003	0.006±0.001	0.004±0.011	13.150±0.059	0.1	13.133±0.095	3.4	484.24±3.08
4.2	6.3127	0.0000±0.0002	0.014±0.002	0.003±0.011	12.821±0.053	0.0	12.817±0.075	1.8	474.00±2.45
4.6	4.6029	0.0001±0.0005	0.015±0.004	0.003±0.011	12.885±0.108	0.2	12.864±0.144	1.3	475.53±4.68
5.0	2.5498	0.0001±0.0012	0.028±0.003	0.004±0.011	12.742±0.130	0.4	12.697±0.253	0.7	470.12±8.25
6.0	2.7419	0.0004±0.0010	0.017±0.004	0.003±0.011	12.952±0.095	0.7	12.861±0.192	0.8	475.44±6.23
12.0	1.6448	0.0008±0.0016	0.029±0.003	0.004±0.011	13.240±0.148	1.4	13.055±0.306	0.5	481.73±9.92
Aliquot:B									
2.4	7.0515	0.0024±0.0004	0.012±0.001	0.006±0.011	11.644±0.046	6.1	10.930±0.101	2.0	411.57±3.39
2.8	62.0923	0.0001±0.0001	0.001±0.000	0.002±0.011	12.280±0.022	0.1	12.264±0.025	17.5	455.94±0.82
3.0	29.7775	0.0000±0.0001	0.003±0.000	0.003±0.011	11.759±0.031	0.0	11.758±0.036	8.4	439.24±1.18
3.3	7.0029	0.0002±0.0004	0.002±0.001	0.004±0.011	11.808±0.091	0.3	11.772±0.119	2.0	439.69±3.95
3.5	57.5608	0.0001±0.0000	0.002±0.000	0.002±0.011	11.797±0.026	0.1	11.782±0.028	16.2	440.04±0.92
3.7	11.3199	0.0000±0.0002	0.002±0.001	0.004±0.011	11.771±0.043	0.0	11.766±0.055	3.2	439.49±1.84
3.9	10.6197	0.0001±0.0003	0.004±0.001	0.005±0.011	11.793±0.057	0.1	11.781±0.077	3.0	439.99±2.56
4.2	5.5519	0.0001±0.0005	0.002±0.002	0.003±0.011	11.763±0.050	0.2	11.739±0.110	1.6	438.62±3.65
4.6	4.6737	0.0001±0.0005	0.005±0.002	0.006±0.011	11.799±0.102	0.2	11.780±0.153	1.3	439.98±5.06
5.5	3.0601	0.0001±0.0006	0.000±0.000	0.006±0.011	11.816±0.088	0.2	11.789±0.181	0.9	440.28±6.01
12.0	14.6262	0.0000±0.0001	0.001±0.001	0.002±0.011	11.848±0.033	0.0	11.844±0.047	4.1	442.08±1.56
AB-02-293 Muscovite; J=.02925380[d] (Z7591; UTM 53784-4443)									
Aliquot: C									
2.0	0.0561	0.0501±0.0117	20.549±9.051	0.074±0.023	15.967±1.743	51.4	7.754±4.658	0.1	368.84±200.53
2.4	0.7537	0.0097±0.0019	0.118±0.636	0.015±0.011	11.589±0.149	19.2	9.364±0.599	1.0	436.77±24.81
2.8	7.1533	0.0010±0.0002	0.085±0.057	0.002±0.011	9.758±0.041	2.0	9.561±0.068	9.5	444.92±2.82
3.0	6.0956	0.0004±0.0002	0.134±0.072	0.002±0.011	9.554±0.052	0.4	9.519±0.074	8.1	443.20±3.07
3.5	22.6758	0.0002±0.0000	0.029±0.015	0.002±0.011	9.625±0.031	0.5	9.578±0.032	30.2	445.63±1.31
3.9	3.6759	0.0003±0.0002	0.211±0.110	0.003±0.011	9.386±0.060	0.0	9.385±0.097	4.9	437.64±4.00
4.2	6.8516	0.0004±0.0002	0.010±0.062	0.001±0.011	9.573±0.034	0.3	9.541±0.058	9.1	444.09±2.41
4.6	16.4352	0.0001±0.0000	0.055±0.024	0.002±0.011	9.526±0.022	0.0	9.529±0.027	21.9	443.60±1.12
5.0	2.4616	0.0008±0.0003	0.205±0.161	0.002±0.011	9.472±0.058	0.4	9.435±0.111	3.3	439.73±4.61
5.5	1.6092	0.0005±0.0005	0.490±0.317	0.002±0.011	9.490±0.102	0.1	9.479±0.142	2.1	441.54±5.87
6.5	5.5769	0.0004±0.0001	0.200±0.103	0.003±0.011	9.574±0.038	0.2	9.553±0.060	7.4	444.61±2.50
12.0	1.7199	0.0007±0.0004	0.345±0.222	0.002±0.011	9.501±0.096	0.1	9.491±0.170	2.3	442.04±7.02

a: As measured by laser in % of full nominal power (10W)
b: Fraction ^{39}Ar as percent of total run
c: Errors are analytical only and do not reflect error in irradiation parameter J
d: Nominal J, referenced to PP-20=1072 Ma (Roddick, 1983)
All uncertainties quoted at 2σ level
UTM measurements are in NAD-27 coordinates

Chapter 3: Evaluation of Early Palaeozoic orogenic event(s) in the Corner Brook Lake block: implications for tectonic models for the Newfoundland Appalachians

3.1. Abstract

The Corner Brook Lake block (CBLB) of the internal Humber Zone in western Newfoundland occupies a central position in the Laurentian realm of the Appalachian-Caledonian mountain chain. New U-Pb ID-TIMS data from the CBLB crystalline basement include the 606.1 ± 1.5 Ma Disappointment Hill tonalite, which is coeval with nearby alkali-granite plutons, and an unnamed felsic gneiss with well-defined intercepts at 1503.6 ± 2.9 Ma and 604.9 ± 4.8 Ma. Moreover, ca. 430-422 Ma $^{40}Ar/^{39}Ar$ cooling ages on variously sheared units and a 427.5 ± 2 Ma (U-Pb on monazite) emplacement age for a post-tectonic pegmatite dyke, corroborate previously reported data, demonstrating that the CBLB underwent important west-vergent deformation and associated peak metamorphism during the Silurian Salinic orogeny, not during the Ordovician Taconic orogeny. There are no available radiometric ages or petrographic fabrics present that would indicate any significant Taconic dynamo-thermal event to have affected the CBLB rocks. This is in sharp contrast with the surrounding tectonic segments of the Laurentian realm, most notably the juxtaposed Dashwoods segment, which experienced a major tectono-thermal event during the Middle Ordovician, but less intense and localized deformation during the Early Silurian. The CBLB most likely occupied an upper crustal setting during the Ordovician, where it may have experienced brittle deformation that could have easily been eradicated by the strong Salinic orogenic event. Therefore, the CBLB and Dashwoods could not have been juxtaposed until after the Early Silurian (ca. 425 Ma). Large-scale (hundreds of kilometres) transcurrent movement on tectonic boundaries in addition to the well-documented

convergent tectonics can better explain the distinct individual tectonic histories of these terranes and their current juxtaposition.

3.2. Introduction

In the original plate-tectonic model proposed for the Newfoundland Appalachians by Dewey (1969), the Laurentian margin was suggested to have experienced a single orogenic event during the Ordovician: the Taconic orogeny, which was believed to have been associated with the collision between Laurentia and Gondwanaland following closure of the Iapetus Ocean. With continued research over the past four decades, this basic model has been moulded and shaped into a complex geodynamic model that resembles the present-day southwest Pacific Ocean setting, which includes multiple orogenic events that have affected various terranes, continental margins, volcanic arcs and ocean basins (Williams and Hatcher, 1982; van Staal et al., 1998). In spite of all the modifications, the basic aspect of the original model that the Laurentian margin was strongly deformed during the Taconic orogeny has remained (Williams, 1995; Waldron et al., 1998a; van Staal, 2007). However, geological evidence from the Corner Brook Lake block (CBLB) of the internal Humber Zone is not consistent with this scenario.

The CBLB occupies a central position in the Laurentian realm of the Newfoundland Appalachians (Figure 3.1; Cawood et al., 1995; van Staal et al., 2007). The rocks of the CBLB have been strongly deformed and metamorphosed under greenschist to amphibolite facies conditions, and as such no fossil control exists. Based on regional correlation with similar, yet less-deformed sedimentary rocks of the external Humber Zone to the west, the CBLB was commonly considered to have experienced deformation and metamorphism during the Ordovician Taconic orogeny (e.g. Hibbard, 1983; Williams, 1995, and references therein). Subsequent introduction of $^{40}Ar/^{39}Ar$ and U/Pb geochronological data for the area demonstrated that the CBLB experienced mainly an Early Silurian Salinic dynamo-thermal event (Cawood et al., 1994). The absence of a noticeable Taconic dynamo-

thermal event would contradict most existing tectonic models of the Newfoundland Appalachians, since these models imply that a hard collision occurred at the Laurentian margin of Newfoundland during the Ordovician (e.g. Dewey, 1969; Hibbard, 1983; Stockmal et al., 1987; Waldron et al., 1998a).

Hence the question: is there any geochronological evidence in the CBLB for the presence of a Taconic dynamo-thermal event? To answer this question, we have undertaken fieldwork and have applied several radiometric dating techniques – including $^{40}Ar/^{39}Ar$, and U/Pb single-grain ID-TIMS – to different minerals, in order to better constrain the thermo-chronological history of the CBLB. Fieldwork was mainly conducted in the area south of Grand Lake (Figure 3.1), which covers the southern part of the CBLB, where exposures of its crystalline basement and cover rocks are equally distributed. The area to the north of Grand Lake was studied in detail by Cawood et al. (1994) and Cawood and van Gool (1998). The results confirm that there is no evidence for the presence of a noticeable Taconic dynamo-thermal event in the rocks of the CBLB. In this chapter, the new results are presented, possible explanations for the absence of such a dynamo-thermal event are proposed and their implications for tectonic models of the Early Palaeozoic evolution of the Laurentian margin are discussed.

3.3. Geologic setting

The CBLB (after Cawood et al, 1995) is a largely fault-bounded block that forms the northern part of the Steel Mountain Inlier or Terrane (Figure 3.1 and 3.2) and has also been referred to as the Long Range Complex (Martineau, 1980). To the south, the CBLB is in contact with the Steel Mountain anorthosite complex, along the Caribou Brook shear zone (Figure 3.2; Brem et al., 2003). To the west, the CBLB is juxtaposed with Ordovician passive margin carbonates of the external Humber Zone along the Grand Lake and Humber River fault, which coincides with a break in the metamorphic field gradient (Cawood et al., 1996). To the east, the long-lived Cabot Fault Zone truncates the CBLB. The

only non-tectonic contact occurs to the northeast, where an unconformity separates the rocks of the CBLB from Early Carboniferous siliciclastic sedimentary rocks (Deer Lake basin). The southern part of the CBLB, which is exposed south of Grand Lake, can be subdivided into two distinguishable sub-units: a crystalline basement and its tectonically overlain metaclastic sequence (Figure 3.2).

The CBLB is commonly characterized as having a para-autochthonous 'Grenvillian' basement with overlying rift-drift sediments of the Iapetus Ocean basin and as such it is interpreted as representing the leading edge of the Laurentian craton. However, a recent interpretation (Chapter 4) suggests that the CBLB may in fact represent a displaced fragment, allochthonous to the position it currently occupies. These two different interpretations of tectonic setting will be further assessed in light of the new data and interpretations in the discussion part of this chapter.

3.3.1. Proterozoic crystalline basement

The oldest rocks in the area form part of the Corner Brook Lake complex and comprise two-pyroxene granulite gneisses and granitoid (tonalite to granodiorite) gneisses (Figure 3.3A; Appendix D). These dominant lithologies are interlayered with minor migmatitic paragneisses, amphibolite layers, quartzites and calc-silicate gneisses. The age of the high-grade units is reportedly constrained by orthopyroxene-bearing granitoid intrusives, such as the Disappointment Hill charnockite (location 1 on Figure 3.2B), which yielded a U-Pb zircon age of 1498 $^{+9}/_{-8}$ Ma (Currie et al., 1992). A similar Pinwarian protolith age of 1510 ± 6 Ma was obtained for the Corner Brook Lake granitoid gneiss (Figure 3.2A; Cawood et al., 1996). Locally within the gneiss complex, a dominantly meta-plutonic association is exposed, consisting of tonalite, monzonite, gabbro and agmatite (Figure 3.3B). This metaplutonic association bears close resemblance to the Middle Ordovician granitoids of the Notre Dame Arc in the Dashwoods Subzone (Dunning et al., 1989; van Staal et al., 2007). The presence of Ordovician intrusions in the internal Humber Zone would directly tie the CBLB with the Notre Dame Arc and would imply that deformation in the internal Humber Zone post-dated the Middle Ordovician

(Brem et al., 2003). A sample of an undeformed tonalite was taken for U-Pb geochronology (sample AB-01-040; Section 3.4.1.2.).

The Mesoproterozoic units appear to have been intruded by Late Neoproterozoic granitoid plutons, which include the ca. 602 Ma Round Pond granite (Figure 3.2A; Williams et al., 1985) and the ca. 608 Ma Hare Hill granite (location 2 on Figure 3.2B; Currie et al., 1992). The composition of these igneous rocks is dominantly alkali granite to syenite (Figure 3.3C). The gneissose units are locally cut by north-trending schistose amphibolite dykes, which are commonly correlated with the Neoproterozoic Long Range dyke swarm in the Long Range Inlier (e.g. Owen and Greenough, 1991). However, in the CBLB these mafic intrusions have not been dated and therefore the correlation should be taken with caution. Some dykes, which were originally thought to belong to the Long Range dyke swarm (ca. 610 Ma; Stukas and Reynolds, 1974; Kamo et al., 1989), actually intrude the Early Silurian Taylor Brook gabbro (Owen, 1992; Heaman et al., 2002) and are thus significantly younger.

Most observed contacts within the CBLB basement are tectonic in nature (Figures 3.2, and 3.4A and B; see also Martineau, 1980; Currie and van Berkel, 1992). Continuous tectonic contacts, such as the Caribou Brook shear zone and the Tulks Pond shear zone (Figures 3.2B and 3.4; Brem et al., 2003), contain steeply ENE-dipping shearing fabrics (S_{BSZ}; Figure 3.5A) and steeply plunging mineral and stretching lineations (L_{BSZ}; Figure 3.5B). Shear sense indicators associated with these fabrics, including S-C' (Figure 3.4B) and S-C (Figure 3.4C) shear bands, and winged objects, consistently indicate a reverse, east-side-up movement. These shear zones affected all crystalline units, including the late Neoproterozoic granitoid rocks (Figure 3.3C); thus the maximum age of deformation on these shear zones was latest Neoproterozoic (< ca. 600 Ma). This interpretation contrasts with previous reports, in which the Hare Hill Complex is assumed to have intruded after intense deformation and metamorphism (Currie and van Berkel, 1992).

3.3.2. Metasedimentary Thrust Stack

In the eastern half of the CBLB, quartzo-feldspathic gneiss units are tectonically interleaved with and act as basement to overlying metasedimentary rocks (see also Owen and Greenough, 1991; Piasecki, 1991). The metasedimentary rocks form part of the Mount Musgrave Group, which can be divided into a lower metaclastic (South Brook Formation) and an upper metacarbonate unit (Breeches Pond Formation; Cawood and van Gool, 1998). Only the former is exposed in the area south of Grand Lake. The dominantly metaclastic South Brook Formation consists of pebble to small-cobble conglomerate layers (Figure 3.6A), quartzites, and predominant psammites and pelites (Figure 3.6B). Some calcareous schists and marble layers, and interlayered granitic sheets are also present. The South Brook metasedimentary rocks are unfossiliferous and have been interpreted as being rift-related sediments. A detrital zircon study has demonstrated that the maximum age of deposition is latest Neoproterozoic (< 578 Ma; Cawood and Nemchin, 2001). To the north, a granodiorite gneiss (Figure 3.2A; Lady Slipper 'pluton' of Cawood et al., 1996), which may form part of a bimodal suite, is inferred to be at the base of the metasedimentary cover sequence. This unit yielded a latest Precambrian U-Pb zircon emplacement age ($555\ ^{+3}/_{-2}$ Ma; Cawood et al., 1996).

The metamorphic grade in the CBLB metasedimentary units varies from greenschist facies conditions in the west (muscovite + biotite) to lower amphibolite facies conditions near the Cabot Fault Zone (kyanite + garnet + staurolite). Quantitatively, peak metamorphic conditions have been estimated to be ca. 650°C and ca. 7-9 kbar (Owen and Greenough, 1991; Cawood et al. 1995).

The dominant foliation in the metasedimentary rocks (S_{SED-1}) is defined by micas, such as muscovite and biotite, and closer to the Cabot Fault Zone by kyanite. The foliation strikes NE and dips moderately to the ESE (Figure 3.5C). Mineral and stretching lineations associated with the S_{SED-1} foliation have variable orientations, but generally plunge towards the SSE (Figure 3.5D). Shear sense indicators associated with these fabrics, including shear bands (Figure 3.7A) and spiral garnets (Figure 3.7B), are consistent with regional east-over-west thrusting. Similar observations have been made for

the area immediately north of Grand Lake (S_1 and L_S in Domain 4 and 5 of Cawood and van Gool, 1998). Individual thrust sheets are apparent in the present-day geomorphology along Grand Lake and Corner Brook Lake.

Garnet porphyroblasts have overgrown the main S_{SED-1} foliation (see also Piasecki, 1991; Cawood and van Gool, 1998), but have been affected by the S_{SED-2} crenulation cleavage (Figure 3.7C). The presence of spiral garnets in one outcrop (Figure 3.7B) suggests that garnet growth was coeval with at least part of S_{SED-1} (see also Figure 32C in Cawood and van Gool, 1998). Owen and Greenough (1991) demonstrated that only a single phase of garnet growth affected both metasedimentary cover and its associated quartzo-feldspathic basement.

The S_{SED-2} fabric is a crenulation cleavage, axial planar to a local folding event that is well-developed near the Cabot Fault Zone, but also occurs near the base of individual thrust sheets further west. Crenulation and fold hinges (F_{SED-2}) are subhorizontal and commonly trend NNE, but deviations between N and E trends are present (Figure 3.5E). In general, D_{SED-2} is characterized by asymmetric folding of the S_{SED-1} fabric, with short limbs dipping steeply to the west and long limbs dipping shallowly to the east (Figure 3.6B). Small muscovite and biotite porhyroblasts have grown parallel to the axial plane of the S_{SED-2} cleavage. S_{SED-2} was overgrown by staurolite and titanite (Figure 3.7C), which combined with garnet and kyanite represent the peak metamorphic assemblage. The fold asymmetry in combination with the F_{SED-2} fold hinge orientation is consistent with prolonged west-vergent deformation.

In summary, these observations suggest that D_{SED-1} and D_{SED-2} in the CBLB thrust stack form part of a single continuous dynamo-thermal event. The structural observations are consistent with those made in the area north of Grand Lake (Cawood and van Gool, 1998): D_{SED-1} corresponds with Cawood and van Gool's D_1, and D_{SED-2} is equivalent with their D_2-D_3. The subsequent deformation phase in the CBLB (D_4 of Cawood and van Gool, 1998) has not been identified south of Grand Lake.

3.4. Geochronology

3.4.1. U-Pb ID-TIMS geochronology

3.4.1.1. Analytical techniques

Analytical techniques utilized for U-Pb ID-TIMS geochronology in this study are summarized here. Detailed descriptions for these analytical procedures can be found in Appendix A. Single, whole-grain zircon, monazite and titanite U-Pb analyses were performed at the Jack Satterly Laboratory, University of Toronto. Standard mineral separation techniques were followed, including methods described by Krogh (1973, 1982). Data were calculated, regressed and plotted using in-house software (UtilAge by D.W. Davis) with regression based on Davis (1982). Results are presented in Table 3.1 and Figure 3.8 (A to D).

3.4.1.2. Disappointment Hill tonalite (AB-01-040; zircon)

The tonalite bodies that are exposed in the Disappointment Hill Complex appear pristine, are relatively undeformed, contain blue quartz, and locally incorporate mafic to ultramafic xenoliths that include an indigenous fabric (Figure 3.3B; Brem et al., 2003). In order to ascertain the age of the tonalite, two separate samples were taken from undeformed exposures, approximately 50 metres apart. Both samples yielded ample zircon grains, which are of simple morphology, euhedral, elongate, and variable in size; the grains in sample AB-01-040B tend to be larger in size. A few zircon grains optically show a core-overgrowth relationship. In total six analyses were performed; three grains from each sample (Table 3.1). All analyses yielded concordant and similar $^{207}Pb/^{206}Pb$ dates between 601 and 611 Ma (Table 3.1; Figure 3.8A). Two fractions yielded large $^{207}Pb/^{235}U$ errors (Grains A1 and A3). However, the $^{206}Pb/^{238}U$ age and the error-of-discordance for both fractions are consistent with the other analyses (Table 3.1). In fact, the $^{206}Pb/^{238}U$ ages and associated errors of all six analyses are very

consistent with each other. The weighted average $^{206}Pb/^{238}U$ age of 606.1 ± 1.5 Ma is therefore interpreted as the age of emplacement of the tonalite.

Thus, the Late Neoproterozoic emplacement age for the Disappointment Hill tonalite unmistakably demonstrates that it could not have formed part of the Ordovician Notre Dame Arc as tentatively inferred in the field (Section 3.3.1). In fact, the tonalite is coeval with the Neoproterozoic alkali-granite plutons in the CBLB, such as the Hare Hill granite.

3.4.1.3. Unnamed felsic gneiss (AB-01-130; zircon)

The sample is from an exposure in the southern part of the Disappointment Hill complex. A phase of this quartz-feldspar-rich gneiss appears to have intruded an agmatic tonalite related to the Disappointment Hill tonalite (sample AB-01-040). The gneissic sample taken for geochronology stemmed from an isolated outcrop and did not have demonstrated contacts with its neighbouring lithologies. It yielded ample euhedral zircon grains and fragments. These grains are of simple morphology and of normal size (100-200 μm), and numerous grains contain small inclusions.

A total of five analyses were performed, all of which yielded various discordant data (0.1-10.2% discordant; Table 3.1). A best-fit regression line fitting four of the five analyses within error (excluding Grain C10) yields an upper intercept of 1503.6 ± 2.9 Ma and a lower intercept of 604.9 ± 4.8 Ma (75% probability of fit; Figure 3.8B). Four analyses near the upper intercept are 7-10% discordant and have $^{207}Pb/^{206}Pb$ ages ranging between 1427 and 1516 Ma (Table 3.1). The Th/U ratios of these analyses are characteristic of magmatic zircons (Th/U = 0.32-0.41; Heaman et al., 2002). The lower intercept is defined by a single but near-concordant zircon (Grain C7; Table 3.1; Figure 3.8A), which distinguishes itself from the upper intercept analyses by its extremely high Th/U value of 2.65. Such a value is not characteristic for zircon in granitoid magmas or even for metamorphic zircon, which tends to have a Th/U ratio lower than magmatic zircon (Hoskin and Schaltegger, 2003). The grain may reflect hydrothermal alteration or recrystallization of a Mesoproterozoic grain (Hoskin & Schaltegger, 2003),

but more likely, the grain crystallized in a vein or neosome (D.W. Davis, pers. comm., 2007). The latter interpretation would imply that metamorphism and possibly deformation occurred in the CBLB at ca. 606 Ma. Even though its origin is unknown, the age of Grain C7 is clearly important within the sample. A regression line using only 3 of 5 analyses (Grains C8, C9, and C11) yields a discordia line with intercepts at ca. 1508 and ca. 627 Ma (no probability of fit), corroborating the best-fit regression line.

The upper intercept of this best-fit line of 1503.6 ± 2.9 Ma may be interpreted as the protolith age of the felsic gneiss. This is compatible with other Pinwarian (ca. 1.5 Ga) ages for the CBLB. The lower intercept of 604.9 ± 4.8 Ma in interpreted as an important thermal event, which may represent the age of regional deformation. This event is coeval with the emplacement of the Neoproterozoic granitoid plutons in the CBLB basement. A mixing line can be constructed using 10 of 11 analyses from samples AB-01-040 and AB-01-130 (excluding Grain C10), yielding an upper intercept of 1503.6 ± 2.7 Ma, and a lower intercept of 604.9 ± 2.3 Ma (96% probability of fit).

3.4.1.4. Post-tectonic pegmatite dyke (AB-03-405; monazite)

A pink pegmatite dyke truncating the main S_{SED-1} fabric of South Brook metapsammitic rocks is exposed approximately 2 km west of the Cabot Fault Zone (Figure 3.6C). This dyke is three metres wide, strikes northwest, dips sub-vertically, and consists of K-feldspar, quartz, muscovite and chlorite. Near the margins, the dyke is rich in quartz. The contacts of the dyke show subhorizontal brittle striations, but internally the dyke is undeformed. A sample for U-Pb dating was taken from the centre of the dyke. Only a few fragments of zircon were recovered, none of which are of good quality. In contrast, the sample yielded ample monazite. The monazite grains are subhedral, of various sizes, and clear to slightly tinted. Most grains have an orange-brown (iron oxide) coating on their surface. Six monazite grains of various shape and size were handpicked for single grain analysis.

All analyses plot near concordia, but most are reversely discordant (-3.2 to 0.9% discordant; Table 3.1; Figure 3.8C). More importantly, the $^{207}Pb/^{235}U$ ages show a 60 million year spread between 478 and 426.5 Ma. The $^{206}Pb/^{238}U$ ages are not being considered here, because these ages could be biased due to excess thorogenic ^{206}Pb stemming from the decay of ^{230}Th (Schärer, 1984). There is no correlation between the $^{207}Pb/^{235}U$ age, the Th/U ratio, the U-concentration, or grain size. Also, abrasion (Grain D12) and treatment of selected grains with HNO_3 in an attempt to remove the iron coating from the surface (Grains D15 and D17), does not appear to have affected the results.

BSEM (Back-Scattered Electron Microscope) images of randomly selected monazite grains show that numerous grains are internally zoned. These heterogeneous grains sometimes show euhedral cores with brighter overgrowths (Figure 3.9A), separated by irregular boundaries that may be indicative of resorption (Figure 3.9B). Most grains contain inclusions, such as quartz, feldspar, zircon, xenotime, and uraninite (Figure 3.9C). The presence of these radiogenic U-bearing inclusions may have contributed to the spread in ages. Some grains show inclusion-rich and inclusion-free zones (Figure 3.9C).

Given the heterogeneity of the grains, the $^{207}Pb/^{235}U$ ages are most likely mixed ages between the actual emplacement age and older xenocrystic ages. The smallest analyzed grain (Grain D12), which yielded the youngest $^{207}Pb/^{235}U$ age of 426.5 ± 1.0 Ma, has a very high U-concentration of 18465 ppm, and is most likely to have crystallized from the pegmatite melt. Additionally, the largest analyzed grain (Grain D13) has a $^{207}Pb/^{235}U$ age of 428.1 ± 1.3 Ma, which is within error of Grain D12. Based on the average of these two analyses, the crystallization age of this pegmatite is interpreted to be 427.5 ± 2 Ma.

3.4.1.5. Hare Hill alkali granite (86-Z-1; titanite)

The Neoproterozoic Hare Hill granite (location 2 in Figure 3.2) was reported to have two multigrain(?) analyses of titanite with imprecise U-Pb TIMS ages between 500 and 440 Ma (Currie et

al., 1992). In an attempt to reproduce these ages, three titanite fractions (two single-grain and one multigrain) from the original Hare Hill mineral separates were analyzed (sample 86-Z-1 of Currie et al., 1992). The mineral separate contains ample pale-brown titanite grains of various size and shape. Optically, these grains appear to form a single homogeneous population although the grains show variations in concentrations of Y and Nb by BSEM.

The ID-TIMS age precision is limited by low concentrations of U (<10 ppm) and high concentrations of common Pb, something that has also been observed in the zircon fractions from this sample (see Table 1 in Currie et al., 1992). However, the average $^{206}Pb/^{238}U$ age of 621 ± 22 Ma (Figure 3.8D; assuming a Stacey and Kramers' [1975] value for initial common Pb) is consistent with the Neoproterozoic zircon age from this sample and distinctly older than Ordovician. The relatively unfractionated Th/U values calculated for these titanite grains are consistent with a magmatic, rather than a metamorphic origin (Abraham et al., 1994).

3.4.2. $^{40}Ar/^{39}Ar$ geochronology

3.4.2.1. Analytical techniques

Analytical techniques utilized for $^{40}Ar/^{39}Ar$ geochronology in this study are summarized here. Detailed descriptions for these analytical procedures can be found in Appendix C. Laser $^{40}Ar/^{39}Ar$ step-heating analyses were performed at the Geological Survey of Canada, Ottawa. Data collection protocols of Villeneuve and MacIntyre (1997) and Villeneuve and others (2000) were followed. Error analysis procedures are outlined in Roddick (1988) and Scaillet (2000). Results are presented in Table 3.2 and Figure 3.10 (A to D). All age errors are given at the 95% confidence interval.

3.4.2.2. Hornblende - biotite ± garnet quartzo-feldspathic gneiss (AB-01-131; hornblende)

This sample comes from a basement gneiss in the southwestern part of the Disappointment Hill complex (location 7 in Figure 3.2). The typical S_{BSZ} fabric in the sample, striking NNW and dipping steeply towards the east, is defined by locally chloritized green-brown biotite and subhedral poikilitic hornblende grains. Some hornblende grains have overgrown the gneissic S_{BSZ} fabric at high angle, suggesting a late syn- to postdeformational growth. The matrix is mainly composed of inequigranular and polygonal, recrystallized feldspar and quartz, in addition to occasional plagioclase porphyroclasts. There is also a sparse amount of anhedral garnet present in the matrix.

The first few low temperature steps in an aliquot of hornblende analyzed from this sample revealed the presence of excess Ar and are marked by higher Ca/K ratios. The subsequent, higher temperature steps yield a well-defined plateau, comprising 70.3% of the total gas and defining an age of 430 ± 4 Ma (Table 3.2; Figure 3.10A). Interestingly, one of the initial excess Ar steps in this sample shows an apparent age (single step comprising ca. 30% of the total gas) at ca. 620 Ma, which is similar to the emplacement ages of several igneous bodies in the area, such as the Hare Hill granite (ca. 608 Ma; Currie and van Berkel, 1992) and the Disappointment Hill tonalite (ca. 606 Ma; see above).

3.4.2.3. Sheared muscovite conglomerate (AB-02-158; muscovite)

This is a sheared muscovite conglomerate along the south shore of Grand Lake at the base of the sedimentary thrust sheets (location 6 in Figure 3.2). The conglomerate layer is a few metres thick, showing a fining-upward character, and the strained clasts are of pebble size (cm-scale). The conglomerate is sheared over basement rocks (quartzo-feldpathic gneiss) at Grand Lake, but is interpreted as being para-autochtonous with respect to its basement (cf. Piasecki, 1991).

Muscovite and (chloritized) biotite define an anastomosing S_{SED-1} foliation, which surrounds the strained conglomerate pebbles. Some muscovite grains are bent and deformed, suggesting growth before or during D_{SED-1} deformation, but generally the grains are undeformed and show parallel extinction. A few grains have overprinted the foliation at high angle, and thus post-date the D_{SED-1}.

Quartz grains are dynamically recrystallized, K-feldspar grains show perthitic exsolution, and plagioclase crystals contain deformation twins.

Two aliquots of muscovite analyzed from this sample yielded a well-defined plateau region, with the exception of a few of the high temperature steps in each of the aliquots, which are marked by higher Ca/K ratios and may indicate degassing of a contaminating phase. The plateau region defined by the two aliquots comprises 91.9% of the gas and defines an age of 424 ± 4 Ma (Table 3.2; Figure 3.10B).

3.4.2.4. Caribou Brook shear zone (AB-02-321; hornblende)

This sample comes from a shear zone that is interpreted as being a splay of the Caribou Brook shear zone, the tectonic zone that separates the Steel Mountain anorthosite from the Disappointment Hill crystalline units (location 8 in Figure 3.2; Figure 3.4A). Hornblende and biotite minerals define the C-surfaces in the sample, although a few hornblende crystals overprint the foliation. Associated shear-sense indicators, including asymmetric folding of the shear fabric, suggest reverse, east-side-up deformation.

Two aliquots of hornblende were analyzed from this sample. The two aliquots yielded a plateau region, comprising 97.7% of the gas, which defines an age of 426 ± 5 Ma (Table 3.2; Figure 3.10C). The second aliquot contains a small amount of excess argon in the first low temperature step. There is some scatter in the final high temperature steps in both aliquots, also marked by higher Ca/K ratios, which may indicate the presence of a contaminating degassing phase. The resulting Silurian plateau age of 426 ± 5 Ma is interpreted as representing the age of deformation.

3.4.2.5. Biotite-muscovite-garnet schist (AB-02-376; biotite)

In the centre of the Disappointment Hill complex, a biotite-muscovite-garnet-bearing shear zone is exposed (location 9 in Figure 3.2). This NNE-striking and steeply dipping shear zone with downdip mica mineral lineation shows a regionally consistent east-side-up reverse movement (Figure 3.4C). The foliation is defined by biotite and muscovite, and minor (retrogressive) chlorite that are interpreted as being synkinematic. Euhedral garnet grains that are present in a statically recrystallized matrix of quartz and feldspars pre-date the mica foliation (Figure 3.4D). Additionally, a few plagioclase porphyroclasts are present.

An aliquot of biotite analyzed from this sample yielded a well-defined plateau, comprising 90.3% of the total gas, that defines an age of 422 ± 4 Ma (Table 3.2; Figure 3.10D). Given the degree of deformation, which most likely took place under upper greenschist facies conditions, the biotite age is interpreted as a cooling age of the rock below the biotite closure temperature for argon (ca. 300°C; McDougall and Harrison, 1999). However, since the biotite grains postdate the peak metamorphic conditions indicated by the garnet, this earliest Late Silurian age might represent the age of the fabric and therefore the age of east-side-up deformation in the CBLB basement.

3.5. Discussion of Geochronological and Petrographic Results

The geochronological results show that Early Silurian Salinic orogenesis has affected crystalline basement and its cover rocks in the southwestern part of the CBLB. These observations confirm those of Cawood et al. (1994), who first demonstrated the importance of the Salinic orogeny in this area. An important part of the dominant west-vergent deformation (S_{SED-1}) in the CBLB can be constrained between ca. 434 Ma (age of a deformed pegmatite dyke, interpreted as syn-tectonic; Cawood et al., 1994) and ca. 427 Ma (age of the post-tectonic pegmatite dyke; sample AB-03-405). Subsequent latest Early Silurian rapid uplift of the CBLB (Cawood and van Gool, 1998) may have been accommodated by S_{BSZ} reverse basement shear zones, such as those in the southwestern part of the CBLB, as

evidenced by ages from samples AB-02-321 (hornblende) and potentially AB-02-376 (biotite; ca. 426 and 422 Ma $^{40}Ar/^{39}Ar$ cooling ages, respectively).

3.5.1. Absence of Ordovician Dynamo-Thermal Event

The combined geochronological data (Cawood et al., 1994; introduced herein) show no evidence for an Ordovician dynamo-thermal event to have affected the rocks of the CBLB and as such do not support the interpretation that the CBLB was involved in an important Ordovician collisional event. The post-tectonic pegmatite dyke (AB-03-405) does show two 'Ordovician-aged' monazite grains (Grains A5 and A6; Table 3.1). However, most monazite grains in this sample are heterogeneous and these results most likely represent mixed ages from a xenocrystic component of unknown age and provenance.

In addition to the Hare Hill sample discussed above (sample 86-Z-1; Currie et al., 1992), only two publications have reported Ordovician radiometric ages for rocks of the CBLB. First, Wanless et al. (1965) reported a biotite (K-Ar) cooling age of 452 ± 20 Ma for a granitic schist near the western end of Grand Lake (location 10 in Figure 3.2), but this age has been recalculated based on new decay constants to be Early Silurian (428 ± 20 Ma; Cawood, 1993). Second, Williams et al. (1985) reported a possible Middle Ordovician Rb-Sr whole rock age for the Round Pond granite (Figure 3.2A), which yielded a U-Pb on zircon crystallization age of 602 ± 10 Ma. The authors assumed an initial $^{87}Sr/^{86}Sr$ ratio of 0.71 (470 Ma) and 0.72 (455 Ma), and interpreted this Rb-Sr age to represent isotopic or partial isotopic resetting during the Ordovician Taconic deformation. Quantitatively and qualitatively, such a single age is meaningless, especially given that the Rb-Sr whole-rock method has been shown to behave as an open-system in many cases (Dickin, 2005).

Besides geochronological constraints, there are also petrographic constraints that do not support the presence of a noticeable Taconic dynamo-thermal event in the CBLB. In medium- to high-grade terranes poikiloblastic garnet grains commonly preserve evidence for poly-phase dynamo-thermal

events (e.g. Jamieson, 1990; Passchier and Trouw, 1996). However, only a single, peak metamorphic assemblage is present in the metasedimentary rocks of the CBLB. In-situ SHRIMP dating of monazite-in-garnet from a Grt-Ky-St schist near the eastern end of the CBLB yielded consistent Early Silurian ages (ca. 430 Ma; V.J. McNicoll, S. Pehrsson and A.G. Brem, unpublished data), indicating that peak metamorphic conditions were reached in the late Early Silurian, not in the Ordovician, thereby supporting U-Pb TIMS monazite data by Cawood et al. (1994). Thus, based on the available geochronological data and petrographic observations, there is no direct evidence that an important Taconic dynamo-thermal event affected the rocks in the CBLB.

3.5.2. Regional Evaluation of the Taconic Event in the Laurentian Realm

The lack of evidence for a penetrative Taconic dynamo-thermal event in the CBLB contrasts sharply with the tectonic history of the adjacent rocks of the Humber Zone to the west and Dashwoods subzone to the east. In the autochthonous external Humber Zone, the Taconic orogeny is evidenced by the transition from carbonate platform to deep foreland basin flysch as represented by the sediments of the Llanvirnian Table Head Group. These rocks demonstrate a complicated record of uplift, faulting, and carbonate platform collapse (Knight et al., 1995, and references therein). Second, the Humber Arm Allochthon (Figure 3.1) contains stratigraphic evidence (cf. Waldron and van Staal, 2001) showing that tectonic loading started in the Middle Arenigian (ca. 475 Ma) and the 469 ± 5 Ma cooling age for the metamorphic sole of the Bay of Islands ophiolite (Dallmeyer and Williams, 1975; recalculated to new decay constant, see Cawood and Suhr, 1992) suggests that ophiolite emplacement and associated west-directed deformation is also Middle Ordovician (Waldron and van Staal, 2001; and references therein). Moreover, the minimum age of west-vergent deformation and subsequent east-vergent folding and thrusting in the Humber Arm Allochthon is earliest Late Ordovician (ca. 455 Ma; Bradley, 2005), pre-dating S_{SED-1} in the CBLB by ca. 30 million years. Third, the Fleur de Lys block in northern Newfoundland (Figure 3.1) contains a pre-Salinic eclogite facies mineral assemblage, which has been

attributed to the underthrusting and burial of the continental margin (Jamieson, 1990; Cawood and Dunning, 1993; Waldron et al., 1998a). Lastly, numerous radiometric dates (U-Pb and $^{40}Ar/^{39}Ar$) have demonstrated that the Dashwoods subzone was affected by coeval Middle Ordovician magmatism (Notre Dame Arc), regional deformation, and associated metamorphism up to granulite facies (van Staal et al., 2007; and references therein). This penetrative dynamo-thermal event has been attributed to arc-continent collision (van Staal et al., 2007; and references therein). In-situ monazite-in-garnet SHRIMP dating from a garnet-muscovite schist near the Cabot Fault Zone in the Dashwoods subzone yielded consistent late Middle Ordovician ages (ca. 461 Ma; V.J. McNicoll, S. Pehrsson and A.G. Brem, unpublished data), demonstrating that peak metamorphic conditions in the Dashwoods subzone were reached 30 million years before peak-metamorphism of the CBLB.

3.5.3. Regional Evaluation of the Salinic Event in the Laurentian Realm

The presence of an important Salinic dynamo-thermal event in the CBLB also contrasts with the tectonic history of the adjacent rocks. In the Humber Arm Allochthon to the west, Early Silurian fabrics are characterized by ca. 440 Ma ductile and brittle normal-sense (west-side-down) faults (D_3 of Bradley, 2005). Similar but geochronologically unconstrained fabrics have been observed in the Old Man's Pond Allochthon (Figure 3.1), where D_3 fabrics are interpreted as having juxtaposed allochthonous sedimentary rocks with the CBLB along the Humber River Fault (Waldron and Milne, 1991). Further to the west, the Early Palaeozoic foreland basin beneath the Gulf of St. Lawrence is characterized by an Early Silurian unconformity (Waldron et al., 1998a).

Similar to the CBLB, the Blair River Complex in Cape Breton Island (Miller et al., 1996) and the Fleur de Lys block in northern Newfoundland (Cawood and Dunning, 1997; Waldron et al., 1998b) have been affected by Salinic deformation and lower amphibolite facies metamorphism. Both tectonic segments have also been affected by Early Silurian magmatism, especially the Fleur de Lys block, where voluminous Early Silurian plutons have recorded the transition from volcanic arc granites (3rd

phase of Notre Dame Arc; e.g. ca. 440 Ma Burlington granodiorite) to post-collisional plutons (e.g. ca. 430 Ma Dunamagon granite; Whalen et al., 2006). The Salinic event in the Dashwoods subzone is also characterized by upper-crustal level magmatism (3rd phase Notre Dame Arc; Whalen et al., 2006), and although regional deformation in the Dashwoods was Taconic, localized deformation did occur during the Salinic (Cormacks Lake complex; Pehrsson et al., 2003). Both Dashwoods and the CBLB are characterized by rapid post-orogenic Early Silurian uplift (Whalen et al., 2006; Cawood et al., 1996 respectively), but only the CBLB has been affected by regional west-vergent deformation. Given the contrasts in Early Silurian tectonic history, especially between Dashwoods and the CBLB, it is highly unlikely that these two segments were juxtaposed before the end of the Salinic orogeny (ca. 425 Ma).

3.6. Implications for Regional Tectonics

The CBLB in the internal Humber Zone is generally being accepted as representing the para-autochthonous leading edge of the Laurentian craton (e.g. Williams, 1995; Waldron et al., 1998a; Waldron and van Staal., 2001). However, a new interpretation introduced in the next chapter proposes that the CBLB represents an exotic, displaced terrane along the Laurentian margin, allochthonous to its present position. This interpretation is based on the noticeable absence of Grenvillian *sensu lato* (1.0-1.3 Ga) U-Pb zircon ages from the CBLB basement, as well as its distinct Ordovician and Silurian history, as discussed in this chapter. Here, both geodynamic settings will be discussed in light of the available data.

3.6.1. The CBLB as Para-Autochthonous Basement and Part of the Leading Edge of the Laurentian Craton

3.6.1.1. Tectonic Setting during the Taconic

To explain the noticeable absence of the Taconic from the CBLB, it must have occupied an upper crustal setting during the Ordovician (cf. Cawood et al., 1996). In such a setting, the crystalline basement and its Palaeozoic cover rocks would have been buried to – at most – low metamorphic grade. Any brittle or low-grade metamorphic fabric imprinted on these rocks could have been obliterated relatively easily during the strong Salinic orogenic imprint. Pre-D_1 brittle-ductile Taconic thrust faults that could potentially be related to such a setting have been reported from the western part of the CBLB (Page 42 in Cawood and van Gool, 1998).

Several scenarios could explain such an upper crustal setting: (1) The subduction/collision zone was at a considerable distance to the east (in present-day reference frame) from the present position of the CBLB during the Ordovician (Figure 3.12A). In this convergent scenario in which little strike-slip is incorporated, the Humber Zone in central Newfoundland would only have experienced thin-skinned upper-crustal deformation, whereas the Dashwoods subzone would represent part of the collision zone. The intervening part of the Humber Zone that was involved in Taconic orogenesis was either excised or buried beneath Dashwoods. This setting would apply if – for example – the CBLB were situated in a deep re-entrant with the collision concentrated in nearby promontories (van Staal et al., 2007). The Long Range Inlier may have formed the promontory along the Laurentian margin with which Dashwoods collided during the Early and Middle Ordovician (Chapter 2). The allochthonous Long Range Inlier is interpreted to have had a clockwise rotation of 10°-20° relative to its Neoproterozoic position (Murthy et al., 1992; Waldron and Stockmal, 1994). Also, its abrupt southern termination has been attributed to a pre-existing transverse fault in the continental margin (Cawood and Botsford 1991; Waldron and Stockmal, 1994). This scenario is also consistent with the interpretation that the Bay of Islands ophiolite formed in a 2nd or 3rd order re-entrant (Cawood and Suhr, 1992), which would have

been the area immediately to the south of the Long Range Inlier. (2) The Dashwoods microcontinent and its associated Notre Dame Arc may not have been opposite to the CBLB during the Ordovician. For example, the Dashwoods may not have formed a continuous ribbon-continent along the length of the Northern Appalachians. Such discontinuity of tectonic elements is very common for a southwest Pacific Ocean style geodynamic setting (Figure 3.11; Hall and Blundell, 1996; van Staal et al., 1998). If this discontinuity is true, then post-Taconic orogen-parallel movements of several hundred kilometres are needed to explain the present-day geological setting. (3) A combination of the Taconic scenarios suggested above.

3.6.1.2. Tectonic Setting during the Salinic

Early Silurian Salinic deformation in Dashwoods is not as strong as in the CBLB, but local deformation has occurred. In contrast, Salinic deformation structures in the CBLB include west-vergent thrusting of the sedimentary rocks and basement slivers, and reverse faulting in the basement rocks. Folding and thrusting are characteristic of accretion-related Salinic structures in central Newfoundland (van Staal, 2007; and references therein). Geodynamically, the Salinic orogeny involved the collision between the peri-Gondwanan microcontinent of Ganderia and the composite Laurentian margin, as represented by the Annieopsquatch Accretionary Tract (Lissenberg et al., 2005). In this scenario, a promontory of Ganderia may have collided with the Laurentian margin in closer proximity to the CBLB than Dashwoods (Figure 3.12B), which can explain the differences in Salinic deformation style between them. This implies that: (1) the CBLB and Dashwoods could not have been juxtaposed until – at least – after the late Early Silurian (ca. 425 Ma), and (2) several hundreds of kilometres of post-Salinic transcurrent movement along the Cabot Fault Zone should have occurred, a possibility already raised above based on the tectonic setting during the Taconic.

3.6.2. The CBLB as a Suspect Terrane

The provenance of the CBLB exotic fragment is not well constrained (Section 4.5). Given the currently available data, the best interpretation is that during the Late Neoproterozoic, the CBLB was situated along the Laurentian margin, in close proximity to the Pinware terrane and north of the Grenville magmatic front (Figure 3.13; Section 4.5). If this is true then at least 500 km of dextral orogen-parallel movement during the Early Palaeozoic Appalachian orogeny is needed to explain its present-day position in the Newfoundland Appalachians. Initiation of southward movement of the CBLB could have started during Early Ordovician (ca. 488 Ma) convergence in the Humber seaway (Waldron and van Staal, 2001). By the start of the Middle Ordovician arc-continent collision between the Dashwoods-Notre Dame Arc and the Laurentian margin in Newfoundland (ca. 470 Ma; van Staal et al., 2007), the CBLB should have been located to the south of this collision zone, in order to have avoided a pervasive Taconic imprint. Also, if during arc-continent collision the CBLB was positioned north of Dashwoods, it should have bypassed Dashwoods along its eastern margin between the Middle Ordovician and Early Silurian, but during this timeframe, the geodynamic setting along the eastern margin was characterized by overall sinistral convergence (Zagorevski et al., 2006; Lissenberg and van Staal., 2006; van Staal, 2007); hence, this scenario is unlikely to have occurred. Subsequent docking of the CBLB to the composite Laurentian margin took place during the Early Silurian Salinic orogeny, as evidenced by the west-vergent structures and metamorphism in the CBLB. As proposed above, a promontory of the Gander margin may have collided with the Laurentian margin in closer proximity to the CBLB than to Dashwoods. Regardless of the provenance of the CBLB, large-scale orogen-parallel transcurrent movements should have occurred to explain the present-day position of the CBLB within the Laurentian realm.

3.6.3. Implications for Current Tectonic Models

In most tectonic models that have been proposed for the Early Palaeozoic development of the Laurentian margin of the Newfoundland Appalachians, the emphasis is predominantly on divergent and convergent processes, so-called 'accordion tectonics' (Bailey et al., 2004), hence most tectonic models are mainly shown as geologic cross sections (e.g. Dewey et al., 1969; Hibbard, 1983; Stockmal et al., 1987; Stockmal et al., 1998; Waldron and van Staal, 2001). These models clearly explain the intra-terrane deformational, metamorphic and magmatic history, but they cannot explain all facets of the tectonic histories between individual terranes where convergence has had a significant oblique component.

Large-scale strike-slip movements along tectonic zones and especially along terrane boundaries have been predicted in the Appalachians, based on a comparison with the southwest Pacific Ocean geodynamic setting (Figure 3.11; van Staal et al., 1998). The concept of strike-slip tectonics and associated suspect terranes has been used to explain marked inter-terrane disparities in the North American Cordillera (e.g. Haggart et al., 2006) and also in other parts of the Appalachian-Caledonian mountain chain, for example the Goochland and surrounding terranes in the U.S. Appalachians (Bartholomew and Tollo, 2004), Laurentian terranes in the British and Irish Caledonides (e.g. Hutton, 1987) and Ganderian fragments in the Canadian Appalachians (e.g. Lin et al., 2007). However, strike-slip tectonics has only been considered in a few reconstructions of the Newfoundland Appalachians (e.g. Currie and Piasecki, 1989; Stockmal et al., 1990; Cawood et al., 1995; Waldron et al., 1998a), which are generally shown either in map view or in 3D block diagrams.

A key restriction on using transcurrent movements in tectonic models is that their magnitudes have not been and cannot easily be quantitatively constrained. For terrane bounding fault zones, such as the Baie Verte Line-Cabot Fault Zone, that are long-lived, kinematically complex, and do not appear to have been stitched by igneous rocks, quantifying movement over any time interval is very difficult. Thus in most models, transcurrent movements have been shown to exist along the major terrane

boundaries, but their extent has been left unattended (e.g. Currie and Piasecki, 1989; Cawood et al., 1995; van Staal et al., 1998). It is also generally assumed that terranes and tectono-stratigraphic zones are continuous along strike within the Canadian Appalachians (e.g. Cawood et al., 1995), but such along-strike continuity may be deceptive and erroneous (Figure 3.11; van Staal et al., 1998). Where actual 'plausible' displacements for Early Palaeozoic transcurrent movements have been incorporated into the models, these are usually in the order of 100 km (Waldron et al., 1998a). With such an amount of displacement along the Cabot Fault Zone, the CBLB and the Dashwoods block are still in close proximity to each other and overlap of tectono-magmatic events would be expected.

A last important point is that only a few of the Early Palaeozoic tectonic models have incorporated the post-Acadian dextral movement on the Cabot Fault Zone associated with the opening of Carboniferous basins such as the Deer Lake basin and the Bay St. George subbasin (Figure 3.1). These movements have been well documented (e.g. Knight, 1983; Hyde et al., 1988; Langdon and Hall, 1994) and may be up to ca. 200 km (Bradley, 1982; Knight, 1983; Stockmal et al., 1990). After removing 140 km of dextral Carboniferous movement on the Cabot Fault Zone (cf. Stockmal et al., 1990), a restoration that represents the pre-Alleghanian Late Devonian geological setting, Dashwoods and its Notre Dame Arc are still juxtaposed with the CBLB (Figure 3.14). An additional 150 km of dextral movement would have to be removed in order to have a clear separation between the CBLB and the Dashwoods subzone. This 150 km cannot be explained by Alleghanian movement alone.

Thus the possibility of significant (hundreds of kilometres) pre-Alleghanian orogen-parallel movement, in addition to the well-documented Early Palaeozoic convergent motions, implies that presently neighbouring terranes could have been far apart during subduction and collision (van Staal et al., 1998). In western Newfoundland, such movement is likely evidenced by dextral mylonite fabrics in the Cabot Fault Zone (Brem et al., 2004; Chapter 5). Considering such a possibility may have significant implications for tectonic interpretation of the Early Palaeozoic evolution of the Newfoundland Appalachians.

3.7. Conclusions

The conclusions can be summarized as follows:

1. New U-Pb geochronological data show that the CBLB basement consists of Pinwarian (ca. 1500 Ma) orthogneisses and Late Neoproterozoic (ca. 605 Ma) intrusions.
2. The CBLB in the study area is affected by a single dynamo-thermal event that is characterized by west-vergent deformation and a coeval greenschist to lower amphibolite facies peak metamorphism. This orogenic event is constrained between ca. 434 Ma and 427 Ma.
3. Four new $^{40}Ar/^{39}Ar$ cooling ages between 422 and 430 Ma from various units in the CBLB corroborate the Salinic peak metamorphic and post-metamorphic cooling ages obtained by Cawood et al. (1994). Two cooling ages of ca. 426-422 Ma from shear zones in the crystalline basement of the CBLB (S_{BSZ}) may actually represent the age of east-side-up deformation that accompanied the rapid cooling of the CBLB.
4. There is neither geochronological nor petrographic evidence for a pre-Silurian Palaeozoic dynamo-thermal orogenic event in the CBLB. Either the Taconic deformation in the CBLB was dominantly brittle and masked by the dominant Salinic orogeny, or during the Ordovician the CBLB may have been situated in a (distant) part of Laurentia where the effects of Taconic convergence were weak or absent.
5. The contrasting tectonic histories of the CBLB and the Dashwoods block indicate that these units were not juxtaposed until the Late Silurian at the earliest. Post-Early Silurian transcurrent movement along the Cabot Fault Zone of – at least – several hundreds of kilometres is probably required to explain the disparities between these two units and their subsequent juxtaposition.
6. The interpretation that the CBLB represents a displaced exotic fragment in the Newfoundland Appalachians (Chapter 4) can explain the apparent absence of a Taconic event and the presence of the distinct Salinic event in the CBLB, and necessitates large-scale orogen-parallel movement. This accords with conclusions drawn from forward modeling of the southwest Pacific Ocean

geodynamic setting as an analogue for the Appalachian-Caledonian mountain belt (Figure 3.11; van Staal et al., 1998), and also agrees with strike-slip tectonic models proposed for the southern Appalachians (Bartholomew and Tollo, 2004) and the European Caledonides (e.g. Hutton, 1987).

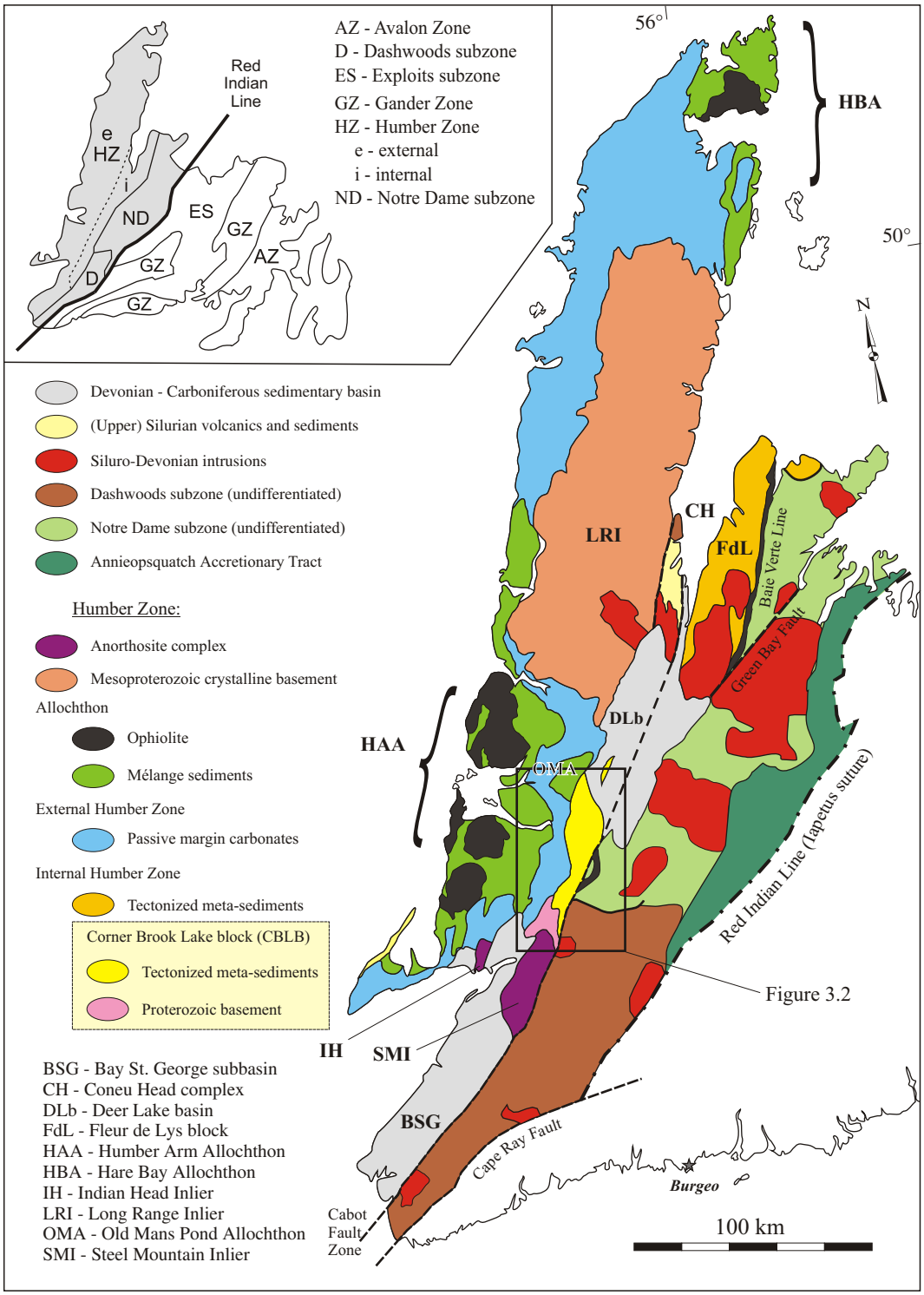

Figure 3.1 Simplified geological map of western Newfoundland, showing the main tectonic elements of the Laurentian realm in the Newfoundland Appalachians. Modified after Waldron et al. (1998). Inset shows the tectono-stratigraphic division of the Newfoundland Appalachians. Modified after Williams et al. (1988).

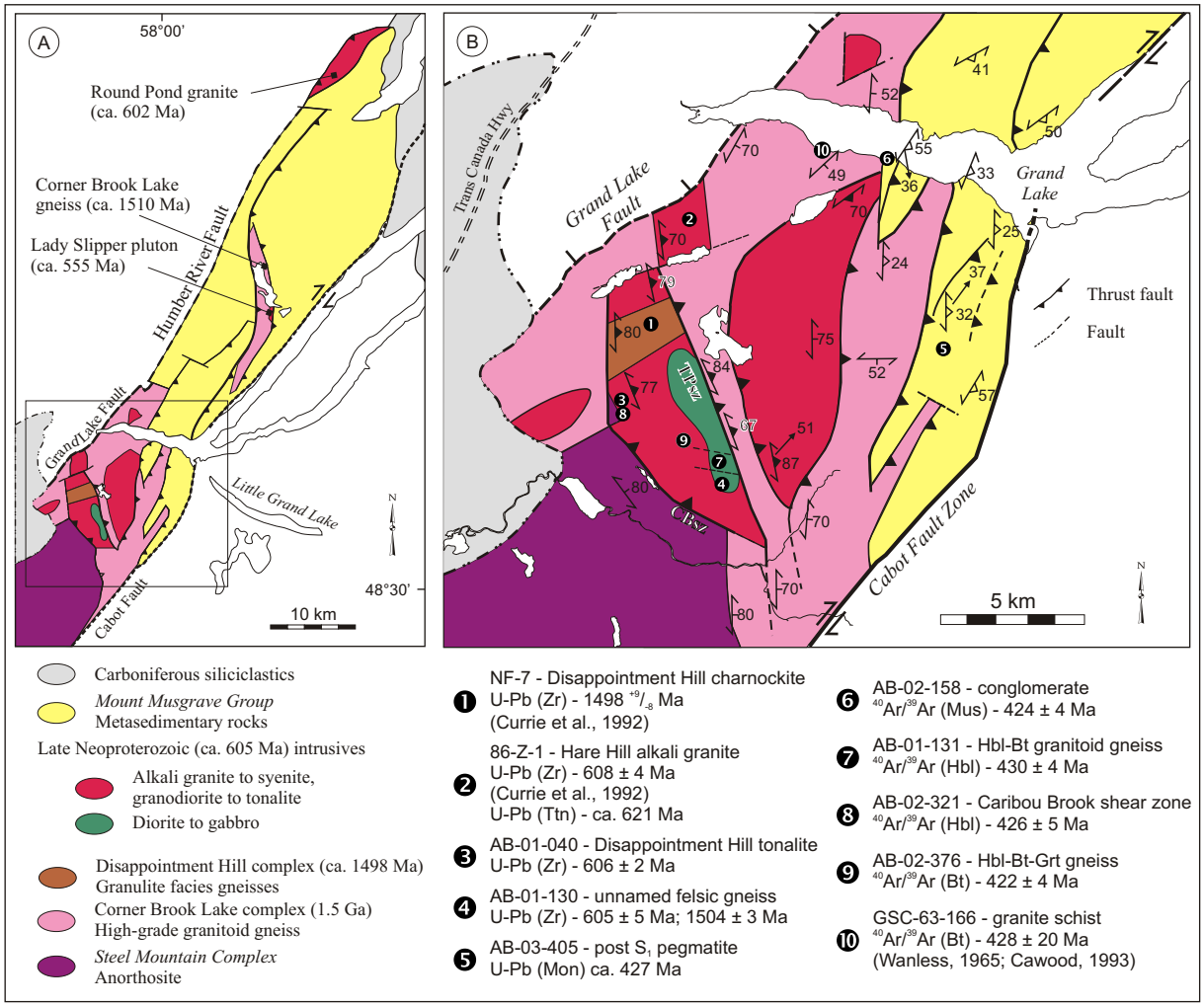

Figure 3.2 (**A**) Geological map of the Corner Brook Lake block (CBLB). (**B**) Simplified geological map of the southern part of the CBLB. Numbers indicate the locations of the geochronological samples introduced and discussed in this chapter. Mineral abbreviations: Abbreviations: CBsz - Caribou Brook shear zone; TPsz - Tulks Pond shear zone; Bt - biotite; Hbl - hornblende; Mon - monazite; Mus - muscovite; Ttn - titanite; and Zr - Zircon.

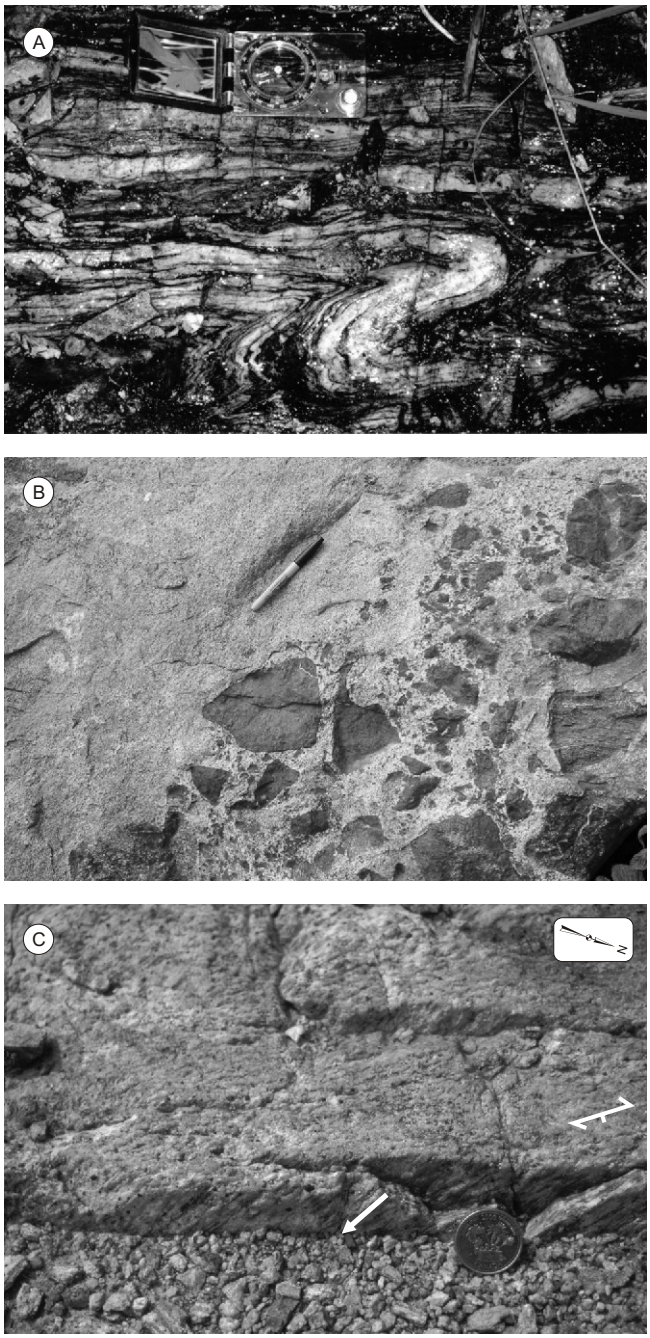

Figure 3.3 Field photographs of lithologies typical for the Corner Brook Lake block basement. (**A**) Folded orthogneiss of the Corner Brook Lake complex (AB-01-005). (**B**) Agmatic tonalite related to the Disappointment Hill complex (AB-01-040). This lithology bears close resemblance to agmatites of the Early Palaeozoic Notre Dame Arc of the Dashwoods subzone. (**C**) Late Neoproterozoic alkali granite of the Hare Hill igneous suite. The strained fabric in this sample demonstrates that the CBLB crystalline basement was affected by an important Palaeozoic deformational event (AB-01-012).

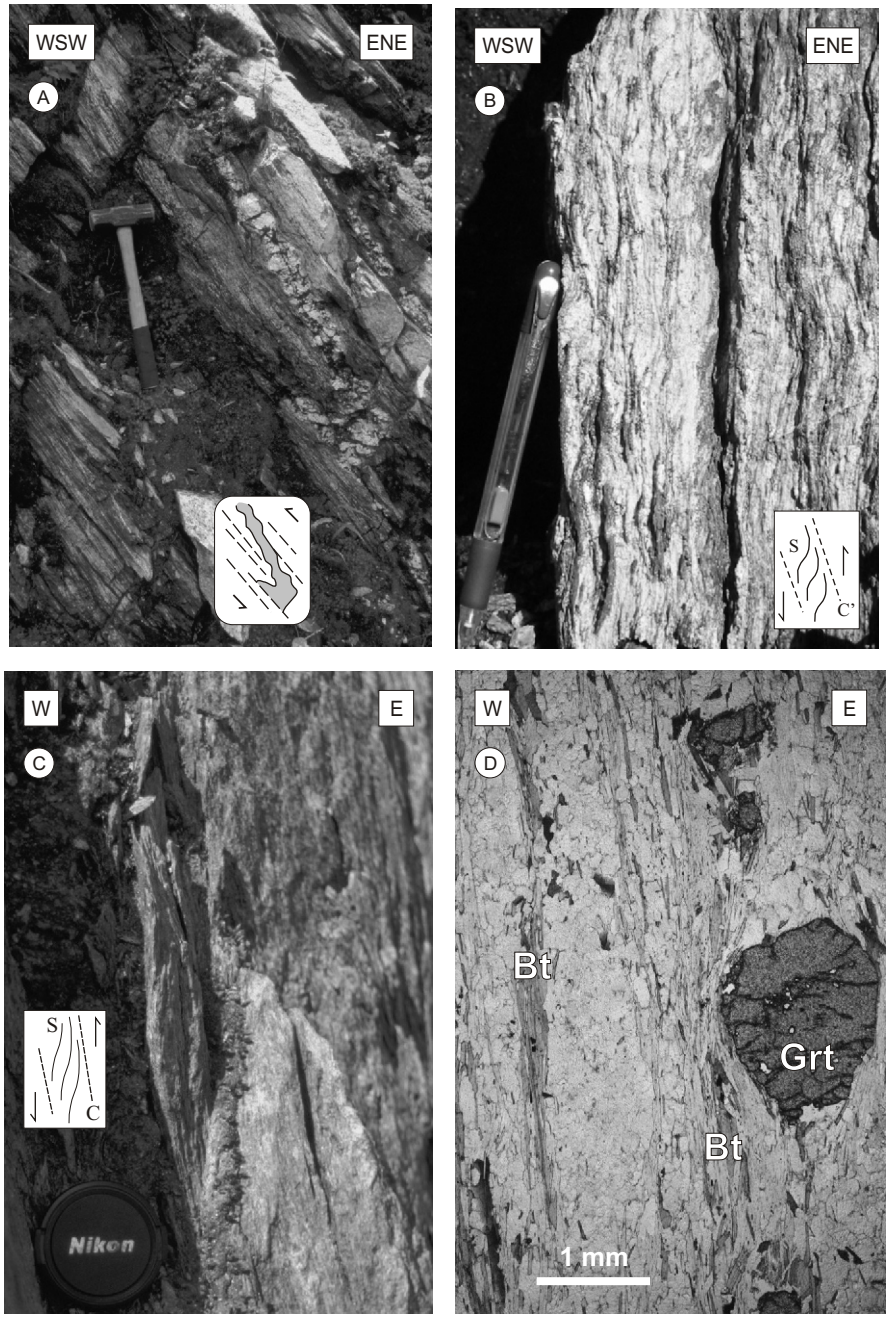

Figure 3.4 Field photographs and photomicrograph of shear zones (S_{BSZ}) in the Corner Brook Lake block basement. (**A**) Caribou Brook shear zone. A boudinaged vein is at clockwise orientation from main shearing foliation, suggesting reverse east-side-up deformation. Note: the photograph is flipped from its outcrop exposure for better comparison (AB-01-037). (**B**) Tulks Pond shear zone. S-C′ shear bands suggesting an east-side-up movement on a steeply dipping shear zone (AB-01-144). (**C**) Small shear zone with the crystalline basement. Possibly related to uplift of region (AB-02-376). (**D**) Photomicrograph of (C) showing Bt crystals defining a foliation that wraps around (postdates) Grt porphyroblasts (AB-02-376).

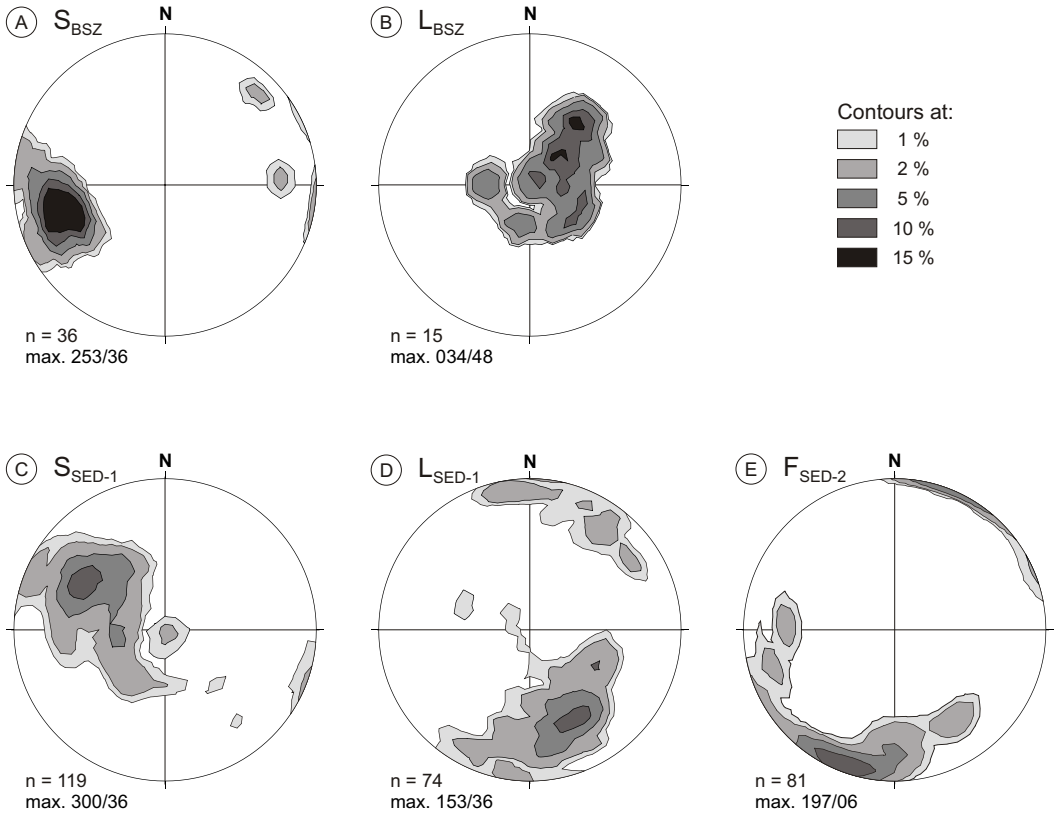

Figure 3.5 Equal-area lower-hemisphere projections of: (**A**) poles to foliation of the shear fabric (S_{BSZ}) in continuous shear zones in the CBLB crystalline basement; (**B**) mineral and stretching lineations (L_{BSZ}) in continuous shear zones in the CBLB crystalline basement; (**C**) poles to foliation of the dominant S_{SED-1} foliation in the Mount Musgrave metasedimentary rocks; (**D**) L_{SED-1} mineral and stretching lineations associated with the dominant S_{SED-1} foliation; and (**E**) F_{SED-2} hinges of crenulation and localized folds.

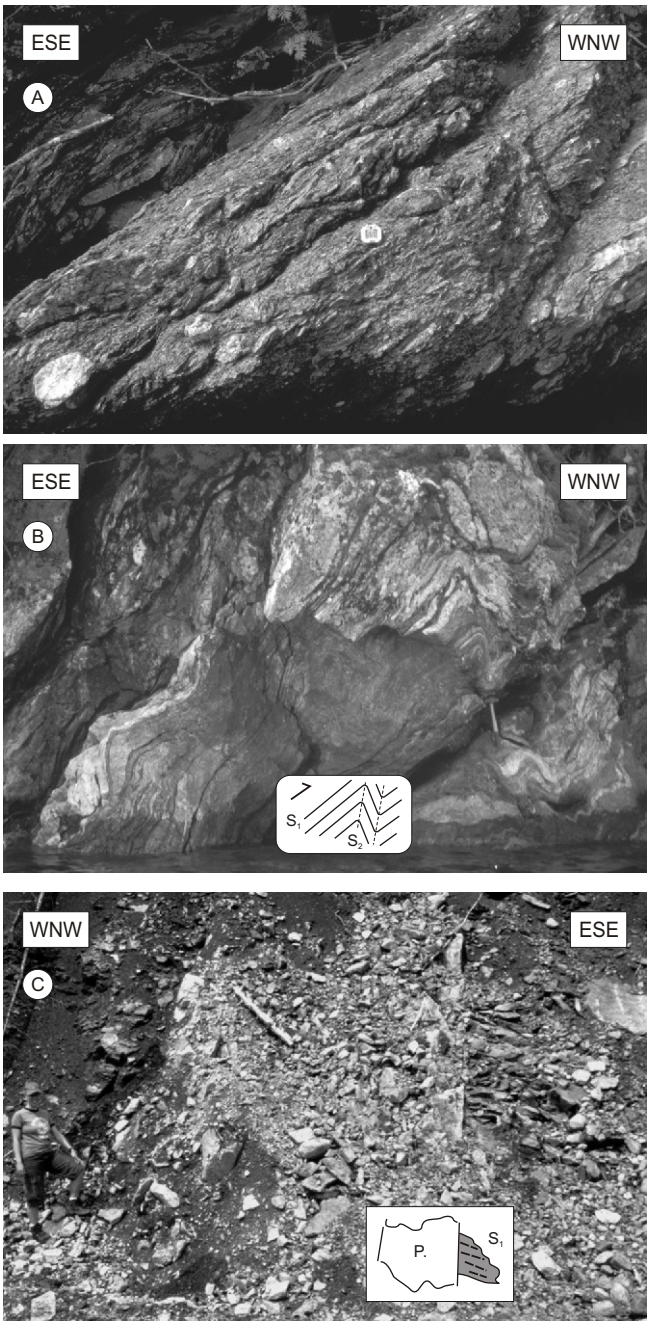

Figure 3.6 Field photographs of lithologies in the Corner Brook Lake block. (**A**) Sheared pebble conglomerate near the base of a thrust stack (AB-01-184). (**B**) Strongly deformed meta-psammitic rock typical of the South Brook Formation along the southern shore of Grand Lake. Note the asymmetric folding of S_{SED-1} with long, shallowly east dipping limbs and short, steeply west dipping limbs (AB-02-163). (**C**) Undeformed post-tectonic pegmatite dyke truncating the strong S_{SED-1} fabric of the metasediments. A sample from the centre of the dyke was taken for U-Pb ID-TIMS geochronology (AB-03-405).

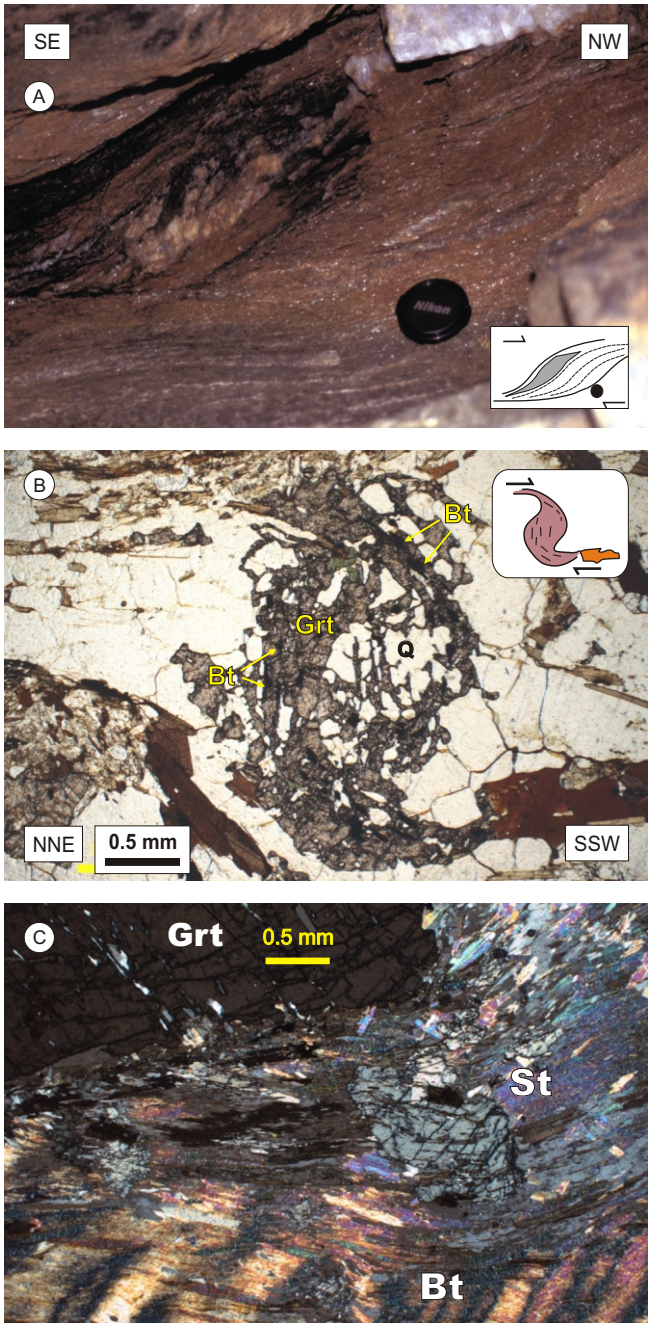

Figure 3.7 Photographs of deformational fabrics and metamorphic minerals in metasedimentary rocks of the South Brook Formation, south of Grand Lake. (**A**) Decimeter scale shear bands in a metapsammitic layer showing east-over-west thrusting (AB-02-168). (**B**) Spiral garnet (Grt) including a trail (S_i) of recrystallized quartz (Q) and biotite (Bt). Near the base of a thrust sheet, suggesting syn-peak metamorphism conditions for southwest-vergent deformation (AB-01-046). (**C**) Commonly observed metamorphic assemblage: garnet (Grt) overprinting the S_{SED-1}, which is defined by micas and biotite (Bt); but garnet has been affected by S_{SED-2} (crenulation cleavage), which has been overprinted by staurolite (St) (AB-02-169).

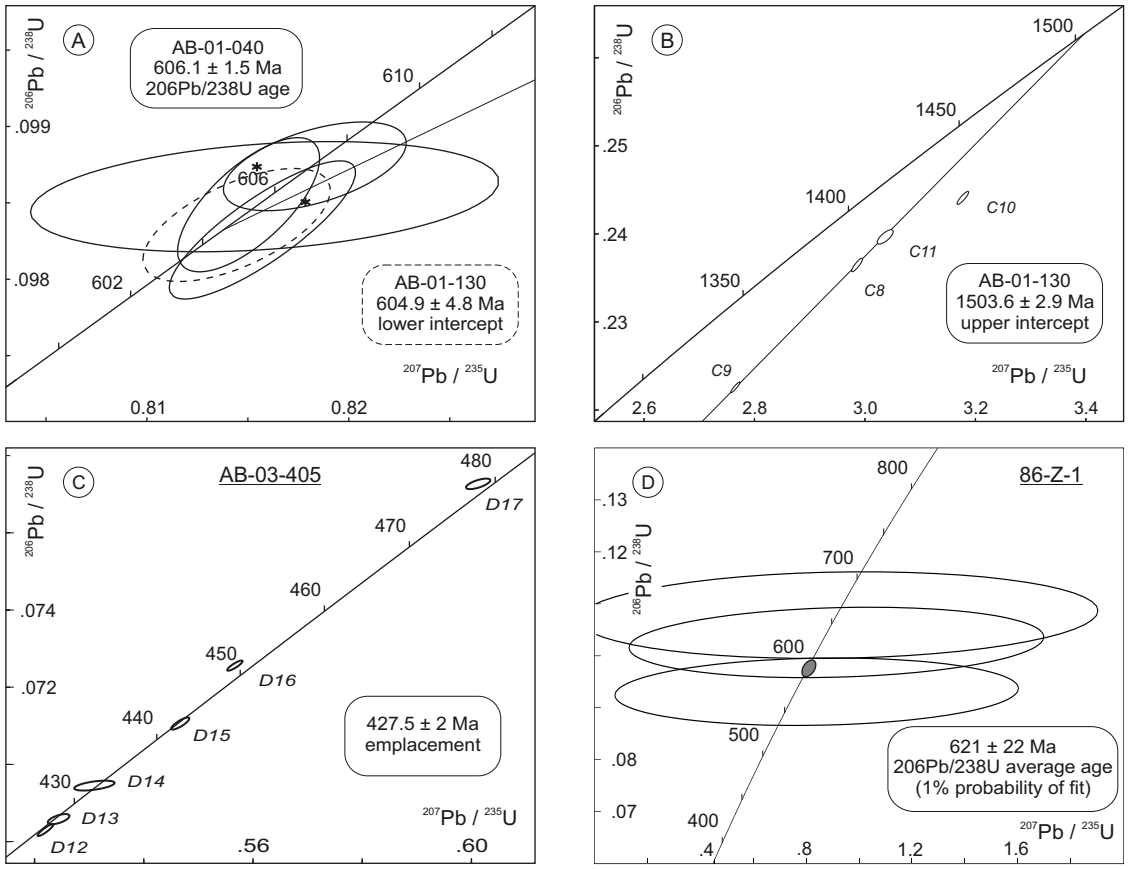

Figure 3.8 U-Pb TIMS Concordia diagrams for samples from the CBLB (results in Table 3.1). (**A**) Disappointment Hill tonalite (sample AB-01-040; zircon). Error ellipses for Grains A1 and A3 are omitted for clarity (see text), and their centers are plotted as stars. Grain C7 defining the lower intercept of the unnamed granitoid gneiss (sample AB-01-130; zircon) is plotted as a dashed ellipse. (**B**) Upper intercept of the unnamed felsic gneiss (sample AB-01-130; zircon). (**C**) Post-tectonic pegmatite dyke (sample AB-03-405; monazite). (**D**) Hare Hill granite (sample 86-Z-1; titanite). Grey-filled ellipse on Concordia shows average of U-Pb ID-TIMS zircon analyses from Currie et al. (1992), which is interpreted as being the age of emplacement for the granite.

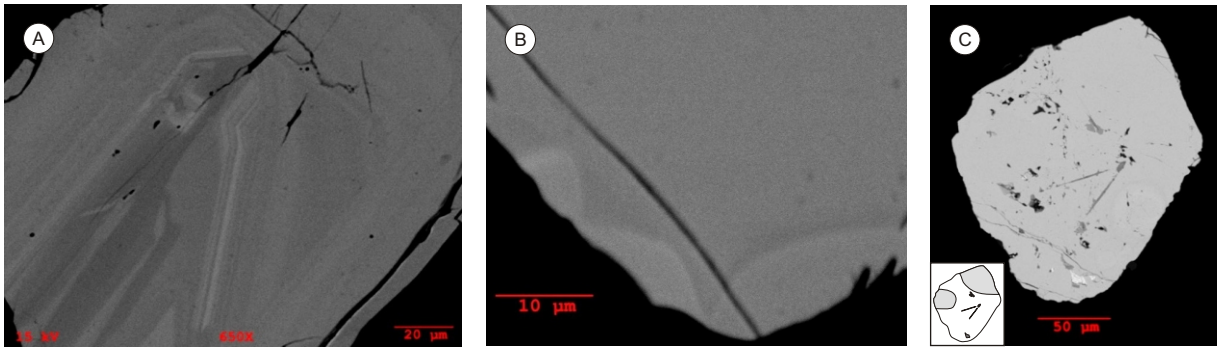

Figure 3.9 Back-scattered electron microscope (BSEM) images of heterogeneous monazite grains from the post-tectonic pegmatite dyke (sample AB-03-405). (**A**) Grain showing an oscillatory zoned core with a featureless overgrowth. (**B**) Grain showing an irregular boundary between core and overgrowth indicative of resorption. (**C**) Grain showing zonation based on inclusion-rich and -free areas. The dark-grey inclusions (including the rod-shaped ones) near the centre of the grain are zircon inclusions. The bright area towards the bottom is a uraninite inclusion.

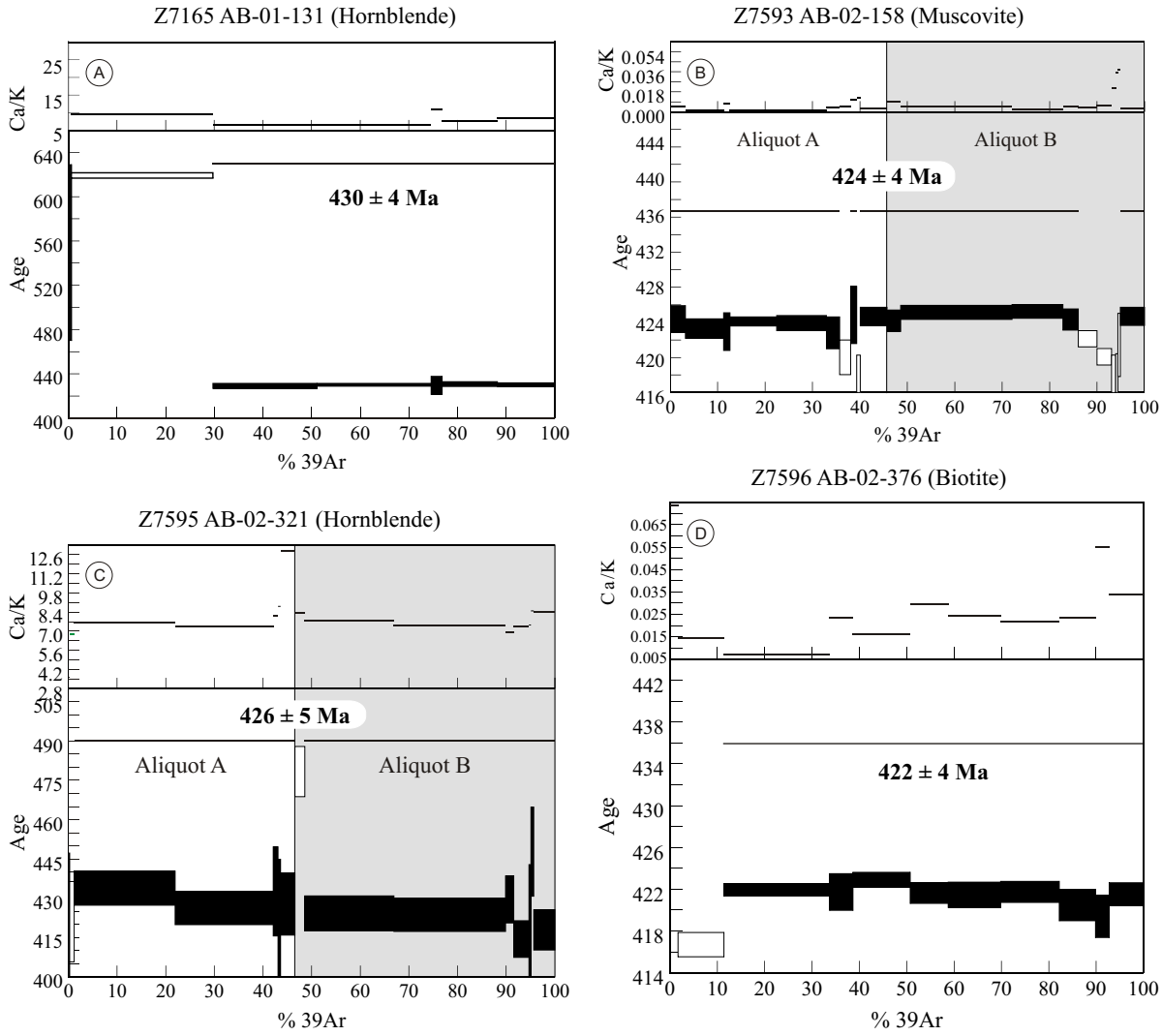

Figure 3.10 $^{40}Ar/^{39}Ar$ geochronology age spectra for samples from the CBLB (results in Table 3.2). (**A**) Hornblende - biotite ± garnet quartzo-feldspathic gneiss (sample AB-01-131; hornblende). (**B**) Sheared muscovite conglomerate (sample AB-02-158; muscovite). (**C**) Caribou Brook shear zone (sample AB-02-321; hornblende). (**D**) Biotite-muscovite-garnet schist (sample AB-02-376; biotite).

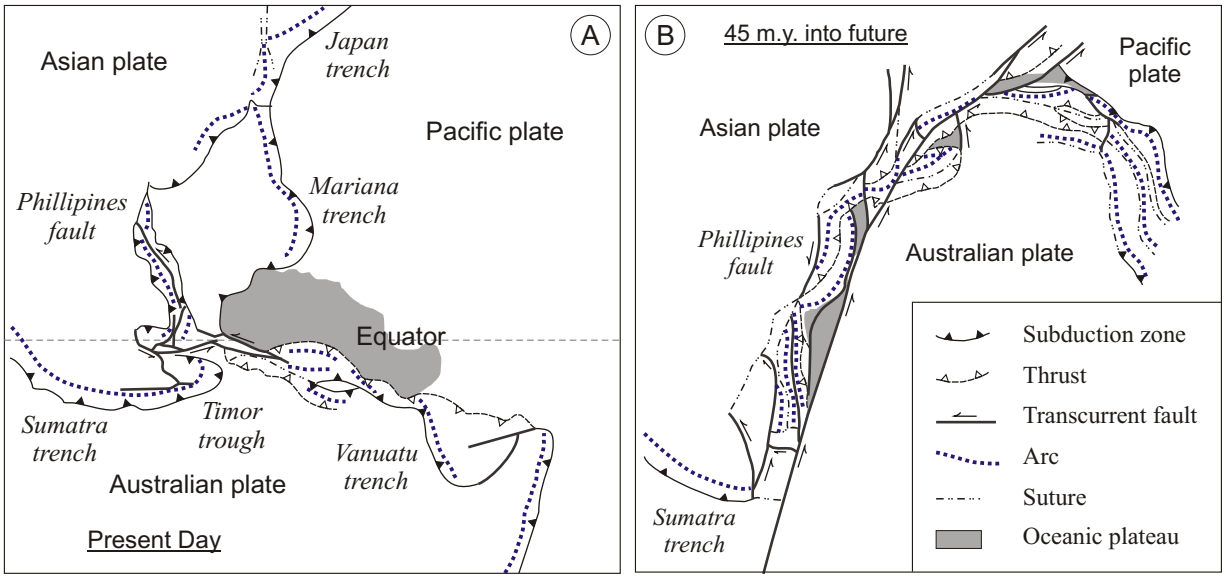

Figure 3.11 Schematic tectonic map of the future orogen produced by the collision between Australia and Asia collision based on forward modeling. (**A**) The present day plate configuration**.** (**B**) The plate configurations projected 45 m.y. into the future. Note the dispersal of once continuous tectonic elements as an effect of large-scale orogen-parallel transcurrent movements, and the resulting linearity of the 'mountain belt'. Modified from van Staal et al. (1998).

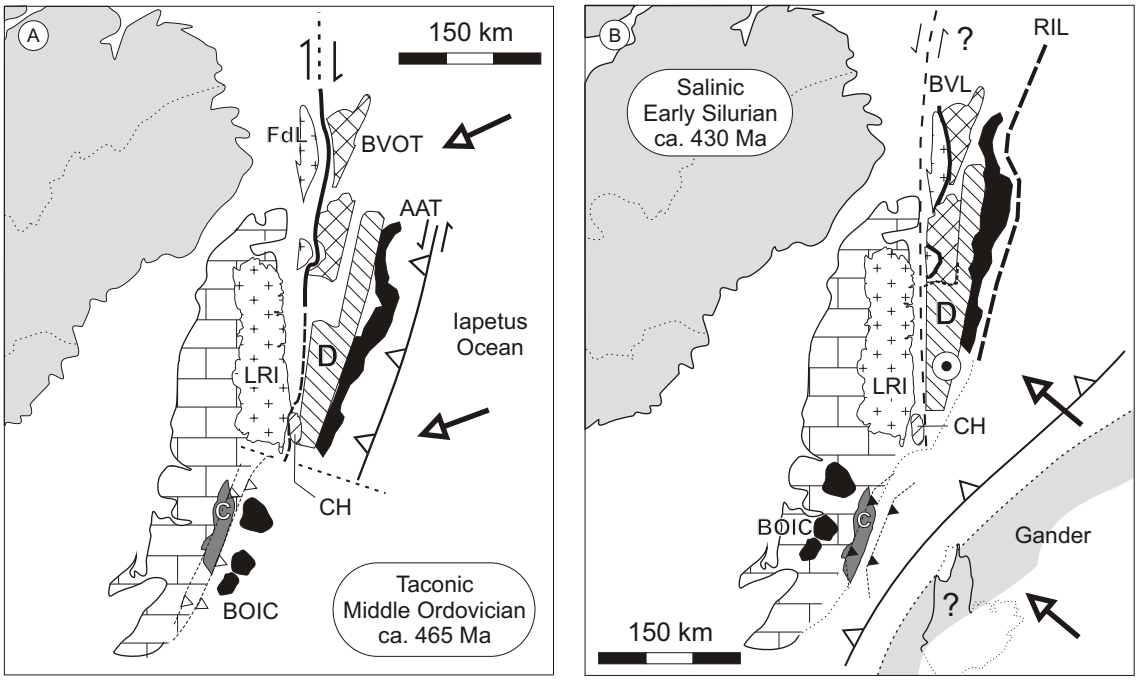

Figure 3.12 Schematic tectonic diagrams for: (**A**) the Middle Ordovician Taconic orogeny, and (**B**) the Early Ordovician Salinic orogeny, assuming that the CBLB represents the para-autochthonous leading edge of the Laurentian craton. The diagrams demonstrate possible tectonic settings that can explain the differences in Early Palaeozoic dynamo-thermal histories between the Dashwoods and CBLB. See text for details. Abbreviations: AAT - Annieopsquatch Accretionary Tract; BOIC - Bay of Islands Complex; BVL - Baie Verte Brompton Line; BVOT - Baie Verte Oceanic Tract; C - Corner Brook Lake Block; CH - Coney Head Complex; D - Dashwoods; FdL - Fleur de Lys block; LRI - Long Range Inlier; and RIL - Red Indian Line.

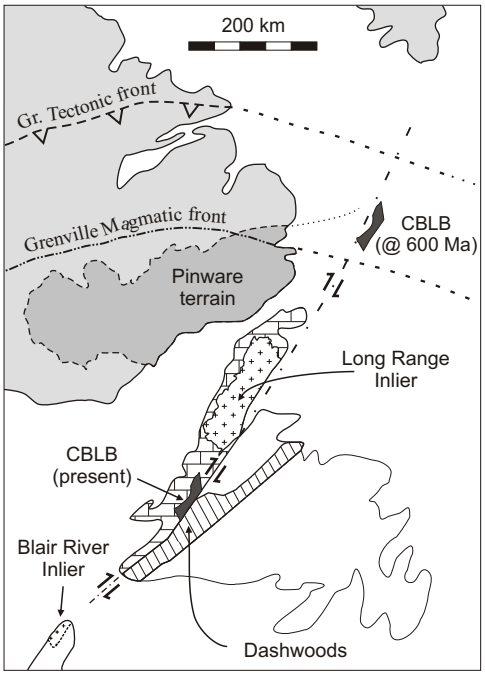

Figure 3.13 Simplified diagram of the western Newfoundland Appalachians showing the main tectonic segments discussed herein. The diagram shows the most probable Late Neoproterozoic position of the CBLB suspect terrane (see Chapter 4 for discussion). The diagram demonstrates that ca. 500 km of dextral orogen-parallel movement is needed to explain the present-day position of the CBLB.

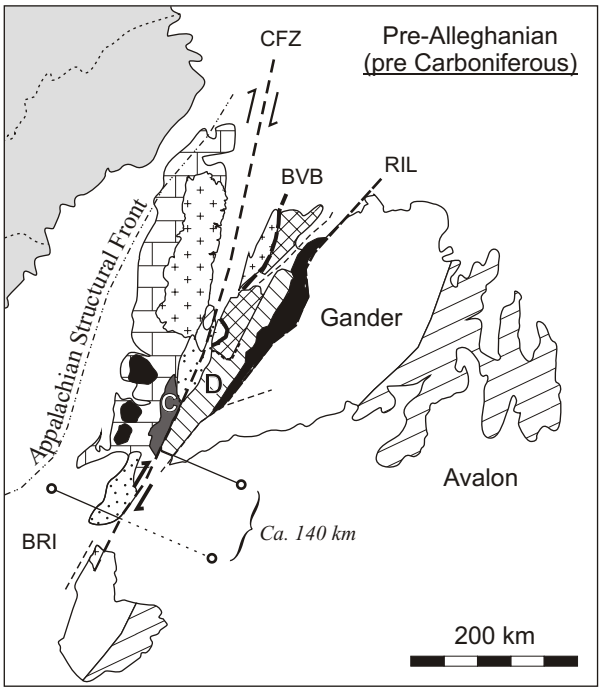

Figure 3.14 Palinspastic reconstruction after removing 140 km of dextral Carboniferous movement on the Cabot Fault Zone, representing the Late Devonian pre-Alleghanian stage (ca. 360 Ma). The diagram shows the partial juxtaposition of the CBLB and the Dashwoods block. Abbreviations: ASF - Appalachian Structural Front; BRI - Blair River Inlier; BVB - Baie Verte Brompton Line; C - Corner Brook Lake Block; CFZ - Cabot Fault Zone; D - Dashwoods; and RIL - Red Indian Line. Modified after Stockmal et al. (1990).

Table 3.1: U-Pb ID-TIMS isotopic data for zircon, monazite and titanite from rocks of the CBLB, western Newfoundland.

No.	Description	Weight (mg)	U (ppm)	Th/U	Pbtot (pg)	PbCom (pg)	206Pb/204Pb	206Pb/238U	207Pb/235U
A	**AB-01-040A - Disappointment Hill tonalite (UTM 53821-4157)**								
1	1 Abr zr flat, no incl. **	0.5	237.2	0.32	11.7	3.05	264.2	0.0987	0.8155
2	1 Abr zr, two incl in top **	1.2	166.8	0.37	19.9	0.21	6023.6	0.0985	0.8150
3	1 Abr zr, no incl. **	0.9	201.4	0.32	20.7	13.07	105.1	0.0985	0.8179
B	**AB-01-040B - Disappointment Hill tonalite (UTM 53821-4157)**								
4	1 Abr zr, large, no incl.	24.3	151.1	0.60	415.9	37.79	617.5	0.0985	0.8158
5	1 Abr zr, many incls, irregular shape	11.2	65.3	0.45	74.4	2.02	2311.9	0.0987	0.8183
6	1 Abr zr, not well abr, no incl. **	6.6	136.4	0.40	90.2	1.64	3480.6	0.0983	0.8157
C	**AB-01-130 - Unnamed felsic gneiss (UTM 53793-4188)**								
7	1 Abr zr, some rnd incl.	3.3	114.7	2.65	60.4	0.79	3040.4	0.0984	0.8144
8	1 Abr zr, equant, no incl. **	1.9	286.8	0.34	132.1	0.48	17183.8	0.2365	2.9857
9	1 Abr zr, large, elon, some incl.	4.5	141.2	0.32	144.2	0.80	11390.6	0.2226	2.7653
10	1 Abr zr, round elliptical clear. **	2.2	206.4	0.41	115.9	0.98	7277.3	0.2441	3.1772
11	1 Abr zr, prism. flat, 1 large incl. **	2.1	126.5	0.36	65.7	1.81	2273.0	0.2397	3.0367
D	**AB-03-405 - Post-tectonic pegmatite dyke (UTM 53834-4267)**								
12	1 mon; stained, incl, rnd edges; abr; HNO3	2.2	18465	4.03	5556	7.66	23310	0.068	0.5220
13	1 mon; ylw, clr, tri, straight crack; HNO3	11.1	2378	9.31	6238	11.38	10249	0.069	0.524
14	1 mon; ylw, tri, stains; 2nd choice	2.2	906.6	8.77	457	5.04	1789.8	0.07	0.531
15	1 mon; frag, clr, transp; HNO3	4.4	5001	3.79	3025	10.18	9889.4	0.071	0.547
16	1 mon; ylw, clr, round, stain	6.8	2405	3.90	2332	6.57	11631	0.073	0.557
17	1 mon; prismatic, ylw; HNO3	3.1	1155	3.12	485	4.48	3984.4	0.077	0.601
E	**86-Z-1 - Hare Hill granite - original mineral separates from Currie et al. (1992)**								
18	1 ttn; pale brown, ang	44	8.07	3.22	259	202.07	28.02	0.0940	0.852
19	1 ttn; hexagonal, multiple incl	41	6.62	3.42	251	199.25	26.98	0.109	0.9360
20	10 ttn grains; light brown, euh	34	7.96	3.09	212	165.05	28.33	0.104	0.929

UTM measurements are in NAD-27 coordinates
abr = abraded, ang = angular, clr = clear, elon = elongate, euh = euhedral, frag = fragment, incl = inclusion, mon = monazite, opq = opaque, rnd = round, tri = triangular, ttn = titanite, ylw = yellow, zr = zircon
* = before dissolution, grain was treated with HNO_3 to remove the hematite (?) coating from the grains
** = no column chemistry (Krogh, 1973) performed on zircon
PbCom is common Pb, assuming the isotopic composition of laboratory blank
Th/U calculated from radiogenic $^{208}Pb/^{206}Pb$ ratio and $^{207}Pb/^{206}Pb$ age assuming concordance
% Disc., is per cent discordance for the given $^{207}Pb/^{206}Pb$ age
Decay constants are from Jaffey et al. (1971)

Table 3.1: Continued.

No.	206Pb 238U	2σ	207Pb 235U	2σ	207Pb 206Pb	2σ	Disc %	Error Corr.	Lab No.
	age (Ma) calculated							Coeff.	
A	**AB-01-040B - Disappointment Hill tonalite**								
1	606.8	2.5	605.5	20.0	600.9	89.1	-1.0	0.7684	dwd4320
2	605.5	3.4	605.3	2.6	604.3	7.3	-0.2	0.8282	dwd4321
3	605.9	4.4	606.9	43.6	610.7	196.7	0.8	0.8117	dwd4322
B	**AB-01-040B - Disappointment Hill tonalite**								
4	605.9	3.6	605.7	6.9	605.2	29.8	-0.1	0.4269	dwd4323
5	607.0	1.9	607.1	2.5	607.5	9.8	0.1	0.5732	dwd4324
6	604.6	7.1	605.7	5.8	609.7	7.5	0.9	0.9618	dwd4325
C	**AB-01-130 - Unnamed felsic gneiss**								
7	604.8	2.2	604.9	2.6	605.6	9.8	0.1	0.6105	dwd4388
8	1368.3	4.0	1404.0	2.5	1458.5	3.0	6.9	0.8830	dwd4390
9	1295.5	3.2	1346.2	2.3	1427.8	2.2	10.2	0.9244	dwd4754
10	1407.9	3.8	1451.6	2.5	1516.2	3.0	7.9	0.8791	dwd4755
11	1384.9	4.2	1416.9	3.6	1465.3	6.1	6.1	0.7421	dwd4756
D	**AB-03-405 - Post-tectonic pegmatite dyke**								
12	425	0.9	426.5	1.0	429.7	2.6	0.9	0.9091	dwd4738
13	427.6	0.8	428.1	1.3	430.7	6.8	0.7	0.6007	dwd4737
14	432.8	0.8	432.4	2.5	430.3	13.9	-0.6	0.5284	dwd4764
15	442.5	0.9	442.8	1.1	444.3	3.8	0.4	0.8277	dwd4736
16	451.6	0.8	449.4	0.9	438.2	2.9	-3.2	0.8706	dwd4763
17	479.8	0.8	478.0	1.4	469.5	6.3	-2.3	0.6616	dwd4762
E	**86-Z-1 - Hare Hill granite**								
18	579.3	38.1	625.5	480	796.1	1603	28.5	0.0033	dwd4867
19	667.3	48.5	670.8	611	682.3	1381	2.3	0.0035	dwd4868
20	636.9	40.4	666.9	495	769.5	1550	18.1	0.0034	dwd4869

Table 3.2: $^{40}Ar/^{39}Ar$ isotopic data for analyses on muscovite, biotite and hornblende from rocks of the CBLB, western Newfoundland.

Power[a]	Vol. ^{39}Ar x10^{-11} cc	$^{36}Ar/^{39}Ar$	$^{37}Ar/^{39}Ar$	$^{38}Ar/^{39}Ar$	$^{40}Ar/^{39}Ar$	$\%^{40}Ar$ ATM	$*^{40}Ar/^{39}Ar$	f_{39}[b] (%)	App. Age Ma[c]
AB-131 Hornblende; J=J=.01442010[d] (Z7165; UTM 53800-4189)									
Aliquot:A									
2.4	0.0643	0.1416±0.0126	36.753±4.662	0.487±0.041	340.750±10.649	12.3	298.908±10.028	0.2	3012.22±49.14
3.0	0.0665	0.2119±0.0178	31.938±308.405	0.169±0.021	127.237±6.028	49.2	64.622±6.804	0.2	1187.97±91.63
3.9	0.0724	0.0651±0.0157	40.546±258.675	0.282±0.027	43.921±3.243	43.8	24.691±4.130	0.2	549.49±79.23
4.6	10.1123	0.0012±0.0001	5.094±0.096	0.400±0.002	28.747±0.124	1.2	28.403±0.129	29.1	619.32±2.38
5.0	7.4407	0.0008±0.0002	3.397±59.514	0.272±0.002	18.867±0.106	1.3	18.626±0.110	21.4	429.20±2.27
5.5	8.1583	0.0004±0.0001	3.448±0.123	0.269±0.002	18.802±0.060	0.7	18.677±0.067	23.5	430.26±1.37
6.0	0.7830	0.0037±0.0014	5.753±120.079	0.285±0.008	19.745±0.335	5.6	18.643±0.395	2.3	429.56±8.09
7.0	3.9477	0.0014±0.0003	3.872±57.960	0.294±0.003	19.128±0.102	2.2	18.700±0.104	11.4	430.72±2.13
12.0	4.1050	0.0007±0.0003	4.394±60.979	0.292±0.002	18.875±0.075	1.1	18.671±0.083	11.8	430.13±1.71
AB-02-158 Muscovite; J=.02283120[d] (Z7593; UTM 53899-4256)									
Aliquot:A									
2.4	0.8880	0.0065±0.0014	0.038±0.010	0.023±0.011	11.932±0.256	16.0	10.018±0.483	0.1	371.61±16.19
2.8	22.7725	0.0005±0.0001	0.003±0.000	0.003±0.011	11.734±0.037	1.1	11.608±0.046	3.1	424.11±1.50
3.0	59.3207	0.0001±0.0000	0.001±0.000	0.002±0.011	11.596±0.031	0.2	11.575±0.033	8.0	423.06±1.08
3.3	9.8606	0.0000±0.0002	0.004±0.001	0.002±0.011	11.576±0.041	0.1	11.569±0.068	1.3	422.86±2.20
3.5	72.6431	0.0001±0.0000	0.001±0.000	0.002±0.011	11.625±0.016	0.2	11.607±0.017	9.8	424.10±0.56
3.9	77.8777	0.0000±0.0000	0.001±0.000	0.002±0.011	11.596±0.024	0.0	11.595±0.026	10.5	423.68±0.84
4.2	20.5225	0.0001±0.0001	0.002±0.001	0.002±0.011	11.585±0.049	0.2	11.561±0.054	2.8	422.60±1.75
4.6	16.9998	0.0000±0.0002	0.002±0.001	0.002±0.011	11.484±0.047	0.0	11.479±0.059	2.3	419.91±1.91
5.0	9.3087	0.0001±0.0003	0.006±0.001	0.004±0.011	11.623±0.069	0.0	11.622±0.097	1.3	424.57±3.17
6.0	5.6877	0.0003±0.0004	0.007±0.003	0.004±0.011	11.432±0.072	0.5	11.379±0.107	0.8	416.64±3.48
12.0	41.6040	0.0000±0.0000	0.001±0.000	0.002±0.011	11.618±0.029	0.0	11.616±0.031	5.6	424.38±1.01
Aliquot:B									
2.4	1.2242	0.0105±0.0016	0.066±0.006	0.018±0.011	14.061±0.234	23.5	10.751±0.264	0.2	396.00±8.73
2.8	19.9520	0.0004±0.0001	0.005±0.001	0.003±0.011	11.743±0.029	1.2	11.602±0.036	2.7	423.93±1.17
3.0	173.4490	0.0000±0.0000	0.002±0.000	0.002±0.011	11.646±0.019	0.1	11.631±0.024	23.5	424.87±0.77
3.4	79.3850	0.0000±0.0000	0.001±0.000	0.002±0.011	11.638±0.023	0.0	11.634±0.023	10.8	424.97±0.76
3.5	23.9777	0.0000±0.0001	0.003±0.000	0.002±0.011	11.610±0.029	0.0	11.606±0.036	3.3	424.07±1.18
3.9	29.0843	0.0000±0.0000	0.002±0.000	0.003±0.011	11.522±0.027	0.0	11.541±0.027	3.9	421.94±0.89
4.2	22.5283	0.0001±0.0001	0.003±0.000	0.002±0.011	11.526±0.021	0.4	11.480±0.028	3.1	419.94±0.91
4.6	6.5904	0.0003±0.0003	0.011±0.002	0.003±0.011	11.525±0.049	1.0	11.409±0.077	0.9	417.63±2.50
6.0	3.6800	0.0003±0.0003	0.020±0.005	0.004±0.011	11.616±0.075	0.8	11.520±0.107	0.5	421.25±3.49
5.0	3.6088	0.0007±0.0003	0.018±0.004	0.005±0.011	11.558±0.110	1.7	11.361±0.129	0.5	416.06±4.22
12.0	37.5949	0.0001±0.0000	0.002±0.000	0.001±0.011	11.652±0.029	0.3	11.617±0.031	5.1	424.42±1.01

a: As measured by laser in % of full nominal power (10W)
b: Fraction ^{39}Ar as percent of total run
c: Errors are analytical only and do not reflect error in irradiation parameter J
d: Nominal J, referenced to PP-20=1072 Ma (Roddick, 1983)
All uncertainties quoted at 2σ level
UTM measurements are in NAD-27 coordinates

Table 3.2: Continued.

Power[a]	Volume ^{39}Ar x10^{-11} cc	$^{36}Ar/^{39}Ar$	$^{37}Ar/^{39}Ar$	$^{38}Ar/^{39}Ar$	$^{40}Ar/^{39}Ar$	$\%^{40}Ar$ ATM	$*^{40}Ar/^{39}Ar$	f_{39}[b] (%)	App. Age Ma[c]
AB-02-321 Hornblende; J=.02286800 (Z7595; UTM 53820-4154)									
Aliquot:A									
2.4	0.0697	0.0024±0.0217	2.550±0.386	0.384±0.066	39.820±5.948	1.8	39.101±8.684	0.1	1152.41±189.50
3.0	0.2679	0.0154±0.0077	1.878±0.101	0.113±0.016	12.666±0.644	22.7	9.786±2.458	0.2	364.33±82.87
3.5	1.4192	0.0063±0.0014	3.507±0.055	0.232±0.013	12.997±0.156	11.6	11.492±0.470	0.9	420.96±15.37
3.9	31.6479	0.0000±0.0001	3.984±0.039	0.238±0.011	11.880±0.028	0.0	11.887±0.201	20.7	433.81±6.52
4.2	30.8019	0.0001±0.0001	3.832±0.039	0.233±0.011	11.663±0.040	0.1	11.652±0.196	20.2	426.17±6.38
4.6	1.5061	0.0004±0.0015	4.207±0.072	0.220±0.013	11.604±0.152	0.0	11.848±0.524	1.0	432.55±17.00
5.0	0.7616	0.0022±0.0027	4.577±0.115	0.234±0.014	11.316±0.257	0.0	11.345±0.877	0.5	416.13±28.74
12.0	4.5364	0.0008±0.0005	6.703±0.078	0.234±0.011	11.819±0.074	1.0	11.699±0.364	3.0	427.68±11.85
				Aliquot:B					
3.0	3.0647	0.0025±0.0008	4.337±0.069	0.240±0.011	14.021±0.114	5.3	13.277±0.304	2.0	478.35±9.61
3.5	27.9940	0.0001±0.0001	4.047±0.044	0.225±0.011	11.614±0.033	0.2	11.591±0.205	18.4	424.17±6.69
3.9	35.0200	0.0000±0.0001	3.862±0.042	0.222±0.011	11.573±0.037	0.0	11.575±0.195	23.0	423.65±6.37
4.0	2.5631	0.0000±0.0005	3.606±0.050	0.204±0.012	11.481±0.105	0.0	11.754±0.277	1.7	429.48±9.02
4.2	4.7557	0.0007±0.0004	3.810±0.049	0.226±0.011	11.494±0.068	1.8	11.291±0.214	3.1	414.36±7.01
4.6	0.6594	0.0003±0.0021	3.874±0.125	0.182±0.012	11.210±0.334	0.0	11.411±0.750	0.4	418.28±24.54
6.0	0.8676	0.0001±0.0011	4.408±0.145	0.187±0.013	12.044±0.272	0.0	12.320±0.529	0.6	447.79±17.01
12.0	6.6549	0.0004±0.0004	4.390±0.052	0.199±0.011	11.532±0.052	1.2	11.398±0.236	4.4	417.86±7.72
AB-02-376 Biotite; J=.02292120 (Z7596; UTM 53807-4177)									
Aliquot:A									
2.8	31.1054	0.0004±0.0001	0.008±0.001	0.055±0.011	11.436±0.025	0.9	11.336±0.035	9.7	416.70±1.17
3.3	15.8801	0.0000±0.0001	0.012±0.002	0.054±0.011	11.492±0.047	0.0	11.489±0.053	4.9	421.74±1.74
2.4	5.4674	0.0045±0.0003	0.039±0.004	0.054±0.011	10.861±0.055	12.1	9.545±0.098	1.7	356.93±3.34
3.0	71.6644	0.0001±0.0000	0.004±0.001	0.055±0.011	11.509±0.017	0.1	11.496±0.018	22.3	421.95±0.60
3.5	38.8496	0.0001±0.0001	0.009±0.001	0.056±0.011	11.555±0.017	0.3	11.525±0.022	12.1	422.90±0.72
3.9	25.7488	0.0000±0.0001	0.016±0.001	0.056±0.011	11.482±0.024	0.0	11.486±0.030	8.0	421.63±0.97
4.2	35.6321	0.0001±0.0001	0.013±0.001	0.054±0.011	11.503±0.033	0.2	11.481±0.037	11.1	421.47±1.20
4.6	39.7133	0.0001±0.0001	0.011±0.000	0.054±0.011	11.497±0.026	0.1	11.490±0.031	12.4	421.75±1.01
5.0	24.5388	0.0001±0.0001	0.012±0.001	0.054±0.011	11.460±0.038	0.1	11.451±0.045	7.6	420.48±1.48
6.0	9.3198	0.0001±0.0002	0.029±0.002	0.054±0.011	11.428±0.042	0.1	11.418±0.062	2.9	419.40±2.02
12.0	23.2460	0.0001±0.0001	0.018±0.001	0.053±0.011	11.498±0.027	0.1	11.483±0.033	7.2	421.52±1.09

Chapter 4: The Corner Brook Lake block in the Newfoundland Appalachians: a suspect terrane along the Laurentian margin and evidence for large-scale orogen-parallel motion

4.1. Abstract

The Corner Brook Lake block (CBLB) of the internal Humber Zone in the western Newfoundland Appalachians is unique along the Laurentian margin in that it: (1) lacks evidence for a Grenvillian (ca. 1.0 Ga) crystalline basement, (2) contains abundant late Neoproterozoic (ca. 600 Ma) granitoid plutons, and (3) has a regionally distinct Early Palaeozoic tectonic history. We suggest that this fault-bounded block represents an exotic, suspect terrane, and that large-scale orogen-parallel movement of at least several hundreds of kilometres took place during the Appalachian orogeny.

4.2. Introduction

The Humber Zone of the Appalachian mountain belt in eastern North America is commonly interpreted as representing part of the leading edge of the Laurentian craton to the Iapetus Ocean basin and/or associated seaways during the latest Neoproterozoic - Early Palaeozoic (Williams, 1995; Waldron and van Staal, 2001). It is underlain by the remnants of deformed Late Neoproterozoic-Ordovician rift, drift and passive margin igneous and sedimentary rocks that have been deposited onto crystalline basement. This crystalline basement is well exposed in several inliers in the Humber Zone of the Newfoundland Appalachians (Figure 4.1; Erdmer and Williams, 1995), which are generally accepted as representing (para-) autochthonous basement and correlated with the neighbouring Grenville Structural Province to the west (Gower and Krogh, 2002).

Whereas the voluminous Long Range Inlier has been demonstrated to be composed of Grenvillian crust (Heaman et al., 2002), compiled U-Pb zircon ages for various crystalline units in the Corner Brook Lake block (CBLB; Figure 4.1) of the Steel Mountain Inlier, demonstrate that the CBLB does not fit the description for para-autochthonous 'Grenvillian' basement. In fact, several lines of evidence discussed herein suggest that the CBLB represents a significantly displaced, exotic fragment within the Appalachian-Caledonian mountain belt that may have had over several hundred kilometres of displacement. Most current tectonic models for the Appalachians are focused on orthogonal divergent and convergent motions, without incorporating significant transcurrent movement (see review in Section 3.6.3), mainly because of a lack of piercing points. Therefore, the results presented herein may have profound implications.

4.3. Geology of the Corner Brook Lake Block

The elongate CBLB is almost entirely fault-bounded. The only non-tectonic boundary occurs in the northeast, where Carboniferous siliciclastic rocks unconformably overlie highly deformed metasedimentary rocks of the CBLB (Figure 4.1B). To the southwest, the CBLB is in contact with the Steel Mountain anorthosite complex of inferred Elsonian age (ca. 1.25 Ga; in Currie et al., 1992) along steep, NNW-trending shear zones, which have accommodated east-side-up reverse movement (Brem et al., 2003; Section 3.3.1). To the west, it is in contact with Cambro-Ordovician passive margin sedimentary rocks along the Grand Lake Fault and its northern extension, the Humber River Fault. The contact itself has not been observed, but carbonate beds that are regionally less deformed have been transposed in close proximity to the fault suggesting a tectonic zone. The boundary also represents an important metamorphic break between low-grade units to the west (external Humber Zone; after Cawood et al., 1994) and the intensely deformed and metamorphosed units of the CBLB (internal Humber Zone; Cawood et al., 1996). To the east, the CBLB is separated from the western Dunnage

Zone along the Cabot Fault Zone. This complex crustal-scale transcurrent fault was active from Late Ordovician (Chapter 2) until at least the Late Carboniferous (Chapter 5; and references therein).

The crystalline basement of the CBLB is predominantly exposed in the southern part (Figure 4.1B). It is mainly composed of granulite-facies quartzofeldspathic gneiss and associated amphibolite layers. Locally, it also includes quartzite layers and calc-silicate paragneissic units. A high-grade felsic intrusive unit (Disappointment Hill charnockite) yielded an upper intercept U-Pb zircon age of 1498 $^{+9}/_{-8}$ Ma, interpreted as the age of emplacement (Currie et al., 1992). Demonstrable intrusive relationships are rare, as most contacts within the CBLB are tectonic (see also Section 3.3.1). The Mesoproterozoic units appear to have been intruded by pegmatite dykes and alkaline granite plutons related to the Late Neoproterozoic Hare Hill complex (ca. 608 Ma; Currie et al., 1992). A coeval high-level granite is exposed in the northern part of the CBLB, where it is spatially associated with bimodal volcanic and intrusive rocks (Williams et al., 1985). Mafic (now amphibolite) dykes intruded the igneous and metamorphic units. The dykes are geochemically and lithologically similar to the tholeiitic Long Range dykes in the Long Range Inlier (ca. 605 Ma; Stukas and Reynolds 1974; Owen and Greenough, 1991), but in the CBLB these mafic intrusions have not been dated.

Together, these crystalline units form the basement to a strongly deformed and metamorphosed rift-drift sedimentary sequence of the Mount Musgrave Group. The latter comprises a predominantly lower metaclastic unit (South Brook Formation), including a thin basal conglomerate, that is overlain by a thick sequence of metacarbonate rocks (Breeches Pond Formation; Cawood et al, 1996). No fossils have been found, but the unit is commonly correlated with less-deformed and -metamorphosed equivalents of the external Humber Zone (e.g. Hibbard, 1983; Cawood et al., 1994; Waldron et al., 1998), which contain Laurentian faunas (Nowlan and Neuman, 1995, and references therein). A detrital zircon study from a clastic layer near the base of the South Brook Formation constrains the maximum age of deposition to be ca. 572 Ma (Cawood and Nemchin, 2001). The sample has a dominant population of Grenvillian-aged zircon grains and is interpreted as having a typical Laurentian detrital zircon signature, even though 1.5 Ga Pinwarian age zircons, which are present in the

underlying basement (see below), appear to be absent from the sediments. A granodiorite gneiss, which may form part of a bimodal suite at the base of the cover sequence, yielded a latest Precambrian U-Pb zircon emplacement age ($555\ ^{+3}/_{-2}$ Ma; Cawood et al., 1996).

4.4. Unique Characteristics of the Corner Brook Lake Block

4.4.1. Absence of Grenvillian Ages

Seven U-Pb ages available from units in the CBLB indicate consistently that its crystalline basement is composed of two Proterozoic age components with ages of ca. 600 Ma and ca. 1.5 Ga (Table 4.1). More importantly, concordant Grenvillian ages *sensu stricto* (980-1080 Ma; Gower and Krogh, 2002) or *sensu lato* (ca. 1.0 to 1.3 Ga; Tollo et al., 2004) are absent from the basement of the CBLB, nor is there evidence for discordia lines with Grenvillian upper or lower intercept ages (Table 4.1). The only Grenvillian age in the CBLB is an upper intercept age (ca. 1021 Ma) for an Early Silurian deformed pegmatite dyke that intruded overlying metasedimentary rocks of the South Brook Formation (Cawood et al., 1994). The latter contains numerous Grenville-age detrital zircon grains (Cawood and Nemchin, 2001); therefore the significance of this single Grenville intercept age is highly conjectural.

The absence of Grenvillian ages in the basement of the CBLB is in sharp contrast with other Laurentian basement segments in the region (Figure 4.3). Directly east of the Cabot Fault, the basement to the Dashwoods subzone has a combined 1.5 Ga and 1.0 Ga signature from igneous units, similar to the Long Range Inlier (Chapter 2). To the southwest, the Blair River Inlier in Nova Scotia is also composed of various plutonic and metamorphic rocks of Grenvillian age (978-1080 Ma; Figure 4.2), and an older Mesoproterozoic component of circa 1.5 Ga is indicated based on Sm-Nd depleted mantle model ages (Miller et al., 1996, and references therein). The para-autochthonous Long Range Inlier of the external Humber Zone in northern Newfoundland is unmistakably composed of both 1.5

and 1.0 Ga igneous and metamorphic units (Figure 4.2; Heaman et al., 2002). It closely resembles the geochronological composition of the nearby Pinware terrane in southeast Labrador and Québec (Figures 4.2 and 4.3; Tucker and Gower, 1994; Wasteneys et al., 1997; Heaman et al., 2004). In addition to the noticeable absence of Grenvillian U-Pb ages from the CBLB, sparse Sm-Nd isotopic data from three units of the CBLB basement also show dissimilarity to the Mesoproterozoic units (Grenville Province crust) in the Long Range Inlier and the Pinware terrane (Table 4.2; Figure 4.4), although the depleted mantle ages (T_{DM} = 1.16 to 1.38 Ga; Table 4.2) may suggest some Grenvillian influence.

The Pinware terrane and the Long Range Inlier form part of the interior magmatic belt of the Grenville Province, which is characterized by extensive and long-lived Grenvillian *sensu lato* magmatism and moderate but pervasive metamorphism (Figure 16 in Gower and Krogh, 2002). If the CBLB is truly para-autochthonous basement in the Newfoundland Appalachians, then it should have formed part of this interior magmatic belt, and Grenvillian magmatic ages (either concordant or defined by discordant lines) and possibly metamorphic ages should be partly, if not dominantly present. Yet, such a Grenvillian signature appears to be missing from the CBLB basement.

4.4.2. Distinct Palaeozoic Tectonic History

In addition to its unique basement signature, the CBLB also has a distinct Early Palaeozoic tectonic history that differs from its neighbouring units (Chapter 3). To the west, stratigraphic evidence from the external Humber Zone and structural evidence from the Humber Arm Allochthon (e.g. Bradley, 2005), demonstrate that the Laurentian margin of the Newfoundland Appalachians was being loaded and deformed during the Middle Ordovician Taconic orogeny (Waldron et al., 1998a). To the north, the Fleur de Lys block (internal Humber Zone; Figure 4.1) contains a pre-Salinic (pre-Early Silurian) eclogite facies mineral assemblage, attributed to the burial of the continental margin sediments during the Ordovician (Jamieson, 1990; Waldron et al., 1998a). East of the CBLB, the

Dashwoods subzone has clearly been affected by Ordovician regional deformation, associated regional metamorphism and coeval arc magmatism, which have been related to arc-continent collision and accretion of oceanic assemblages (van Staal, 2007, and references therein). During the Early Silurian Salinic orogeny, the Dashwoods subzone was affected by local deformation, voluminous post-orogenic magmatism and rapid uplift (Whalen et al., 2006).

In sharp contrast to these surrounding rocks, the CBLB underwent strong regional west-vergent deformation and associated amphibolite facies peak metamorphism during the Salinic orogeny (Cawood et al., 1994; Chapter 3). Moreover, evidence for a Middle Ordovician tectono-thermal event is absent from the CBLB: no radiometric ages, metamorphic fabrics or igneous units have been found in the CBLB to indicate that the CBLB was affected by the Taconic orogeny (Section 3.5.1).

4.4.3. Corner Brook Lake Block as a Suspect Terrane

Since the CBLB is fault-bounded against other Appalachian terranes (Figure 4.1B), and given the evidence for a distinct age and isotopic signature of the CBLB basement, the CBLB is proposed to represent a suspect terrane. The apparent absence of a Taconic event in the CBLB indicates that it escaped the penetrative tectono-thermal effects of the Taconic collision present elsewhere in the Laurentian realm, adding to the suspect nature of the CBLB. The Early Silurian Salinic event could represent the docking of the CBLB to the Laurentian margin.

4.5. Possible Provenance of the Corner Brook Lake Block

The Late Neoproterozoic age distribution pattern in the CBLB, consisting of 610-600 Ma and ca. 555 Ma granitoid plutons (Table 4.1), is similar to peri-Gondwanan terranes in the northern Appalachians (Figures 4.1A and 4.3). Ganderian terranes, such as the Aspy, Bras d'Or, New River and Brookville terranes (Lin et al., in press, and references therein); and Avalonian terranes, including the

Caledonia terrane (Barr and Kerr, 1997) and the Antigonish and Cobequid Highlands (Murphy et al., 1997), contain numerous 620-600 Ma igneous units and widespread 560-550 Ma arc plutons. The ca. 600 Ma igneous suites in all these terranes are commonly interpreted as having formed in a continental arc magmatic setting, an interpretation that could also be considered for the CBLB alkaline and calc-alkaline plutons, based on lithologies (Brem et al., 2003). The sparse Sm-Nd isotopic data from units of the CBLB basement (Table 4.2; T_{DM} = 1.16 to 1.38 Ga; εNd = -0.9 to +0.6, recalculated for t = 600 Ma) are also similar to most of the Late Neoproterozoic units in the peri-Gondwanan terranes (Figure 4.4; Barr et al., 1998; Murphy and Nance, 2002; Barr et al., 2003a).

Even though some similarities are apparent between the CBLB basement and the peri-Gondwanan terranes, the former is overlain by a sedimentary sequence that contains carbonate units and a detrital zircon signature typical of the Laurentian realm (cf. Cawood and Nemchin, 2001). In contrast, Gander and Avalon are underlain by dominantly metaclastic sedimentary rocks containing Gondwanan faunas (e.g. Nowlan and Neuman, 1995). Therefore, a post-Neoproterozoic peri-Gondwanan provenance for the CBLB is unlikely. Given these sedimentological constraints, a provenance for the CBLB should be sought along the Laurentian margin of the Appalachian-Caledonian orogen.

To the south, basement inliers in the Québec Humber Zone are rare and no U-Pb dates are available. In contrast, the Humber Zone of the United States Appalachians contains numerous, large Precambrian basement inliers (Figure 4.3; Tollo et al., 2004), some of which show Late Neoproterozoic U-Pb igneous ages, such as the Goochland terrane (588-630 Ma), and the Reading Prong (ca. 602 Ma; Bartholomew and Tollo, 2004, and references therein). However, all of these basement inliers are characterized by the dominant presence of Grenvillian *sensu lato* ages and none contains any ca. 1.5 Ga igneous or metamorphic units (Tollo et al., 2004).

In eastern Laurentia, 1.5 Ga ages appear to be restricted to the Pinware terrane of southeast Labrador and the Long Range Inlier in northern Newfoundland, but both have a penetrative Grenvillian imprint throughout (Figure 4.2; Heaman et al., 2002; Gower and Krogh, 2002). If the CBLB were derived from an area north of Newfoundland but close to the Pinware terrane, it must have

been located at least north of the Grenvillian magmatic front (position ‘a’ in Figure 4.3) and possibly even north of the metamorphic front (position ‘b’ in Figure 4.3), for it to lack the Grenvillian tectono-magmatic imprint.

The Northern Highlands and Grampian terranes of the Scottish Caledonides contain several localized 588-611 Ma igneous units, which have intruded the Proterozoic Moine and Dalradian Supergroup sedimentary rocks (Figure 4.3). Some of these units, such as the Ben Vuirich granite, show discordia lines with intercepts ages at 550-600 Ma and 1.45 Ga (Rogers et al., 1989), similar to samples from the CBLB (Table 4.1). However, Laurentian basement in the Irish and Scottish Caledonides, including the offshore Rockall Bank, contains both Paleoproterozoic (1.75-1.8 Ga) and Grenvillian *sensu stricto* magmatic and metamorphic ages (Daly, 2001; Trewin, 2002).

Although the provenance of the CBLB is not well-constrained, the geological arguments presented herein, evidence for dominantly Early Palaeozoic dextral motion along its bounding faults (Chapter 5) and predominant dextral convergence near the Laurentian margin during the final contractional phases of the Appalachian orogeny (e.g. van Staal, 2007) suggest that the CBLB most likely came from the north, possibly from the latitude of Labrador (‘a’ in Figure 4.3).

4.6. Conclusion and Implication

The CBLB is proposed to represent a suspect terrane, instead of the para-autochthonous leading edge of the Laurentian margin in the Newfoundland Appalachians. Even though the available data do not permit a definite interpretation of the provenance of the CBLB, they do indicate that significant orogen-parallel movement of the CBLB (at least hundreds of kilometres) should have taken place during the Early Palaeozoic in order to explain its present position. The possibility of large-scale strike-slip tectonics, in addition to the well-documented convergent motions, may have significant implications for tectonic interpretation of the Early Palaeozoic evolution of the Newfoundland Appalachians.

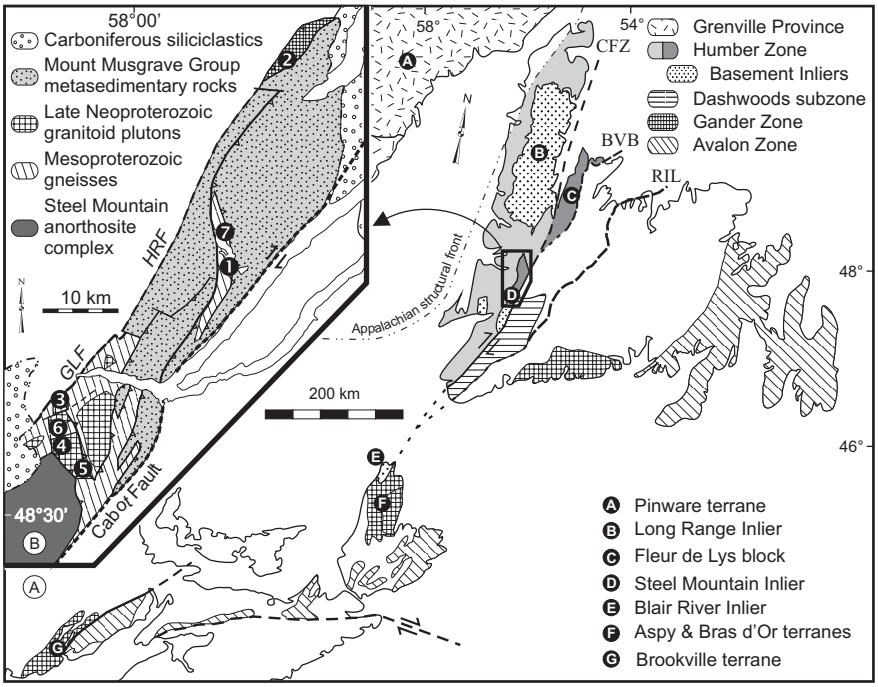

Figure 4.1 (**A**) Tectono-stratigraphic setting of the Northern Appalachians. (**B**) Simplified geology of the Corner Brook Lake block, as part of the Steel Mountain Inlier in western Newfoundland. Numbers refer to U-Pb ages for basement units as summarized in Table 4.1. Abbreviations: BVB - Baie Verte-Brompton Line; CFZ - Cabot Fault Zone; GLF - Grand Lake Fault; HRF - Humber River Fault; RIL - Red Indian Line.

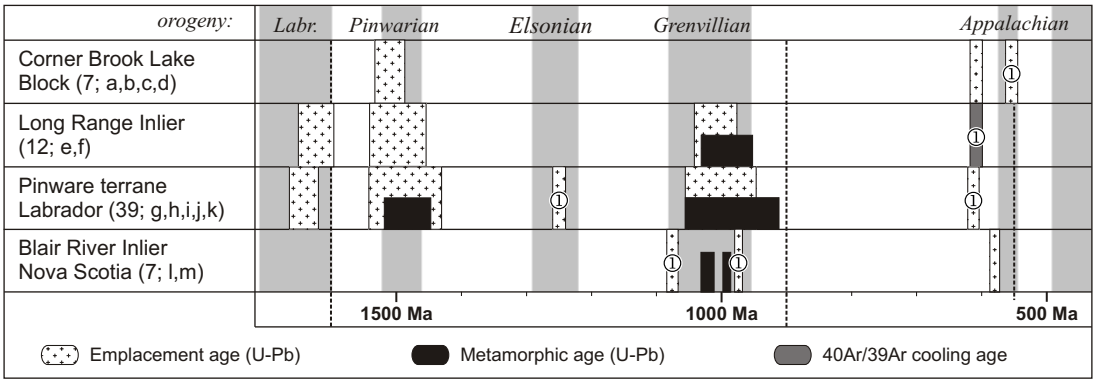

Figure 4.2 Synthesis of U-Pb isotopic data from crystalline basement units in the Laurentian realm of the Northern Appalachians, including southeast Labrador & Quebec, Newfoundland and Nova Scotia. Only Proterozoic ages are plotted. The range of U-Pb ages present in each block is shown (including 2σ errors). Blocks constrained by a single age are labelled as (1). Crystallization and metamorphic ages are based on interpretation by the respective authors. Metamorphic ages include monazite and titanite ages, and lower intercepts for discordant zircon analyses. Time scale and orogenic periods follow Gower and Krogh (2002). Number in brackets indicates the number of analyses used to constrain each terrane. Sources for geochronological data are: (a) Chapter 3; (b) Williams et al., 1985; (c) Currie et al., 1992; (d) Cawood et al., 1996; (e) Stukas and Reynolds, 1974; (f) Heaman et al., 2002; (g) Kamo et al., 1989; (h) Gower et al., 1991; (i) Tucker and Gower, 1994; (j) Wasteneys et al., 1997; (k) Heaman et al., 2004; (l) Miller et al., 1996; and (m) Miller and Barr, 2004. Abbreviation: Labr. - Labradorian. Diagram modified after Heaman et al. (2004).

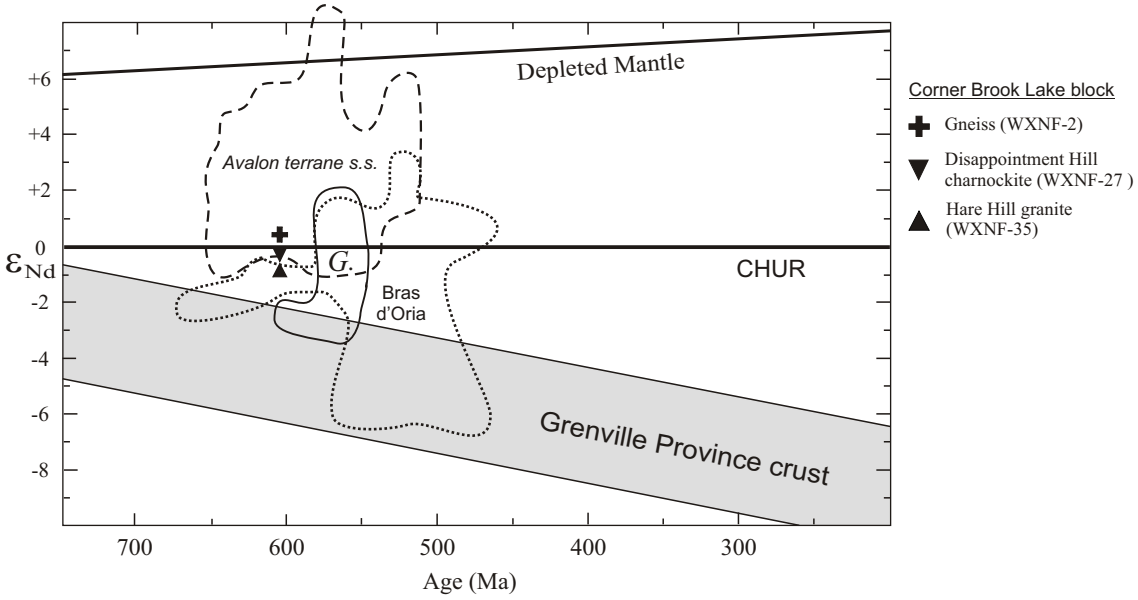

Figure 4.4 Compiled plot of εNd (t = 600 Ma) against time for samples from the CBLB. Data ranges of Neoproterozoic and Early Palaeozoic samples from Gander and Avalon terranes in the Canadian Appalachians and the crustal evolution of the Grenville Province are shown. Data for the CBLB samples in Table 4.2. Diagram modified from J.B. Whalen, personal communication, 2006. Grenville Province crust incorporates data from Dickin (2000, 2004) summarized in Table 4.2. Abbreviation: G - Gander terrane.

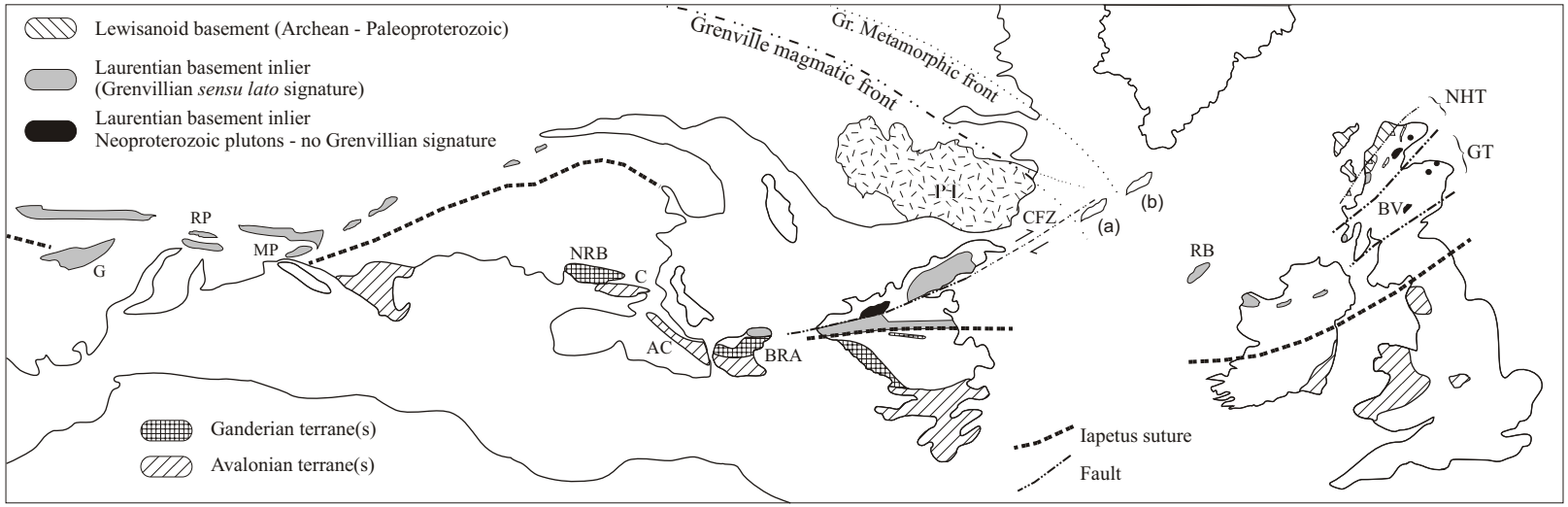

Figure 4.3 Schematic reconstruction of the Appalachian-Caledonian mountain chain during the Early Mesozoic, showing the dispersal of Laurentian basement fragments. Possible provenance of the CBLB along the Laurentian craton margin (see text for details): (a) north of the Grenville magmatic front in close proximity to the Pinware terrane; and (b) north of the Grenville metamorphic front. Grenville magmatic and metamorphic fronts are after Gower and Krogh (2002). Abbreviations: AC - Antigonish and Cobequid Highlands; BRA - Bras d'Or and Aspy terranes; BV - Ben Vuirich granite; Caledonia terrane; CFZ - Cabot Fault Zone; G - Goochland terrane; GT - Grampian terrane; MP - Manhatten prong; NHT - Northern Highlands terrane; NRB - New River and Brookville terranes PT - Pinware Terrane; RB - Rockall Bank; RP - Reading prong.

Table 4.1: Summary of published U-Pb ages for basement units in the CBLB. Number in front of column refers to sample location on Figure 4.2. Sources for geochronological data are: (a) Cawood et al., 1996; (b) Williams et al., 1985; (c) Currie et al., 1992; and (d) Chapter 3.

			U-Pb age (Zr) in Ma		
			Concordant age		
	unit	**rock type**	lower int.	upper int.	**Ref .**
(1)	Lady Slipper pluton	tonalitic gneiss	**555 +3/-5**	*(1400 ± 220)*	a
(2)	Round Pond granite	peralkaline leucogranite	**602 ± 10**		b
(3)	Hare Hill complex	alkali granite	**608 ± 4**		c
(4)	Disappointment Hill complex pluton	tonalite	**606 ± 2**		d
(5)	unnamed	felsic gneiss	**604 ± 4**	**1504 ± 4**	d
(6)	Disappointment Hill complex	charnockite	*(840 ± 25)*	**1498 +9/-8**	c
(7)	Corner Brook Lake complex	banded granitic gneiss	*(730 ± 40)*	**1510 ± 6**	a

Table 4.2: Sm-Nd isotopic analyses for samples from the CBLB basement. Data for Corner Brook Lake block modified from Joseph B. Whalen, personal communication, 2006. Data from the Grenville Province (Dickin, 2000) and the Long Range Inlier (Dickin, 2004) have been summarized for reference.

Sample	lithology	age	UTM (Nad-27) North	UTM (Nad-27) East	^{143}/$_{144}$(m)	^{147}/$_{144}$(m)	^{143}/$_{144}$(i)	εNd (t)	εNd (0.6 Ga)	εNd (1.0 Ga)	εNd (1.5 Ga)	εNd (1.65 Ga)	TDM (Ga)
Corner Brook Lake block													
WXNF - 2	Orthogneiss	-	53888	4221	0.512386	0.12526	0.511482	-4.9	+0.56	+4.23	+8.85	-	1.32
WXNF - 27	Charnockite	1498 Ma	53846	4159	0.512194	0.0882	0.511384	-8.7	-0.34	+5.24	+12.25	-	1.16
WXNF - 35	Alkali granite	608 Ma	53883	4172	0.512282	0.1182	0.511817	-6.9	-0.93	n/a	n/a	n/a	1.38
Grenville Province, Québec and Labrador													
Quebecia (n = 37)		-	-	-	n/a	0.1130 (± 0.025)	0.51201 (± 0.0003)	-	-	-	+2.3 to +4.0	-	1.51 - 1.64
Labradoria (n = 26)		-	-	-	n/a	0.1074 (± 0.014)	0.51186 (± 0.0001)	-	-	-	-	+2.3 to +3.6	1.54 - 1.80
Blanc Sablon area (n = 20)		-	-	-	n/a	0.1101 (± 0.019)	0.51185 (± 0.0002)	-	-	-	-	+2.4 to +3.4	1.66 - 1.79
Grenvillian (?) plutons (n = 7)		-	-	-	n/a	0.1087 (± 0.018)	0.51201 (± 0.0002)	-	-	n/a	-	-	1.46 - 1.65
Long Range Inlier, Newfoundland													
Quebecia (n = 15)		-	-	-	n/a	0.1132 (± 0.025)	0.51203 (± 0.0002)	-	-	-	+3.4 to +4.8	-	1.49 - 1.60
Labradoria (n = 7)		-	-	-	n/a	0.1134 (± 0.015)	0.51185 (± 0.0002)	-	-	-	-2.5 to +2.3	-	1.69 - 2.03
Plutons (n = 4)		-	-	-	n/a	0.1038 (± 0.02)	0.51198 (± 0.0001)	-	-	-	+3.3 to +6.7	-	1.35 - 1.62

Chapter 5: The Kinematics of the Baie Verte-Brompton Line - Cabot Fault Zone tectonic boundary in the Newfoundland Appalachians

5.1. Abstract

The Baie Verte-Brompton Line - Cabot Fault Zone (BCZ) in western Newfoundland is a long-lived crustal-scale tectonic zone that separates the Corner Brook Lake block (CBLB) to the west from the Dashwoods block to the east. Five deformation phases (D_{BCZ}) in the BCZ are recognized, using detailed field and microscopic observations in addition to U-Pb geochronology. These phases demonstrate a progressive evolution of the tectonic zone from mid-crustal levels (D_{BCZ-1} gneisses and D_{BCZ-2} mylonites) to high-crustal levels (D_{BCZ-5} cataclasites). The BCZ has recorded a protracted history of dominant oblique-dextral transcurrent movement, as evidenced by well-developed Late Ordovician - earliest Silurian (post-Taconic) D_{BCZ-1} and late Early Silurian to Early Devonian (post-Salinic) D_{BCZ-2} fabrics. Large-scale Early Palaeozoic orogen-parallel dextral movement along the BCZ can explain the marked differences in tectonic histories between the CBLB and Dashwoods.

5.2. Introduction

In previous chapters, it has been proposed that large-scale orogen-parallel transcurrent movements have had an important role in the Appalachian orogeny. This may be especially important for the crustal-scale Baie Verte-Brompton Line - Cabot Fault Zone (BCZ), which separates the Corner Brook Lake block (CBLB) to the west from the Dashwoods block to the east (Figure 5.1; Appendix D). To better understand the tectonic evolution of the peri-Laurentian realm, it is important to understand the kinematic history of the BCZ.

Currently, there is no consensus on the pre-Carboniferous tectonic history of the BCZ in western Newfoundland (see also Hibbard, 1983; Goodwin and Williams, 1990) and there are several reasons for this. First, major tectonic boundaries are often represented by a complex zone of mylonite, cataclasite, and discrete faults that have developed over a prolonged period of time as a result of several distinct deformation phases (Stewart et al., 1999). The earlier history of a reactivated fault zone is often difficult to elucidate, because of the overprinting effects of later deformation within the fault zone, and the BCZ is no exception to this rule. Second, the sequence and styles of deformation in the BCZ are very complex and vary between locales. In fact, opposing ductile senses of shear even within one locale have been reported (e.g. Goodwin and Williams, 1990; Piasecki, 1995). Third, the absolute timing of deformation phases, especially older phases, is very poorly constrained. Fourth, there are no clear piercing points across the BCZ that would allow for a quantification of finite movement on the BCZ over any time interval. Fifth, only fragmental information along the trace of the BCZ exists, i.e. there is no regional synthesis that has incorporated all local and regional data.

In order to constrain the kinematics of deformation, we have conducted detailed field studies and thin section analyses, in addition to appropriate geochronological analyses (see also Chapters 2 and 3), along a trace of 150 km along the BCZ in southwestern Newfoundland (Appendix D). The results show that the BCZ has recorded a protracted history of dominantly dextral movement, which spanned at least 150 million years, and evolved from ductile (straight gneiss and mylonite), through brittle-ductile, to brittle deformation (cataclastite and discrete fractures).

5.3. Definitions

The presence of an important tectonic zone in western Newfoundland was first recognized by Alexander Murray and James Howley in the 1880's (Hibbard, 1983). Since then, several different denominators have been used to describe this tectonic zone that separates the Corner Brook Lake block (CBLB; internal Humber Zone) from the western Dunnage Zone (Figure 5.1).

The Baie Verte-Brompton Line is – by definition – the genetic Middle Ordovician boundary between the Humber and Dunnage zones and is characterized by the presence of dismembered ophiolite slivers (Williams and St-Julien, 1982). It is well exposed in the Baie Verte peninsula in northern Newfoundland, but south of the Deer Lake basin, Baie Verte ophiolites are absent, except for an exposure on Glover Island (Figure 5.1). Farther to the south, the trace of the Baie Verte-Brompton Line swings towards the Québec Appalachians, where it is more continuous and better exposed (Williams and St-Julien, 1982; Williams, 1995).

The term Cabot Fault (Zone) was introduced to describe the rectilinear and narrow belt of large faults that bisects western Newfoundland (Wilson, 1962), a feature that is clearly present on aeromagnetic maps (see below), from other geophysical studies, and on air and satellite photographs. Moreover, it is spatially associated with Carboniferous sedimentary basins, including the Deer Lake basin and Bay St. George subbasin (Figure 5.1). The Long Range Fault in southwestern Newfoundland is the westernmost strand of the Cabot Fault, which separates Carboniferous basin sediments from the tectonized elements of the Dashwoods subzone (Riley, 1962; Knight, 1983). The composite term 'Long Range Fault (Cabot Fault)' has also been used (Piasecki, 1995). North of the Deer Lake basin, the Cabot Fault Zone consists of several larger splays (Figure 5.1), two of which are notable. First, the Doucers Valley Fault Complex (or Taylor Brook Fault; Hyde et al., 1988) is the westernmost strand and separates the White Bay allochthon (including the Coney Head complex; Dunning, 1987) to the east from the Mesoproterozoic Long Range Inlier to the west (Kerr and Knight, 2004). Second, the Hampden Fault, usually shown as the main strand of the Cabot Fault, represents the western boundary of the Fleur de Lys block. Towards the east, the Baie Verte-Brompton Line and the Green Bay Fault are generally considered as splays of the Cabot Fault (e.g. Hyde et al., 1988; Goodwin and Williams, 1996).

In the study area in southwest Newfoundland, the Cabot Fault Zone only locally coincides with the Ordovician Baie Verte-Brompton Line. For consistency with previous chapters and to encompass its entire deformation history, the composite term Baie Verte-Brompton Line - Cabot Fault Zone (BCZ)

that was introduced in Chapter 2 is used to describe the tectonic zone that separates the CBLB (internal Humber Zone) from the Dashwoods subzone (Dunnage Zone). It must be noted that in some instances in this chapter, the distinction between Baie Verte-Brompton Line and Cabot Fault Zone is retained in order to describe features that specifically relate to each tectonic zone.

5.4. Characteristics of the BCZ

The BCZ is apparent on seismic profiles across the orogen. On offshore lines across the Cabot Strait south of Newfoundland the absence of internal reflectors and the presence of flower structures demarcate the trace of the main strand of the BCZ (Figure 5.2; Figure 8 in Langdon and Hall, 1994). On onland seismic lines, such as the Lithoprobe seismic lines, the BCZ is also distinguishable (Figure 5.2; Waldron et al., 1998a; van der Velden et al., 2004). In fact, based on the evident truncations of various prominent reflectors in the subsurface up to 12s TWT (ca. 35 km depth), the BCZ can be considered as a crustal-scale tectonic boundary (van der Velden et al., 2004).

Geomorphologically, the BCZ is a topographic depression flanked by steep slopes, a demarcation that is clearly visible in the field (Figure 5.3A), on aerial photographs, and on satellite images. The western channel of Grand Lake coincides with the trace of the BCZ, where some strands are exposed along its western shore (Appendix D). As mentioned above, the trace of the BCZ is also apparent on aeromagnetic images, where it is characterized as a sharp rectilinear anomaly (Figure 5.1).

South of the Deer Lake basin, the BCZ is a wide tectonic zone, up to a few kilometres (Appendix D), consisting of anastomosing ductile shear zones that are crosscut and overprinted by intense high-level brittle-ductile and brittle shear zones. The features associated with the latter deformation appear to be restricted to the immediate vicinity of the Humber Zone-Dunnage Zone boundary, whereas the ductile fabrics are better preserved away from the boundary (Brem et al., 2002).

5.5. Deformation in the BCZ

Based on crosscutting relationships, absolute ages and differences in deformation mechanisms observed in the field and in thin sections, the structural fabrics were divided into five different deformation phases: D_{BCZ-1} strongly tectonized gneissic fabrics, which are only observed in the Dashwoods subzone rocks; D_{BCZ-2} schistose shear bands and mylonite fabrics, which are observed along the trace of the BCZ; D_{BCZ-3} transcurrent brittle-ductile shear zones; D_{BCZ-4} a local west-side-down normal shear zone; and D_{BCZ-5} cataclasite zones and discrete brittle faults.

5.5.1. Strongly Tectonized Gneisses (D_{BCZ-1})

The western part of the Dashwoods subzone is characterized by gneissic to migmatitic meta-sedimentary rocks and variably foliated igneous units. Within these units, locally bands of strongly tectonized gneisses are present (sub-) parallel to the BCZ. These are restricted to the first few kilometres east of the boundary. These shear zones have been described and evaluated in Chapter 2, and will be summarized here.

The localized high-strain zones are steeply dipping and generally strike NE (orogen parallel), but deviations from this direction to northerly and easterly strikes occur (Figure 5.4A). The foliation is commonly curviplanar. Stretching lineations defined by elongate quartz-feldspar aggregates, and mineral lineations defined by biotite and/or hornblende, vary in orientation, but dominantly plunge moderately to steeply towards the southwest (Figure 5.3B; Figures 5.4B and C). Shear-sense indicators, such as the conjugate set of late syntectonic pegmatite dykes (Figure 5.3C), sheath folds (Figure 5.3D), winged objects, and S-C structures (cf. Passchier and Trouw, 1996) associated with these lineations indicate a prominent dip-slip to oblique-dextral and southeast-side-down movement. This dextral sense of shear is corroborated by Z-folds (L_{BCZ-1B}) related to open-to-tight asymmetric folding of the mylonitic foliation (Figure 5.3D).

5.5.2. Greenschist and Lower Amphibolite Facies Mylonites (D_{BCZ-2})

The D_{BCZ-2} deformation in the BCZ is characterized by schistose S-C and S-C' mylonites (Figures 5.5 and 5.6). These mylonite units have been identified all along the trace of the Cabot Fault Zone in the study area and form anastomosing zones in close proximity to the Humber Zone–Dunnage Zone boundary. The deformation affected rocks of both the CBLB and Dashwoods subzone.

The shear zone foliations (C-surfaces) are very consistent in orientation along the trace of the BCZ. They dip steeply and strike NNE, which parallels the regional trace of the BCZ (Figure 5.4E). Lineations are defined by elongate quartz and/or feldspar aggregates, muscovite, chlorite, and occasionally hornblende and biotite. The metamorphic mineral assemblages mainly depend on the host-rock and can vary per locale. In some locales, e.g. in the Hbl-bearing anorthositic gabbro of the Steel Mountain anorthosite, minerals defining a lineation were rotated into their present orientation and thus do not represent a metamorphic assemblage associated with shearing. The lineations vary in orientation, but dominantly plunge shallowly to moderately towards the south (Figures 5.4F and G). Similar observations were made by G.C. Riley (1962, page 49) and other researchers along the Long Range Fault (e.g. Knight, 1983). Numerous shear-sense indicators have been observed, including oblique foliations (Figure 5.6A), shear bands and S-C' fabrics (Figure 5.6B), winged objects (commonly feldspar porphyroclasts), synthethic and antithetic fractures (Figures 5.6C and D) and drag folds. The shear-sense indicators associated with the lineations demonstrate a dominant oblique-dextral movement for D_{BCZ-2} (Figure 5.6), but locally some oblique-sinistral movements have been observed as well (Figure 5.7B; see below for discussion).

The D_{BCZ-2} structures can be subdivided into two sub-groups, based on their appearance in thin sections: D_{BCZ-2A}, a higher-grade phase in which both quartz and feldspar show ductile behaviour; and D_{BCZ-2B}, a lower-grade phase in which feldspars deform brittlely, whereas quartz behaves ductilely. It must be noted that these two subdivisions are transitional; they do not form discrete deformation phases and some overlap of fabrics between them may occur.

5.5.2.1. Ductile deformation of feldspars (D_{BCZ-2A})

D_{BCZ-2A} is characterized by dynamic recrystallization of plagioclase and K-feldspar porphyroclasts. Along the margins of the grain various equigranular and euhedral crystals of feldspars have recrystallized, giving it a core-mantle texture (Vernon, 2004). Some plagioclase porphyroclasts contain mechanical twins, where the twin-lamellae are at high angle to the main foliation. The centres of the porphyroclasts contain various anhedral feldspar phases that have exsolved from the main crystal, thereby rendering these crystals a poikilitic texture, in some locales to such a degree that original feldspar porphyroclasts have almost entirely been consumed (Figure 5.5C).

Quartz aggregates tend to have an (in)equigranular interlobate texture (cf. Passchier and Trouw, 1996). They are predominant in quartz bands (remnant quartz veins?), but also in asymmetric tails of poikilitic feldspar (Figure 5.5C). Quartz grains are relatively large in size compared to the recrystallized feldspars. Most quartz grains are optically free of internal dislocations and are commonly composed of subgrains. These observations suggest that grain boundary migration and subgrain rotation facilitated the dynamic recrystallization of quartz. A strand of the BCZ that developed in a quartz-rich psammite of the South Brook Formation in the CBLB (Section 3.3.2) shows another texture assigned to this sub-phase: an oblique foliation, in which recrystallized quartz grains define S-surfaces and sparse elongate feldspars parallel C-surfaces (Figure 5.6A). A similar oblique foliation, but with a higher degree of recrystallization of the quartz grains, was observed by Cawood and van Gool (1998, see Figure 32B) in the area immediately south of the Deer Lake basin.

Metamorphic mineral assemblages associated with these deformation textures are muscovite, biotite (generally chloritized) and minor chlorite. As mentioned above, these assemblages can vary per locale and mainly depend on the protolith in which the D_{BCZ-2A} shear zone has developed. No attempt has been made to better quantify the metamorphic grade. Based on the general observations described here, the metamorphic conditions are estimated as being middle greenschist to lower amphibolite

facies. Given the appearance of some fabric-forming minerals (chloritized biotite and chlorite) associated with the quartz-feldspar aggregates, some of these D_{BCZ-2A} fabrics may have formed under retrograde conditions.

5.5.2.2. Brittle deformation of feldspars (D_{BCZ-2B})

The D_{BCZ-2B} subphase is characterized by the brittle deformation of feldspars. The feldspars clearly form porphyroclasts, are generally smaller in size than the D_{BCZ-2A} feldspars, do not have the poikilitic texture and are distinguishable as tailed objects (e.g. Figure 5.7A). Minor recrystallization and perthitic exsolution textures are still present within K-feldspar crystals, but are not common. In contrast to feldspar, quartz shows features characteristic of ductile deformation. Quartz crystals and aggregates form elongate quartz ribbons in which subgrains and undulose extinction are typical (Figures 5.7B and C); some core-mantle textures (Vernon, 2004) are present. Fabric-forming metamorphic minerals associated with these lower-grade mylonites are muscovite and/or chlorite (Figure 5.6C and D), with biotite only sparsely present. Some D_{BCZ-2B} mylonites are associated with irregular quartz veins and silicifications parallel to the foliation (Figure 5.7C). Based on these observations, the metamorphic conditions are estimated as being at least lower greenschist facies.

5.5.3. Brittle-ductile Shear Zones (D_{BCZ-3})

Brittle-ductile shear zones are not restricted to the BCZ, but are locally present throughout the study area. In the BCZ these rectilinear shear zones dip steeply (Figure 5.8A) and are up to 50 cm wide. These tectonites can usually be traced for tens of metres (outcrop permitting) and are characterized by the drag of pre-existing (D_{BCZ-1} or D_{BCZ-2}) fabrics when viewed on horizontal surfaces (Figure 5.8B). Even though the strike of each shear zone is fairly consistent within each outcrop, both the trend and shear-sense of D_{BCZ-3} brittle-ductile shear zones appear random throughout the BCZ

(Figure 5.8A). As such, they do not appear to form a single conjugate system. Most D_{BCZ-3} tectonites are also characterized by the ample presence of quartz within and in close proximity to the main zone of shearing, where it is concentrated in irregular veins and vugs or en echelon veins (Figure 5.8C).

5.5.4. West-side-down Brittle-ductile Normal Shearing (D_{BCZ-4})

In the southern part of the BCZ, a relatively undisturbed section across the Long Range Fault is exposed. To the west of the contact, rocks of the Robinsons River Formation (Middle to Upper Visean Codroy Group; Knight, 1983) are shallowly west dipping, but in close proximity to the contact with the rocks of the Dashwoods subzone these are dipping steeply towards the west (Figure 5.9A; Appendix D). East of the contact, muscovite-chlorite schists with a D_{BCZ-2B} mylonitic fabric (Figures 5.6C and D) have been overprinted by a decimetre-to-metre scale S-C' fabric (Figure 5.9B). The shear foliation (C-surfaces) dips steeply to the west. Down-dip (west-side-down) movement is corroborated by the down-dip alignment of dark-green chlorite crystals that are present on the curved S-surfaces.

From the area south of Grand Lake, Piasecki (1995) reported steeply east dipping brittle-reverse faults ('D_2' fabrics), which demonstrated east-over-west movement. This phase can be correlated with D_{BCZ-4}, when interpreting that these 'D_2' fabrics were overturned with respect to D_{BCZ-4}.

5.5.5. Cataclasite Zones and Discrete Brittle Faults (D_{BCZ-5})

Throughout the region, brittle fractures and faults are omnipresent, but are concentrated in the BCZ these, especially along the immediate boundary between the Humber and Dashwoods (sub)zones. Along the trace of the BCZ, the intensity of brittle fracturing varies (Figure 5.10), resulting in localized areas with cataclasites and areas with less-intense 'minor' brittle fracturing. Such heterogeneity in concentration of brittle deformation along the trace of the fault can be explained by the presence of restraining jogs or by differences in plastic behaviour of the rocks affected. In the cataclastic zones

(´shatter belts´ of Piasecki, 1995), fracturing occurs throughout and all rocks have been affected, except for the Carboniferous sedimentary rocks in the Bay St. George subbasin. Fractures and fault planes are generally small (cm- to dm-scale) and very irregular, and contain brittle striations as well as newly formed chlorite or quartz. Rusty iron-staining of many fractures is pervasive. Irregular small quartz-chlorite veins are variably present. In thin section, some pseudotachylite 'veins' have been observed (Figure 5.10B). In zones of less intense cataclastic deformation, individual fractures and fault planes are more continuous and wider spaced throughout the outcrop than in the cataclasite zone (Figure 5.10C). Such fractures and faults also occur in the Carboniferous sedimentary rocks. The orientations of these faults and associated brittle striations are inconsistent and appear random, comparable with the brittle-ductile D_{BCZ-3} phase (see above). Hence, no sense of shear could be deduced from the brittle faults within the BCZ.

5.6. Timing of Deformation

5.6.1. D_{BCZ-1} Oblique-dextral Shearing

The timing of the middle crustal D_{BCZ-1} deformation phase (Figure 5.11) is constrained to be earliest Late Ordovician (ca. 455 Ma) to earliest Silurian (younger than ca. 446 Ma; Chapter 2). First, the folded pegmatite dyke of the conjugate set of late syntectonic pegmatite dykes (Figure 5.3C), which demonstrates a dextral sense-of-shear, yielded an emplacement age of ca. 455 Ma (Section 2.5.2.2). Second, a ca. 446 Ma foliated granodiorite sheet (Section 2.5.2.4) that is interlayered with strongly tectonized metasedimentary rocks, contains evidence for west-side-up deformation (Figure 5.3D; Section 2.4.1), suggesting that high-strain oblique-dextral D_{BCZ-1} deformation in the BCZ occurred in a protracted fashion over a time period of at least 10 m.y. into the earliest Silurian (Figure 5.12).

5.6.2. D_{BCZ-2} Dextral Shearing

The age of D_{BCZ-2} deformation can be bracketed between at least the latest Early Silurian (ca. 430 Ma) and the earliest Carboniferous (Early Visean; ca. 340 Ma); an important part of D_{BCZ-2} most likely took place before the Emsian (ca. 410 Ma; see below; Figure 5.12). The older (maximum) age constraint is based on the observation that the D_{BCZ-2} mylonite fabrics have developed in the metapsammitic rocks of the CBLB (Figure 5.6A) and most likely have overprinted its dominant Early Silurian Salinic fabric (S_{SED-1}; Chapter 3). Therefore the D_{BCZ-2} mylonite phase must be younger than ca. 430 Ma.

Immediately after the Salinic event, the CBLB (Chapter 3; Cawood et al., 1994) and Dashwoods-Notre Dame Arc (Whalen et al., 2006) were rapidly uplifted. The rocks of the CBLB, which were at peak metamorphic (lower amphibolite facies; Section 3.3.2) conditions by ca. 430 Ma, attained sub-greenschist facies conditions by ca. 424-422 Ma, based on $^{40}Ar/^{39}Ar$ muscovite and biotite ages (samples AB-02-158 and AB-03-376 respectively; Section 3.4.2). Since the CBLB rocks have been affected by D_{BCZ-2} shearing, which is characterized by lower greenschist to amphibolite facies fabrics (Figure 5.11; see above), and since the muscovite closure temperature for argon (ca. 350°C; McDougall and Harrison, 1999) roughly corresponds with the lower greenschist facies boundary (Figure 5.11), an important part of the D_{BCZ-2} phase is likely to have taken place during the Late Silurian (Figure 5.12). The age of movement is corroborated by a monazite analysis from a schistose muscovite granite located in the BCZ (sample AB-01-029; Section 2.5.2.1; Appendix D), which yielded an earliest Devonian $^{206}Pb/^{238}U$ age of 414 ± 3 Ma (Grain A9 in Figure 2.6B and Table 2.1) and is interpreted as reflecting either lead-loss or monazite growth related to movement in the BCZ.

Some of the D_{BCZ-2B} mylonitic strands of the BCZ formed under low-to-medium greenschist facies conditions and may have formed after the Early Devonian. The maximum age of deformation for these fabrics is interpreted as being Middle to Late Devonian, based on a regional correlation with the Romaines Brook Fault to the west. This NNE-striking fault is the eastern boundary of the Indian Head

Inlier (Figures 1.1 and 5.1; Palmer et al., 2002). The latest stage of movement is characterized by mylonitic (C-S) fabrics that have developed in Cambro-Ordovician limestone and demonstrate a dextral sense of shear. Here, the age of dextral movement is constrained between the final emplacement of the Humber Arm Allochthon which is certainly post-Pridolian (ca. 417 Ma), but more likely post-Emsian (ca. 391 Ma; Stockmal et al., 1998), and undeformed overlying Early Visean strata (ca. 342 Ma; Palmer et al., 2002).

In the Baie Verte peninsula in northern Newfoundland, the Baie Verte-Brompton Line (Figure 5.1) has registered a complex deformation history that includes ductile transcurrent (both dextral and sinistral), and dip-slip movements (Hibbard, 1983; Goodwin and Williams, 1990; Piasecki, 1995). No direct geochronological ages have been associated with these deformational phases, but it has been postulated that two ductile dextral strike-slip motions have occurred, the younger of which is associated with greenschist facies deformation and is younger than Early Silurian (Goodwin and Williams, 1996).

5.6.3. D_{BCZ-3} to D_{BCZ-5} Brittle-ductile and Brittle Fabrics

The timing of deformation on the D_{BCZ-3} to D_{BCZ-5} phases is difficult to constrain. The only solid constraint is that these fabrics post-date the D_{BCZ-2} mylonite fabrics, and therefore must be younger than at least the Late Silurian (ca. 420 Ma).

5.6.3.1. D_{BCZ-3} Brittle-ductile shear zones

The D_{BCZ-3} phase of brittle-ductile shear zones overprints the D_{BCZ-2} fabric. Such shear zones have not been identified in the Carboniferous strata of the Bay St. George subbasin (see also Knight, 1983), hence, D_{BCZ-3} is most likely Devonian in age (Figure 5.12). Similar ductile-brittle shear zones (HSZ_3 in Gaboury et al., 1996) were observed in the Hammer Down prospect, a mesothermal gold deposit in

northern Newfoundland that is spatially associated with second-order splays of the Green Bay Fault (Figure 5.1). These HSZ_3 structures and associated sulphide-rich quartz veins are also spatially associated with high strain fabrics (HSZ_1 in Gaboury et al., 1996), which could be similar to D_{BCZ-3} and D_{BCZ-1} fabrics, respectively, in southwestern Newfoundland. The older (maximum) age constraint on the HSZ_3 veins is ca. 437 Ma (Ritcey et al., 1995).

5.6.3.2. D_{BCZ-4} Normal faulting

No overprinting relationships were observed between D_{BCZ-4} and D_{BCZ-3} or D_{BCZ-5}; therefore, its relative age was assigned based on the plasticity of deformation (brittle-ductile D_{BCZ-4} vs. brittle D_{BCZ-5}). The D_{BCZ-4} phase demonstrates downward movement of the Bay St. George sedimentary basin. Based on sedimentological and stratigraphical data, two phases of normal faulting have been identified for this basin (Figure 9 in Hyde et al., 1988): first, during initial subsidence of the basin, which occurred during the latest Devonian and the Early Tournaisian (ca. 350-360 Ma), when sediments of the Anguille and Horton groups were deposited; second, during the Westphalian (ca. 300-315 Ma) when sediments of the Barachois Group were deposited during subsidence of the basin. Based on this, the D_{BCZ-4} is tentatively interpreted to be Carboniferous in age (Figure 5.12), but data are lacking to allow for a better correlation of the D_{BCZ-4} fabrics with either of these extensional phases.

5.6.3.3. D_{BCZ-5} Brittle deformation

High-level brittle deformation is usually the latest stage(s) of orogenic events. Hence, the D_{BCZ-5} phase (cataclasites and discrete brittle fracture planes) is most likely Carboniferous to Early Permian in age, but could be as young as Mesozoic (P.F.Williams et al., 1995). Theoretically, it could be as old as Early Devonian. Fabrics associated with this phase likely record a prolonged history of upper crustal movement along the BCZ that may span at least 100 m.y. Based on chronostratigraphic evidence from

the Carboniferous sediments in the Bay St. George subbasin, the BCZ is assumed to have accommodated three separate phases of dextral transpressional faulting during the Carboniferous to Early Permian (Figure 5.12; Langdon and Hall, 1994).

5.6.4. Discussion on Sinistral Deformation

Some sinistral shear-sense indicators have been observed in rocks formed as a result of the D_{BCZ-1} and D_{BCZ-2} phases. The lineations and foliations associated with these kinematic indicators are similar in orientation to fabrics associated with dextral kinematic indicators (Figures 5.4C and G). However, the sinistral kinematic indicators are relatively rare and are less pronounced than the dextral shear-sense indicators. Most of the sinistral indicators are locally present in the area between Grand Lake and the Burgeo Road (Piasecki, 1995; Appendix D), but these have also been observed along the Bay St. George subbasin further to the south. Sinistral movement along the BCZ could have occurred during the Early Palaeozoic, and it may have been overprinted by subsequent, more intense deformation (D_{BCZ-1} or more likely D_{BCZ-2}). This interpretation agrees with the one made by Piasecki (1988; 1995) and is consistent with observations made along the Baie Verte-Brompton Line north of the Deer Lake basin (Goodwin and Williams, 1990). This interpretation also agrees with regional tectonic considerations, such as the postulated Early Silurian sinistral convergence between Gander and the Laurentian margin (e.g. van Staal, 2007). Unfortunately, the observations from the study area are sparse and localized, and no accurate overprinting relationships exist with the other deformation phases. Therefore, sinistral movement may have occurred along the BCZ in southwestern Newfoundland, most likely during the Late Ordovician and/or Early Silurian (Figure 5.12), but this is inconclusive due to the sparseness of evidence.

Several interpretations exist that can explain the presence of localized sinistral shear-sense indicators in the BCZ. First, shear sense indicators in the northeastern margin of the Steel Mountain anorthosite demonstrate an oblique-sinistral sense of shear. The associated shear fabrics vary between

NNE-striking (in close proximity to the BCZ) and NNW-striking (to the west, away from the BCZ) (Appendix D; Currie and van Berkel, 1992). An outcrop of anorthosite gneiss from this border phase, which is exposed along the Burgeo Road (Piasecki 1995, page 340; Appendix D), was used as part of the evidence for sinistral shear-sense in the BCZ (D_1 of Piasecki, 1988; 1995). However, the regional swing in the strike of the sinistral shear fabrics (Appendix D) could be interpreted as representing drag due to dextral movement along the BCZ. In this interpretation, the sinistral fabrics would misrepresent the movement along the BCZ. The sinistral deformational event may actually represent an older phase of deformation, for example the Silurian docking of the CBLB to the Steel Mountain (Chapter 3) or even an unidentified Proterozoic event.

Second, sinistral shearing may have been synchronous with, but a local side effect of, overall dextral shearing. Theoretical models suggest that within a host shear zone, such as the BCZ, locally induced spin may be strong enough to induce a sense of non-coaxiality, which results in antithetic (here sinistral) shear fabrics that are at low angle to the main (dextral) shear zone (based on Case III of Jiang and White, 1995). This interpretation was assumed most applicable for the Late Ordovician $D_{BCZ\text{-}1}$ deformation phase (Section 2.4).

Finally, tight-to-isoclinal folding that post-dates the main dextral shear ($D_{BCZ\text{-}1}$ and $D_{BCZ\text{-}2}$) may have folded the fabric in such a way that once dextral kinematic indicators now give a sinistral sense of shear. For this to occur, the fold axis must be sub-parallel to the shallowly SW plunging mineral and stretching lineations that are associated with the dextral fabrics. Some small-scale (cm-scale) fold hinges are consistent with this scenario (Figures 5.4D and H; Figure 5.7B) and evidence for larger scale (dam-scale) folding of the fabric has been observed in one outcrop, coincidentally an exposure where sinistral kinematic indicators have been observed. Post-shearing upright folding around subhorizontal orogen-parallel fold axes was proposed to have occurred in the Dashwoods subzone (Piasecki, 1988). Thus, later folding of original $D_{BCZ\text{-}1}$/$D_{BCZ\text{-}2}$ fabrics is likely to have occurred. However, this mechanism cannot account for all observed sinistral kinematic indicators, since not all outcrops where sinistral fabrics have been developed show evidence of folding.

5.7. Discussion

In previous chapters, it was proposed that large-scale orogen-parallel movements of at least 500 km may have taken place in the Northern Appalachians, most likely along the BCZ (Chapters 3 and 4). Such a magnitude of transcurrent motion on the BCZ would allow for terranes that are currently situated outside of the Newfoundland Appalachians to have been positioned adjacent to the Laurentian margin in Newfoundland at some point during the Early Palaeozoic, and also for terranes that are currently situated adjacent to the Laurentian margin in Newfoundland to have originated from outside of the Newfoundland Appalachians. Thus, for terrane correlations as well as palinspastic and tectonic reconstructions of the northern Appalachians, it is important to understand the lateral continuity of the BCZ outside the island of Newfoundland.

5.7.1. Lateral Continuation of the Baie Verte-Brompton Line

In the Newfoundland Appalachians, the ophiolites representing the Baie Verte-Brompton Line are only discontinuously exposed in the Baie Verte peninsula and as a small sliver on Glover Island (Figure 5.1; Appendix D). Towards the south, the suture reappears in the Gaspé Peninsula (Québec), where it is well-exposed and laterally traceable into the southern Québec Appalachians (Williams and St. Julien, 1982). The Mont Albert and Thetford Mines ophiolites represent the Baie Verte-Brompton Line in Québec. The northern continuation of the Baie Verte-Brompton Line in the Appalachian-Caledonian mountain chain is generally interpreted as being the Clew Bay-Fair Head Line (Ireland) and Highland Border Complex (Scotland) (Dewey and Shackleton, 1984; Winchester et al., 1992; van Staal et al., 1998).

5.7.2. Initiation of the Cabot Fault

As discussed above, the Baie Verte-Brompton Line and Cabot Fault Zone do not coincide along the length of the Appalachian orogen. The Baie Verte-Brompton Line is unmistakably a Middle Ordovician suture characterized by the presence of ophiolites (Williams and St. Julien, 1982; Williams, 1995) and discontinuously follows the trace of the Cabot Fault (Figure 5.1). The Cabot Fault Zone has a linear expression on aeromagnetic images across western Newfoundland (Figure 5.1), which coincides in the field with D_{BCZ-2} mylonite and/or D_{BCZ-5} brittle fabrics. This linear expression is not as pronounced under the Carboniferous sediments in the Deer Lake basin and in the Cabot Strait. Given these observations, the D_{BCZ-2} mylonite fabrics are interpreted as marking the linear anomaly that is the Cabot Fault. Thus the Cabot Fault was – most likely – initiated in late Early to Late Silurian (ca. 430-414 Ma), during or immediately after the west-vergent thrusting in the CBLB (Chapter 3).

5.7.3. Lateral Continuation of the Cabot Fault

The Cabot Fault was initially interpreted to continue southwards into Cape Breton (Wilkie Brook Fault) through New Brunswick (Caledonia Fault) and into Massachusetts (Wilson, 1962). Based on aeromagnetic images (Figure 5.1), the Cabot Fault does appear to link up with the Wilkie Brook Fault (see also Figure 1 in van Staal, 2007), an observation corroborated by interpretations from seismic profiles across the Cabot Strait (Langdon and Hall, 1994). A strand of the Cabot Fault may potentially link up with the Aspy Fault, which is located immediately east of the Wilkie Brook Fault (Pascucci et al., 2000). Also, an important strand of the BCZ might be situated west of the Blair River Inlier, which could explain the truncation of this autochthonous(?) Grenvillian basement inlier (Erdmer and Williams, 1995; Miller et al., 1996). These two hypotheses have not been tested. Further towards the south, the aeromagnetic lineament that represents the Wilkie Brook Fault is truncated by the east-west striking Cobequid-Chedabucto Fault (Figure 5.1; van Staal, 2007). This important tectonic boundary has recorded Middle Devonian-Early Carboniferous dextral transcurrent motion related to the Middle

Devonian Neoacadian docking of the Meguma terrane, and has been reactivated during the Mesozoic (Murphy and Keppie, 1998). Correlation of the Cabot Fault south of this lineament is purely speculative, but should be sought towards the west given the dextral sense of shear on the Cobequid-Chedabucto Fault.

The northern continuation of the Cabot Fault is poorly constrained, given the insular position of Newfoundland and the Mesozoic opening of the Atlantic Ocean, which is most likely to have truncated any possible continuation of the Cabot Fault Zone towards the northeast into the Irish and British Caledonides. The relatively straight eastern margin of the Long Range Inlier (Figures 1.1 and 5.1) would suggest that the Cabot Fault follows this coast line, similar to the western arm of Grand Lake. A linear magnetic anomaly near the northern tip of Newfoundland ('m' in Figure 5.1) might represent the continuation of the Cabot Fault. However, the high intensity of this anomaly may suggest that it represents the ophiolitic Baie Verte-Brompton Line instead. Summarizing, the lateral continuation of the Cabot Fault outside of Newfoundland is not well-constrained.

5.8. The BCZ in a Regional Geodynamic Context

Convergence and collision of various tectonic segments with the Laurentian craton margin throughout the Appalachian orogeny has taken place in dominantly dextral convergent settings (van Staal et al., 1998; van Staal, 2007). The initial orogenic phase (Taconic 1; Cawood et al., 1996; van Staal, 2007), which involved the emplacement of ophiolites onto the Laurentian margin and Dashwoods microcontinent during the Late Cambrian - earliest Ordovician, occurred in an oblique dextral convergent setting (Harris, 1995; van Staal, 2007). Subsequent closure of the Humber seaway (Taconic 2; Waldron and van Staal, 2001; van Staal, 2007) involved oblique-dextral convergence between the Dashwoods microcontinent and the Laurentian margin. Consequently, during late Middle Ordovician arc-continent collision, the Dashwoods microcontinent and its Notre Dame Arc had a southward translation with respect to the Laurentian margin along the BCZ, as evidenced by the

conjugate set of ca. 455 Ma late syntectonic pegmatite dykes (Chapter 2). The Clew Bay-Fair Head line in the Irish Caledonides (Chew and Schaltegger, 2005) and the Shickshock Sud fault zone in the Québec Appalachians, a fault system spatially associated with the BCZ (Sacks et al., 2004), also have accommodated oblique-dextral movement during the Late Ordovician.

The only – yet important – exception to overall dextral convergence in the northern Appalachians during the Palaeozoic, was the latest Ordovician to Early Silurian (Salinic; 447-430 Ma) sinistral convergence between the Gander terrane and the Laurentian margin (Doig et al., 1990; van Staal, 2007). Evidence for sinistral movement in the BCZ is not conclusive (see above). However, if such movement did occur in the BCZ (e.g. Piasecki, 1995), then it is most likely to have taken place during this Early Silurian Salinic stage (cf. Cawood et al., 1995).

Immediately after emplacement of the Salinic thrust sheets in the CBLB (Chapter 3), the Cabot Fault was initiated. Characterized by D_{BCZ-2} greenschist facies mylonites along the trace of the fault, this phase can be related to the Early Devonian Acadian dextral convergence of Avalon with the composite margin of Laurentia (Holdsworth, 1994; van Staal, 2007). Similar post-Silurian movement has also been observed in the Green Bay Fault, where dextral offset of Silurian volcanic rocks is interpreted to amount up to 50 km (Hibbard, 1983; Szybinski, 1995; Ritcey et al., 1995). However, the observations for the Newfoundland Appalachians contrast with the Irish (and Scottish?) Caledonides, where coeval Early Devonian (ca. 412 Ma) movement on the Clew Bay-Fair Head Line is interpreted as being sinistral (Hutton, 1987; Chew and Schaltegger, 2005). Both these settings differ from the D_1 deformation in the Eastern Highlands shear zone in Cape Breton Island, a tectonic zone that is situated east of the Wilkie Brook fault (Figure 5.1) and separates the Ganderian Aspy and Bras d'Or terranes (Lin, 1993). This shear zone has documented Late Silurian-Early Devonian (425-415 Ma) east-over-west movement with a minor sinistral component (Lin, 2001).

Subsequent Middle Devonian Neoacadian convergence between composite Laurentia and the Meguma terrane is demonstrated to be dextral as evidenced by fabrics in the Cobequid-Chedabucto Fault (Murphy and Keppie, 1998; van Staal, 2007). Dextral movement (D_{BCZ-2B} or D_{BCZ-3}) may have

taken place on the BCZ. Late Devonian to Early Carboniferous (Neoacadian) movement on the Eastern Highlands shear zone was also oblique-dextral (Lin et al., 1998), as evidenced from their D_2 fabrics that appear similar to the D_{BCZ-2} mylonites.

During the Carboniferous, convergence between Laurentia and Gondwana, which caused continent-continent collision in the southern Appalachians (Alleghanian orogeny), is characterized by upper-crustal dextral transpressional faulting in the BCZ and sedimentation in genetically related strike-slip basins in the northern Appalachians (Bradley, 1982; Knight, 1983; Langdon and Hall, 1994).

5.9. Conclusions

The results of this chapter can be summarized as follows:

1. In the BCZ south of the Deer Lake Basin, five different deformation phases have been identified, which demonstrate the evolution of a fault zone from mid-crustal levels (D_{BCZ-1} gneissose and D_{BCZ-2} schistose mylonites) to upper crustal brittle deformation (D_{BCZ-5} cataclasites; Figure 5.11). Its history spans over 150 million years, from at least late Middle Ordovician (ca. 455 Ma) to possibly younger than earliest Permian (ca. 290 Ma).
2. In contrast with previous reports, movement in the BCZ throughout its history is dominantly – although not exclusively – oblique-dextral, and corresponds with the dominant oblique-dextral convergence of the 'composite' Laurentian margin with various tectonic segments during the Appalachian orogeny. Dominant Early Palaeozoic dextral deformation in the BCZ may have profound implications for terrane correlations and tectonic reconstructions in the northern Appalachians, especially considering that large-scale orogen-parallel motions along this crustal-scale tectonic zone have occurred.

3. The important D_{BCZ-2} mylonite fabrics, which are present along the trace of the Cabot Fault, correspond with a linear expression on aeromagnetic images and suggest that the Cabot Fault was initiated during the late Early to Late Silurian.

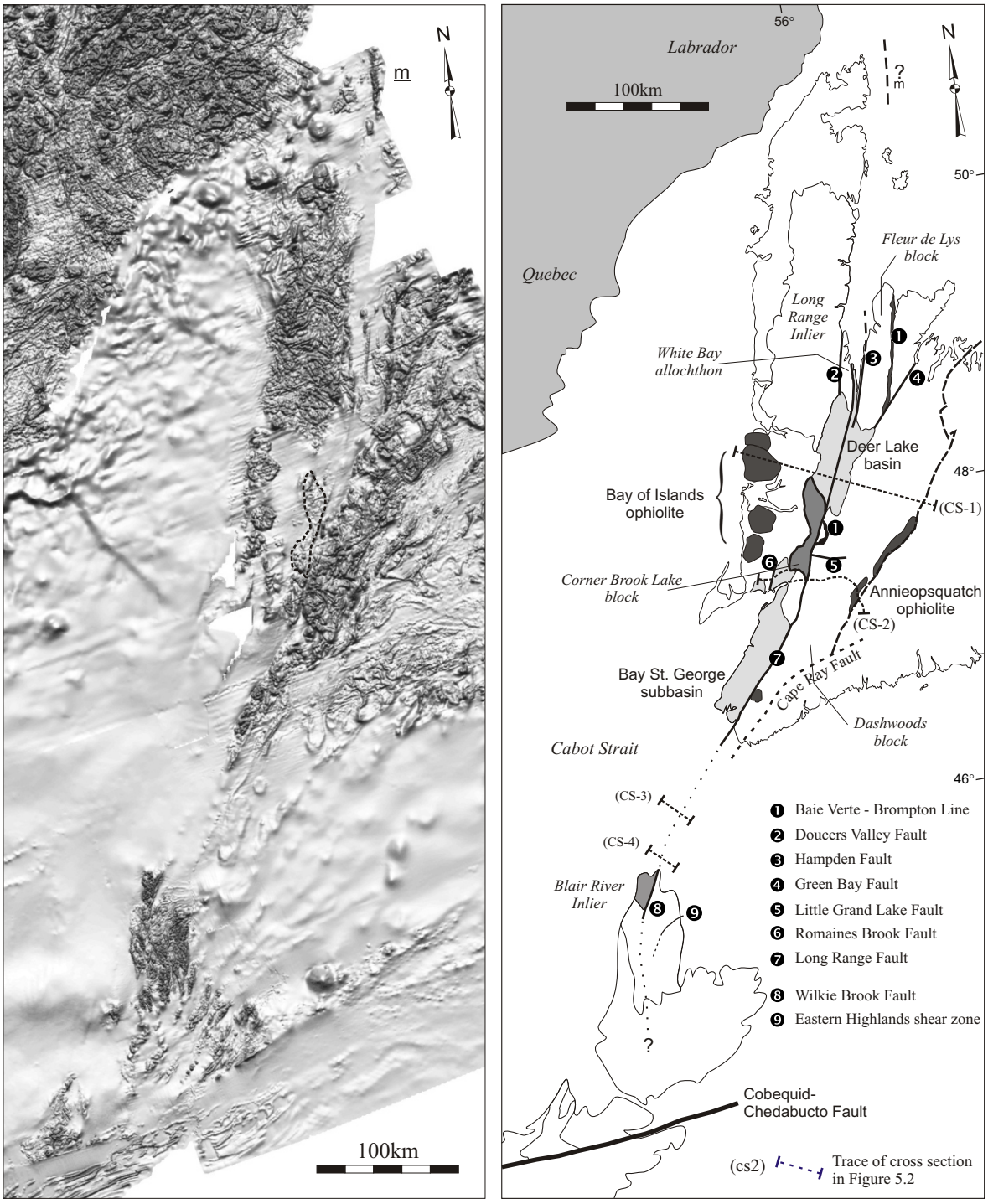

Figure 5.1 Aeromagnetic map (left) and interpretation (right) of the Laurentian realm in west Newfoundland and Cape Breton Island. Position of the Corner Brook Lake block is outlined on the aeromagnetic image. Geological Survey of Canada.

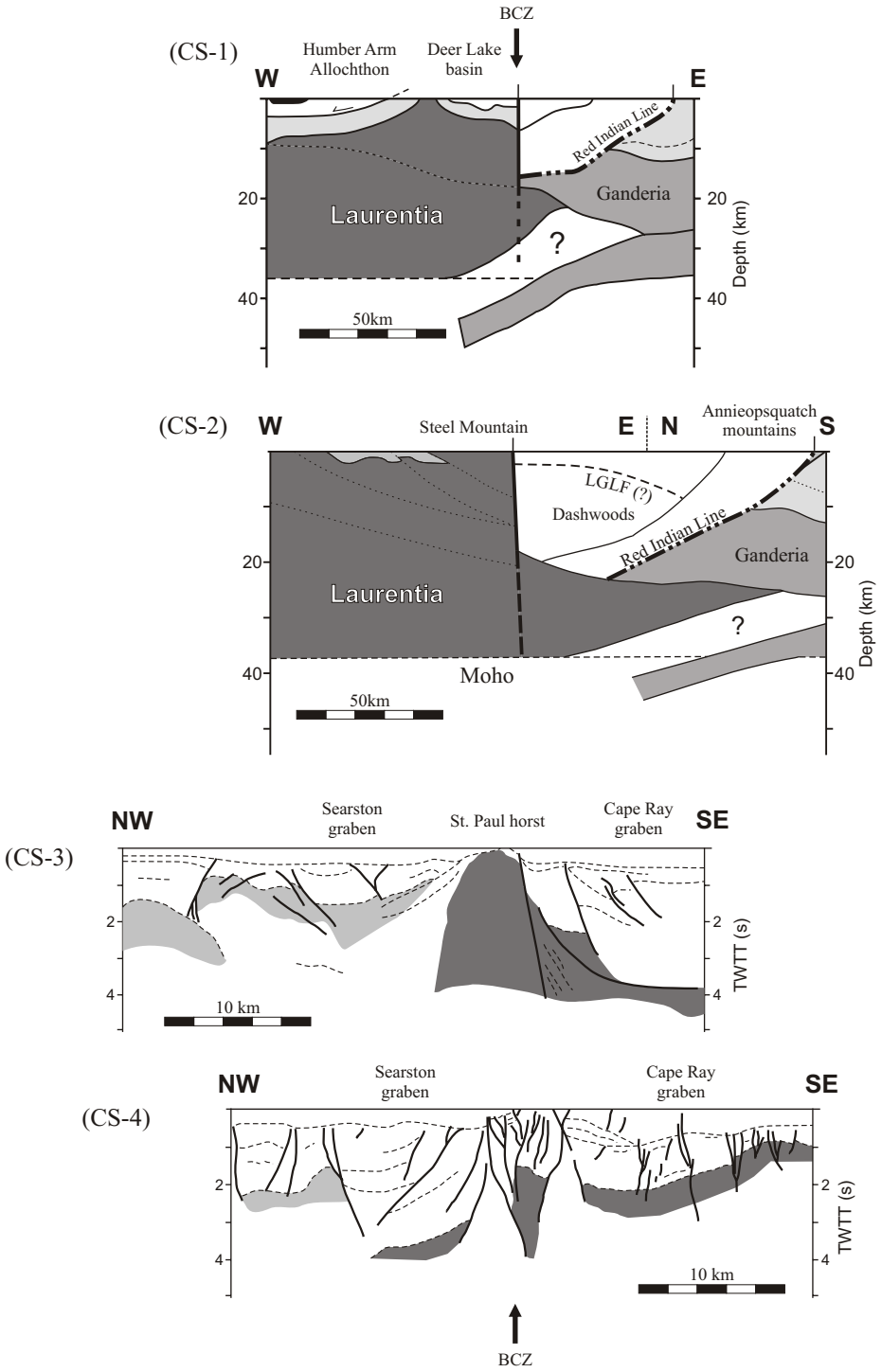

Figure 5.2 Interpretative cross sections based on seismic reflection studies across the BCZ in and south of the Newfoundland Appalachians. The diagrams show the crustal-scale character of the BCZ. The surface trace of each section is shown in Figure 5.1. Note the differences in scale. CS-1 and CS-2 (Lithoprobe 1989) modified from van der Velden et al. (2004). CS-3 and CS-4 (PetroCanada 81-1115 and 81-1121 respectively) modified from Langdon and Hall (1994).

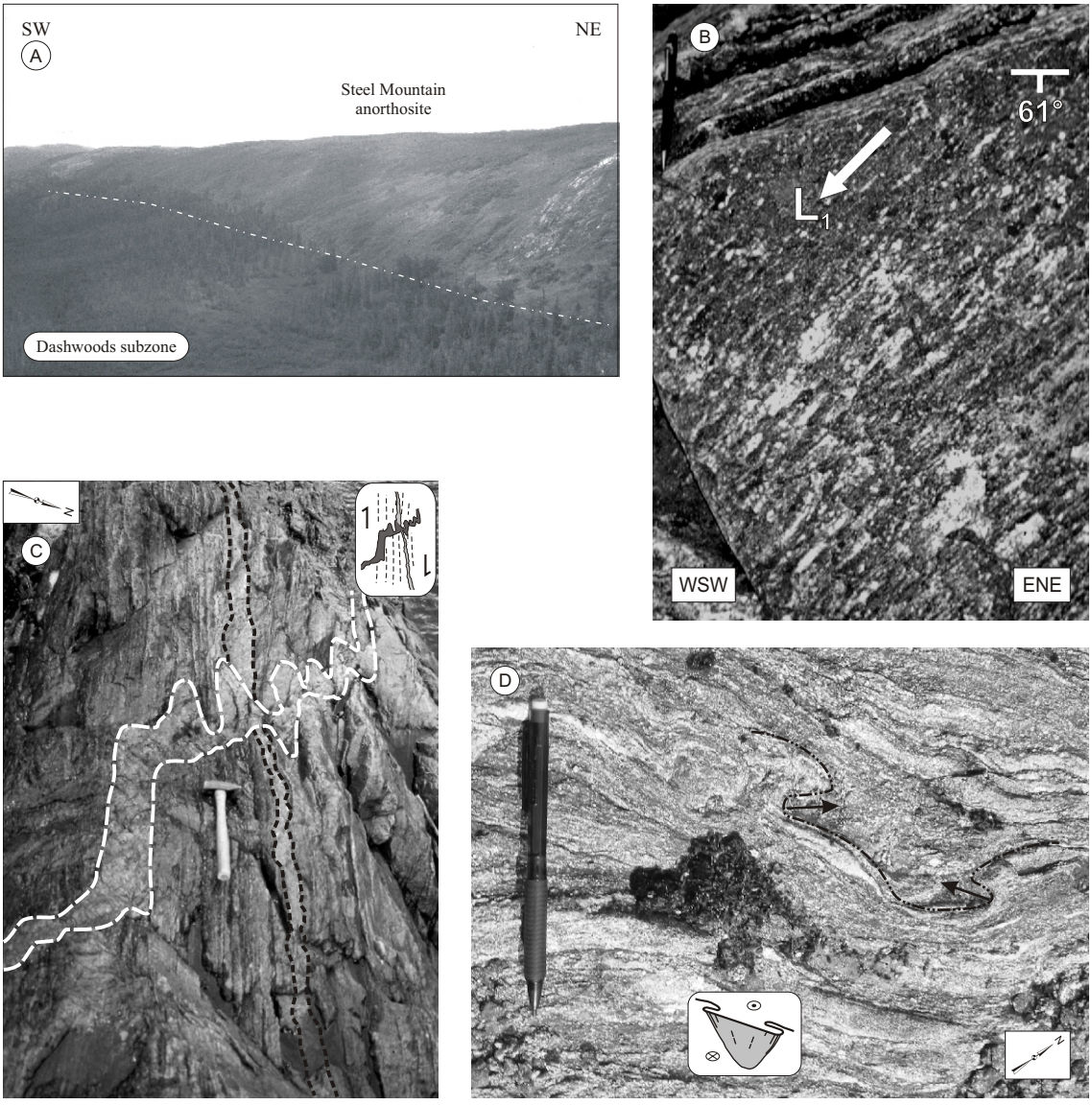

Figure 5.3 Field photographs showing the geomorphology of the BCZ and the D_{BCZ-1} fabric (see also Chapter 2). (**A**) The geomorphology of the BCZ as seen along the Steel Mountain anorthosite complex (near AB-01-100). (**B**) L_1 stretching lineation of quartz-feldspar aggregates plunging moderately SW on the gneissic foliation (AB-01-104). (**C**) Conjugate set of ca. 455 Ma late syntectonic pegmatite dykes. The geometry demonstrates a dextral sense of shear for D_{BCZ-1} (AB-01-104). (**D**) Sheath fold in high-strain zone developed in paragneiss, with vertical foliation, down-dip mineral lineation, northeast plunging Z-fold axis and southwest plunging S-fold-axis. Such geometry is indicative of a northwest-side-up movement (AB-02-228).

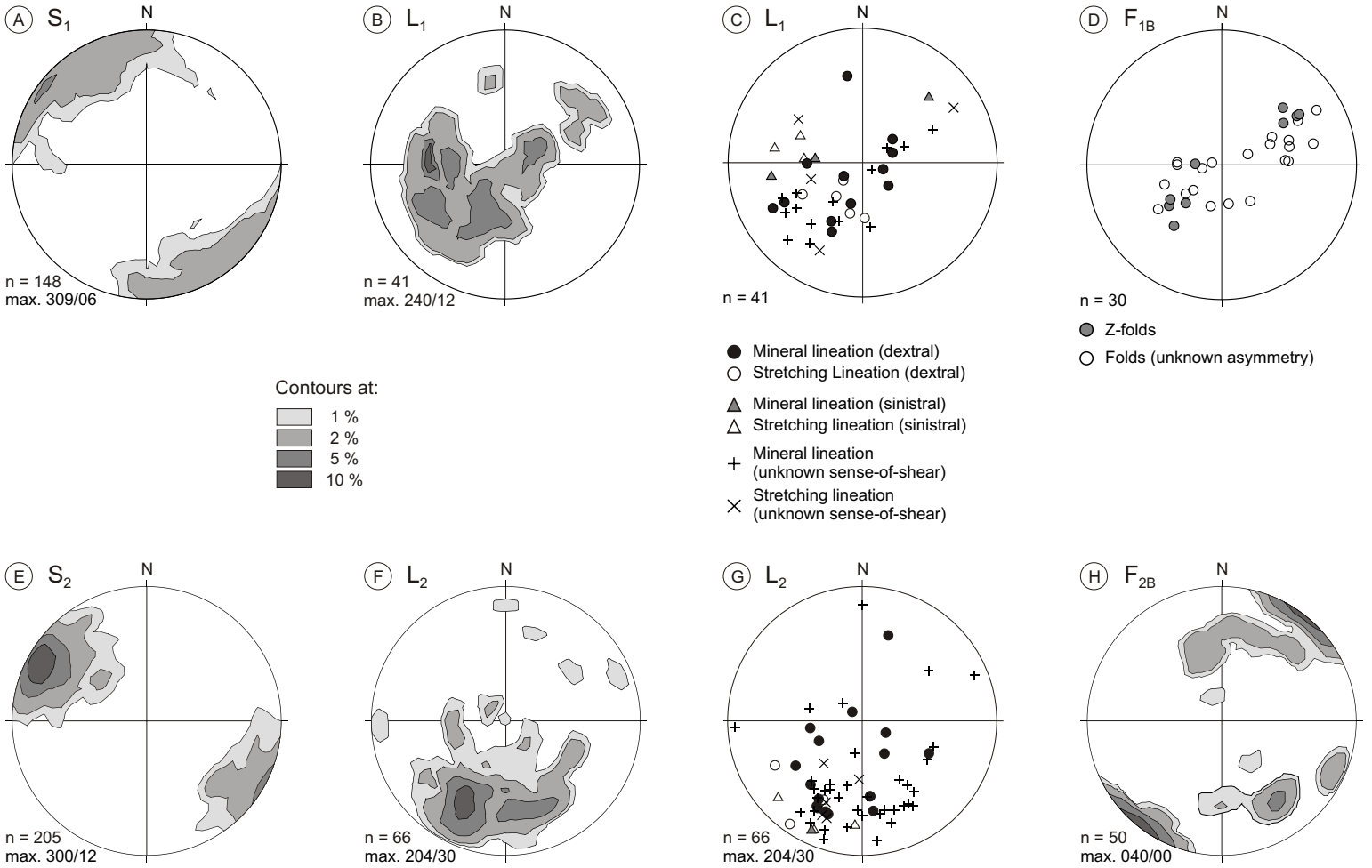

Figure 5.4 Equal-area lower-hemisphere projections of gneissose D_{BCZ-1} (A to D) and schistose D_{BCZ-2} (E to H) mylonites in the BCZ. (**A**) Contours of poles to S_1 foliation. (**B**) Contours of L_1 lineations. (**C**) L_1 lineations, showing the orientation of sinistral and dextral kinematic indicators. (**D**) Fold axes of F_{1B} asymmetric folds. (**E**) Contours of poles to S_2 foliation. (**F**) Contours of L_2 lineations. (**G**) L_2 lineations, showing the orientation of sinistral and dextral kinematic indicators. (**H**) Fold axes of F_{2B} folds.

Figure 5.5 Photographs showing characteristics of D_{BCZ-2} fabrics. (**A**) Field photograph of dextral D_{BCZ-2} S-C mylonite, along the western shore of Grand Lake. Picture taken down towards the northeast (AB-02-172). (**B**) Photograph of oriented hand sample showing an σ-shaped object indicative of dextral shear. Image is perpendicular to the foliation; the lineation plunges shallowly to the left into the page (AB-01-089). (**C**) Photomicrograph of D_{BCZ-2A} plagioclase porphyroclast (white Pl) showing dynamic recrystallization of quartz and feldspars (yellow Pl) within the grain, giving it a poikilitic texture. (AB-01-062).

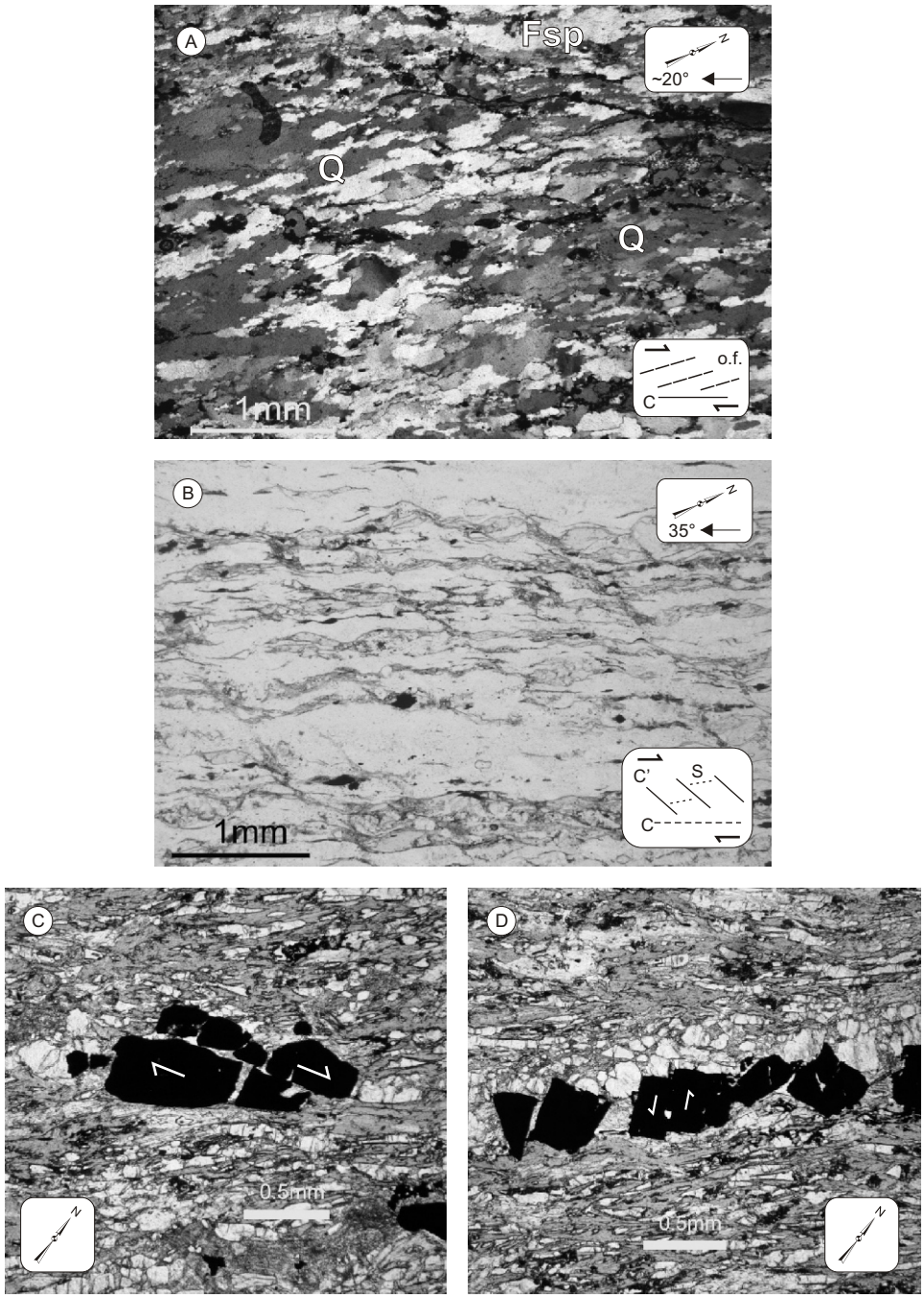

Figure 5.6 Photomicrographs of dextral D_{BCZ-2} fabrics in the BCZ. (**A**) Oblique foliation (o.f.) developed in metapsammitic rock of the South Brook Formation, indicating a dextral sense of shear. These metasedimentary rocks were emplaced during the Early Silurian Salinic orogeny (Chapter 3), therefore the D_{BCZ-2} is interpreted as being post-Salinic (<ca. 430 Ma) in age (AB-01-111). (**B**) S-C' mylonite fabric showing a dextral sense of shear (AB-01-057). (**C**) synthetic and (**D**) antithetic fractures developed in pyrite crystals (opaque) in a muscovite-chlorite schist, indicating dextral sense of shear. The pyrite in the outcrop is associated with late-D_{BCZ-2} quartz veins (AB-03-399).

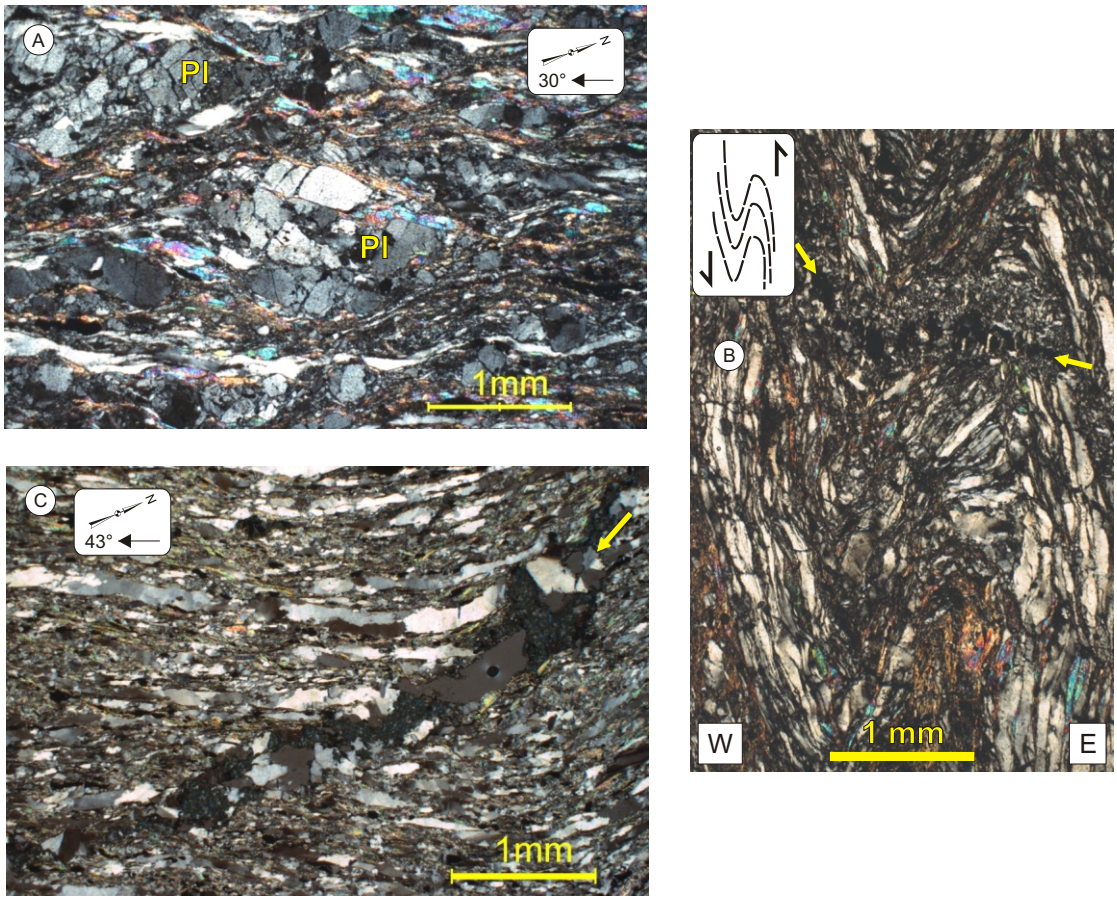

Figure 5.7 Photomicrographs of features associated with D_{BCZ-2} fabrics. (**A**) Internally fractured plagioclase porphyroclast (Pl) in a D_{BCZ-2B} mylonite fabric (AB-02-170). (**B**) Tight asymmetric (S-type) folding of D_{BCZ-2B} fabric, corroborating sinistral (east-side-up) sense of shear observed in outcrop. The D_{BCZ-2B} fabric is crosscut by a quartz-chlorite vein (yellow arrow) which appears to have intruded during the latest stages of folding (AB-01-059). (**C**) D_{BCZ-2B} mylonite, rich in quartz parallel to the foliation. The D_{BCZ-2B} fabric is truncated at low angle by a quartz-chlorite vein (AB-01-090).

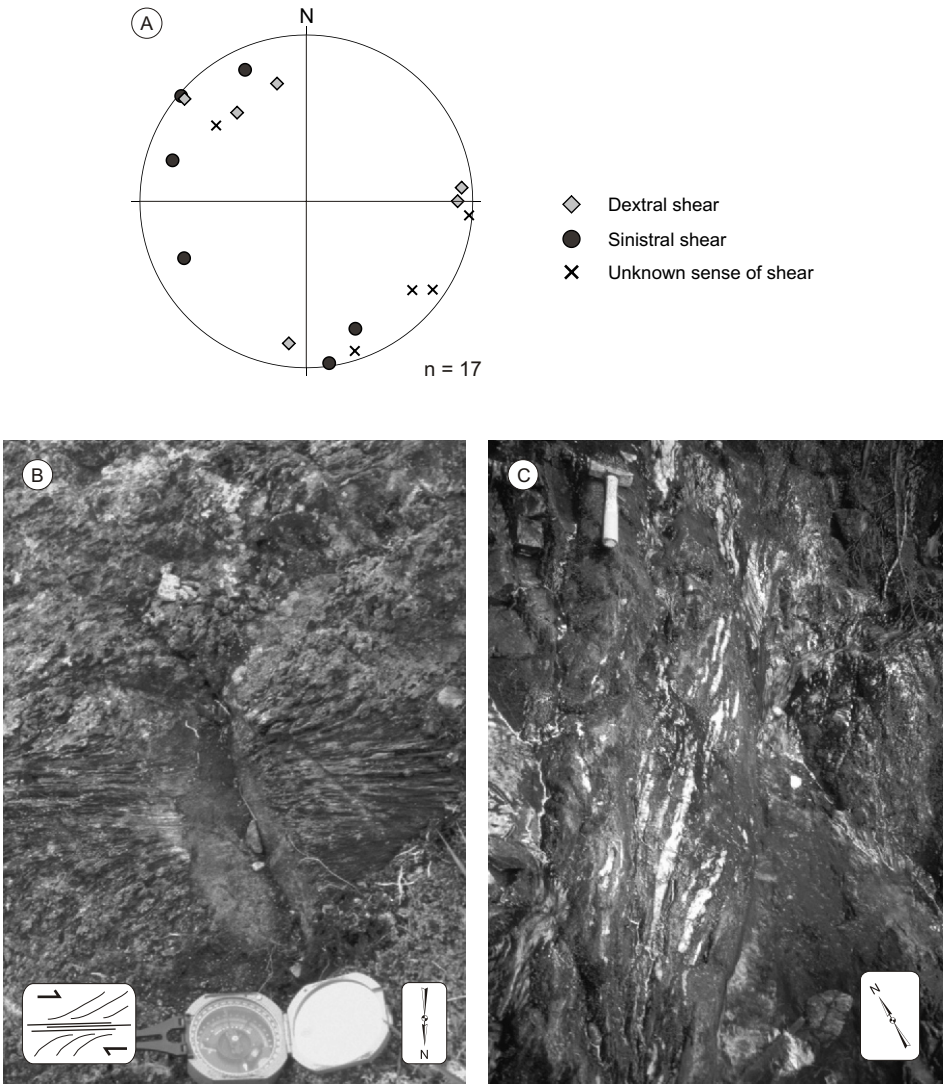

Figure 5.8 (**A**) Equal-area lower hemisphere projection of D_{BCZ-3} brittle-ductile shear zones showing the randomness in the strike of the shear zones and their senses of shear. (**B**) Field photograph of brittle-ductile D_{BCZ-3} shear zone in the Steel Mountain anorthosite showing drag of the pre-existing fabric, suggesting a dextral sense of shear (AB-01-097). (**C**) Field photograph of closely spaced en-echelon quartz veins within a brittle-ductile D_{BCZ-3} shear zone (AB-01-137).

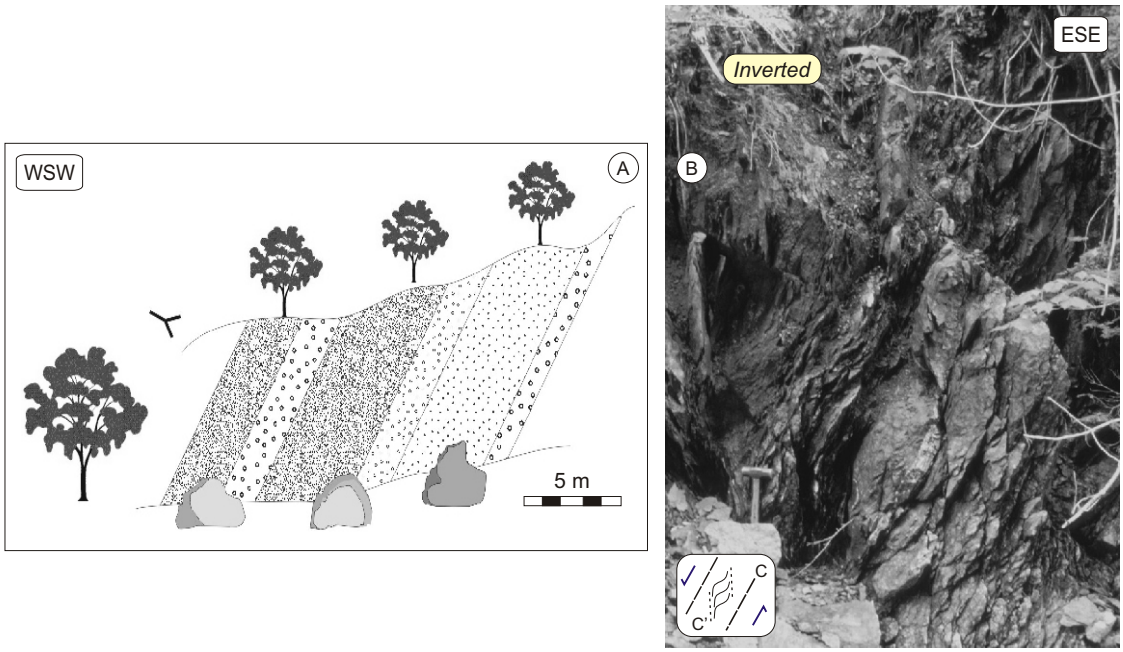

Figure 5.9 Composite diagram of D_{BCZ-4} west-side-down normal faulting in the BCZ along the Carboniferous Bay St. George subbasin. (**A**) Sketch diagram of steeply west-dipping clastic sediments of the Visean Codroy Group. (**B**) D_{BCZ-4} west-side-down brittle-ductile normal faulting in Dashwoods subzone rocks adjacent to Carboniferous Bay St. George subbasin (AB-03-399). Please note that in outcrop this photograph was taken to the south, and the image has been flipped horizontally for display reasons. Distance between diagrams (A) and (B) is ca. 50 m.

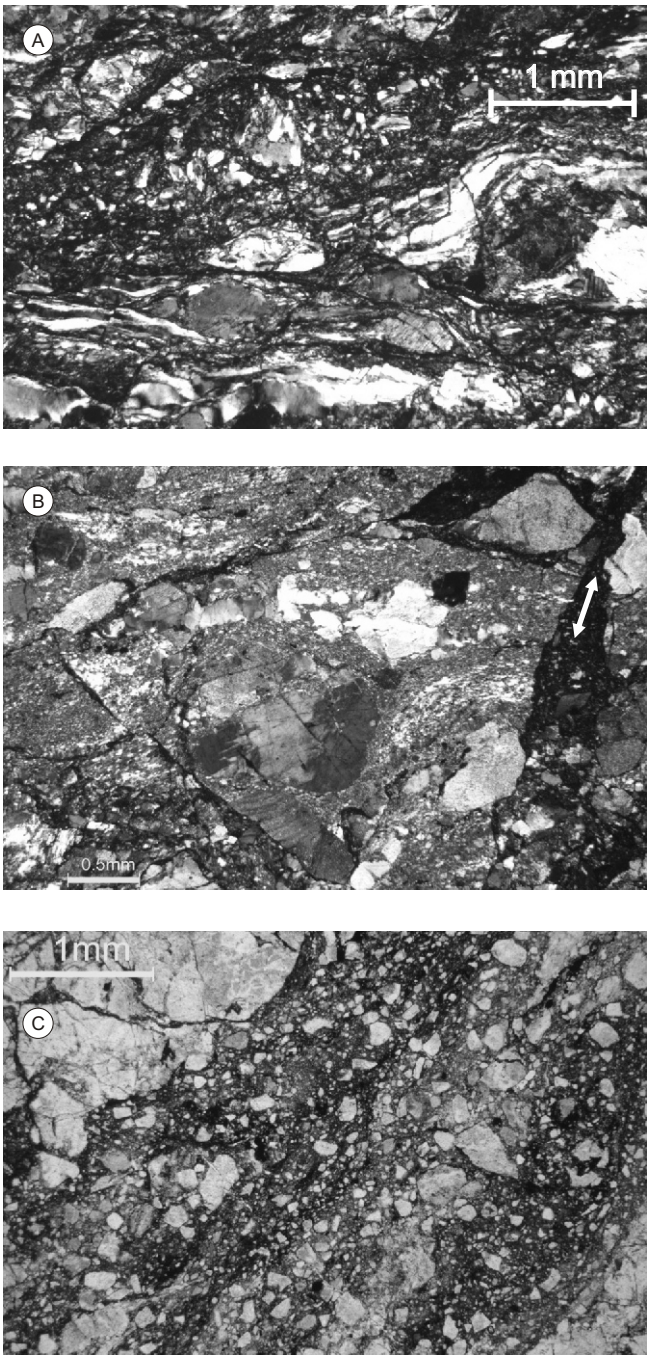

Figure 5.10 Photomicrographs of D_{BCZ-5} brittle fabrics. (**A**) Brittle fracturing of a D_{BCZ-2} mylonitic fabric (AB-01-110). (**B**) Irregular pseudotachylite fracturing (arrow) of a pre-existing ductile (D_{BCZ-2}) and the brittle fabric (AB-01-123). (**C**) Dominant cataclastic fracturing (AB-01-096).

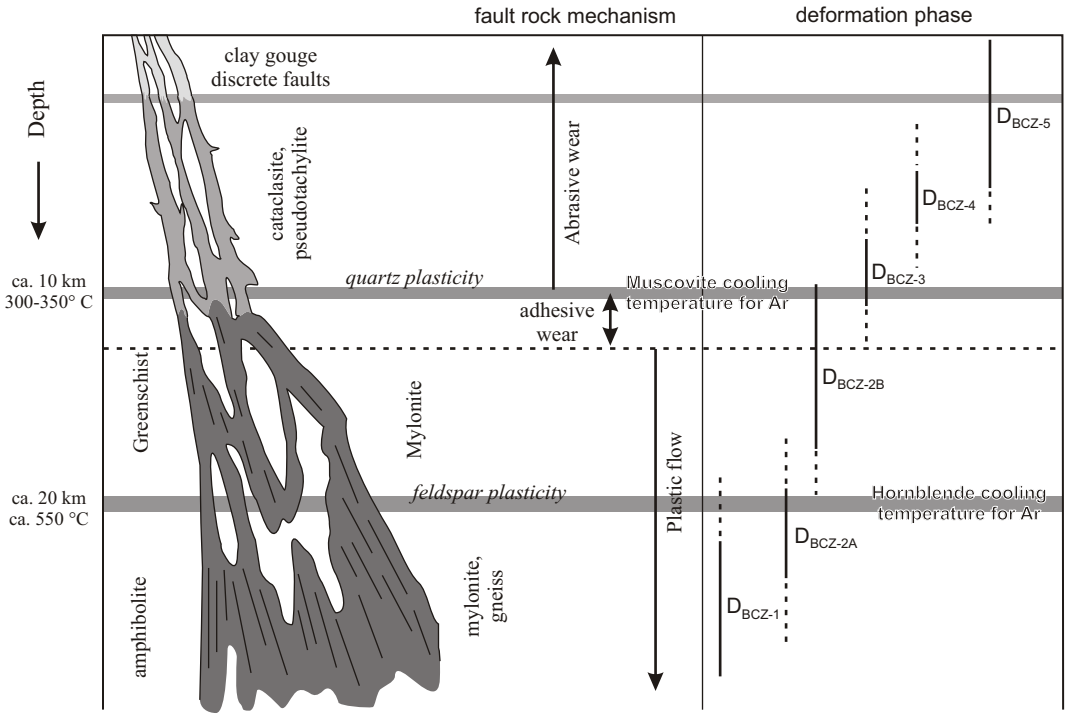

Figure 5.11 Schematic depth-profile of the BCZ as a crustal-scale tectonic zone. The diagram shows the D_{BCZ-1} to D_{BCZ-5} deformational events with respect to their interpreted crustal-level. Modified after Vernon (2004).

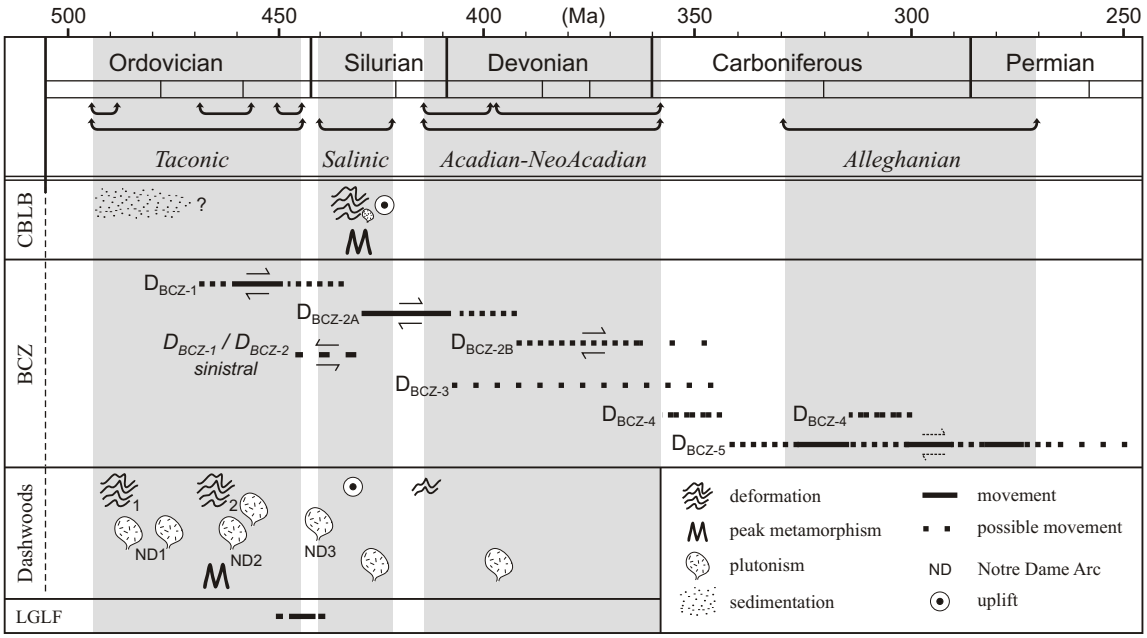

Figure 5.12 Chronological summary of the D_{BCZ-1} to D_{BCZ-5} deformational events in the BCZ in southwestern Newfoundland. Also displayed for reference are: the dynamo-thermal events from the Corner Brook Lake block (CBLB; Chapter 3), the single deformation event along the Little Grand Lake Fault (LGLF; Chapter 2), and the tectono-magmatic events from the Dashwoods block (Chapter 2; Pehrsson et al., 2003; and Figure 2 in van Staal, 2007).

Chapter 6: Summary and Tectonic Model for the Laurentian Margin of the Newfoundland Appalachians

6.1. Introduction

This thesis was aimed at studying the differences in dynamo-thermal histories of the Corner Brook Lake block (CBLB; internal Humber Zone) and Dashwoods subzone (western Dunnage Zone). In the previous chapters, the tectonic history of both segments has been discussed. In addition, the kinematic evolution of the BCZ, the tectonic zone that separates the CBLB from Dashwoods, has been characterized. The results indicate that strike-slip tectonics has played a more important role during the Early Palaeozoic Appalachian orogeny than is presently appreciated. In this final chapter, the main observations and conclusions from each previous chapter are summarized, and a schematic Late Neoproterozoic - Early Palaeozoic tectonic history focusing on the Laurentian margin of the Newfoundland Appalachians is proposed.

6.2. Summary of Conclusions

6.2.1. Dashwoods Subzone – Microcontinent (Chapter 2)

- The Dashwoods subzone, interpreted as representing an Early Palaeozoic microcontinent (Waldron and van Staal, 2001), is underlain by a crystalline basement with U-Pb ages of ca. 1.0 Ga (Grenvillian *sensu stricto*) and ca. 1.5 Ga (Pinwarian), which closely resembles the Long Range Inlier in northern Newfoundland.
- U-Pb ID-TIMS and SHRIMP geochronological analyses on variously sheared igneous rocks from the Dashwoods subzone have demonstrated the presence of numerous ca. 460 Ma latest Middle

Ordovician granitoid plutons. These igneous rocks form part of the regionally voluminous 2nd phase of the Notre Dame Arc.

- The conjugate set of late syntectonic pegmatite dykes that crosscuts a mylonitic foliation constrains the minimum age of the main phase of deformation in the Dashwoods subzone to be ca. 455 Ma, and demonstrates a Late Ordovician dextral sense of shear along the BCZ.
- During the Late Ordovician-earliest Silurian, Dashwoods had a southward translation relative to the Humber Zone.

6.2.2. Little Grand Lake Fault (LGLF) – Northern Dashwoods Boundary (Chapter 2)

- The LGLF accommodated south-side-up reverse movement during a single deformation phase.
- Deformation on the LGLF is constrained between ca. 463 Ma (age of emplacement of the host-rock) and ca. 440 Ma ($^{40}Ar/^{39}Ar$ cooling ages on muscovite). Given the retrograde character of the fabric, movement is most likely to have occurred between latest Ordovician and earliest Silurian (ca. 450-440 Ma), post-dating the main orogenic event in the Dashwoods and synchronous with the southward translation of Dashwoods relative to the Humber Zone.

6.2.3. Corner Brook Lake Block (CBLB) – Internal Humber Zone (Chapters 3 and 4)

- The CBLB has been affected by Early Silurian Salinic west-vergent deformation (D_{SED-1} and D_{SED-2}) and associated amphibolite facies metamorphism. There is neither geochronological nor petrographic evidence for a penetrative Taconic dynamo-thermal event to have affected the rocks of the CBLB. Therefore, the CBLB remained at upper-crustal levels during the Ordovician and could not have been involved in a significant tectono-metamorphic event until the Early Silurian (cf. Cawood et al., 1994).

- The CBLB is underlain by a regionally unique basement, with a U-Pb signature of 600 Ma and 1.5 Ga ages. More importantly, it is devoid of Grenvillian *sensu lato* (ca. 1.0-1.3 Ga) ages that are regionally omnipresent. Hence it cannot represent para-autochthonous basement in the Newfoundland Appalachians, such as the Long Range Inlier.
- The CBLB is interpreted as representing a suspect terrane, based on its unique basement signature and distinct Early Palaeozoic dynamo-thermal history. The CBLB shares several similarities with the Proterozoic basement of Ganderian terranes, but given the currently available geological data on its Palaeozoic cover, the CBLB is best interpreted as a Laurentian fragment.
- During the Late Neoproterozoic the CBLB was most likely positioned along the Laurentian craton margin north of the Grenville magmatic front in close proximity to the Pinware terrane (Figures 3.13 and 4.3).

6.2.4. Baie Verte-Brompton Line - Cabot Fault Zone (BCZ) (Chapters 2 and 5)

- The BCZ is a long-lived (ca. 455 to 290 Ma) and kinematically complex crustal-scale tectonic zone that has accommodated predominant oblique-dextral movement. Five phases of deformation have been identified in the area south of the Deer Lake basin and demonstrate a progressive evolution of the tectonic zone from mid-crustal levels (D_{BCZ-1} gneisses and D_{BCZ-2} mylonites) to high-crustal levels (D_{BCZ-5} cataclasites).
- Late Ordovician - earliest Silurian (ca. 455 to <446 Ma) D_{BCZ-1} is characterized by high-strain gneisses, which show evidence for an oblique-dextral sense of shear. Movement may have started earlier during the Middle Ordovician (ca. 465 Ma), since deformation in these Dashwoods gneisses was synchronous with peak metamorphism (C.R. van Staal, personal communication, 2006). The dextral movement facilitated the southwards translation of the Dashwoods microcontinent during and after arc-continent collision.

- Post-Salinic late Early Silurian - earliest Devonian (ca. 430-410 Ma) D_{BCZ-2} is characterized by greenschist facies mylonites that are present along the trace of the Cabot Fault and have recorded a dextral transcurrent movement. These fabrics correspond with a regional aeromagnetic lineament and could be regarded as representing the initiation of the Cabot Fault.
- Dominant Early Palaeozoic dextral deformation in the BCZ (D_{BCZ-1} and D_{BCZ-2}) may have profound implications for terrane correlations in, and tectonic reconstructions of, the northern Appalachians, especially when large-scale orogen-parallel motions have occurred along this crustal-scale tectonic zone.

6.3. Late Neoproterozoic to Early Palaeozoic Evolution of the Laurentian Margin of the Newfoundland Appalachians

Using the new observations and interpretations, combined with previously published data and models, a tectonic history for the Laurentian margin of the Newfoundland Appalachians can be constructed. The model presented here (Figure 6.1) is focused on the Laurentian realm of the Newfoundland Appalachians. The size of some segments is enlarged (e.g. Coney Head complex) and in several instances previously introduced tectonic segments are omitted from subsequent cartoons (e.g. Lush's Bight oceanic tract, Figure 6.1F), both for the purpose of clarity. The southern continuation into Cape Breton of western Dunnage Zone tectonic elements, most notably the Dashwoods block, is uncertain. These tectonic elements may have been: (1) discontinuous in their original Neoproterozoic-Palaeozoic geodynamic setting (see Section 3.6.1; van Staal, 2007); (2) buried beneath the Blair River Inlier and/or the Aspy terrane in Cape Breton (e.g. Lin et al., in press); or (3) exhumed and eroded after collision (Lin et al., in press). Therefore, the lateral continuity of western Dunnage Zone elements is not addressed in this reconstruction. All compass directions given are in present-day reference frame.

During the Late Neoproterozoic (ca. 610-600 Ma), the Laurentian margin of eastern Canada was characterized by anorogenic rift-related magmatism, as evidenced by the ca. 615 Ma Long Range dykes in Labrador (Kamo et al., 1989) and the Long Range Inlier (Stukas and Reynolds, 1974), and possibly by the various ca. 605 Ma granitoid plutons in the CBLB (e.g. Williams et al., 1985; Currie et al., 1992). This phase represents the prelude to the opening of the main Iapetus Ocean basin at ca. 570 Ma (Figure 6.1A; Cawood et al., 2001). Subsequent latest Neoproterozoic (ca. 550 Ma) rift-related magmatism (Lady Slipper pluton; Cawood et al., 1996) and sedimentation marked the departure of the Dashwoods block from the Laurentian margin (ca. 550-530 Ma; Waldron and van Staal, 2001), thereby creating the Humber seaway. Dashwoods likely rifted from a position near the Long Range Inlier, based on the comparable signature of its unexposed basement with the Long Range Inlier (Section 2.6.4). As mentioned in Chapter 3, the allochthonous Long Range Inlier is interpreted to have had a clockwise rotation of 10-20° relative to its Neoproterozoic position (Murthy et al., 1992; Waldron and Stockmal, 1994). Also, its abrupt southern termination has been attributed to a pre-existing transverse fault in the continental margin (Cawood and Botsford 1991; Waldron and Stockmal, 1994). Hence, the Long Range Inlier likely represented a promontory in the Humber seaway, and the area immediately to the south represented a re-entrant (e.g. Figure 6.1B). During the Neoproterozoic rifting stages, the CBLB would have been situated along the Laurentian margin to the north of the Long Range Inlier in close proximity to the Pinware terrane (Figure 6.1A and B; Section 4.5).

Convergence on the Laurentian side of the Iapetus Ocean started in the Early to Middle Cambrian. Initiation of an east-dipping subduction zone located east of Dashwoods created the supra-subduction zone Lush's Bight oceanic tract (510-501 Ma; Figure 6.1C), which was subsequently emplaced onto the Dashwoods microcontinent in the Late Cambrian (ca. 495 Ma; Taconic 1; Figure 6.1D; Waldron and van Staal, 2001; van Staal, 2007).

After obduction of the Cambrian oceanic rocks, subduction relocated into the Humber seaway, where a new east-dipping subduction zone was initiated (Figure 6.1D). This generated the ca. 490 Ma supra-subduction zone Baie Verte oceanic tract (Waldron and van Staal, 2001; van Staal, 2007), which

includes the Grand Lake ophiolite complex (Appendix D). Closure of the Humber seaway occurred in a dextral convergent setting (Cawood and Suhr, 1992; Dewey, 2002) and was accompanied by coeval arc magmatism in the Dashwoods (489-477 Ma; 1st phase of the continental Notre Dame Arc; Dubé et al., 1994; van Staal, 2007) and in the Baie Verte oceanic tract (487-476 Ma; oceanic Snooks Arm arc; Bédard et al., 2000). Both arcs may have formed part of a continuous arc system, comparable to the present day Banda and Sunda arc system in Indonesia (Section 2.6.3; van Staal et al., 2007).

The obliquity of the dextral convergence between Dashwoods and the Laurentian margin most likely initiated and sustained the southward movement of the CBLB fragment (Figure 6.1D). The CBLB would have moved through the Humber seaway as an independent continental sliver. During continued convergence in the Humber seaway, roll-back of the downgoing slab into a 2nd order re-entrant created the ca. 485 Ma Bay of Island ophiolite (Cawood and Suhr, 1992, Bédard and Kim, 2002; van Staal, 2007). This re-entrant is conceivably the area south of the Long Range Inlier discussed above (Figure 6.1E).

Convergence of Dashwoods with the Laurentian margin continued into the Middle Ordovician and resulted in the sedimentary and tectonic loading of the external Humber Zone, initial emplacement of allochthons and associated obduction of ophiolites, including the Bay of Islands ophiolite (Waldron et al., 1998a), and sustained southward movement of the CBLB (Figure 6.1F). Evidence for the actual Middle Ordovician (ca. 470 Ma) collision between Dashwoods and the Laurentian margin (Figure 6.1G) is well-preserved in the Dashwoods subzone, as evidenced by regional deformation and high-grade metamorphism (Taconic 2; Pehrsson et al., 2003; van Staal et al., 2007). Deformation is coeval with voluminous arc magmatism (466-459 Ma; 2nd phase of Notre Dame Arc; Section 2.6; Dunning et al., 1989; van Staal et al., 2007). Collision is most likely to have occurred at the Long Range Inlier promontory (Figure 6.1G). The Coney Head complex, which is positioned in the White Bay Allochthon opposite to the Long Range Inlier (Figure 1.1), is an allochthonous segment containing a ca. 474 Ma tonalite (Dunning, 1987) that is lithologically and geochronologically similar to the Notre Dame Arc lithologies. Based on this, the Coney Head complex is tentatively interpreted as

representing a piece of Dashwoods. After the Middle Ordovician collision, the complex was likely detached from Dashwoods due to transcurrent movement on the BCZ, hence it remained close to the collision zone west of the BCZ. At the time of collision, the CBLB should have been located south of this collision zone in order to have avoided a strong Taconic deformational imprint (Section 3.6.2). Thus it would have moved at least 500 km in approximately 20 m.y., which corresponds with a velocity of ca. 2.5 cm/y. Such a velocity is similar to modern day analogues, for example the Mentawai sliver plate in the Sumatra trench, Indonesia (Malod and Kemal, 1996).

During the Arenig, probably after active subduction in the Humber seaway had ceased, a west-dipping subduction zone was initiated outboard (east) of Dashwoods (van Staal, 2007). In this new setting, the Annieopsquatch Accretionary Tract ophiolites and arc/back-arc igneous complexes (ca. 480-473 Ma; Lissenberg et al., 2005) were formed (Figure 6.1F), and were subsequently accreted to the eastern margin of Dashwoods in Middle Ordovician (Figure 6.1G; 468-459 Ma; Lissenberg et al., 2005). Final closure of the Iapetus Ocean was accomplished in Late Ordovician (455-450 Ma) when the peri-Gondwanan Victoria-Popelogan Arc collided with the composite Laurentian margin along the Red Indian Line (Taconic 3; Zagorevski et al, 2006), marking the end of the Taconic orogeny (van Staal et al., 2007). During this period, Dashwoods had a southward translation with respect to the Laurentian margin as evidenced by the D_{BCZ-1} fabrics in the BCZ (Figure 6.1H; Section 2.6.2; Chapter 5). Contemporaneously, the LGLF accommodated reverse movement bringing up the higher-grade Dashwoods and its Notre Dame Arc, with respect to the Snooks Arm Arc and its Baie Verte oceanic tract basement (Figure 6.1H; Notre Dame subzone; Section 2.6.3). During this pre-Salinic period, the tectonic history of the CBLB is uncertain. It is likely to have had a southward translation similar to Dashwoods (Figure 6.1H). However, its position was likely not too far away from the external Humber Zone south of the Long Range Inlier (Figure 6.1H), because it was soon to be accreted to the external Humber Zone during the Salinic orogeny (see below).

Continued westward subduction of peri-Gondwanan crust material beneath the eastern composite Laurentian margin produced 446-435 Ma calc-alkaline magmatism (3rd phase of Notre Dame Arc), which includes the ca. 446 Ma foliated granodiorite sheet (Section 2.5.2.4). During the Early Silurian, the Gander margin (van Staal, 1994) converged with the composite Laurentian margin, the leading edge of which is now represented by the Annieopsquatch Accretionary Tract (Figure 6.1I; Lissenberg et al., 2005). Convergence between Gander and Laurentia occurred in a sinistral setting (Doig et al., 1990; van Staal, 2007), which may have initiated sinistral movement along the BCZ (Section 5.6.6). The Gander terrane likely collided with Laurentia in closer proximity to the CBLB than to the Dashwoods (Figure 6.1I). This resulted in west-vergent thrusting and associated amphibolite facies metamorphism in the CBLB at ca. 430 Ma (Chapter 3; Cawood et al., 1994), thereby docking the CBLB fragment to the external Humber Zone. Based on simple palinspastic reconstructions, it is not unlikely that the Aspy terrane in Cape Breton (a Ganderian terrane) was in close proximity to the CBLB during collision (Figure 6.1I; Brem et al., 2006). In contrast, Dashwoods only experienced local deformation during regional uplift. Subsequent voluminous bimodal magmatism (433-429 Ma) throughout the Notre Dame subzone was associated with break-off of the Gander margin slab (Whalen et al., 2006).

Immediately after the docking of the CBLB, the Cabot Fault Zone was initiated, as evidenced by the well-developed D_{BCZ-2} mylonite fabrics along the trace of the BCZ (Chapter 5). Important post-Salinic dextral deformation (D_{BCZ-2}) in the Cabot Fault Zone allowed Dashwoods and its Notre Dame Arc to move southwards with respect to the CBLB and the Long Range Inlier, resulting in the partial juxtaposition of Dashwoods with the CBLB (Figure 6.1J). In addition to this orogen-parallel movement, the entire Laurentian realm, including the external Humber Zone (mid-Silurian erosion; Waldron et al., 1998a), the CBLB (Chapter 3; Cawood and van Gool, 1998) and the western Dunnage Zone (Whalen et al., 2006) experienced rapid uplift to sub-greenschist facies conditions. In the CBLB, this uplift may have been accommodated by reverse faulting (S_{BSZ}) in the basement rocks (Section 3.5).

During the Acadian (Early Devonian) and Neoacadian (Middle-Late Devonian) orogenies, the CBLB and Dashwoods were both at high-crustal levels, and already partially juxtaposed, due to the post-Salinic dextral orogen-parallel movements in the BCZ discussed above. The external Humber Zone contains evidence for Middle Devonian (Acadian) thick-skinned west-vergent deformation, which has been interpreted as resulting from the collision between the Avalon composite terrane and Laurentia (Stockmal et al., 1998; Waldron et al., 1998a). This thick-skinned event involved the final emplacement of the allochthons in the external Humber Zone (cf. Waldron et al., 1998a) as well as the final rotation (10-20º clockwise rotation) and emplacement of the Long Range Inlier (Figure 6.1K; Section 3.6.1; Waldron and Stockmal, 1994). Even though no evidence is available, both the CBLB and the Dashwoods are likely to have been affected by this orogenic event.

The final stage of the Appalachian orogeny involved continent-continent collision between Gondwanaland and Laurentia. In the western Newfoundland Appalachians, the effects of this tectonic event are restricted to the Cabot Fault Zone and the associated sedimentary basins, the Bay St. George and Deer Lake basins (Knight, 1983; Hyde et al., 1988). Transcurrent movement along the BCZ allowed for opening of strike-slip basins, as likely evidenced by the D_{BCZ-4} normal shearing in the BCZ (Section 5.6.4). The BCZ accommodated dextral transpressional deformation (Hyde et al., 1988; Langdon and Hall, 1994; Cawood and van Gool, 1998), which resulted in faulting and folding of sedimentary rocks within the basins, and formed brittle faults and cataclastic zones in the BCZ (D_{BCZ-5}). Circa 140 km of cumulative dextral deformation along the BCZ (Section 3.6.2; Stockmal et al., 1990) allowed for the final juxtaposition of the CBLB and Dashwoods into its present-day configuration (Figure 6.1L).

6.4. Epilogue

Ever since I obtained the ca. 606 Ma emplacement age for the Disappointment Hill tonalite (Section 3.4.1.2), the geology of the CBLB basement has intrigued me. At first, I considered that the

CBLB represented a piece of Avalon, based on its Late Neoproterozoic age. After having reviewed other available geological data, I had to abandon this hypothesis. However, the distinct Proterozoic similarities between the CBLB and the composite peri-Gondwanan Gander terrane, which includes the Bras d'Or, Aspy, Brookville and New River terranes in Maritime Canada, are noteworthy. As mentioned in Section 4.5, basement in both the CBLB and Gander share a number of similarities. (1) Two distinct igneous pulses at ca. 550 Ma and ca. 605 Ma are found. (2) The ca. 600 Ma Late Neoproterozoic granitoid intrusions may be interpreted as representing a continental volcanic arc. For the Gander terrane this has readily been established, but for the CBLB, this pulse has been interpreted as representing rift-related magmatism (after Williams et al., 1985). (3) Sm-Nd isotopic data (ε_{Nd} at 600 Ma and T_{DM} model ages) are comparable, yet these are different from the Grenville Province (Figure 4.4). (4) Both terranes are overlain by Late Neoproterozoic sedimentary packages of which the detrital zircon signatures are not too dissimilar (compare Cawood and Nemchin, 2001; Barr et al., 2003b).

Unfortunately, most of the data is insufficient, either qualitatively or quantitatively, and therefore inconclusive as to the genetic link between the CBLB and Gander. Moreover, the overlying carbonate sequence in the CBLB (Breeches Pond Formation) is most likely of Laurentian affinity (cf. Nowlan and Neuman, 1995), an interpretation that is very difficult to ignore. Therefore with the currently available data, the most viable interpretation is that the CBLB represents a Laurentian fragment. Nonetheless, the clear similarities between the CBLB and Gander remain intriguing and I believe this would make for an interesting research project. Such a project would have to involve detailed geochemical and isotopic studies (including Sm-Nd), as well as paleomagnetic studies, which are currently not available for the CBLB. Also, the contact of the carbonate sequence (Breeches Pond Formation; passive margin carbonates) with the underlying units of the CBLB, currently believed to be primary (as opposed to tectonic), should be re-examined.

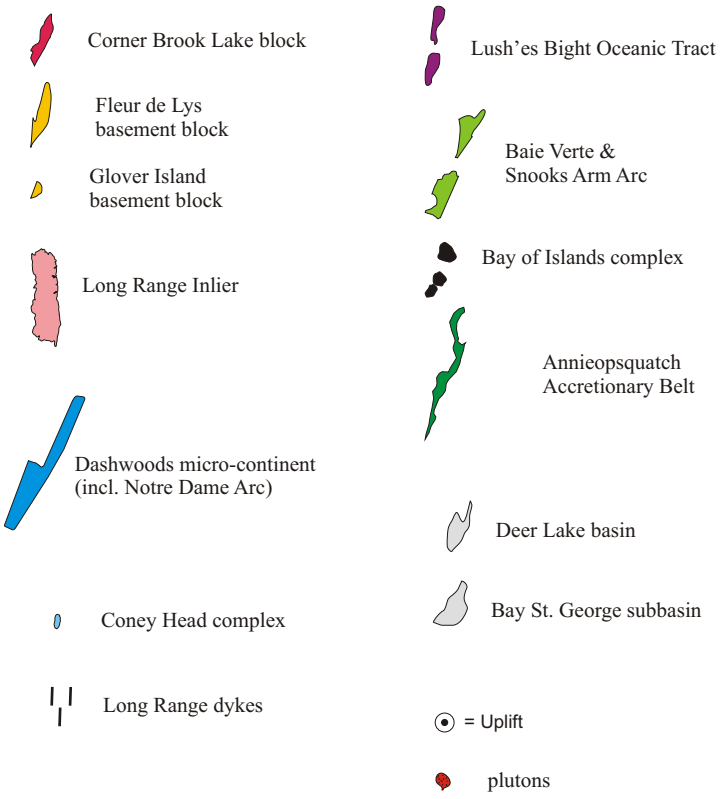

Legend to **Figure 6.1** "Schematic Late Neoproterozoic to Early Palaeozoic tectonic history for the Laurentian margin of the Newfoundland Appalachians."

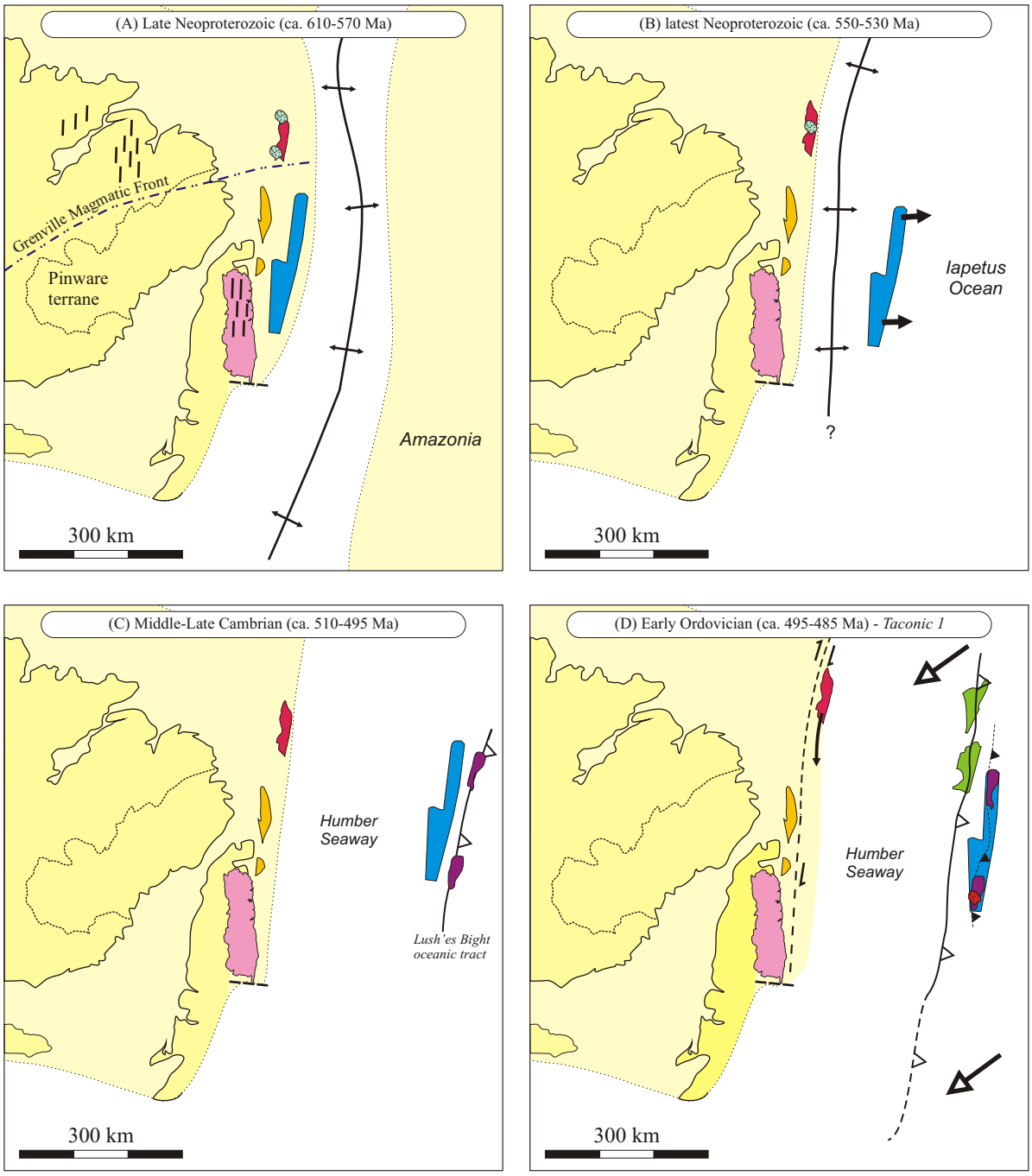

Figure 6.1 Schematic Late Neoproterozoic to Early Palaeozoic tectonic history for the Laurentian margin of the Newfoundland Appalachians. See Section 6.3 for detailed descriptions. (**A**) Late Neoproterozoic opening of Iapetus Ocean and associated basins. (**B**) Latest Neoproterozoic departure of the Dashwoods and opening of the Humber seaway. (**C**) Inception of convergence east of Dashwoods. (**D**) Obduction of the Lush's Bight oceanic tract, relocation of subduction zone into the Humber seaway and associated formation of the Baie Verte oceanic tract. Inception of southward movement of the CBLB through the Humber seaway due to oblique convergence between Dashwoods and the Laurentian margin. First phase of Notre Dame Arc stitches the Lush's Bight oceanic tract.

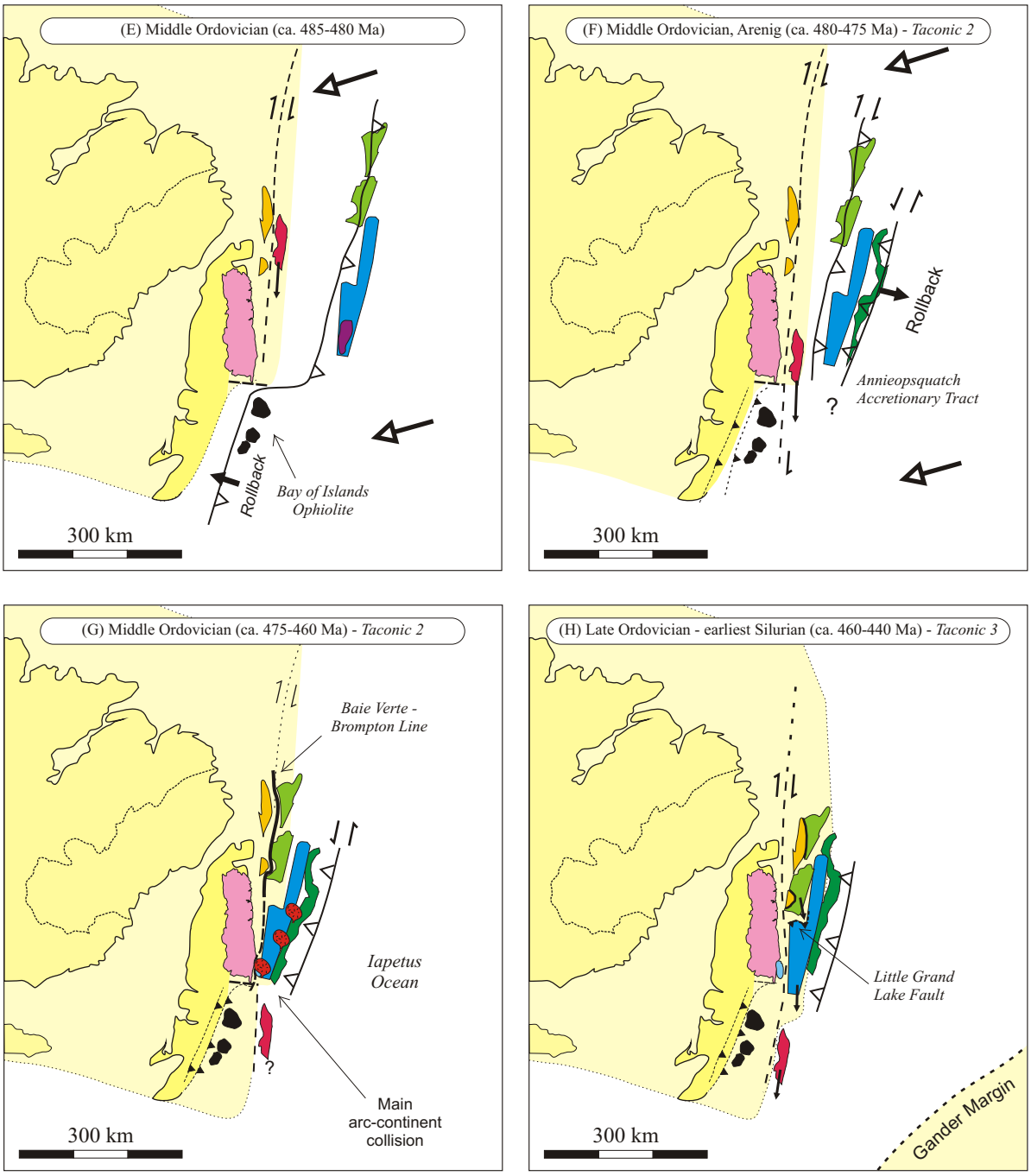

Figure 6.1 continued (**E**) Continued dextral convergence between Dashwoods and Laurentia, continued southward movement of the CBLB through Humber Seaway, rollback into the re-entrant south of the Long Range Inlier allowed for the Bay of Islands ophiolite to be formed. (**F**) Sedimentary loading of the external Humber Zone, emplacement of thin-skinned tectonic slices including ophiolite obduction (Bay of Islands), and formation of Annieopsquatch Accretionary Tract east of Dashwoods. (**G**) Arc-continent collision between Dashwoods and Laurentia at the Long Range Inlier, regional deformation and high-grade metamorphism in Dashwoods, coeval with voluminous tonalitic magmatism (2nd phase Notre Dame Arc), and continued accretion in Annieopsquatch Accretionary Tract east of Dashwoods. (**H**) Post-collisional state in which Dashwoods moved southward with respect to the Laurentian margin (D_{BCZ-1}), and LGLF accommodated south-side up movement, moving Dashwoods up with respect to the Notre Dame subzone.

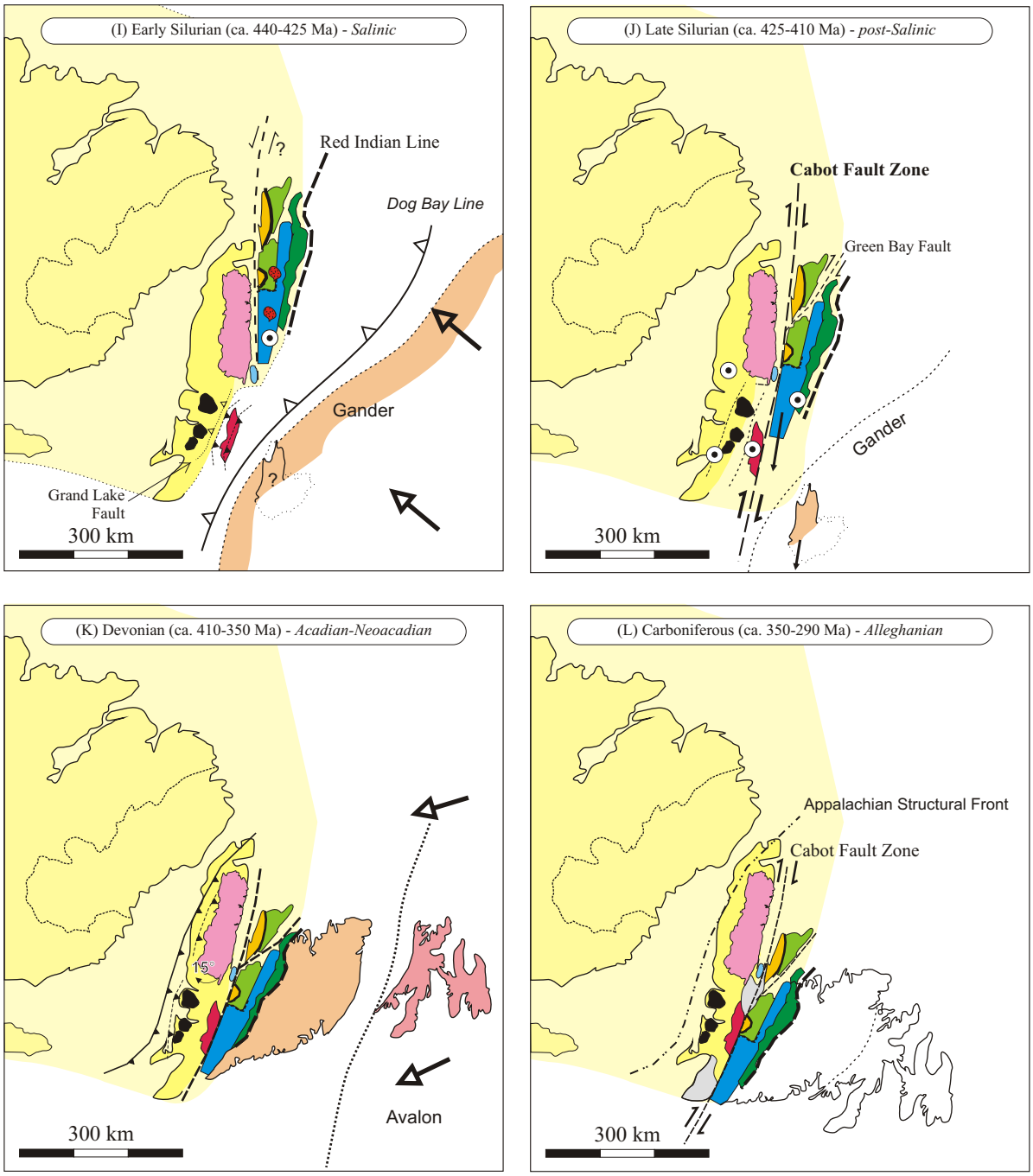

Figure 6.1 continued (**I**) Salinic sinistral convergence between Gander and Laurentia, strong west-vergent deformation (D_{SED-1} and D_{SED-2}) and associated metamorphism in the CBLB, and plutonism (3rd phase of Notre Dame Arc) and regional uplift affecting the Dashwoods block. (**J**) Rapid post-Salinic uplift of the region, including Dashwoods, CBLB, and the external Humber Zone, synchronous with important orogen-parallel dextral movement (D_{BCZ-2}) along the BCZ, allowing Dashwoods to be partially juxtaposed with the CBLB. (**K**) Collision of Avalon and Meguma (not shown here) with the composite Laurentian margin, thick-skinned west-vergent deformation in external Humber Zone, final emplacement of allochthons, and rotation of Long Range Inlier. (**L**) Alleghanian opening of and deformation in sedimentary basins spatially associated with the Cabot Fault Zone, and ca. 150 km dextral transcurrent movement along the BCZ resulting in the present-day configuration of the Newfoundland Appalachians.

References

Abraham, A.P.G., Davis, D.W., Kamo, S.L., and Spooner, E.T.C. (1994) Geochronological constraints on Late Archean magmatism, deformation and gold-quartz vein mineralization in the northwestern Anialik River greenstone belt and igneous complex, Slave Province, NWT. Canadian Journal of Earth Sciences, vol. 31, pp. 1365-1383.

Bailey, C., Owens B., and Shirvell, C.R. (2005) Northern ancestry for the Goochland terrane as a displaced fragment of Laurentia: COMMENT. Geology, Online FORUM, e70.

Barr, S.M., and Kerr, A. (1997) Late Precambrian plutons in the Avalon Terrane of New Brunswick, Nova Scotia, and Newfoundland. *In* The nature of magmatism in the Appalachian Orogen. *Edited by* A.K. Sinha, J.B. Whalen and J.P. Hogan, J.P. Geological Society of America, Memoir 191, pp. 45-74.

Barr, S.M., Raeside, R.P., and White, C.E. (1998) Geological correlations between Cape Breton Island and Newfoundland, northern Appalachian orogen. Canadian Journal of Earth Sciences, vol. 35, pp. 1252-1270.

Barr, S.M., White, C.E., and Miller, B.V. (2003a) Age and geochemistry of late Neoproterozoic and Early Cambrian igneous rocks in southern New Brunswick: similarities and contrasts. Atlantic Geology, vol. 39, pp. 55-73.

Barr, S.M., Davis, D.W., Kamo, S., and White, C.E. (2003b) Significance of U-Pb detrital zircon ages in quartzite from peri-Gondwanan terranes, New Brunswick and Nova Scotia, Canada. Precambrian Research, vol. 126, pp. 123-145.

Bartholomew, M.J., and Tollo, R.P. (2004) Northern ancestry for the Goochland Terrane as a displaced fragment of Laurentia. Geology, vol. 32, pp. 669-672.

Bédard, J. H., Lauzière, K., Tremblay, A., Sangster, A., Douma, S. L., and Dec, T. (2000) Betts Cove Ophiolite and its cover rocks, Newfoundland. Geological Survey of Canada, Bulletin 550, 76 pages.

Bédard, J.H., and Kim, J. (2002) Boninites in the NE Appalachian Notre Dame Subzone ophiolites: tectonic models for Iapetus terranes. Geological Society of America, Abstracts with Programs, vol. 34, p. A60.

Bird, J.M., and Dewey, J.F. (1970) Lithosphere plate-continental margin tectonics and the evolution of the Appalachian Orogen. Geological Society of America Bulletin, vol. 81, pp. 1031-1060.

Bradley, D.C. (1982) Subsidence in late Palaeozoic basins in the northern Appalachians. Tectonics, vol. 1, pp. 107-123.

Bradley, J.C. (2005) Structural history of the Humber Arm Allochthon in the Corner Brook area, western Newfoundland. Master's thesis, University of Alberta, Edmonton AB, Canada, 166 pages.

Brem, A.G., Lin, S., and van Staal, C.R. (2002) Humber Zone - Dunnage Zone relationships and the Long Range Fault, south of Grand Lake, western Newfoundland: preliminary results. Newfoundland Geological Survey, Current Research, Report 02-1, pp. 135-144.

Brem, A.G., Lin, S., and van Staal, C.R. (2003) Structural relationships south of Grand Lake, Newfoundland. Newfoundland Geological Survey, Current Research, Report 03-1, pp. 1-13.

Brem, A.G., Lin, S., van Staal, C.R., Davis, D.W., and McNicoll, V.J. (2004) Different styles and ages of deformation in the Cabot Fault Zone of Western Newfoundland: Geological Association of Canada Annual Meeting, Abstracts, vol. 29, pp. 135.

Cawood, P.A., and Botsford, J.W. (1991) Facies and structural contrasts across Bonne Bay cross-strike discontinuity, western Newfoundland. American Journal of Science, vol. 291, pp. 737-759.

Cawood, P.A., and Suhr, G. (1992) Generation and obduction of ophiolites: constraints for the Bay of Islands Complex, western Newfoundland. Tectonics, vol. 11, pp. 884-897

Cawood, P.A. (1993) Acadian Orogeny in West Newfoundland: definition, character, and significance. Geological Society of America, Special Paper 275, pp. 135-152.

Cawood, P.A., and Dunning, G.R. (1993) Silurian age for movement on the Baie Verte Line: implications for accretionary tectonics in the Northern Appalachians. Geological Society of America, Abstracts with Programs, vol. 25, pp. 422.

Cawood, P.A., Dunning, G.R., Lux, D., and van Gool, J.A.M. (1994) Timing of peak metamorphism and deformation along the Appalachian margin of Laurentia in Newfoundland: Silurian, not Ordovician. Geology, vol. 22, pp. 399-402.

Cawood, P.A., van Gool, J.A.M., and Dunning, G.R. (1995) Collisional tectonics along the Laurentian margin of the Newfoundland Appalachians. Geological Association of Canada, Special Paper 41, pp. 283-301.

Cawood, P.A., van Gool, J.A.M., and Dunning, G.R. (1996) Geological development of the eastern Humber and western Dunnage zones: Corner Brook-Glover Island region, Newfoundland. Canadian Journal of Earth Sciences, vol. 33, pp. 182-198.

Cawood, P.A., and van Gool, J.A.M. (1998) Geology of the Corner Brook - Glover Island region, Newfoundland. Geological Survey of Canada, Bulletin 427, 96 pages.

Cawood, P.A., and Nemchin, A.A. (2001) Paleogeographic development of the East Laurentian margin: constraints from U-Pb dating of detrital zircons in the Newfoundland Appalachians. Geological Society of America Bulletin, vol. 113, pp. 1234-1246.

Chew, D.M., and Schaltegger, U. (2005) Constraining sinistral shearing in NW Ireland: a precise U-Pb zircon crystallization age for the Ox Mountains granodiorite. Irish Journal of Earth Sciences, vol. 23, pp. 55-63.

Cross, T.A., and Pilger Jr., R.H. (1982) Controls of subduction geometry, location of magmatic arcs, and tectonics of arc and back-arc regions. Geological Society of America Bulletin, vol. 93, pp. 545-562.

Cumming, G.L., and Richards, J.R. (1975) Ore lead in a continuously changing Earth. Earth and Planetary Science Letters, vol. 28, pp. 55-171.

Currie, K.L., and Piasecki, M.A.J. (1989) Kinematic model for southwestern Newfoundland based upon Silurian sinistral shearing. Geology, vol. 17, pp. 938-941.

Currie, K.L. and van Berkel, J.T. (1992) Notes to accompany a geological map of the southern Long Range, southwestern Newfoundland: Geological Survey of Canada, Paper 91-10, 10 pages. *Includes* Geology, southern Long Range Mountains, Newfoundland. Geological Survey of Canada, Map 1815A, scale 1:100 000.

Currie, K.L., van Breemen, O., Hunt, P.A., and van Berkel, J.T. (1992) Age of high-grade gneisses south of Grand Lake, Newfoundland. Atlantic Geology, vol. 28, pp. 153-161.

Dallmeyer, R.D., and Williams, H. (1975) $^{40}Ar/^{39}Ar$ ages from the Bay of Islands metamorphic aureole: their bearing on the timing of Ordovician ophiolite obduction. Canadian Journal of Earth Sciences, vol. 12, pp. 1685-1690.

Daly, J.S. (2001) Precambrian. *In* The Geology of Ireland. *Edited by* C.H. Holland. Dunedin Academic Press Ltd, Edinburgh, pp. 7-45.

Davis, D.W. (1982) Optimum linear regression and error estimation applied to U-Pb data. Canadian Journal of Earth Sciences, vol. 19, pp. 2141-2149.

Dewey, J.F. (1969) Evolution of the Appalachian/Caledonian orogen. Nature (London), vol. 222, pp. 124-129.

Dewey, J.F., and Shackleton, R.S. (1984) A model for the evolution of the Grampian tract in the early Caledonides and Appalachians. Nature (London), vol. 312, pp. 115-121.

Dewey, J.F. (2002) Transtension in arcs and orogens. International Geology Reviews, vol. 44, pp. 402-439.

Dickin, A.P., and Raeside, R.P. (1990) Sm-Nd analysis of Grenville gneisses from Cape Breton Island, Nova Scotia. Proceedings of the LITHOPROBE-EAST Transect Meeting, St. John's, Newfoundland, pp. 37-38.

Dickin, A.P. (2000) Crustal formation in the Grenville Province: Nd-isotope evidence. Canadian Journal of Earth Sciences, vol. 37, pp. 165–181.

Dickin, A.P. (2004) Mesoproterozoic and Paleoproterozoic crustal growth in the eastern Grenville Province: Nd isotopic evidence from the Long Range Inlier of the Appalachian orogen. *In* Proterozoic tectonic evolution of the Grenville Orogen in North America. *Edited by* R.P. Tollo, L. Corriveau, J.M. McClelland, and M.J. Bartholomew. Geological Society of America, Memoir 197, pp. 495-503.

Dickin, A.P. (2005) Radiogenic Isotope Geology. Cambridge University Press, 2nd edition, 510 pages.

Doig, R., Nance, R.D., Murphy, J.B., and Casseday, R.P. (1990) Evidence for Silurian sinistral accretion of Avalon composite terrane in Canada. Journal of the Geological Society, London, vol. 147, pp. 927-930.

Dubé, B., Dunning, G. R., Lauziere, K., and Roddick, J.C. (1996) New insights into the Appalachian Orogen from geology and geochronology along the Cape Ray fault zone, southwest Newfoundland. Geological Society of America Bulletin, vol. 108, pp. 101-116.

Dunning, G.R. (1987) U/Pb geochronology of the Coney Head Complex, Newfoundland. Canadian Journal of Earth Sciences, vol. 24, pp. 1072-1075.

Dunning, G.R., Wilton, D.H.C., and Herd, R.K. (1989) Geology, geochemistry and geochronology of a Taconic batholith, southwestern Newfoundland. Transactions of the Royal Society of Edinburgh: Earth Sciences, vol. 80, pp.159-168.

Dunning, G.R., O'Brian, S.J., Colman-Sadd, S.P., Blackwood, R.F., Dickson, W.L., O'Neill, P.P., and Krogh, T.E. (1990) Silurian orogeny in the Newfoundland Appalachians. Journal of Geology, vol. 98, pp. 895-913.

Erdmer, P., and Williams, H. (1995) Grenville basement rocks (Humber Zone). *In* Geology of the Appalachian-Caledonian Orogen in Canada; Chapter 3: Lower Paleozoic and older rocks. *Edited by* H. Williams, pp. 50-61.

Evans, J., and Zalasiewicz, J. (1996) U-Pb, Pb-Pb and Sm-Nd dating of authigenic monazite: implications for the diagenetic evolution of the Welsh Basin. Earth and Planetary Science Letters, vol. 144, pp. 421-433.

Fox, D., and van Berkel, J.T. (1988) Mafic-ultramafic occurrences in metasedimentary rocks of southwestern Newfoundland. Geological Survey of Canada, Current Research, Paper 88-1B, pp. 41-48.

Gaboury, D., Dubé, B., Laflèche, M.R., and Lauzière, K. (1996) Geology of the Hammer Down mesothermal gold deposit, Newfoundland Appalachians, Canada. Canadian Journal of Earth Sciences, vol. 33, pp. 335-350.

Goodwin, L.B., and Williams, P.F. (1990) Strike-slip movement along the Baie Verte Line. *In* Lithoprobe Report. *Edited by* J. Hall. Vol. 13, pp. 75-84.

Goodwin, L.B., and Williams, P.F. (1996) Deformation path partitioning within a transpressive shear zone, Marble Cove, Newfoundland. Journal of Structural Geology, vol. 18, pp. 975-990.

Gower, C.F., and Krogh, T.E. (2002) A U-Pb geochronological review of the Proterozoic history of the eastern Grenville Province. Canadian Journal of Earth Sciences, vol. 39, pp. 795-829.

Haggart, J., Enkin, R.J., and Monger, J.W.H., *editors* (2006) Paleogeography of the North American Cordillera: evidence for and against large-scale displacements. Geological Association of Canada, Special Paper 46, 429 pages.

Hall, L.A.F., and van Staal, C.R. (1999) Geology, southern end of Long Range Mountains (Dashwoods subzone), Newfoundland. Geological Survey of Canada, Open File 3727, scale 1:50 000.

Hall, R., and Blundell, D.J., *editors* (1996) Tectonic Evolution of Southeast Asia. Geological Society Special Publication 106, 566 pages.

Harris, D.H.M. (1995) Caledonian transpressional terrane accretion along the Laurentian margin in Co. Mayo, Ireland. Journal of the Geological Society, London, vol. 152, pp. 797-806.

Heaman, L.M., Erdmer, P., and Owen, J.V. (2002) U-Pb geochronologic constraints on the crustal evolution of the Long Range Inlier, Newfoundland. Canadian Journal of Earth Sciences, vol. 39, pp. 845-865.

Heaman, L.M., Gower, C.F., and Perreault, S. (2004) The timing of Proterozoic magmatism in the Pinware terrane of Southeast Labrador, easternmost Quebec, and northwest Newfoundland. Canadian Journal of Earth Sciences, vol. 41, pp. 127-150.

Hibbard, J.P. (1983) Geology of the Baie Verte Peninsula, Newfoundland. Newfoundland Department of Mines and Energy, Memoir 2, 279 pages.

Hirth, G., and Tullis, J. (1992) Dislocation creep regimes in quartz aggregates. Journal of Structural Geology, vol. 14, pp. 145-159.

Hirth, G., Teyssier, C., and Dunlap, W.J. (2001) An evaluation of quartzite flow laws based on comparisons between experimentally and naturally derived rocks. International Journal of Earth Sciences, vol. 90, pp. 77-87.

Holdsworth, R.E. (1994) Structural evolution of the Gander-Avalon terrane boundary: a reactivated transpression zone in the NE Newfoundland Appalachians. Journal of the Geological Society, London, vol. 151, pp. 629-646.

Hoskin, P.W.O., and Schaltegger, U. (2003) The composition of zircon and igneous and metamorphic petrogenesis. *In* Zircon. *Edited by* J.M. Hanchar and P.W.O. Hoskin. Reviews in Mineralogy and Geochemistry, vol. 53, pp. 27-62.

Hutton, D.H.W. (1987) Strike-slip terranes and a model for the evolution of the British and Irish Caledonides. Geological Magazine, vol. 124, pp. 405-425.

Hyde, R.S., Miller, H.G., Hiscott, R.N., and Wright, J.A. (1988) Basin architecture and thermal maturation in the strike-slip Deer Lake Basin, Carboniferous of Newfoundland. Basin Research, vol. 1, pp. 85-105.

Jaffey, A.H., Flynn, K.F., Glendenin, L.E., Bentley, W.C., and Essling, A.M. (1971) Precision measurement of half-lives and specific activities of ^{235}U and ^{238}U. Physical Review C, vol. 4, pp. 1889-1906.

Jamieson, R.A. (1990) Metamorphism of an early Palaeozoic continental margin, western Baie Verte Peninsula, Newfoundland. Journal of Metamorphic Geology, vol. 8, pp. 269-288.

Jiang, D., and White, J.C. (1995) Kinematics of rock flow and the interpretation of geological structures with particular reference to shear zones. Journal of Structural Geology, vol. 17, pp. 1249-1265.

Kamo, S.L., Gower, C.F., and Krogh, T.E. (1989) Birthdate for the Iapetus Ocean? A precise U-Pb zircon and baddeleyite age for the Long Range dikes, Southeast Labrador. Geology, vol. 17, pp. 602-605.

Kerr, A., and Knight, I. (2004) Preliminary report on the stratigraphy and structure of the Cambrian and Ordovician rocks of the Coney Arm area, western White Bay, NTS map area 12H/15. Newfoundland Geological Survey, Current Research, Report 04-1, pp. 127-156.

Knight, I. (1983) Geology of the Carboniferous Bay St. George Subbasin, western Newfoundland. Newfoundland Department of Mines and Energy, Memoir 1, 358 pages.

Knight I., James, N.P., and Williams, H. (1995) Cambrian-Ordovician carbonate sequence (Humber Zone). *In* Geology of the Appalachian-Caledonian Orogen in Canada; Chapter 3: Lower Paleozoic and older rocks. *Edited by* H. Williams, pp. 67-87.

Krogh, T.E. (1973) A low-contamination method for hydrothermal decomposition of zircon and extraction of U and Pb for isotopic age determinations. Geochimica et Cosmochimica Acta, vol. 37, pp. 485-494.

Krogh, T.E. (1982) Improved accuracy of U-Pb zircon ages by the creation of more concordant systems using an air abrasion technique. Geochimica et Cosmochimica Acta, vol. 46, pp. 637-649.

Langdon, G.S. and Hall, J. (1994) Devonian-Carboniferous tectonics and basin deformation in the Cabot Strait area, Eastern Canada. AAPG Bulletin, vol. 78, pp. 1748-1774.

Lin, S. (1993) Relationship between the Aspy and Bras d'Or "terranes" in the northeastern Cape Breton Highlands, Nova Scotia. Canadian Journal of Earth Sciences, vol. 30, pp. 1773-1781.

Lin, S., Jiang, D., and Williams, P.F. (1998) Transpression (or transtension) zones of triclinic symmetry: natural example and theoretical modelling. Geological Society Special Publication 135, pp. 41-57.

Lin, S. (2001) $^{40}Ar/^{39}Ar$ age pattern associated with differential uplift along the Eastern Highlands shear zone, Cape Breton Island, Canadian Appalachians. Journal of Structural Geology, vol. 23, pp. 1031-1042.

Lin, S., Davis, D.W., Barr, S.M., Chen, Y., van Staal, C.R., and Constantin, M. (2007) U-Pb geochronological constraints on the geological evolution and regional correlation of the Aspy terrane, Cape Breton Island, the Canadian Appalachians. American Journal of Science, vol. 307, *in press*.

Lissenberg, C.J., Zagorevski, A., McNicoll, V.J., van Staal, C.R., and Whalen, J.B. (2005) Assembly of the Annieopsquatch Accretionary Tract, Newfoundland Appalachians: Age and geodynamic constraints from syn-kinematic intrusions. Journal of Geology, vol. 113, pp. 553-570.

Lissenberg, C.J., and van Staal, C.R. (2006) Feedback between deformation and magmatism in the Lloyds River Fault Zone: an example of episodic fault reactivation in an accretionary setting, Newfoundland Appalachians. Tectonics, vol. 25, TC4004, doi:10.1029/2005 TC001789, 18 pages.

Ludwig, K.R. (1998) On the treatment of concordant uranium-lead ages. Geochimica et Cosmchimica Acta, vol. 62, pp. 665-676.

Ludwig, K.R. (2001) User's manual for Isoplot/Ex rev. 2.49: a Geochronological Toolkit for Microsoft Excel. Berkeley Geochronology Center, Berkeley USA, Special Publication 1a, 55 pages.

Malod, J.A., and Kemal, B.M. (1996) The Sumatra margin: oblique subduction and lateral displacement of the accretionary prism. *In* Tectonic Evolution of Southeast Asia. *Edited by* R. Hall and D.J. Blundell. Geological Society Special Publication 106, pp. 19-28.

Martineau, Y.A. (1980) The relationships among rock groups between the Grand Lake Trust and Cabot Fault, West Newfoundland. Master's thesis, Memorial University of Newfoundland, St. John's NF, Canada, 150 pages.

McDougall, I., and Harrison, T.M. (1999) Geochronology and thermochronology by the $^{40}Ar/^{39}Ar$ method. New York, Oxford University Press, Inc., 269 pages.

McKerrow, W.S., and van Staal, C.R. (2000) The Palaeozoic time scale reviewed. *In* Orogenic Processes: Quantification and Modelling in the Variscan Belt. *Edited by* W. Franke, V. Haak, O. Oncken and D. Tanner. Geological Society Special Publication 179, pp. 5-8.

Miller, B.V., Dunning, G.R., Barr, S.M., Raeside, R.P., Jamieson, R.A., and Reynolds, P.H. (1996) Magmatism and metamorphism in a Grenvillian fragment: U-Pb and $^{40}Ar/^{39}Ar$ ages from the

Blair River Complex, northern Cape Breton Island, Nova Scotia, Canada. Geological Society of America Bulletin, vol. 108, pp. 127-140.

Miller, B.V., and Barr, S.M. (2004) Metamorphosed gabbroic dikes related to the opening of Iapetus Ocean at the St. Lawrence Promontory: Blair River Inlier, Nova Scotia, Canada. Journal of Geology, vol. 112, pp. 277-288.

Murphy, J.B., Keppie, J.D., Davis, D., and Krogh, T.E. (1997) Tectonic significance of new U–Pb age data for Neoproterozoic igneous units in the Avalonian rocks of northern mainland Nova Scotia, Canada. Geological Magazine, vol. 134, pp. 113-120.

Murphy, J.B., and Keppie, J.D. (1998) Late Devonian palinspastic reconstruction of the Avalon-Meguma terrane boundary: implications for terrane accretion and basin development in the Appalachian Orogen. Tectonophysics, vol. 284, pp. 221-231.

Murphy, J.B., and Nance, R.D. (2002) Sm-Nd isotopic systematics as tectonic tracers: an example from West Avalonia in the Canadian Appalachians. Earth Science Reviews, vol. 59, pp. 77-100.

Murthy, G., Gower, C., Tubrett, M., and Paetzold, R. (1992) Paleomagnetism of Eocambrian Long Range dykes and Double Mer Formation from Labrador, Canada. Canadian Journal of Earth Sciences, vol. 29, pp. 1224-1234.

Nowlan, G.S., and Neuman, R.B. (1995) Chapter 10: Paleontological contributions to Paleozoic paleogeographic and tectonic reconstructions. *In* Geology of the Appalachian-Caledonian Orogen in Canada. *Edited by* H. Williams, pp. 815-842.

Owen, J.V. (1992) Geology of the Long Range Inlier, Newfoundland. Geological Survey of Canada, Bulletin 395, 89 pages.

Owen, J.V., and Greenough, J.D. (1991) Recrystallization of quartzofeldspathic rocks in a Palaeozoic thrust belt, Grand Lake, Newfoundland: implications for garnet-biotite thermometry. Lithos, vol. 33, pp. 225-239.

Palmer, S.E., Waldron, J.W.F., and Skilliter, D.M. (2002) Post-Taconian shortening, inversion and strike slip in the Stephenville area, western Newfoundland Appalachians. Canadian Journal of Earth Sciences, vol. 39, pp. 1393-1410.

Pascucci, V., Gibling, M.R., and Williamson, M.A. (2000) Late Paleozoic to Cenozoic history of the offshore Sydney Basin, Atlantic Canada. Canadian Journal of Earth Sciences, vol. 37, pp. 1143–1165.

Passchier, C.W., and Trouw, R.A.J. (1996) Microtectonics. Berlin-Heidelberg, Springer Verlag, corrected 2nd printing, 289 pages.

Pehrsson, S.J., van Staal, C.R., Herd, R., and McNicoll, V.J. (2003) The Cormacks Lake Complex, Dashwoods Subzone: a window into the deeper levels of the Notre Dame Arc. Newfoundland Geological Survey, Current Research, Report 03-1, pp. 115-125.

Piasecki, M.A.J. (1988) Strain-induced mineral growth in ductile shear zones and a prelimenary study of ductile shearing in western Newfoundland. Canadian Journal of Earth Sciences, vol. 25, pp. 2118-2129.

Piasecki, M.A.J., Williams, H., and Colman-Sadd, S.P. (1990) Tectonic relationships along the Meelpaeg, Burgeo, and Burlington Lithoprobe transects in Newfoundland. Newfoundland Geological Survey, Report of Activities, Report 90-1, pp. 327-339.

Piasecki, M.A.J. (1991) Geology of the southwest arm of Grand Lake, western Newfoundland. Geological Survey of Canada, Current Research, Report 91-01D, pp. 1-8.

Piasecki, M.A.J. (1995) Dunnage Zone boundaries and some aspects of terrane development in Newfoundland. *In* Current Perspectives in the Appalachian-Caledonian Orogen. *Edited by* J.P. Hibbard, C.R. van Staal and P.A. Cawood. Geological Association of Canada, Special Paper 41, pp. 323-347.

Pryer, L.L. (1993) Microstructures in feldspars from a major crustal thrust zone: the Grenville Front, Ontario, Canada. Journal of Structural Geology, vol. 15, pp. 21-36.

Renne, P.R., Deino, A.L., Walter, R.C., Turrin, B.D., Swisher, C.C., Becker, T.A., Curtis, G.H., Sharp, W.D., and Jaouni, A-R. (1994) Intercalibration of astronomical and radioisotopic time. Geology, vol. 22, pp. 783-786.

Riley, G.C. (1962) Stephenville map area, Newfoundland. Geological Survey of Canada, Memoir 323, 72 pages.

Ritcey, D.H., Wilson, M.R., and Dunning, G.R. (1995) Gold mineralization in the Paleozoic Appalachian orogen: constraints from geologic, U/Pb, and stable isotope studies of the Hammer Down prospect, Newfoundland. Economic Geology, vol. 90, pp. 1955-1965.

Roddick, J.C., (1983) High-precision intercalibration of $^{40}Ar/^{39}Ar$ standards. Geochimica et Cosmochimica Acta, vol. 47, pp. 887-898.

Roddick, J.C. (1988) The assessment of errors in $^{40}Ar/^{39}Ar$ dating. *In* Radiogenic Age and Isotopic Studies, Report 2. Geological Survey of Canada, Paper 88-2, pp. 7-16.

Roddick, J.C., Cliff, R.A., and Rex, D.C. (1980) The evolution of excess argon in alpine biotites: a $^{40}Ar/^{39}Ar$ analysis. Earth and Planetary Science Letters, vol. 48, pp. 185-208.

Rogers, G., Dempster, T.J., Bluck, B.J., and Tanner, P.W.G. (1989) A high precision U-Pb age for the Ben Vuirich Granite: implications for the evolution of the Scottish Dalradian Supergroup. Journal of the Geological Society, London, vol. 146, pp. 789-798.

Sacks, P.E., Malo, M., Trzcienski Jr., W.E., Pincivy, A., and Gosselin, P. (2004) Taconian and Acadian transpression between the internal Humber Zone and the Gaspé Belt in the Gaspé Peninsula: tectonic history of the Shickshock Sud fault zone. Canadian Journal of Earth Sciences, vol. 41, pp. 635-653.

Scaillet, S. (2000) Numerical error analysis in $^{40}Ar/^{39}Ar$ dating. Chemical Geology, vol. 162, pp. 269-298.

Schärer, U. (1984) The effect of initial ^{230}Th disequilibrium on young U-Pb ages: the Makalu case, Himalaya. Earth and Planetary Science Letters, vol. 67, pp. 191-204.

Stacey, J.S., and Kramers, J.D. (1975) Approximation of terrestrial lead isotope evolution by a two-stage model. Earth and Planetary Science Letters, vol. 26, pp. 207-221.

Stern, R.A. (1997) The GSC Sensitive High Resolution Ion Microprobe (SHRIMP): analytical techniques of zircon U-Th-Pb age determinations and performance evaluation. *In* Radiogenic Age and Isotopic Studies, Report 10. Geological Survey of Canada, Current Research 1997-F, pp. 1-31.

Stern, R.A., and Amelin, Y. (2003) Assessment of errors in SIMS zircon U-Pb geochronology using a natural zircon standard and NIST SRM 610 glass. Chemical Geology, vol. 197, pp. 111-146.

Stewart, M., Strachan, R.A., and Holdsworth, R.E. (1999) Structure and early kinematic history of the Great Glen fault zone, Scotland. Tectonics, vol. 18, pp. 326-342.

Stockmal, G.S., Colman-Sadd, S.P., Keen, C.E., O'Brien, S.J., and Quinlan, G. (1987) Collision along an irregular margin: a regional plate tectonic interpretation of the Canadian Appalachians. Canadian Journal of Earth Sciences, vol. 24, pp. 1098-1107.

Stockmal, G.S., Colman-Sadd, S.P., Keen, C.E., Marillier, F., O'Brien, S.J., and Quinlan, G.M. (1990) Deep seismic structure and plate tectonic evolution of the Canadian Appalachians. Tectonics, vol. 9, pp. 45-62.

Stockmal, G.S., Slingsby, A., and Waldron, J.W.F. (1998) Deformation styles at the Appalachian structural front, western Newfoundland: implications of new industry seismic reflection data. Canadian Journal of Earth Sciences, vol. 35, pp. 1288-1306.

Stukas, V., and Reynolds, P.H. (1974) $^{40}Ar/^{39}Ar$ dating of the Long Range dikes, Newfoundland. Earth and Planetary Science Letters, vol. 22, pp. 256-266.

Szybinski, Z.A. (1995) Paleotectonic and structural setting of the western Notre Dame Bay area, Newfoundland Appalachians. Ph.D. thesis, Memorial University of Newfoundland, St. John’s NF, Canada, 493 pages.

Tollo, R.P., Corriveau, L., McLelland, J.M., and Bartholomew, M.J., *editors* (2004) Proterozoic tectonic evolution of the Grenville Orogen in North America. Geological Society of America, Memoir 197, 820 pages.

Trewin, N.H., *editor* (2002) The Geology of Scotland, 4th edition. Geological Society, London, 576 pages.

Tucker, R.D., and Gower, C.F. (1994) A U/Pb geochronological framework for the Pinware terrane, Grenville province, southwest Labrador. Journal of Geology, vol. 102, pp. 67-78.

van der Velden, A.J., van Staal., C.R., and Cook, F.A. (2004) Crustal structure, fossil subduction, and the tectonic evolution of the Newfoundland Appalachians: evidence from a reprocessed seismic reflection survey. Geological Society of America Bulletin, vol. 116, pp. 1485-1498.

van Staal, C.R. (1994) The Brunswick subduction complex in the Canadian Appalachians: record of the Late Ordovician to Late Silurian collision between Laurentia and the Gander margin of Avalon. Tectonics, vol. 13, pp. 946-962.

van Staal, C.R., Dewey, J.F., MacNiocaill, C., and McKerrow, W.S. (1998) The Cambrian-Silurian tectonic evolution of the northern Appalachians and British Caledonides: history of a complex west and southwest Pacific-type segment of Iapetus. *In* Lyell; the past is the key to the present. *Edited by* D. Blundell and A.C. Scott. Geological Society Special Publication 143, pp. 199-242.

van Staal, C.R., Barr, S.M., Fyffe, L R., McNicoll, V.J., Pollock, J C., Reusch, D.N., Thomas, M.A., Valverde-Vaquero, P., and Whalen, J.B. (2002) Ganderia: an important peri-Gondwanan terrane in the Northern Appalachians. Geological Society of America, Northeastern Section, Abstracts with Programs, vol. 34, pp. 28.

van Staal, C.R. (2005) North American Regional Geology / Northern Appalachians. *In* Encyclopedia of Geology, Volume Four. *Edited by* R.C. Selley, L.R.M. Cocks, and I.R. Plimer. Elsevier Academic Press, Oxford, United Kingdom, pp. 81-92.

van Staal, C.R. (2007) Pre-Carboniferous metallogeny of the Canadian Appalachians. *In* Mineral Deposits of Canada: A Synthesis of Major Deposit-types, District Metallogeny, the Evolution of Geological Provinces, and Exploration Methods. *Edited by* W.D. Goodfellow. Geological Association of Canada, Mineral Deposits Division, Special Publication 5, 32 pages, *in press*.

van Staal C.R., Whalen, J. B., McNicoll, V. J., Pehrsson, S., Lissenberg, C. J., Zagorevski, A., Jenner, G., and van Breemen, O. (2007) The Notre Dame arc and the Taconic Orogeny in Newfoundland. *In* The 4D Framework of Continental Crust. *Edited by* R.D. Hatcher, Jr., M.P. Carlson, J.H. McBride, and J.R. Martínez Catalán. Geological Society of America, Memoir 200, doi: 10.1130/2007.1200(26), *in press*.

Vernon, R.H. (2004) A Practical Guide to Rock Microstructure. Cambridge University Press, 606 pages.

Villeneuve, M.E., and MacIntyre, D.G. (1997) Laser $^{40}Ar/^{39}Ar$ ages of the Babine porphyries and Newman Volcanics, Fulton Lake map area, west-central British Columbia. *In* Radiogenic Age and Isotopic Studies, Report 10. Geological Survey of Canada, Current Research 1997-F, pp. 131-139.

Villeneuve, M.E., Sandeman, H.A., and Davis, W.J. (2000) A method for the intercalibration of U-Th-Pb and $^{40}Ar/^{39}Ar$ ages in the Phanerozoic. Geochimica et Cosmochimica Acta, vol. 64, pp. 4017-4030.

Waldron, J.W.F., and Milne, J.V. (1991) Tectonic history of the central Humber Zone, western Newfoundland Appalachians: post-Taconian deformation in the Old Man's Pond area. Canadian Journal of Earth Sciences, vol. 28, pp. 398-410.

Waldron, J.W.F., and Stockmal, G.S. (1994) Structural and tectonic evolution of the Humber Zone, western Newfoundland: 2. A regional model for Acadian thrust tectonics. Tectonics, vol. 13, pp. 1498-1513.

Waldron, J.W.F., Anderson, S.D., Cawood, P.A., Goodwin, L.B., Hall, J., Jamieson, R.A., Palmer, S.E., Stockmal, G.S., and Williams, P.F. (1998a) Evolution of the Appalachian Laurentian margin: Lithoprobe results in western Newfoundland. Canadian Journal of Earth Sciences, vol. 35, pp. 1271-1287.

Waldron, J.W.F., Jamieson, R A., Stockmal, G.S., and Quinn, L.A. (1998b) Loading the Laurentian margin; correlating foreland basin subsidence with eclogite metamorphism. Atlantic Geology, vol. 34, pp.79.

Waldron, J.W.F., and van Staal, C.R. (2001) Taconian Orogeny and the accretion of the Dashwoods Block: a peri-Laurentian microcontinent in the Iapetus Ocean. Geology, vol. 29, pp. 811-814.

Wanless, R.K., Stevens, R.D., Lachance, G.R., and Rimsaite, R.Y.H. (1965) Age determinations and geological studies. K-Ar isotopic ages, Report 5. Geological Survey of Canada, Paper 64-17, pp. 136.

Wasteneys, H.A., Kamo, S.L., Moser, D., Krogh, T.E., Gower, C.F., and Owen, J.V. (1997) U-Pb geochronological constraints on the geological evolution of the Pinware Terrane and adjacent areas, Grenville Province, Southeast Labrador, Canada. Precambrian Research, vol. 81, pp. 101-128.

Whalen, J.B., and Currie, K.L. (1983) The Topsails igneous terrane of western Newfoundland: Geological Survey of Canada, Current Research, Paper 83-1A, p. 15-23.

Whalen, J.B., Currie, K.L., and van Breemen, O. (1987) Episodic Ordovician - Silurian plutonism in the Topsails igneous terrane, western Newfoundland. Transactions of the Royal Society of Edinburgh: Earth Sciences, vol. 78, pp. 17-28.

Whalen, J.B., Currie, K.L., and Piasecki, M.A.J. (1993) A re-examination of relationships between Dunnage subzones in southwest Newfoundland. Geological Survey of Canada, Current Research, Paper 93-1D, pp. 65-72.

Whalen J.B., Jenner, G.A., Longstaffe, F. J., Gariépy, C., and Fryer, B. J. (1997) Implications of granitoid geochemical and isotopic (Nd, O, Pb) data from the Cambrian-Ordovician Notre Dame arc for the evolution of the Central Mobile belt, Newfoundland Appalachians. *In* The Nature of Magmatism in the Appalachian Orogen. *Edited by* K. Sinha, J.B. Whalen, and J.P. Hogan., Geological Society of America, Memoir 191, pp. 367-395.

Whalen, J.B., McNicoll, V.J., van Staal, C.R., Lissenberg, C.J., Longstaffe, F.J., Jenner, G.A., and van Breemen, O. (2006) Spatial, temporal and geochemical characteristics of Silurian collision-zone magmatism: an example of a rapidly evolving magmatic system related to slab break-off. Lithos, vol. 89, pp. 377-404.

Williams, H. (1979) Appalachian Orogen in Canada. Canadian Journal of Earth Sciences, vol. 16, pp. 792-807.

Williams, H., and St.Julien, P. (1982) The Baie Verte-Brompton Line: early Palaeozoic continent-ocean interface in the Canadian Appalachians. *In* Major structural zones and faults of the Northern Appalachians. *Edited by* P. St-Julien, and J. Beland. Geological Association of Canada, Special Paper 24, pp. 177-208.

Williams, H., and Hatcher Jr., R.D. (1982) Suspect terranes and accretionary history of the Appalachian Orogen. Geology, vol. 10, pp. 530-536.

Williams, H., Gillespie, R.T., and van Breemen, O. (1985) A late Precambrian rift-related igneous suite in western Newfoundland. Canadian Journal of Earth Sciences, vol. 22, pp. 1727-1735.

Williams, H., Colman-Sadd, S.P., and Swinden, H.S. (1988) Tectonic-stratigraphic subdivisions of central Newfoundland. Geological Survey of Canada, Current Research, Paper 88-1B, pp. 91-98.

Williams, H., *editor* (1995) Geology of the Appalachian/Caledonian Orogen in Canada and Greenland. Geological Survey of Canada, The Geology of Canada Volume 6, 944 pages. [also: Geological Society of America, The Geology of North America series, vol. F-1]

Williams, P.F., Goodwin, L.B., and Lafrance, B. (1995) Brittle faulting in the Canadian Appalachians and the interpretation of reflection seismic data. Journal of Structural Geology, vol. 17, pp. 215-232.

Williams, S.H. (1992) Lower Ordovician (Arenig-Llanvirn) graptolites from the Notre Dame Subzone, central Newfoundland. Canadian Journal of Earth Sciences, vol. 29, pp. 1717-1733.

Winchester, J.A., Williams, H., Max, M.D., and van Staal., C.R. (1992) Does the Birchy Complex of Newfoundland extend into Ireland? Journal of the Geological Society, London, vol. 149, pp. 159-162.

Wilson, T. (1962) Cabot Fault, an Appalachian equivalent of the San Andreas and Great Glen Fault and some implications for continental displacement. Nature (London), vol. 195, pp. 135-138.

Wilson, J.T. (1966) Did the Atlantic close and then re-open? Nature (London), vol. 211, pp. 676-681.

Zagorevski, A., Rogers, N., van Staal, C.R., McNicoll, V.J., Lissenberg, C.J., and Valverde-Vaquero, P. (2006) Lower to Middle Ordovician evolution of peri-Laurentian arc and back-arc complexes in the Iapetus: constraints from the Annieopsquotch Accretionary Tract, Central Newfoundland. Geological Society of America Bulletin, vol. 118, pp. 324-342.

Appendix A: **Analytical Techniques for U-Pb ID-TIMS**

Single grain zircon, monazite and titanite U-Pb ID-TIMS analyses were performed at the Jack Satterly Laboratory, University of Toronto and at the Royal Ontario Museum. Mineral concentrates were prepared using standard methods involving crushing, grinding, a Wilfley™ table, heavy liquids, and the Frantz™ isodynamic separator successively. Grains were examined and handpicked using a binocular microscope.

Standard methods of bomb dissolution and U-Pb extraction with HCl in small anion exchange columns were used for zircon (Krogh, 1973, 1982), although several small zircon grains were analyzed without chemical purification (marked ** in Tables 2.1 and 3.1).

Selected monazite grains were dissolved in 6N HCl in Savillex™ capsules, and processed with HCl in small anion exchange columns. Pb and U were loaded together with silica gel onto out-gassed rhenium filaments.

Selected titanite grains were dissolved in 6N HCl in Savillex™ capsules, and processed with HBr in small anion exchange columns. Pb and U were loaded with silica gel onto out-gassed rhenium filaments and analyzed separately.

The isotopic compositions of Pb and U were measured using a single collector Daly detector in a solid source VG354 mass spectrometer. Data were calculated, regressed and plotted using the UTILAge software (D.W. Davis, in-house program) with regression based on Davis (1982). All age errors quoted in the text and in Tables 2.1 and 3.1, and error ellipses in the Concordia diagrams (Figures 2.6, 2.7A and 3.8), are given at the 95% confidence interval.

Appendix B: **Analytical Techniques for U-Pb SHRIMP[1]**

SHRIMP II analyses were conducted at the Geological Survey of Canada (GSC) laboratory in Ottawa, Ontario using analytical procedures described by Stern (1997), with standards and U-Pb calibration methods following Stern and Amelin (2003). Handpicked zircon grains from sample AB-02-293 (z7591) were cast in 2.5 cm diameter epoxy mounts (GSC mount #304) along with fragments of the GSC laboratory standard zircon (z6266, with $^{206}Pb/^{238}U$ age = 559 Ma). The midsections of the zircon grains were exposed using 9, 6, and 1 µm diamond compound, and the internal features of the zircons were characterized with backscatter electrons (BSE) and cathodo-luminescence (CL) utilizing a Cambridge Instruments scanning electron microscope (SEM). Mount surfaces were evaporatively coated with 10 nm of high purity Au. Analyses were conducted using an $^{16}O^-$ primary beam, projected onto the zircon grains at 10 kV. The sputtered area used for analysis was ca. 12 µm in diameter with a beam current of ca. 1.3 nA. The count rates of ten isotopes of Zr^+, U^+, Th^+, and Pb^+ in zircon were sequentially measured over 5 scans with a single electron multiplier and a pulse counting system with deadtime of 35 ns. Off-line data processing was accomplished using customized in-house software. The 1σ external error of $^{206}Pb/^{238}U$ ratios reported in Table 2.2 incorporate a ±1.0 % error in calibrating the standard zircon (see Stern and Amelin, 2003). No fractionation correction was applied to the Pb-isotope data; common Pb correction utilized the measured $^{204}Pb/^{206}Pb$ and compositions modeled after Cumming and Richards (1975). The $^{206}Pb/^{238}U$ ages for the analyses have been corrected for common Pb using both the 204- and 207-methods (Stern, 1997), but there is generally no significant difference in the results (Table 2.2). Isoplot v. 2.49 (Ludwig, 2001) was used to generate a Concordia diagram where the data are plotted with errors at the 2σ-level (Figure 2.7B). The calculated Concordia age and errors quoted in the text are at 2σ with decay constant errors included (Ludwig, 1998).

[1] Text prepared by Vicki J. McNicoll, Geological Survey of Canada

Appendix C: Analytical Techniques for $^{40}Ar/^{39}Ar$ Geochronology[1]

Laser $^{40}Ar/^{39}Ar$ step-heating analysis was carried out at the Geological Survey of Canada laboratories in Ottawa, Ontario.

Samples were processed for $^{40}Ar/^{39}Ar$ analysis of biotite (AB-02-376), muscovite (AB-02-158; AB-02-293) and hornblende (AB-01-131; AB-02-321) phenocrysts by standard mineral separation techniques, including hand-picking of clear, unaltered crystals in the size range 0.5 to 1 mm. Individual mineral separates were loaded into aluminum foil packets along with PP-20 hornblende (Hb3gr equivalent) with an apparent age of 1072 Ma (Roddick, 1983) to act as flux monitor. The sample packets were arranged radially inside an aluminum can. The samples were then irradiated for 70 hours (120 hours for aliquot C of sample AB-02-293) at the research reactor of McMaster University in a fast neutron flux of approximately $3x10^{16}$ neutrons/cm^2.

Upon return from the reactor, samples were split into several aliquots and loaded into individual 1.5 mm-diameter holes in a copper planchet. The planchet was then placed in the extraction line and the system evacuated. Heating of individual sample aliquots in steps of increasing temperature was achieved using a Merchantek MIR10 10W CO_2 laser equipped with a 2 mm x 2 mm flat-field lens. The released Ar gas was cleaned over getters for ten minutes, and then analyzed isotopically using the secondary electron multiplier system of a VG3600 gas source mass spectrometer; details of data collection protocols can be found in Villeneuve and MacIntyre (1997) and Villeneuve and others (2000). Error analysis on individual steps follows numerical error analysis routines outlined in Scaillet (2000); error analysis on grouped data follows algebraic methods of Roddick (1988).

Corrected argon isotopic data are listed in Tables 2.3 and 3.2, and presented as spectra of gas release in Figures 2.7C and D, and Figure 3.10 (Roddick et al., 1980). The gas-release spectrums from samples AB-02-158 (Figure 3.10B), AB-02-293 (Figure 2.7C) and AB-02-321 (Figure 3.10C) contain step-heating data from two aliquots, alternately shaded and normalized to the total volume of ^{39}Ar released. Such plots provide a visual image of replicated heating profiles and the error and apparent age of each step.

Neutron flux gradients throughout the sample canister were evaluated by analyzing the hornblende flux monitors included with each sample packet and interpolating a linear fit against calculated J-factor and sample position. The error on individual J-factor values is conservatively estimated at ±0.6% (2σ). Because the error associated with the J-factor is systematic and not related to individual

[1] Text prepared by Vicki J. McNicoll, Geological Survey of Canada

analyses, correction for this uncertainty is not applied until calculation of dates from isotopic correlation diagrams (Roddick, 1988). All errors are quoted at the 2σ level of uncertainty.

Geology of the Long Range Mountains, southwestern Newfoundland

(Appendix D)

Post-orogenic basin sedimentary rocks
Carboniferous

Deer Lake basin

C_{DL} — Deer Lake Group (Visean)
Red-brown siltstone, mudstone and sandstone

C_A — Anguille Group (Tournaisian)
Fining-upward sequence: basal conglomerate, dominantly grey sandstone and siltstone, and carbonaceous mudstone; minor limestone and dolostone layers

Bay St. George Subbasin

C_B — Barachois Group (Namurian - Westphalian A)
Green-gray and red sandstones; red siltstones, black shales and coal beds

C_C — Codroy Group (Middle - Upper Visean)
Dominantly pink-red arkosic grits, sandstones and siltstones

C_A — Anguille Group (Upper Devonian ? - Tournaisian)
Red and gray sandstones; minor siltstones and conglomerates

Humber Arm Allochthon
Cambro-Ordovician

HAA — Undifferentiated
Black shale and silt

External Humber Zone
Humber Arm Supergroup - Cambro-Ordovician

EHZ — Undifferentiated
Dolomite and limestone; May locally contain *South Brook Formation* or rocks of the *Humber Arm Allochthon*.

Internal Humber Zone - Steel Mountain Inlier

Corner Brook Lake block

Metasedimentary thrust stack

NO_S — Matthews Brook serpentinite
Serpentinized ultramafic rock

Mount Musgrave Group

ϵCO_{BP} — Breeches Pond Formation
Metacarbonate rocks: calcareous schists; calc-mica schist, marble and meta-limestone conglomerate

NO_{SB} — South Brook Formation (<ca. 572 Ma)
Metaclastic rocks: pebble-conglomerate, psammitic and pelitic schists; minor marble and calc-silicate layers

PC_L — Labrador Group
Pebble-conglomerate, grit, and coarse sandstone

Crystalline basement

NP_{LS} — Lady Slipper pluton (ca. 555 Ma)
Granodiorite gneiss and amphibolite

Hare Hill igneous complex (ca. 602-608 Ma)

NP_{HH} — Hare Hill granite (ca. 608 Ma)
Weakly to strongly foliated pink to red alkali granite and syenite, and related gneisses; locally massive and pegmatitic

NP_{DHG} — Disappointment Hill granitoid plutons (ca. 606 Ma)
Pale white to grey granodiorite, tonalite and gneissic variations; tonalitic agmatite containing mafic to ultramafic xenoliths

x — Ultramafic xenolith of troctolitic affinity

NP_{DHM} — Disappointment Hill mafic plutons
Weakly to well-foliated buff-grey diorite, gabbro, and monzonite

MP_{DHC} — Disappointment Hill charnockite (ca. 1498 Ma)
Salic to intermediate two-pyroxene granulite gneiss, and megacrystic orthopyroxene leucogranite

MP_{CBL} — Undifferentiated Corner Brook Lake complex (ca 1.50 Ga)
Quartzo-feldspathic gneiss and migmatite, and associated amphibolite layers; local quartzite and calc-silicate paragneissic layers

Steel Mountain complex

MP_{SMC} — Anorthosite
Pale white to lilac massive anorthosite to (anorthositic) gabbro; marginal cumulate textures; locally gneissose or pegmatitic; intruded by amphibolite dykes

Geological contact (defined; approximate; assumed)

(gradational)

Unconformity

Fault (defined; approximate; assumed)

Baie Verte-Brompton Line - Cabot Fault Zone (BCZ) Tectonic zone

Thrust fault

Brittle fault

Cataclasite zone

Brittle-ductile shear zone (sinistral; dextral)

Main or composite foliation

Foliation in BCZ (D_{BCZ-1}; D_{BCZ-2}; D_{BCZ-3}; D_{BCZ-4}) See Chapter 5

Foliation in CBLB metasediments (S_{SED-1}; S_{SED-2}) See Chapter 3

Foliation in CBLB basement (S_{BSZ}) See Chapter 3

Foliation in Little Grand Lake Fault See Chapter 2

Mineral lineation

Stretching lineation

Fold axis (F_1 or generic; F_2)

Bedding (normal, overturned)

Transposed bedding

Bedding from pillow lavas (younging direction known)

Igneous layering

Axis of anticline

Axis of syncline

Trans Canada Highway

Burgeo Road

Trail / lumber road

Radiometric ages:

$^{40}Ar/^{39}Ar$ age

ca. 443 Ma (M) (introduced herein)

ca. 428 Ma (M) (previously published)

B = Biotite; H = Hornblende; M = Muscovite

U-Pb age (zircon, unless otherwise stated)

463 ± 5 Ma (introduced herein)

608 ± 4 Ma (previously published)

M = Monazite; R = Rutile

N

Mean magnetic declination: 21°W (in 2006)

0 5 10 km

Scale 1 : 100 000

Notre Dame subzone

S_T — Topsails Igneous Suite (ca. 427-429 Ma)
Unfoliated, pink to red medium- to coarse-grained mainly subsolvus granite; alkali granite to syenite

S_{RL} — Rainy Lake complex (includes Glover Island granodiorite) (ca. 435-440 Ma) - Notre Dame Arc 3rd phase
Weakly foliated, fine- to coarse-grained calc-alkaline gabbro, diorite, tonalite and granodiorite

O_T — Tonalite - Notre Dame Arc 1st or 2nd phase
Foliated white tonalite

Glover Group

O_{CP} — Corner Pond Formation (lower to middle Arenig)
Multi-coloured shale, conglomerate, sandstone, felsic volcanics, purple to green pillow basalts; typical red shale near base

O_{TKP} — Tuckamore & Kettle Pond formations
Green pillow basalts, pillow breccia, and mafic tuff; minor diabase dykes; polymictic conglomerate and sandstone; minor volcanics

O_M — Mafic volcanics
Blackgreen pillow basalts, layered to massive gabbro, sheeted diabase dykes

ϵCO_{GLO} — Grand Lake ophiolite complex (ca. 490 Ma)
Layered to massive gabbro, trondhjemite, and mafic dykes

P_B — Undifferentiated basement
Quartzo-feldspathic gneiss and conglomerate

Dashwoods subzone

SD — Pink granite - Siluro-Devonian
Pink, unfoliated medium- to coarse-grained granite

S_{LH} — Lake of the Hills intrusives (ca. 430 Ma)
Pink to red, biotite-amphibole granite

S_{PP} — Puddle Pond Complex (includes Main Gut gabbro) (ca. 431 Ma)
Foliated to unfoliated, dark, medium-grained diorite, gabbro and diabase; locally layered cumulate sequence of anorthosite and norite

uO_G — Granodiorite (ca. 446 Ma) - Notre Dame Arc 3rd phase
Medium- to coarse-grained granodiorite to granite; locally developed as sheets

mO_{SBC} — Southwest Brook Complex (ca. 456-464 Ma) - Notre Dame Arc 2nd phase
Variably foliated white, medium-coarse grained tonalite to granodiorite; agmatic tonalite contains mafic-ultramafic enclaves and sedimentary screens; locally co-mingling structures

m — Meta-sedimentary enclave

x — Amphibolitized mafic-ultramafic xenolith

mO_{LGL} — Little Grand Lake granite (ca. 463 Ma)
Pale coloured, muscovite ± biotite granite to granodiorite

NO_{DPC} — Dennis Pond complex (Mischief mélange) (>ca. 488 Ma)
Chlorite and muscovite bearing schistose mixture of granitoids and metasedimentary rocks; sparse marble and grit-conglomerate layers; also includes regionally developed unlayered, chaotic migmatitic mélange

x — Amphibolitized mafic-ultramafic rafts

NO_{CLC} — Cormacks Lake Complex (ca. 483-489 Ma) - Notre Dame Arc 1st phase
Mainly well-banded granodiorite to tonalite orthogneiss; includes tectonized layered mafic and felsic volcanic rock, and sillimanite-garnet-bearing paragneiss

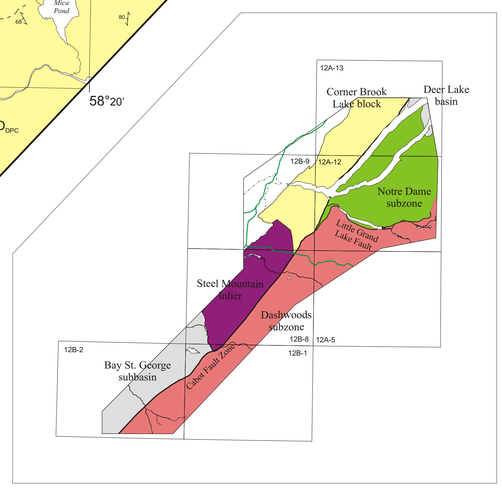

Geological compilation by Arjan G. Brem (2006):

- Field data collected in 2001-2003
- Publications:

Brem, A.G., and van Staal., C.R. (2006) Geology, Harrys River, Newfoundland and Labrador, 12B/09, Geological Survey of Canad, Open File 4921, scale 1:50 000.

Cawood, P.A., and van Gool, J.A.M. (1998) Geology, Corner Brook Lake region, Newfoundland; Geological Survey of Canada, Map 1893A, scale 1:50 000 (accompanying GSC Bulletin 427).

Currie, K.L., and van Berkel, J.T. (1992) Geology, southern Long Range Mountains, Newfoundland; Geological Survey of Canada, Map 1815A, scale 1:100 000 (accompanied by GSC Paper 91-10).

Knight, I. (1982) Geology of the Carboniferous Bay St. George subbasin; Newfoundland Department of Mines and Energy, Map 82-1, scale 1:125 000 (accompanying Memoir 1).

Szybinski, Z.A., Brem, A.G., van Staal., C.R., Whalen, J., McNicoll, V.J., Jenner, G., and Piercey, S. (2006) Geology, Little Grand Lake, Newfoundland and Labrador, 12A/12; Geological Survey of Canada, Open File 1668, scale 1:50 000.

Pehrsson, S.J., Brem, A.G., and van Staal., C.R. (2006) Geology, Main Gut, Newfoundland and Labrador, 12B/09, Geological Survey of Canada, Open File 1666, scale 1:50 000.

van Staal, C.R., Lissenberg, C.J., Pehrsson, S., and Zagorevski, A. (2005) Geology, Puddle Pond, Newfoundland and Labrador, 12A/05. Geological Survey of Canada, Open File 1664, scale 1:50 000.

This geological map forms part of the Ph.D. dissertation titled "*The Late Neoproterozoic to Early Palaeozoic tectonic evolution of the Long Range Mountains in southwest Newfoundland*" by Arjan G. Brem, submitted to the University of Waterloo, Canada (2007).